DYNAMIC STABILITY TEST RESULTS

ON AN O.024 SCALE B-1 AIR VEHICLE

(NASA-CR-145903) DYNAMIC STABILITY TEST RESULTS ON AN 0.024 SCALE B-1 AIR VEHICLE (North American Rockwell Corp.) 147 p HC $6.00 CSCL 01C

N76-13112

Unclas

G3/08 05140

Los Angeles Division
North American Rockwell

NA-72-82

SERIAL NO. 10

DYNAMIC STABILITY TEST RESULTS

ON AN 0.024 SCALE B-1 AIR VEHICLE

PREPARED BY

R. R. Beeman

D J Beck

D. J. Beck
B-1 Project Aerodynamicist

R. B. Lyford, Manager
Aerodynamics

DATE 17 March 1972

NO. OF PAGES 145

Los Angeles Division
North American Rockwell
International Airport, Los Angeles, California 90009, (213) 670-9151

FOREWORD

This report was prepared by the Aerodynamics Group of the Los Angeles Division of North American Rockwell Corporation at Los Angeles, California under Air Force contract No. F33657-70-C-0800, and the NASA Vehicle Dynamics Section of Langley Research Center, Langley Air Force Base, Virginia.

Three Langley Research Center wind tunnels were utilized to obtain the main damping derivatives (C_{mq}, C_{n_r} and C_{ℓ_p}) over the Mach number range of the air vehicle - the Langley 4 foot Unitary Plan wind tunnel (supersonic), the Langley 8 foot Transonic Pressure tunnel and the Langley 7 x 10 foot High Speed tunnel (transonic and subsonic).

Messrs. R. R. Beeman and R. Whitmoyer (NR Aerodynamics) and Mr. Cecil Berthold (NR Wind Tunnel) were assigned to this test under the overall technical direction of Mr. L. Gaines (NR Aerodynamics).

NASA, LRC, Vehicle Dynamics Section personnel conducting the test were Messrs. R. A. Kilgore, E. E. Davenport, J. Adcock and R. Boyden under the supervision of Mr. H. G. Wiley.

SUMMARY

Dynamic longitudinal and lateral-directional stability characteristics of the B-1 air vehicle have been investigated in three wind tunnels at the Langley Research Center. The main rotary derivatives were obtained for an angle of attack range of -3 degrees to +16 degrees for a Mach number range of 0.2 to 2.16. Damping in roll data could not be obtained at the supersonic Mach numbers. The Langley 7 x 10 foot high speed tunnel, the 8 foot transonic pressure tunnel and the 4 foot Unitary Plan wind tunnel were the test sites. An 0.024 scale light-weight model was used on a forced oscillation type balance. Test Reynolds number varied from 0.474 x 10^6/Ft. to 1.55 x 10^6/Ft. through the Mach number range tested.

The results of the investigation showed that the dynamic stability characteristics of the model in pitch and roll were generally satisfactory up to an angle attack of about +6 degrees.. In the wing sweep range from 15 to 25 degrees the positive damping levels in roll deteriorated rapidly above +2 degrees angle of attack. This reduction in roll damping is believed to be due to the onset of separation over the wing as stall is approached.

In the subsonic and transonic speed range, yaw damping levels are negative in some cases (wing $\Lambda = 25°$, $55°$ and $65°$), vertical tail inputs are zero to negative and body input is about twice the estimate. The afterbody of the rotary derivative model is distorted from the air vehicle lines to permit insertion of the balance and to provide clearance between the base and the sting for model oscillation.

The resulting large diameter base is believed to have caused an aerodynamic interference between the model afterbody and the horizontal and vertical tails which significantly altered the vertical tail input to yaw damping. Since the B-1 fuselage has a much different shape than the model in the vicinity of the vertical tail, the yaw damping characteristics measured on the model are probably not representative of the B-1 air vehicle.

TABLE OF CONTENTS

FOREWORD	1
SUMMARY	2
LIST OF ILLUSTRATIONS	4
NOMENCLATURE	6
INTRODUCTION	8
DISCUSSION	9
MODEL DESCRIPTION	9
WIND TUNNELS	9
OSCILLATION BALANCE MECHANISM	10
PRESENTATION OF RESULTS	11
CONCLUSIONS AND RECOMMENDATIONS	13
DIMENSIONAL DATA	14
REFERENCES	19

LIST OF ILLUSTRATIONS

Figure No.	Title	Page
1-5	Model Photographs	26-30
6	View of B-1	31
7&8	Model Drawings	33 & 34
	PITCH DAMPING	
9-12	Effect of Mach no. on Damping in Pitch	35 - 38
13-18	Damping in Pitch Derivatives $\Lambda = 15^{\circ}$, 25°, Mach 0.55 - 0.75	39 - 44
19&20	Effect of Filler Blocks on Damping in Pitch	45 & 46
21&22	Comparison of Tunnels	47 & 48
23-27	Damping in Pitch Derivatives, $\Lambda = 65^{\circ}$; Mach 0.55-1.2	49 - 53
28-32	Effect of L.E. Sweep on Damping in Pitch; Mach 0.55-1.2	54 - 58
33-37	Effect of CG Location on Damping in Pitch, Mach 0.55-1.2	59 - 63
38-45	Damping in Pitch Derivatives $\Lambda = 55^{\circ}$, 65°; Mach 1.8, 2.16	64 - 71
46-49	Effect of Component Build up on Damping in Pitch Derivatives $\Lambda = 55^{\circ}$, 65°, Mach = 1.8, 2.16	72 - 75
50	Effect of Center cf Gravity Variation on Damping in Pitch Derivatives	76
51-53	Horizontal Tail Input to Damping in Pitch Derivatives; Mach 1.8, 2.16	77 - 79
	YAW DAMPING	
54-59	Effect of Horizontal and Vertical Tails on Damping in Yaw Derivatives $\Lambda = 15^{\circ}$, 25°, Mach 0.55 - 0.75	80 - 85
60&61	Effect of Filler Blocks on Damping in Yaw Derivatives $\Lambda = 25^{\circ}$, Mach 0.55, 0.70	86 & 87
62	Effect of SMC vane, Horizontal and Vertical Tails on Damping in Yaw Derivatives $\Lambda = 25^{\circ}$ Mach = 0.70	88
63&64	Damping in Yaw Derivatives, Data Repeatability $\Lambda = 25^{\circ}$	89 & 90
65-67	Effect of Horizontal and Vertical Tails on Damping in Yaw Derivatives $\Lambda = 65^{\circ}$, Mach 0.55 - 0.80	91 - 93
68&69	Effect of Filler Blocks on Damping in Yaw Derivatives $\Lambda = 65^{\circ}$, Mach 0.55, 0.75	94 - 95
70&71	Effect of Horizontal Tail Deflection on Damping in Yaw Derivatives $\Lambda = 65^{\circ}$; Mach = 0.55, 0.75	96 & 97
72-74	Effect of Mach Number on Damping in Yaw Derivatives $\Lambda = 55^{\circ}$, 65°	98 - 100
75-78	Component Build up $\Lambda = 65^{\circ}$, Mach 0.55 - 0.80	101 - 104
79	Comparison of Bodies $\Lambda = 65^{\circ}$, Mach = 0.75	105
80	Effect of Sweep and Steel Rod Stays on Damping in Yaw Derivatives Mach = 0.55	106
81-83	Effect of Sweep on Damping in Yaw Derivatives Mach 0.7 - 0.08	107 - 109

LIST OF ILLUSTRATIONS (Continued)

Figure No.	Title	Page
84&85	Comparison of Various Bodies; Mach 0.55, 0.75	110 - 111
86&87	Component Build-up Mach 0.55, 0.75	112 - 113
88&89	Data Repeatability $\Lambda = 65^{\circ}$, Mach 0.55, 0.75	114 - 115
90-93	Effect of Mach Number and Sweep on Damping In Yaw Derivatives, $\Lambda = 55^{\circ}, 65^{\circ}$, Mach = 1.80, 2.16	116 - 119
94	Effect of Center of Gravity Position on Damping in Yaw $\Lambda = 65^{\circ}$, Mach = 1.80, 2.16	120
95-98	Effect of Component Build up on Damping in Yaw Derivative, Mach = 55°, 65°, Mach = 1.80, 2.16	121 - 124
99-100	Vertical Tail Input to Damping in Yaw Derivatives, $\Lambda = 55^{\circ}, 65^{\circ}$ Mach = 1.80, 2.16	125 - 126
101	Comparison of Yaw Data with Estimates $\Lambda = 65$ Mach = 2.16	127
102	Data Sensitivity to Change in Oscillatory Frequency Mach = 2.16	128
	ROLL DAMPING	
103	Effect of Mach Number on Damping in Roll	129
104-109	Damping in Roll Derivatives, $\Lambda = 15^{\circ}, 25^{\circ}$, Mach 0.55 - 0.75	130 - 135
110-114	Damping in Roll Derivatives, $\Lambda = 55^{\circ}, 65^{\circ}$, Mach 0.55 - 1.20	136 - 140
115-119	Damping in Roll Derivatives, Effect of C.G. Location $\Lambda = 65^{\circ}$; Mach 0.55 - 1.20	141 - 145

NOMENCLATURE

Symbols

ℓ	reference length = 10.33 ft.
C_ℓ	rolling moment coefficient, $\frac{\text{Rolling moment}}{q_\infty S \ell}$
$C_{\ell p} = \frac{\partial C_\ell}{\partial\left(\frac{p\ell}{2V}\right)}$	per radian
C_m	pitching moment coefficient, $\frac{\text{Pitching moment}}{q_\infty S \ell}$
k	reduced frequency parameter, $\frac{\omega\ell}{2V}$ in pitch and yaw
M	freestream Mach number
q	angular velocity of model about body Y-axis, rad/sec
q_∞	freestream dynamic pressure, psf
r	angular velocity of model about body Z-axis, rad/sec
S	reference area = 60.44 ft.^{2}
V	freestream velocity ft/sec
α	angle of attack, degrees or radians; mean angle of attack, deg.
β	angle of sideslip, degrees or radians; mean angle of sideslip, degrees
ω	angular velocity, $2\pi f$, rad/sec
$C_{m_q} = \frac{\partial C_m}{\partial\left(\frac{q\ell}{2V}\right)}$ /rad	
$C_{m_q} + C_{m_{\dot\alpha}}$	damping in pitch parameter, per radian

$C_{m_{\dot{q}}} = \dfrac{\partial C_m}{\partial\left(\dfrac{\dot{q}\ell^2}{4V^2}\right)}$ /rad

$C_{m_\alpha} = \dfrac{\partial C_m}{\partial \alpha}$ /rad

$C_{m_\alpha} - k^2 C_{m_{\dot{q}}}$ oscillatory-longitudinal-stability parameter, per radian

$C_{m_{\dot{\alpha}}} = \dfrac{\partial C_m}{\partial\left(\dfrac{\dot{\alpha}\ell}{2V}\right)}$ /rad

C_n yawing-moment coefficient, $\dfrac{\text{Yawing moment}}{q_\infty S \ell}$

$C_{n_r} = \dfrac{\partial C_n}{\partial\left(\dfrac{r\ell}{2V}\right)}$ /rad

$C_{n_r} - C_{n_{\dot{\beta}}} \cos\alpha$ damping-in-yaw parameter, per radian

$C_{n_{\dot{r}}} = \dfrac{\partial C_n}{\partial\left(\dfrac{\dot{r}\ell^2}{4V^2}\right)}$ /rad

$C_{n_\beta} = \dfrac{\partial C_n}{\partial \beta}$ /rad

$C_{n_\beta} \cos\alpha + k^2 C_{n_{\dot{r}}}$ oscillatory-directional-stability parameter, per radian

$C_{n_{\dot{\beta}}} = \dfrac{\partial C_n}{\partial\left(\dfrac{\dot{\beta}\ell}{2V}\right)}$ /rad

$C_{\ell_p} + C_{\ell_{\dot{\beta}}} \sin\alpha$ damping in roll parameter, per radian

$C_{\ell_{\dot{\beta}}} = \dfrac{\partial C_\ell}{\partial\left(\dfrac{\dot{\beta}b}{2V}\right)}$

INTRODUCTION

Design of guidance and control systems for aerodynamic configurations requires knowledge of the various dynamic stability derivatives through wide ranges of flight speeds. Experimental data and theories are available at low speeds, and a limited amount of data is available at supersonic speeds. However, at transonic speeds no adequate theories for predicting these derivatives are available, especially at angle of attack, and little experimental data exists.

Therefore, wind tunnel test investigations have been conducted by the National Aeronautics and Space Administration and North American Rockwell Corporation to substantiate the levels of the main dynamic stability derivatives of the B-1 air vehicle. The information obtained will be used to determine their effect on the flight dynamics of the air vehicle.

DISCUSSION

MODEL DESCRIPTION

The model is a relatively lightweight 0.024-scale replica of the B-1 air vehicle with provision for sting mounting to the NASA-Langley rigidly forced oscillation system. Aerodynamic similarity is maintained except for the fuselage modifications necessary to accommodate the support sting and oscillating mechanism, figures 1 through 8. The upper fuselage moldline follows the air vehicle lines, reference 1, but a significant deformation of the lower surface was necessary to form the required circular cross section aft of fuselage station 950. Forward of this station, the circular section gradually blends into the air vehicle mold lines at fuselage station 150.

The wing and empennage surfaces are fabricated of aluminum alloy and the forward fuselage section is constructed of laminated fiberglass. The wing is pivoted to provide four discrete sweep positions and the horizontal tail is adjustable to -10°, 0°, and +10° deflection.

The balance mounting bulkhead can be moved in the mounting tube to place the balance center-of-rotation at the longitudinal position corresponding to the full scale air vehicle center of gravity for the various wing sweep positions.

The reference dimensions used in the data calculation are the following:

0.24-Scale	Full Scale
S_W = 1.1209 sq. ft.	1946 sq. ft.
b_W = 39.364 in.	1640.17 in.
$\bar{c}_W$ = 4.417 in.	184.05 in.
F.S. of $.25\bar{c}_W$ = 23.708 in.	987.85 in.
F.S. of $.45\bar{c}_W$ = 24.59 in.	1024.66 in.
F.S. of $.75\bar{c}_W$ = 25.92 in.	1079.88 in.

Additional model and test information is contained in references 2 and 3.

WIND TUNNELS

Three wind tunnels were used to obtain the data presented herein. All three are equipped for control of relative humidity and total temperature of the air in the tunnel to minimize the effects of condensation and for control of total pressure in order to obtain the test Reynolds number.

Langley Unitary Plan Wind Tunnel.-The data at Mach numbers 1.8 and 2.16 were obtained in test section number 1 of the Langley Unitary Plan wind tunnel. This single return tunnel has a test section about 4.0 feet by 4 feet. An asymmetric sliding block, which varies the area ratio, is used to change Mach number from about 1.47 to 2.86. The angle of attack mechanism used for this investigation has a total range of about 25 degrees when used with the oscillation balance mechanism.

Langley 8-foot Transonic Pressure Tunnel.-The data at Mach numbers from 0.40 to 1.20 were obtained in the Langley 8-foot transonic pressure tunnel. The test section of this single return closed-circuit wind tunnel is about 7.0 feet by 7 feet with slotted upper and lower walls to permit continuous operation through the transonic speed range. Test section Mach numbers from about 0.2 to 1.30 can be obtained and kept constant by controlling the speed of the tunnel fan drive motor. The Mach number is reasonably uniform throughout the test section, with a maximum deviation from the average freestream Mach number of approximately 0.01 at the higher Mach numbers.

The sting support strut is designed to keep the model near the center line of the tunnel through a range of sting angles of attack from about -4 to +22 degrees when used with the oscillation balance mechanism.

Langley 7 x 10 foot High Speed Tunnel.-Correlation data for Mach numbers from 0.2 to 0.8 were obtained in the Langley 7 by 10 foot high speed tunnel. It is a single return wind tunnel which operates with atmospheric stagnation pressure and has a conventional, closed, rectangular fixed geometry test section. The sting support strut is designed to keep the model near the center line of the tunnel through a range of sting angles of attack from about -12 to +16 degrees when used with the oscillation balance mechanism.

OSCILLATION BALANCE MECHANISM

Two oscillation balance mechanisms were used for these tests, one for pitch and yaw and the other for roll. The damping terms are measured as a function of how much torque is required to oscillate the models at a certain amplitude. A description of these mechanisms is given in reference 3.

AXIS SYSTEM

The aerodynamic parameters are referred to the body system of axes originating at the oscillation center of the model as shown in figure 7 The reference dimensions are based on the geometric characteristics of the model with the wings in the swept forward position ($\Lambda = 15°$) regardless of the actual test wing-sweep position.

PRESENTATION OF RESULTS

The actual run schedules for the five tests presented in this report are shown on Tables I through V (pages 20 through 25). The tests were as follows:

Table	Test No.	Tunnel	Derivative
I	952	4' UPWT	Pitch & Yaw
II & III	596	8' TPT	Pitch & Yaw
IV	599	8' TPT	Roll
V	934	7 x 10' HST	Yaw & Pitch

Test Reynolds number, based on the wing mean aerodynamic chord was approximately 1,100,000 in the Unitary Plan tunnel, 1,550,000 in the 8' TPT, and between 1,100,000 and 1,450,00 in the 7 x 10 tunnel with the exception of the data taken at Mach 0.2, which was at a Reynolds number of 500,000.

The damping in pitch derivative $C_{m_q} + C_{m_{\dot{\alpha}}}$ and the oscillatory-stability parameter $C_{m_\alpha} - k^2 C_{m_q}$ are presented in figures 9 through 53 for subsonic, transonic and supersonic Mach numbers. The data obtained show positive damping and are in fair agreement with estimated levels at zero angle of attack, and in general show an increase in damping with increase in angle of attack. Component build-up data, such as figures 13 thru 19, show that the horizontal tail contributes approximately 50 percent of the damping in pitch. Plots showing the effect of wing leading edge sweep, Mach number, center of gravity shift and wing input on the damping in pitch parameters are also presented. The effects of Mach number at constant angles of attack are presented on figures 9 through 12 for various leading edge sweep angles. Estimated data are superimposed on these plots.

The damping in yaw derivative $C_{n_r} - C_{n_{\dot{\beta}}}$ and the oscillatory stability parameter $C_{n_\beta} \cos + k^2 C_{n_{\dot{r}}}$ are presented on figures 54 through 102 for subsonic, transonic and supersonic Mach numbers. Inspection of the supersonic data reveal that $C_{n_r} - C_{n_{\dot{\beta}}}$ measured approximately 50 percent more damping than was estimated. The increased damping was due primarily to body input, which was probably influenced by the enlarged model base. Vertical tail input to the damping in yaw parameter was about 70 percent of the estimated data. This reduction in tail damping may be due in part to the distorted model afterbody, as suspected in the subsonic tests. Directional stability, C_{n_β} due to the tail was slightly less than that measured in the trisonic wind tunnel.

The subsonic damping in yaw data measured in the Langley 8' TPT was questionable because of variation with frequency, and zero or negative damping due to vertical tail. The model was shifted to the Langley 7 x 10 HST for further investigation with a stiffer model support system. The variation of $Cn_r - Cn_{\dot{\beta}}$ with frequency was reduced but the vertical tail input to yaw damping was still zero or negative. Removing the horizontal tail improved the vertical tail damping input. A fairing was tested on the vertical tail in the area between the horizontal tail and aft fuselage mold line, page 32 , to partially simulate the three dimensional relief between the horizontal tail and fuselage as it exists on the air vehicle. Data obtained with this "channel filler block" brought the tail on yaw damping level closer to estimated values, fig 68 & 69 Tail input, however, was still less than 50 percent of estimated. The data also show that damping in yaw gets less positive with increase in Mach number from 0.2 to 0.8 for all sweeps. Installation of the "filler blocks" reversed this trend through this Mach number range. Since either the removal or deflection of the horizontal tail, or the addition of the filler blocks on the vertical tail drastically altered the vertical tail input to yaw damping, it is apparent that aerodynamic interference between the fuselage afterbody, horizontal and vertical tails significantly affected the yaw damping of the model configuration. Since the model lines are significantly different than the B-1 air vehicle in this area, the yaw damping characteristics measured on the model are probably not representative of the B-1 air vehicle.

The damping in roll derivative $C_{\ell_p} + C_{\ell_{\dot{\beta}}} \sin\alpha$ is presented on figures 103 through 119. These data were obtained at subsonic through transonic Mach numbers for the wing leading sweep range of the air vehicle. Damping data obtained with the wing in the aft sweep positions, $\Lambda = 65$ and 55 degrees show good agreement with estimated data at a fairly constant level of damping with variation of angle of attack. Data obtained with the forward leading edge sweep positions $\Lambda_{LE} = 25$ and 15 degrees show good agreement with estimated data from -3 to 0 to 2 degrees angle of attack. The damping levels drop rapidly with increasing angle of attack above 0 to 2 degrees. This phenomenon is associated with the onset of airflow separation over the wing as the angle of attack for stall is approached. Force data obtained on other B-1 models indicate the onset of separation at somewhat higher angles of attack than those at which the roll damping begins to deteriorate. This is probably because the force models were tested at higher Reynolds numbers than the rotary derivative model.

CONCLUSIONS

Data obtained with the wing panels swept 15 and 25 degrees showed positive damping in pitch, that generally remained linear with angle of attack for angles below about six degrees. The damping in roll data obtained showed positive damping at angles of attack from -2 to +2 degrees; above these angles of attack the damping deteriorated rapidly. This phenomenon is closely associated with the onset of separation at these sweeps and angles of attack.

Data obtained with the wing panels swept 55 and 65 degrees showed positive damping in pitch and roll and remained linear with angle of attack for angles below about six degrees at subsonic and transonic Mach numbers and about 10 degrees supersonically. No supersonic damping in roll data was obtained.

The aerodynamic damping in pitch and roll measured in these tests appear reasonable, and are substantiated by estimates for the B-1 configuration.

The measured aerodynamic damping in yaw showed some unusual results. The damping due to the body was larger than estimated, but the measured damping due to the vertical tail was less than estimated, and sometimes even negative at Mach numbers between .7 and .8. Component buildup showed the vertical tail input to be strongly affected by aerodynamic interference between the fuselage afterbody and the horizontal and vertical tails. Since the model shape is significantly different than the B-1 air vehicle in this area, the yaw damping characteristics measured on the model are probably not representative of the B-1 air vehicle.

RECOMMENDATIONS

In order to obtain data that can be used during design to define the flight dynamics of the B-1 air vehicle, additional testing must be accomplished. The model lines should be modified to more closely approximate B-1 afterbody lines so that the questionable validity of the initial test data can be clarified. Since the horizontal tail planform was changed subsequent to the construction of this model, this component should also be updated. Also since roll damping was not attainable above $M = 1.2$, additional testing for this parameter should be accomplished over the complete Mach range.

DIMENSIONAL DATA

W_{47} Wing

Model

Reference Area, Ft.^{2}	1.120
Span, Ft.	3.272
Aspect Ratio	9.560
Taper Ratio	.351
Chords, In.:	
Root (B.P. 0.0)	6.075
Tip (B.P. 19.634)	2.135
M.A.C. (B.P. 8.247)	4.420
Fus. Sta. of 0.25 M.A.C., In.	23.705
Fus. Sta. of Wing Pivot (B.P. 3.480), In.	23.256
Leading Edge Sweepback Angle, Deg.	14.992°
Dihedral, Deg.	-1.940°
Incidence, Deg.	0.0°

h_{58} Wing hood

Data for One of Two Sides

Model

Area, Ft^2	.065
Corresponding Wing Area, ft^2	1.120
Wing Sweep, Deg.	15.

B_{51} Body

Model

Length, Ft.	3.40
Max. Width (F.S. 22.8-40.8), In.	3.6
Max. Depth (F.S. 22.8-40.8), In.	3.6
Max. Cross-Sectional Area (F.S. 22.8-40.8), Ft^2	.071
Fineness Ratio	11.333

B_{60} B_{51} with Ogive Forebody

B_{61} B_{51} with Filler Blocks in Channel Between Horizontal Tail and Fuselage (see page 32)

B_{62} B_{51} with Vertical Tail Mounting Plate Faired Forward to Blend More Smoothly into Fuselage

T_R 19 Boundary Layer Transition Grit
N_o. 100 Carborundum Grit

Wing, Horizontal, Vertical (Both Sides)

Width = .05 ∓ In.
.5 In Aft of L.E.

Fuselage Forebody

Width = .05 In
1.5 in Aft. of L.E.

N54 Nacelle
Data for 1 of 2 Sides

Model	
Length (Overall), Ft.	.895
Max. Width, (F.S. 29.39), In.	3.03
Max. Depth, (F.S. 28.20), In.	1.65
Inlet Area, $Ft.^2$	.0124
Capture Area, $Ft.^2$	.0124
Exit Area (Total), $Ft.^2$	.00863
Fus. Sta. of Nacelle Leading Edge, In.	21.77
Nacelle Centerline	
B.P., In. (F.S. 21.77), In.	3.386
W.P., In. (F.S. All), In.	-.840
Offset Angle Nac. C_L (L.E. Inb'd)	.318°

C_{12} Structural Model Control Vane

Total	
Area, Ft^2	.027
Span (Equiv.), Ft.	.25
Aspect Ratio	2.298
Taper Ratio	.100
Chords, Inc.	
Root (B.P. 0.0)	2.053
Tip (B.P. 1.499)	.206
M.A.C. (B.P. .545)	1.381
Fus. Sta. of 0.25 M.A.C. (W.P. .417), In.	5.273
Dihedral Angle, Deg.	-30.0
Incidence Angle, Deg.	0.
Sweepback Angle, Deg.	
Leading Edge	35.022°
0.25 Chord Element	23.458°
Airfoil Section L.E.R. = (.051) (Local Chord)	
T.E.R. = Knife Edge	

Exposed	
Area, Ft^2	.0065
Span (Equiv.), Ft.	.110
Aspect Ratio	1.867
Taper Ratio	.202
Chords, In.	
Root (B.P. .837)	1.021
Tip (B.P. 1.499)	.206
MA.C. (B.P. 1.095)	.704
Fus. Sta of 0.25 M.A. C. (W.P. .0999), In.	5.548

H_{163} Horizontal Tail

Total	
Area, Ft.^{2}	.293
Span (Equiv.), Ft.	1.071
Aspect Ratio	3.918
Taper Ratio	.304
Chords, In.	
Root (B.P. 0.0)	5.030
Tip (B.P. 1.528)	1.528
M.A.C. (B.P. 2.640)	3.591
Fus. Sta. of 0.25 M.A.C. (W.P. 3.024), In.	38.395
Angles, Deg.	
Dihedral	0.0
Incidence	0.0
Leading Edge Sweep	32.500
0.25 Chord Element	26.601
Airfoil Section	
Root (B.P. 0.0)	65A007
Tip (B.P. 6.457)	65A007
Exposed	
Area, Ft.^{2}	.271
Span (Equiv.), Ft.	1.017
Aspect Ratio	3.824
Taper Ratio	.315
Chords, In.	
Root (B.P. .321)	4.855
Tip (B.P. 6.42)	1.528
M.A.C. (B.P. 2.842)	3.481
Fus. Sta. of 0.25 M.A.C. (W.P. 3.024), In.	38.497

V_{46} **Vertical Tail**

Area, Ft.^{2}	.146
Span (Equiv.), Ft.	.409
Aspect Ratio	1.184
Taper Ratio	.304
Equivalent Chords, In.	
Root (W.P. 2.016)	6.362
Tip (W.P. 6.930)	1.937
M.A.C. (W.P. 4.036)	4.543
Fus. Sta. of 0.25 M.A.C. (B.P. 0.0), In.	34.049
Angles, Deg.	
Cant	0.0
Offset	0.0
Leading Edge Sweep	50.777
0.25 Chord Element	45.0
Airfoil Section	
Root (W.P. 2.016)	65A010
(W.P. 3.854)	65A010
Tip (W.P. 6.962)	65A005

D_3 **Dorsal Fin**

Area, Ft.^{2}	.021
Length, In.	11.562

REFERENCES

1. D481-55B-1, " General Arrangement, Three View Drawing of the B-1 Air Vehicle" Dated 14 December 1970.

2. NA-70-550-2, TP/PS 0221-1-002, "Pretest Information for B-1 0.024-Scale Air Vehicle Rotary Derivative Tests in Langley 4 Foot UPWT", Dated 19 April 1971.

3. NA-70-550-2, TP/PS 0221-1-001,"Pretest Information for B-1 0.024-Scale Air Vehicle Rotary Derivative Tests in Langley 8-foot TPT", Dated 17 May 1971.

4. NASA TN D-1231, "A Rigidly Forced Oscillation System for Measuring Dynamic-Stability Parameters in Transonic and Supersonic Wind Tunnels", Dated March 1962.

TABLE I

LANGLEY 4' UPWT TEST NO. 952

ACTUAL RUN SCHEDULES - PITCH AND YAW OSCILLATIONS

CONFIGURATION		Λ	δ_H	C.G. POS. $\%\bar{c}_w$	PITCH MACH NO./RUN NO.		YAW MACH NO./RUN NO.	
					1.8	2.16	1.8	2.16
W47h58B51N54C12D3H163V46	TR19	65°	0°	.27	2	1	22	21
W47h58B51N54C12D3H163V46	TR19	65°	0°	.75	4	3	24	23
W47h58B51N54C12D3--V46	TR19	65°	-	.75	7	6	-	-
W47h58B51N54C12---	TR19	65°	-	.75	-	-	27	26
W47h58B51N54C12D3H163V46	TR19	65°	-10°	.75	9	8	29	28
W47h58B51N54C12D3H163V46	TR19	55°	0°	.75	11	10	31	30
W47h58B51N54C12D3--V46	TR19	55°	-	.75	13	12	-	-
W47h58B51N54C12----	TR19	55°	-	.75	-	-	33	32
B51C12	TR19	-	-	.75	16	14	-	-
B51C12D3H163V46	TR19	-	0°	.75	18	17	20	19

TABLE II

LANGLEY 8' TPT TEST NO. 596

ACTUAL RUN SCHEDULE - PITCH OSCILLATION

CONFIGURATION		Λ	δ_H	C.G. POS. $\%\bar{c}_W$	MACH NUMBER/RUN NUMBER						
					.55	.7	.75	.85	.95	1.03	1.2
W47h58B51N54C12 D3H163V46	TR19	55°	0°	.75	3	-	-	2	5	4	1
W47h58B51N54C12 D3H163V46	TR19	65°	0°	.75	6	-	-	7	10	9	8
W47h58B51N54C12D3--V46	TR19	65°	-	.75	15	-	-	14	13	12	11
W47h58B51N54C12D3H163V46	TR19	65°	0°	.25	20	-	-	19	18	17	16
W47h58B51N54C12D3H163V46	TR19	15°	0°	.25	23	22	21	-	-	-	-
W47h58B51N54C12D3--V46	TR19	15°	-	.25	26	25	24	-	-	-	-
W47h58B51N54C12D3--V46	TR19	25°	-	.45	29	28	27	-	-	-	-
W47h58B51C12D3H163V46	TR19	25°	0°	.45	32	31	30	-	-	-	-
B51C12D3H163V46	TR19	-	0°	.75	37	-	-	36	35	34	33
B51C12D3---V46	TR19	-	-	.75	39	-	-	38	-	-	-

TABLE III

LANGLEY 8' TPT TEST NO. 596 (CONT'D)

ACTUAL RUN SCHEDULE - YAW OSCILLATION

CONFIGURATION		Λ	δ_H	C.G. POS. % $\bar{c}_W$	MACH NUMBER/RUN NUMBER						
					.55	.7	.75	.85	.95	1.03	1.2
W47h58B51N54C12D3H163V46	TR19	55°	0	.75	44	—	—	43	42	41	40
W47h58B51N54C12D3H163V46	TR19	65°	0	.75	49	—	—	48/92**	47	46	45
W47h58B51N54C12-----	TR19	65°	—	.75	54	—	—	53	52	51	50
W47h58B51N54C12D3H163V46	TR19	65°	0°	.25	60	—	59	58	57	56	55
W47h58B51N54C12D3H163V46	TR19	15°	0°	.25	63	62	61	—	—	—	—
W47h58B51N54C12-----	TR19	15°	—	.25	66	65	64	—	—	—	—
W47h58B51N54C12-----	TR19	25°	—	.45	69	68	67/89*	—	—	—	—
W47h58B51N54C12D3H163V46	TR19	25°	0°	.45	72/91**	71	70/90**	—	—	—	—
W47h58B51---C12D3H163V46	TR19	65°	0°	.75	76	—	75	74	—	—	73
B51C12D3H163V46	TR19	—	0°	.75	81	—	—	80	79	78	77
B51C12	TR19	—		.75	86	—	—	85	84	83	82
W47h58B51N54C12D3H163V46	TR19	25°	0°	.45	—	88*	87*	—	—	—	—

*Runs 87, 88 and 89 Made with Pitch Oscillation Rig with Model at $\phi = 270°$

**Runs 90, 91 and 92 Made with 2 more Cables added to the Yaw Oscillation Rig to increase System Stiffness

TABLE IV

LANGLEY 8' TPT TEST NO. 599

ACTUAL RUN SCHEDULE - ROLL OSCILLATION

CONFIGURATION		Λ	δ_H	C.G. Pos $\%\bar{c}_W$	MACH NUMBER/RUN NUMBER						
					.55	.7	.75	.85	.95	1.03	1.2
W47h58B51N54C12D3H163V46	TR19	65°	0°	.75	5	—	—	4	1	3	2
W47h58B51N54C12D3--V46	TR19	65°		.75	10	—	—	9	8	7	6
W47h58B51N54C12D3H163V46	TR19	55°	0°	.75	15	—	—	13	12	14	11
W47h58B51N54C12D3H163V46	TR19	65°	0°	.25	20	—	—	18	17	19	16
W47h58B51N54C12D3H163V46	TR19	15°	0°	.25	23	22	21	—	—	—	—
W47h58B51N54C12D3--V46	TR19	15°	—	.25	26	25	24	—	—	—	—
W47h58B51N54C12D3--V46	TR19	25°	—	.45	29	28	27	—	—	—	—
W47h58B51C12D3H163V46	TR19	25°	0°	.45	32	31	30	—	—	—	—
W47h58B51N54C12D3H163V46	TR19	25°	-10°	.45	35	34	33	—	—	—	—

TABLE V

LANGLEY 7 x 10' HST TEST NO. 934

ACTUAL RUN SCHEDULE - YAW OSCILLATION

CONFIGURATION		Λ	δ_H	C.G.POS. $\%\bar{c}_W$	MACH NUMBER/RUN NUNBER				
					.20	.55	.7	.75	.8
W47h58B51N54C12D3H163V46	TR19	25°	0°	.45	—	6/12,68*	5/69*	4	—
W47h58B51N54C12----	TR19	25°	—	.45	—	9	8	7	—
W47h58B51N54----	TR19	25°	—	.45	—	—	10	—	—
W47h58B51N54--D3H163V46	TR19	25°	0°	.45	—	—	11	—	—
W47h58B51N54C12D3H163V46	TR19	15°	0°	.25	—	15	14	13	—
W47h58B51N54C12----	TR19	15°	—	.25	—	18	17	16	—
B51C12D3H163V46	TR19	—	0°	.75	—	22	21	20	19
B51C12D3--V46	TR19	—	—	.75	—	23	24	25	26
B51C12	TR19	—	—	.75	—	27	—	28	—
B60	TR19	—	—	.75	—	30	—	29	—
B60D3--V46	TR19	—	—	.75	—	31	—	32	—
B60D3H163V46	TR19	—	0°	.75	—	33	—	34	—
B51D3H163V46	TR19	—	0°	.75	—	36	—	35	—
W47h58B51N54C12D3H163V46	TR19	65°	0°	.75	41	37	38	39/67*	40
W47h58B51N54C12D3H163V46	TR19	65°	-10°	.75	—	42	—	43	—
W47h58B51N54C12----	TR19	65°	—	.75	—	44	—	—	45
W47h58B51N54C12D3--V46	TR19	65°	—	.75	—	46	—	48	47
W47h58B51N54C12D3H163V46	TR19	55°	0°	.75	—	49/55**	52	51/54**	50/53**

TABLE V (CONT'D)

CONFIGURATION		Λ	δ_H	C.G.POS. %$\bar{c}_W$	MACH NUMBER/RUN NUMBER .20	.55	.70	.75	.80
W47h58B51N54C12D3H163V46	TR19	65°	0°	.75	—	56/65*	63	57/64*	62
W47h58B61N54C12D3--V46	TR19	65°	—	.75	—	58	—	59	—
W47h58B51N54C12D3H163V46	TR19	65°	+10°	.75	—	61	—	60	—
W47h58B62N54C12D3H163V46	TR19	65°	0°	.75	—	—	—	66	—
W47h58B61N54C12D3H163V46	TR19	25°	0°	.45	—	72	73	—	—
W47h58B61N54C12D3--V46	TR19	25°	—	.45	—	74	75	—	—
W47h58B51N54C12D3--V46	TR19	25°	—	.45	—	71	70	—	—

*Runs 12, 64, 65, and 68 are Check Runs

**Runs 53, 54 and 55 were made at = 4° only with Horizontal Steel Rod Stiffness Instead of Cable

LANGLEY 7 x 10' HST TEST NO. 936

ACTUAL RUN SCHEDULE - PITCH OSCILLATION

CONFIGURATION		Λ	δ_H	C.G.POS. %$\bar{c}_W$	MACH NUMBER/RUN NUMBER .20	.55	.70	.75	.80
W47h58B51N54C12D3H163V46	TR19	25°	0°	.45	—	1	2	—	—
W47h58B61N54C12D3H163V46	TR19	25°	0°	.45	—	3	4	—	—

NASA
L-71-8370

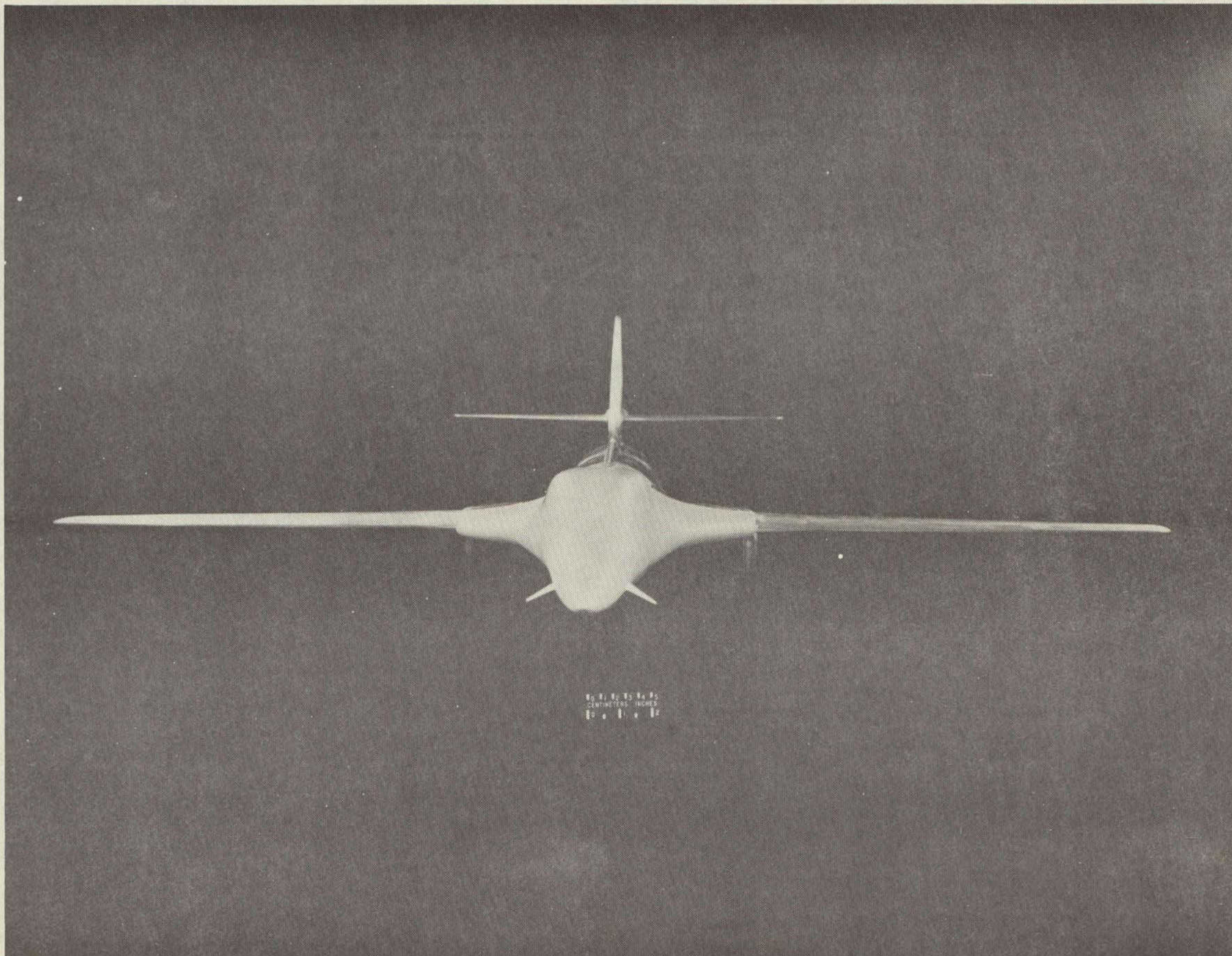

NA-72-82

PAGE 26

NASA
L-71-8371

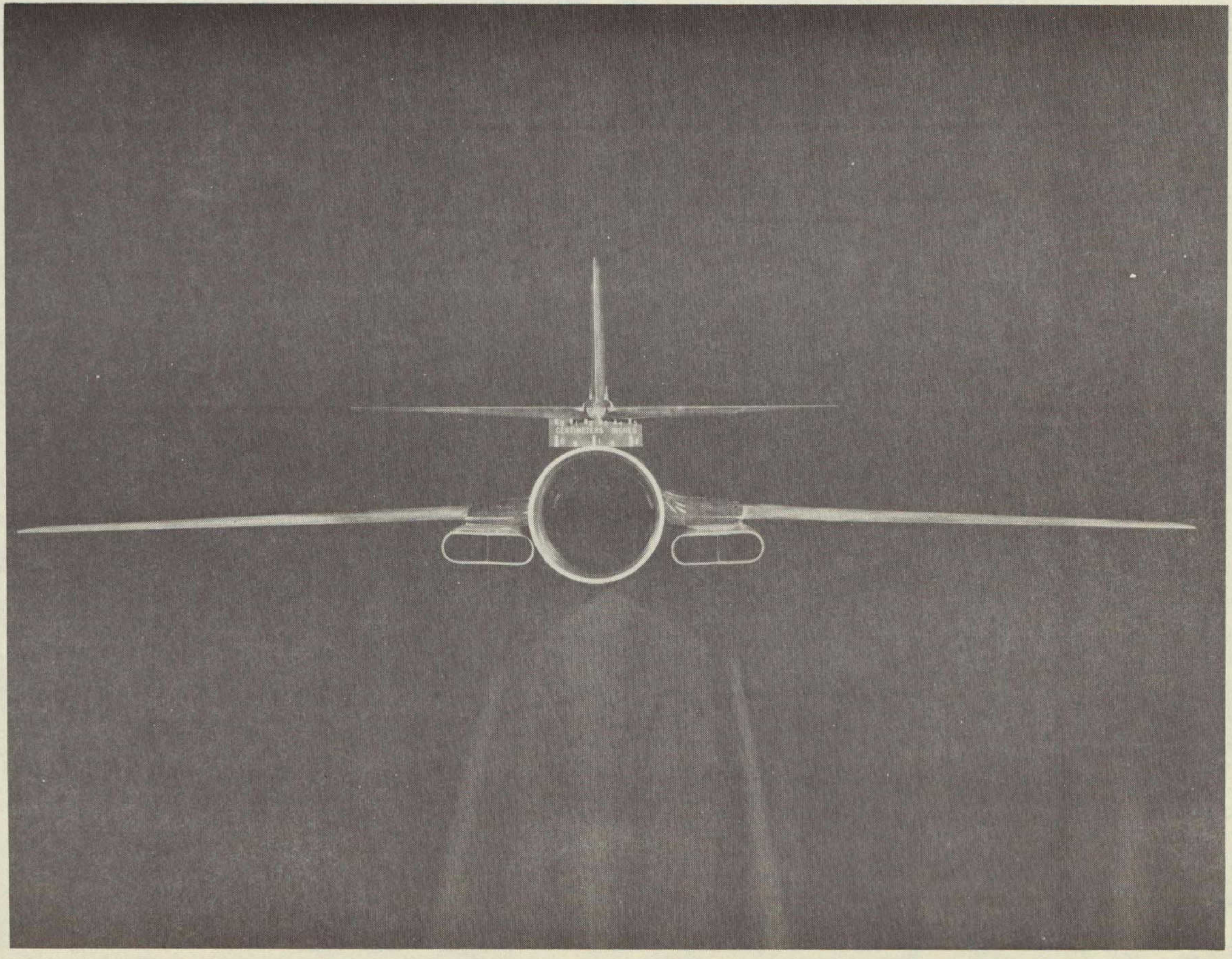

ORIGINAL PAGE IS
OF POOR QUALITY

NA-72-82

NASA
L-71-8372

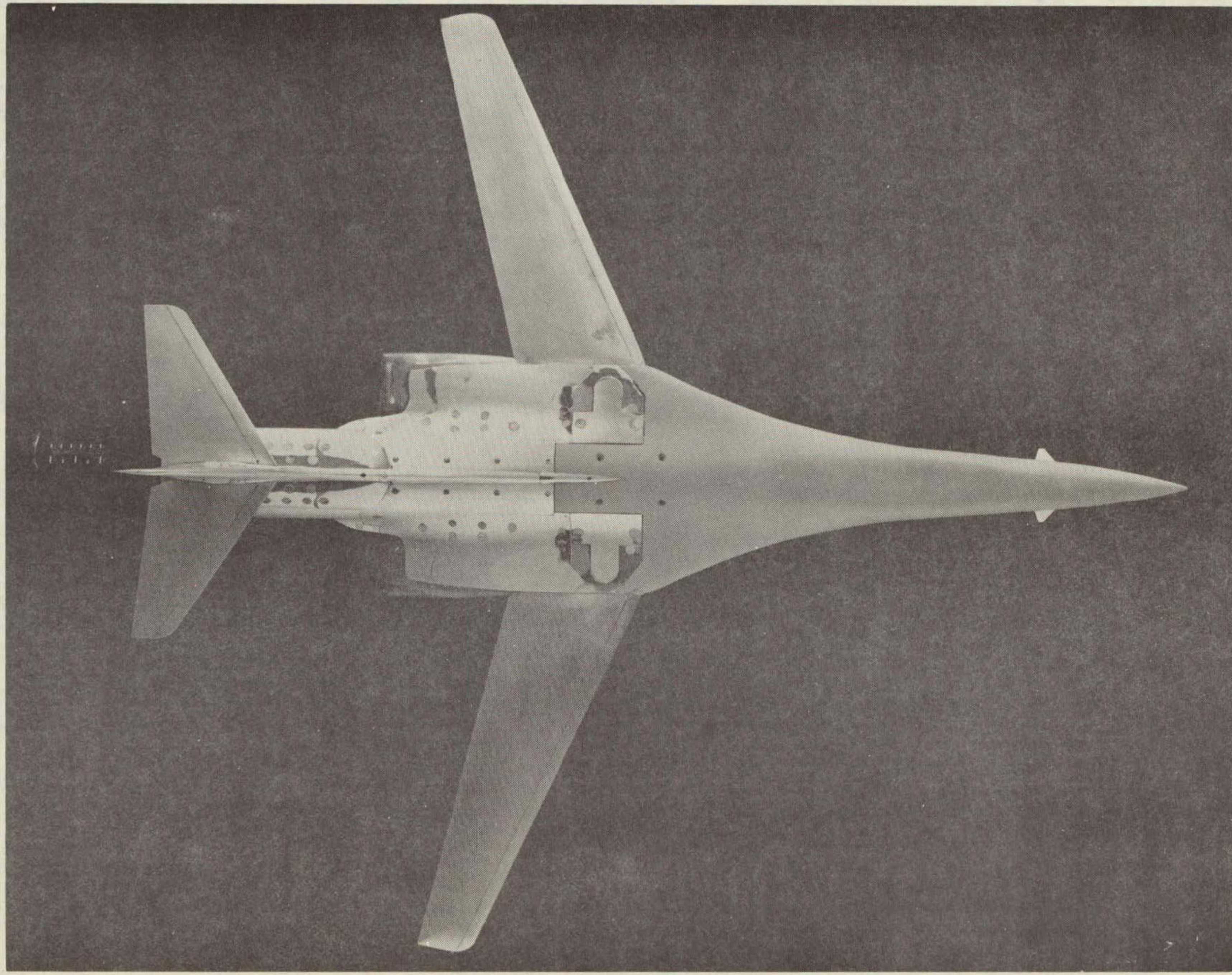

NA - 72-82

NASA
L-71-8373

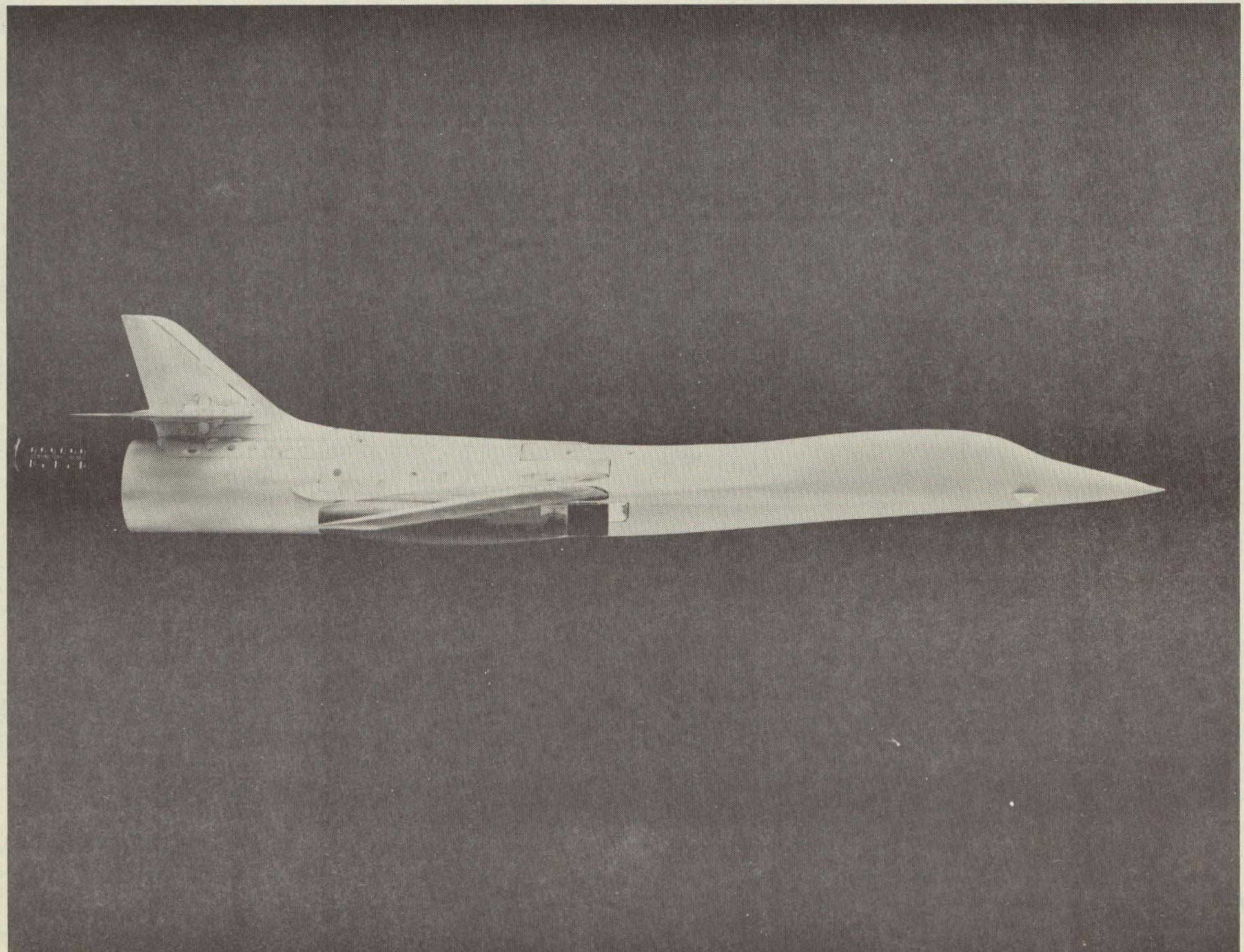

NA-72-82

NASA
L-71-8374

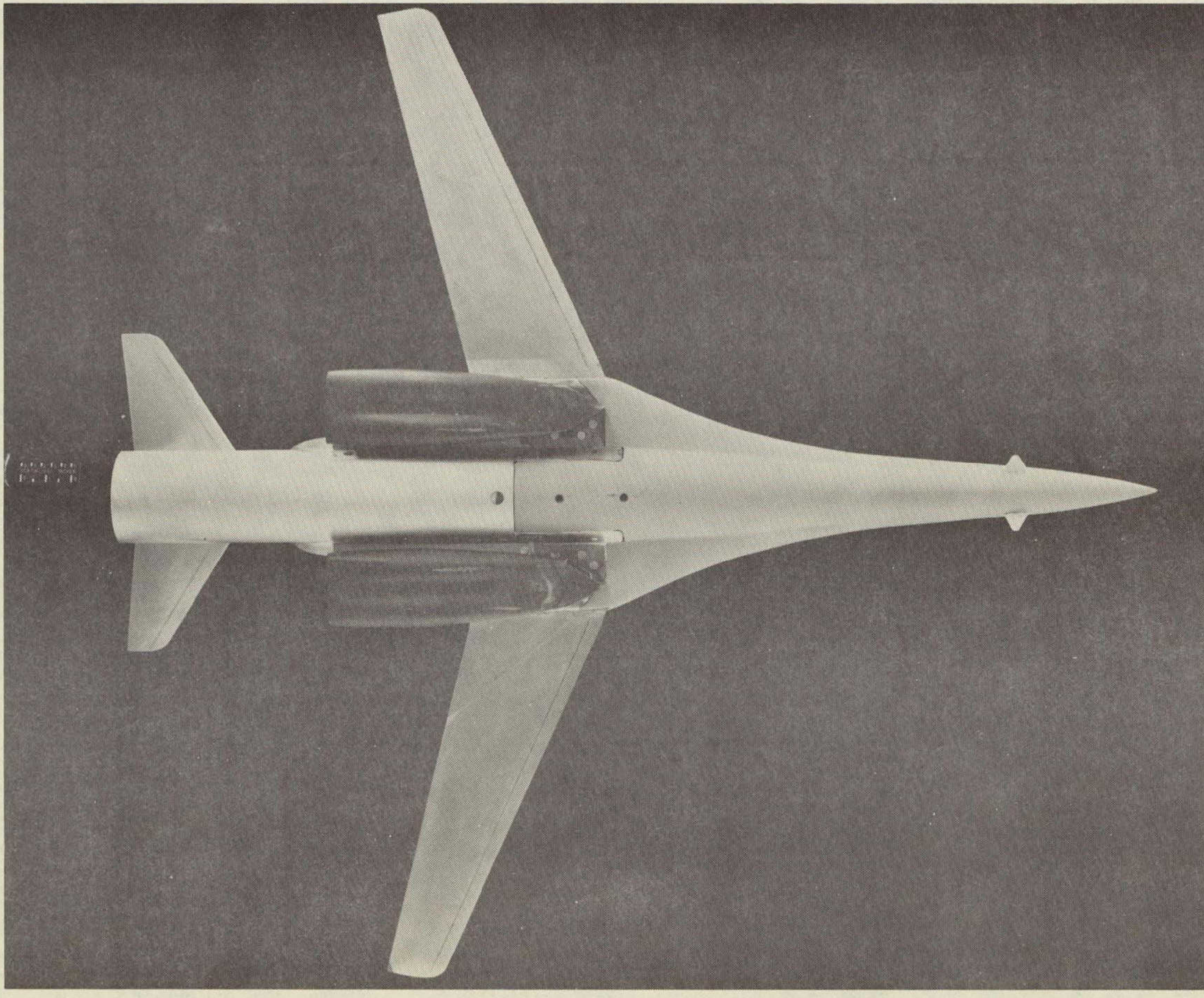

NA-72-82

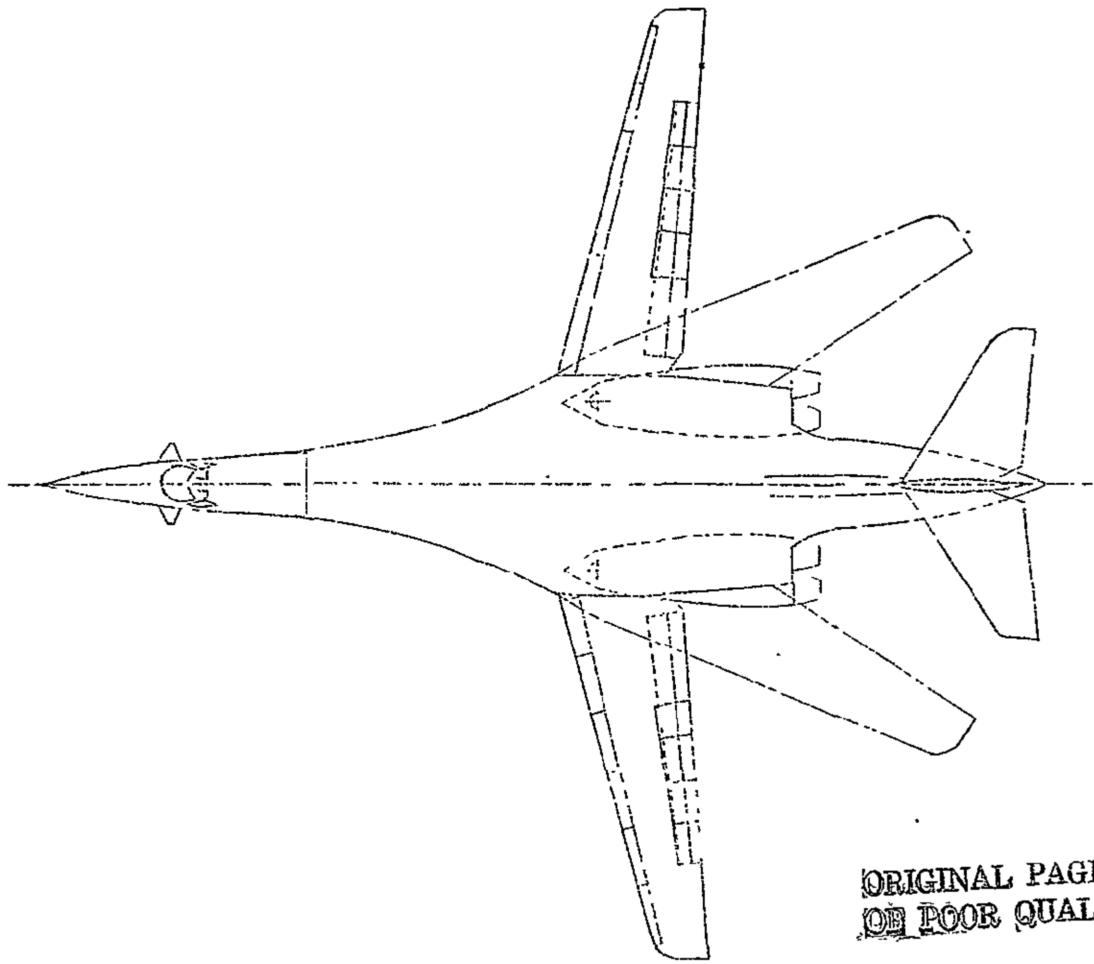

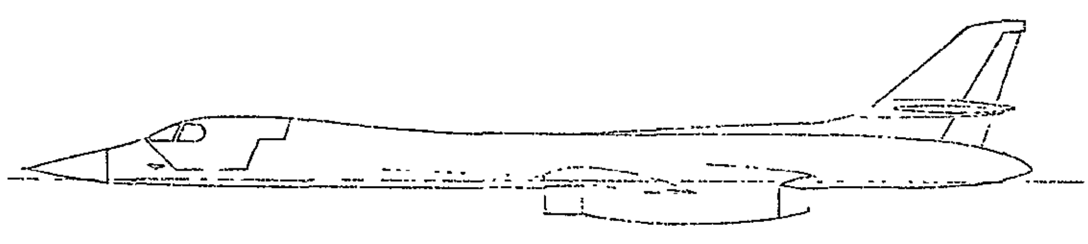

VIEW OF B-1

.024 SCALE ROTARY DERIVATIVE MODEL

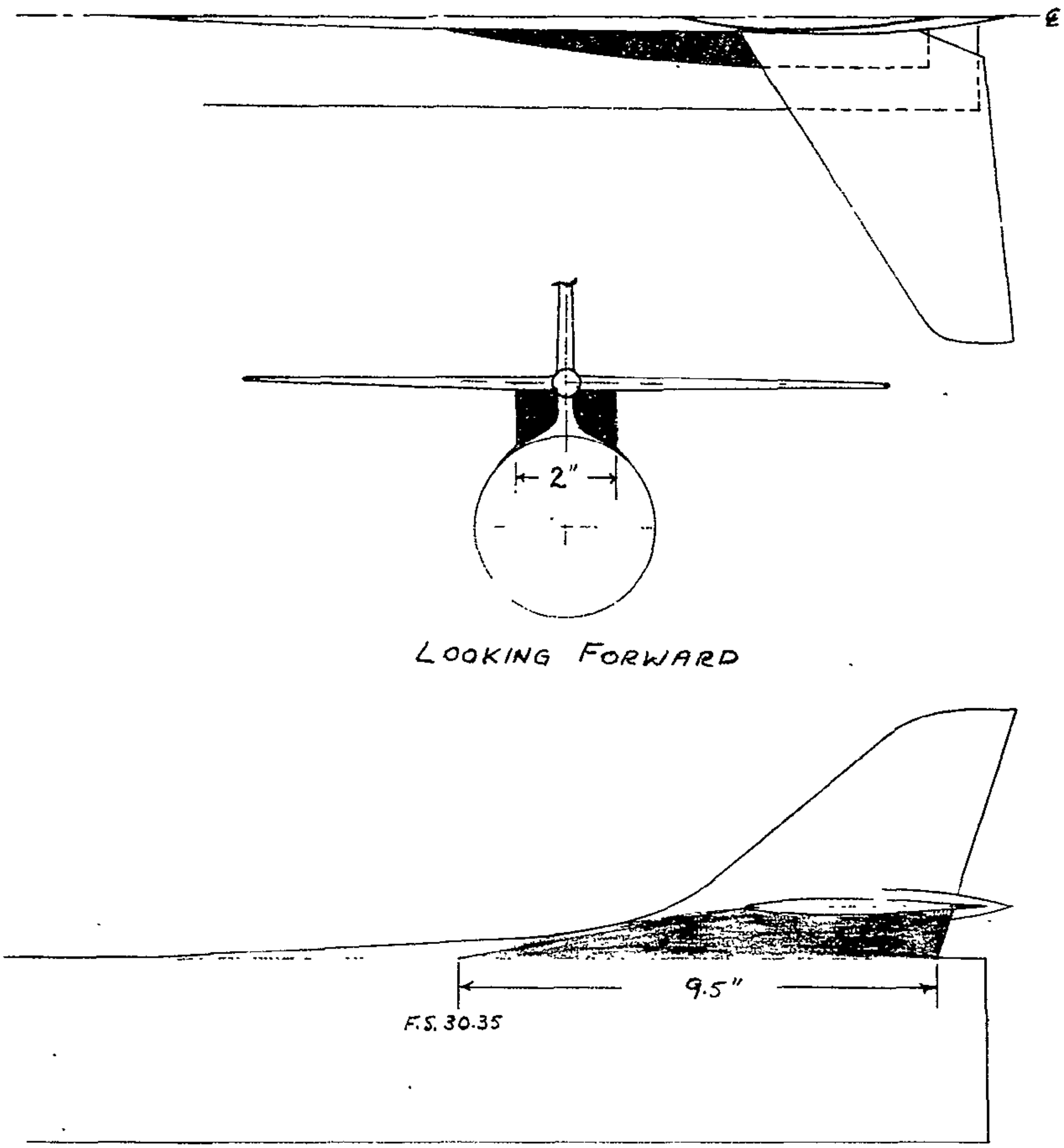

CHANNEL FILLER BLOCKS, B_{61}

FORM 1021-S REV. 10-70

PREPARED BY:	Los Angeles Division North American Rockwell	PAGE NO. 35 OF 145
CHECKED BY:		REPORT NO NA-72-82
DATE:		MODEL NO.

Fig 5

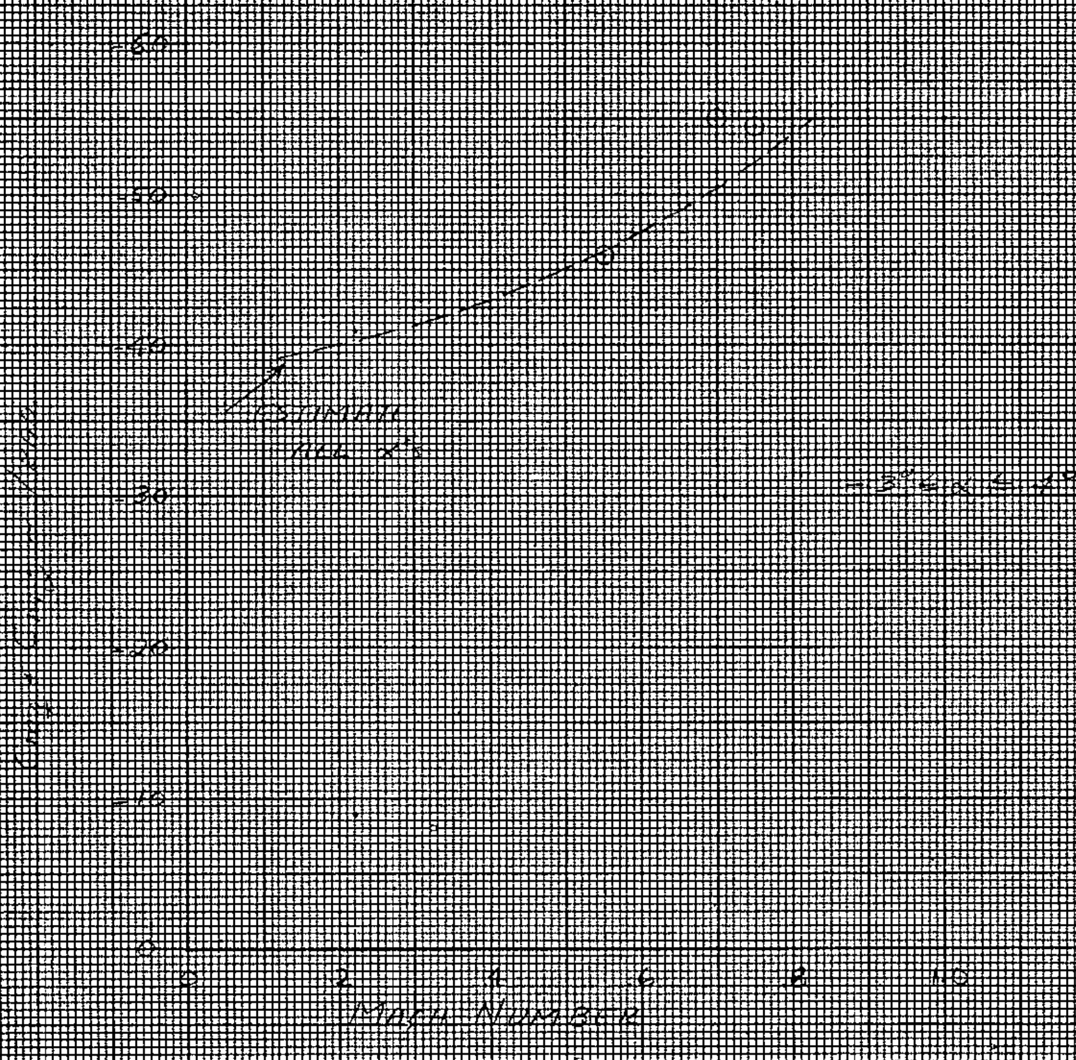

EFFECT OF MACH NUMBER ON DAMPING IN PITCH

TAIL ON WING $\angle_{LE} = 15°$ CG = 25 $\bar{c}$

TEST MS 596

PREPARED BY:	Los Angeles Division North American Rockwell	PAGE NO 36 OF 145
CHECKED BY:		REPORT NO NA-72-82
DATE:		MODEL NO.

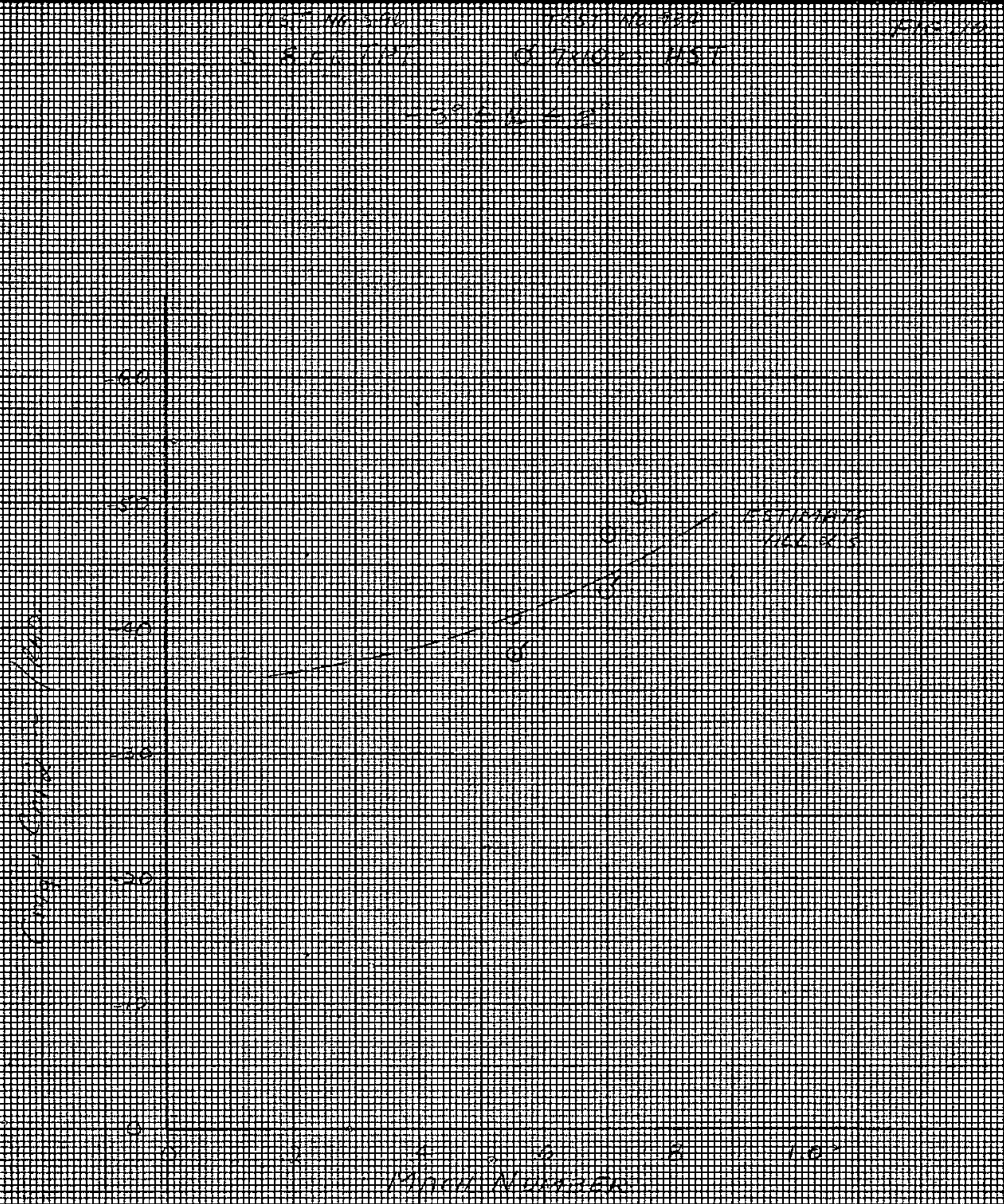

EFFECT OF MACH NUMBER ON DAMPING IN PITCH

TAIL ON WING ALE 25°

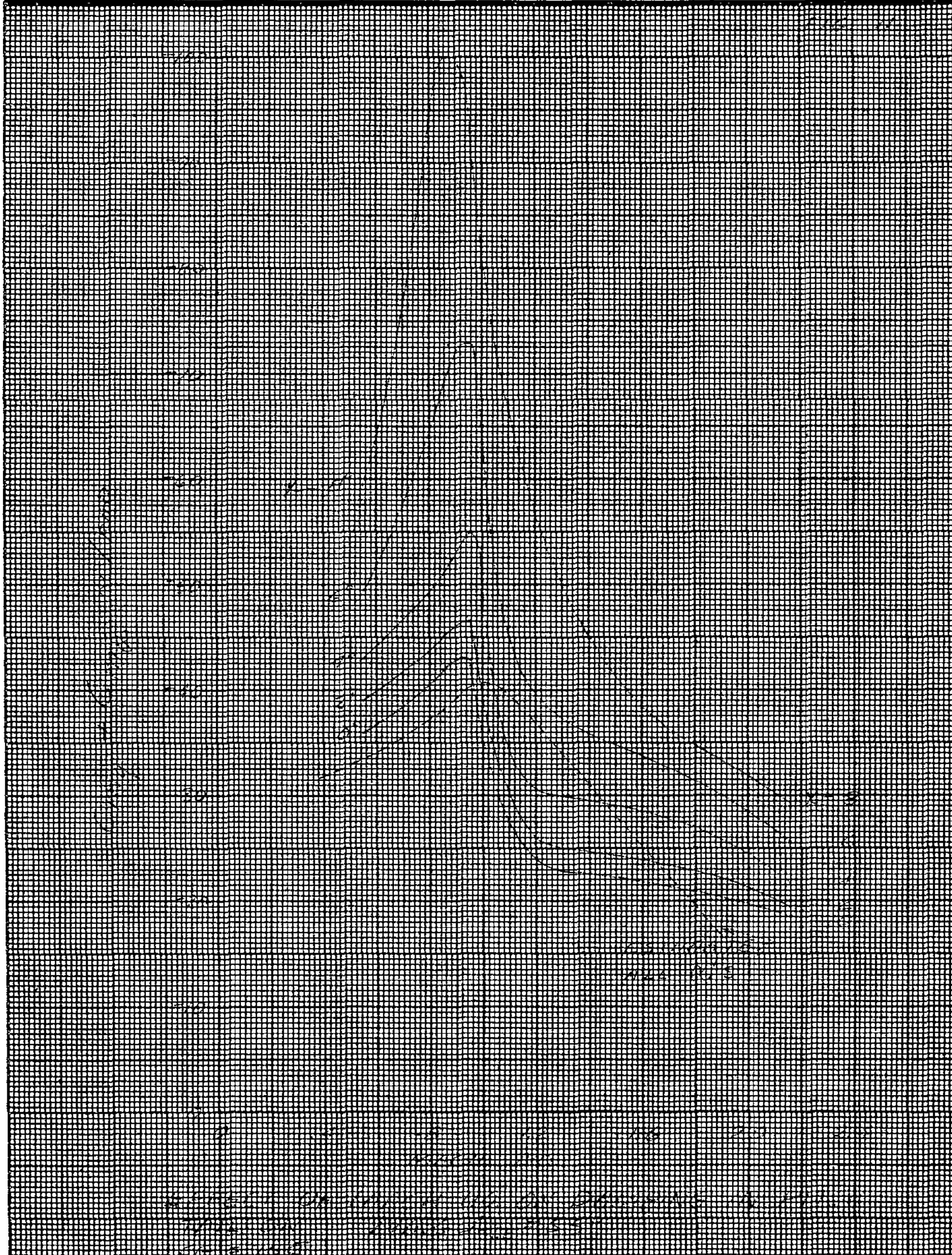

FORM 1021-B REV 10-70

PREPARED BY:	Los Angeles Division North American Rockwell	PAGE NO 38 OF
CHECKED BY:		REPORT NO NA-72-82.
DATE:		MODEL NO.

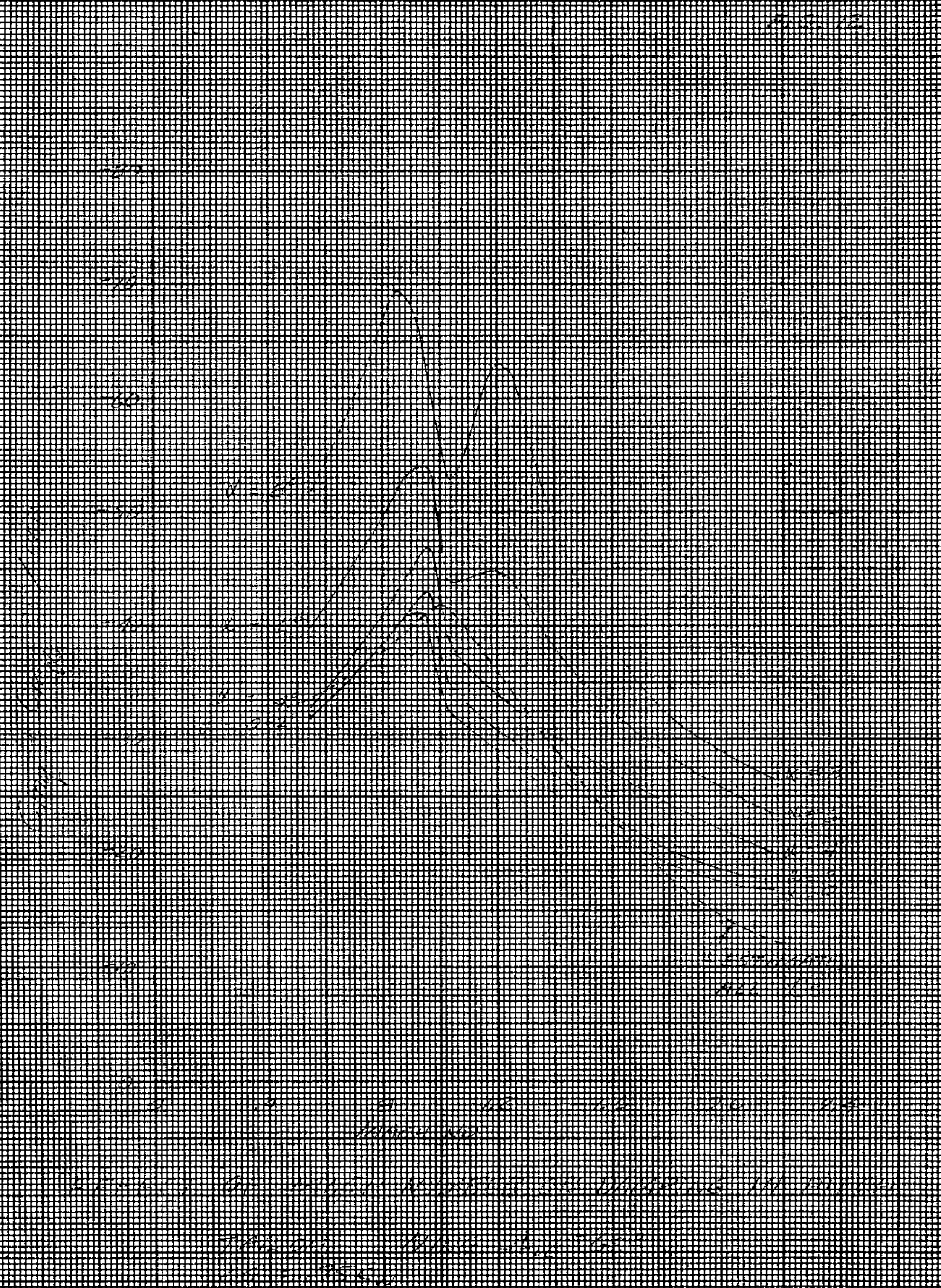

FORM 1021-8 REV 10-70

PREPARED BY:	Los Angeles Division North American Rockwell	PAGE NO 39 OF 145
CHECKED BY:		REPORT NO NA-72-82
DATE:		MODEL NO.

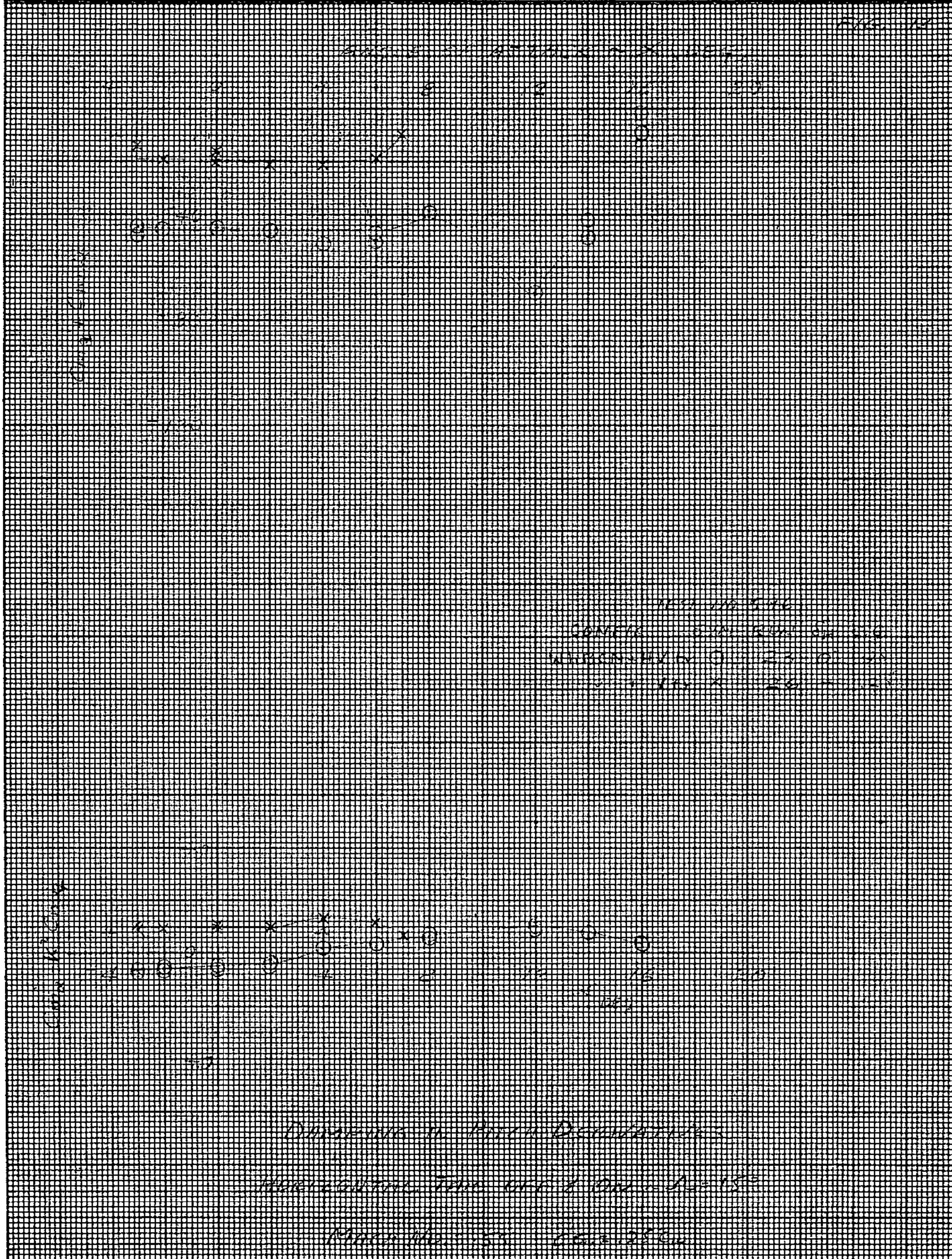

FORM 1021-5 REV. 10-70

PREPARED BY:	Los Angeles Division North American Rockwell	PAGE NO 40 OF 145
CHECKED BY:		REPORT NO NA-72-82
DATE:		MODEL NO.

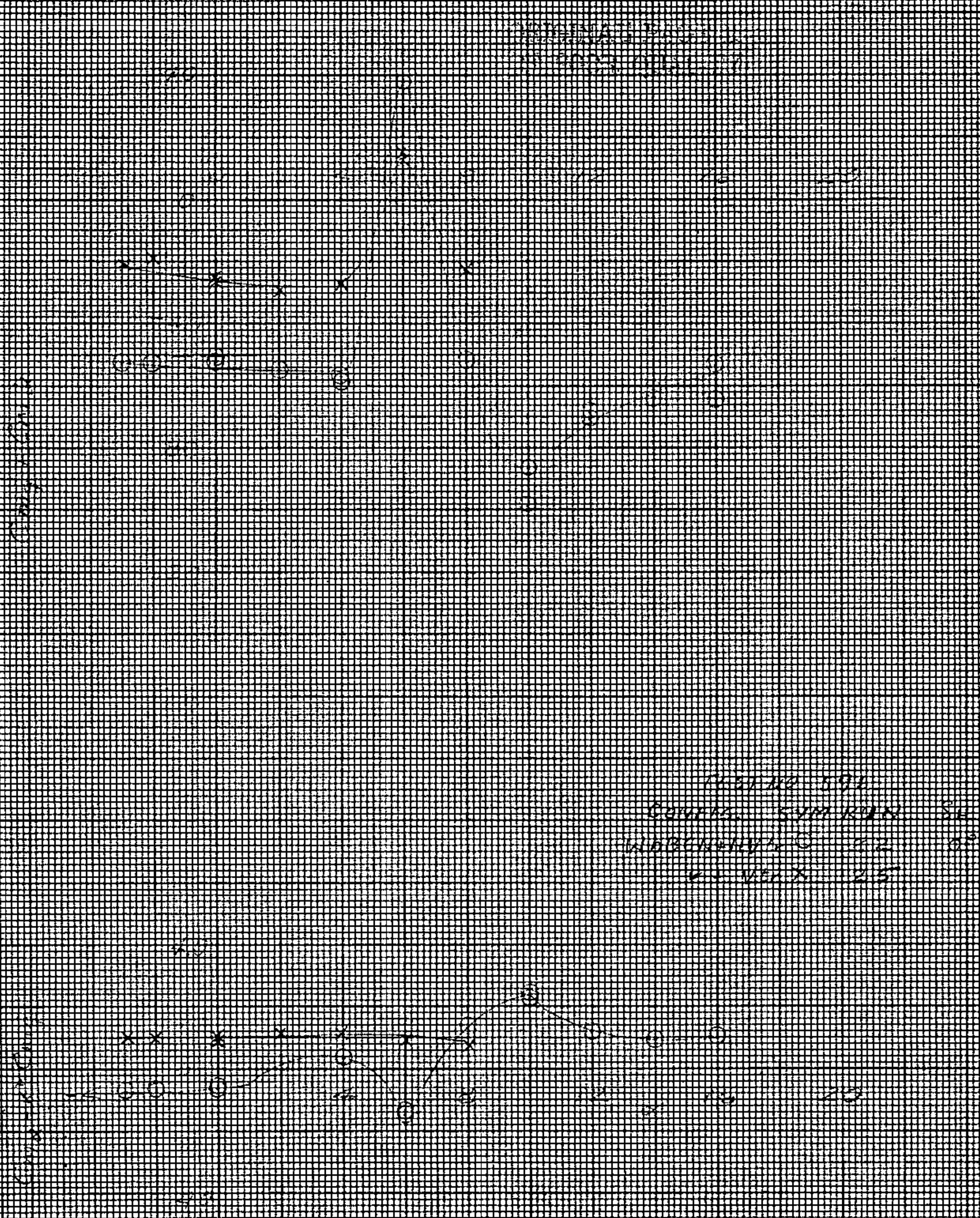

CHANGES IN PITCH DERIVATIVES

HORIZONTAL TAIL [illegible]

[illegible]

MACH NO = .70

FORM 1021-S REV 10-70

PREPARED BY:	Los Angeles Division North American Rockwell	PAGE NO 41 OF 145
CHECKED BY:		REPORT NO NA-72-82
DATE:		MODEL NO

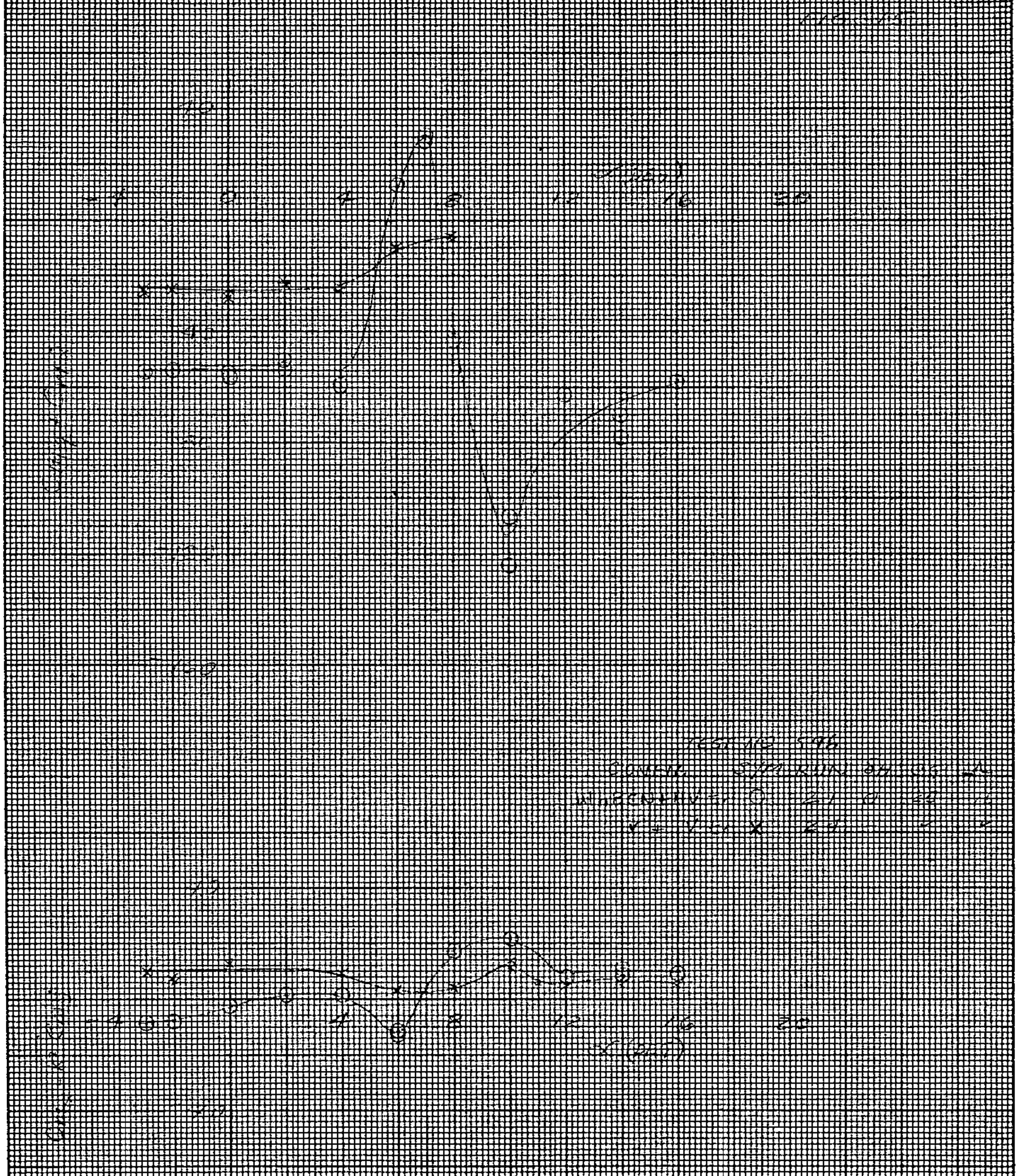

DAMPING IN PITCH DERIVATIVES

FORM 1021-S REV. 10-70

PREPARED BY:	Los Angeles Division North American Rockwell	PAGE NO 42 OF 145
CHECKED BY:		REPORT NO NA-72-82
DATE:		MODEL NO.

FIG. 16

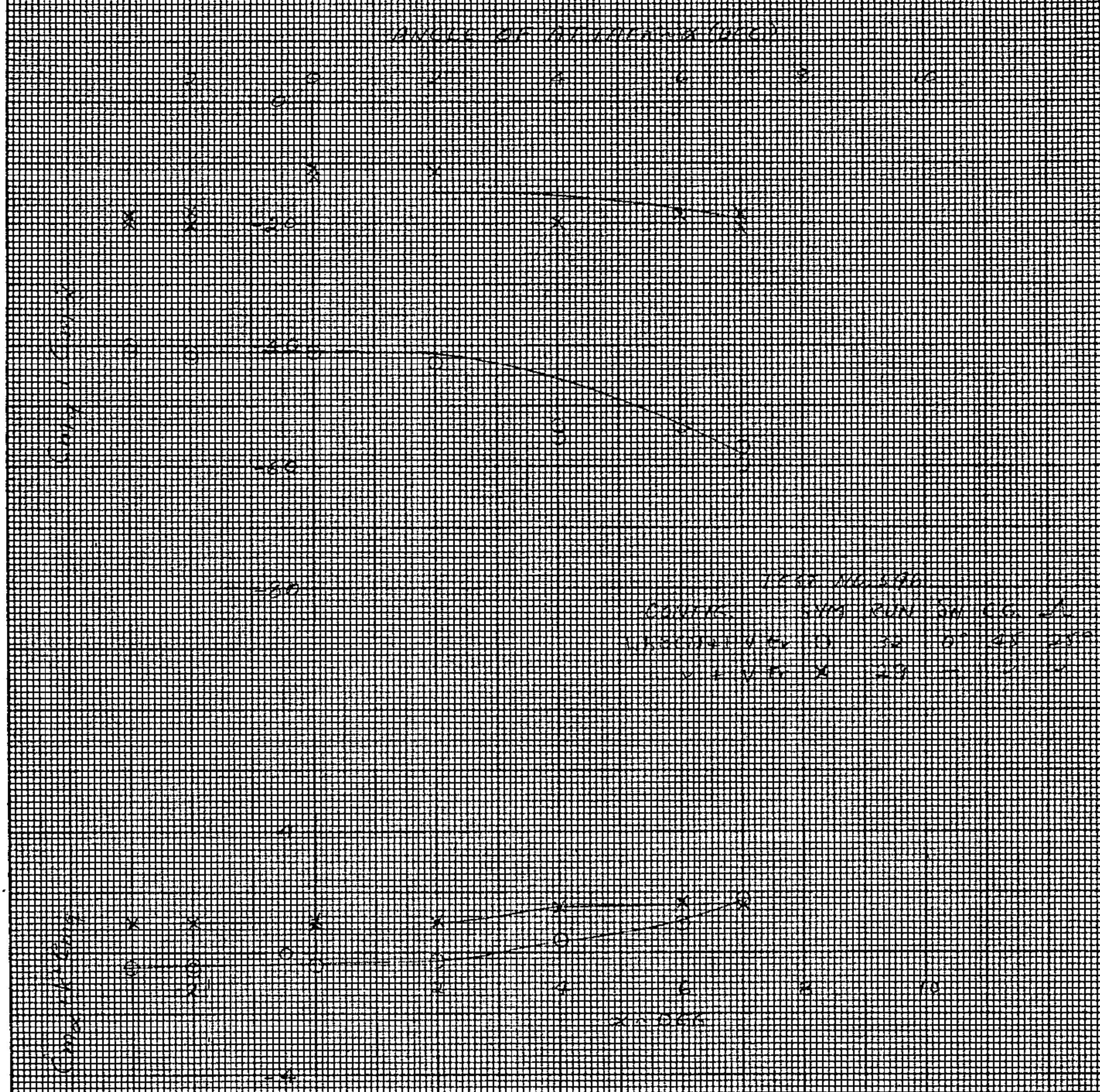

DAMPING IN PITCH DERIVATIVES
HORIZONTAL TAIL OFF 5 DEG
CG = .432
MACH NO = 0.55

FIG. 17

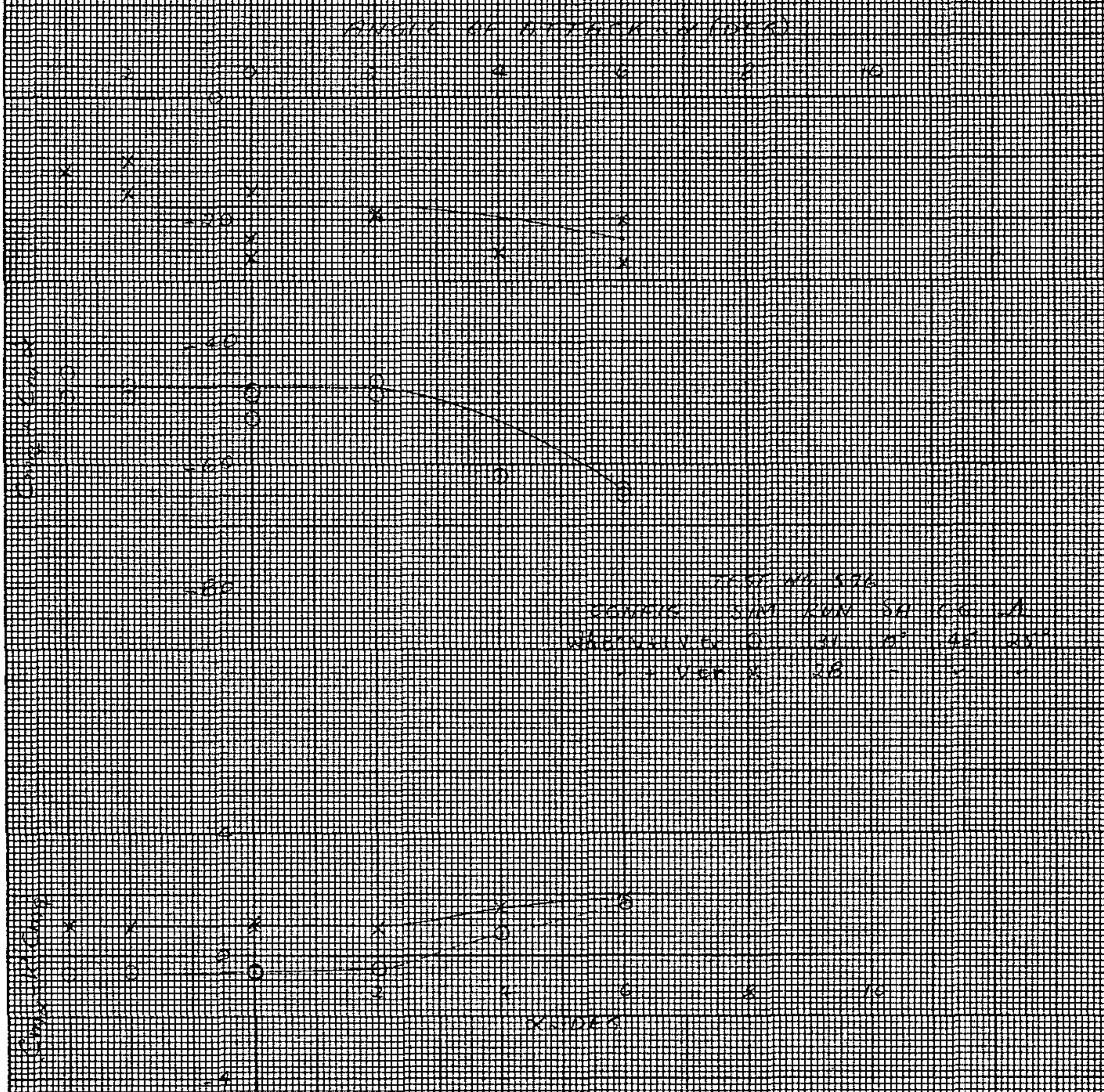

DAMPING IN PITCH DERIVATIVE

HORIZONTAL TAIL OFF-ON

MACH No = 0.4

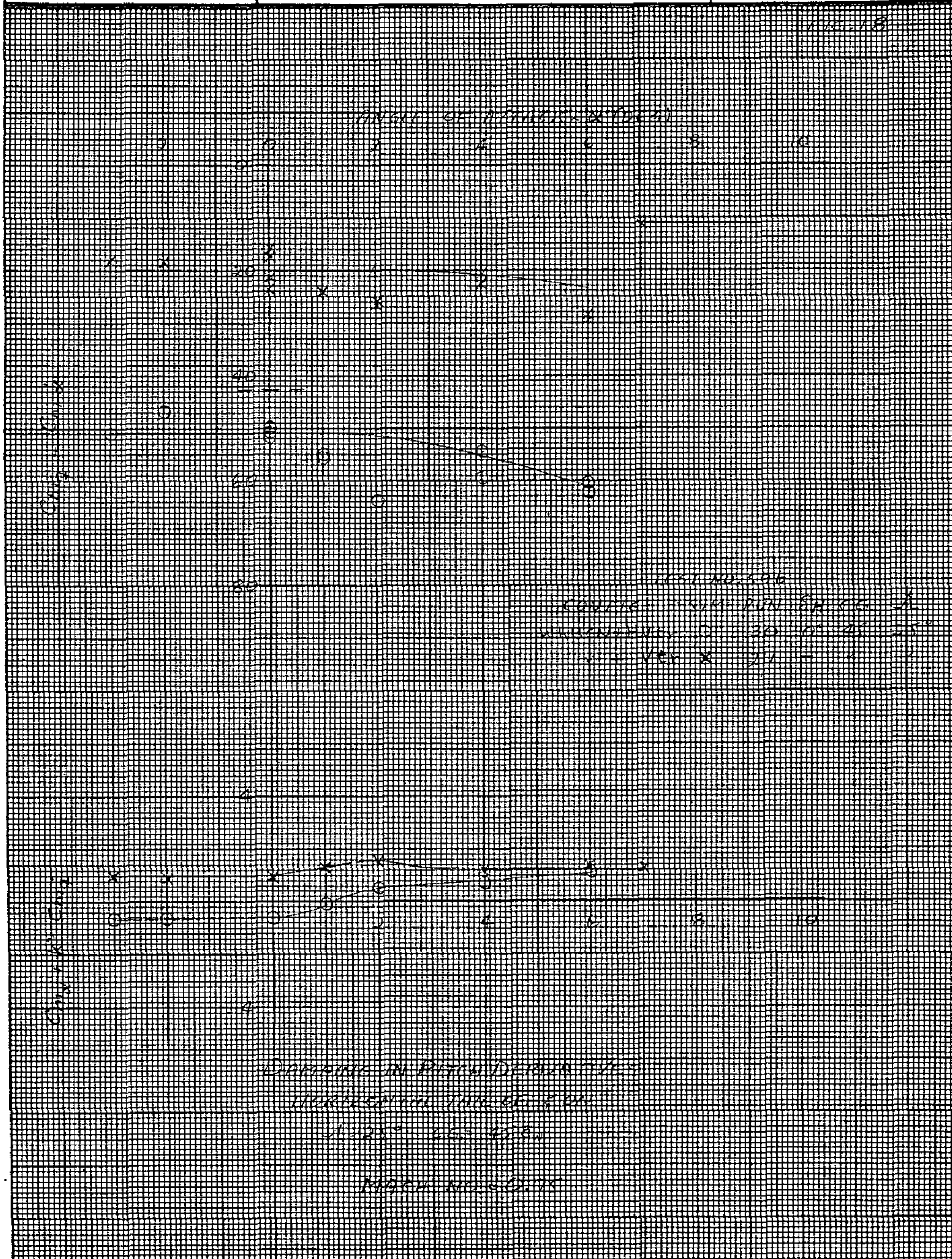
2
0
2
4
6
8
10
20
40
60
80
4
CONFIG
VER
DAMPING IN PITCH DERIVATIVES
MACH NO.

FORM 1021-S REV 10-70

PREPARED BY: C.L.D	Los Angeles Division North American Rockwell	PAGE NO. A-5 OF 145
CHECKED BY:		REPORT NO NA-72-82
DATE: 11-5-71		MODEL NO.

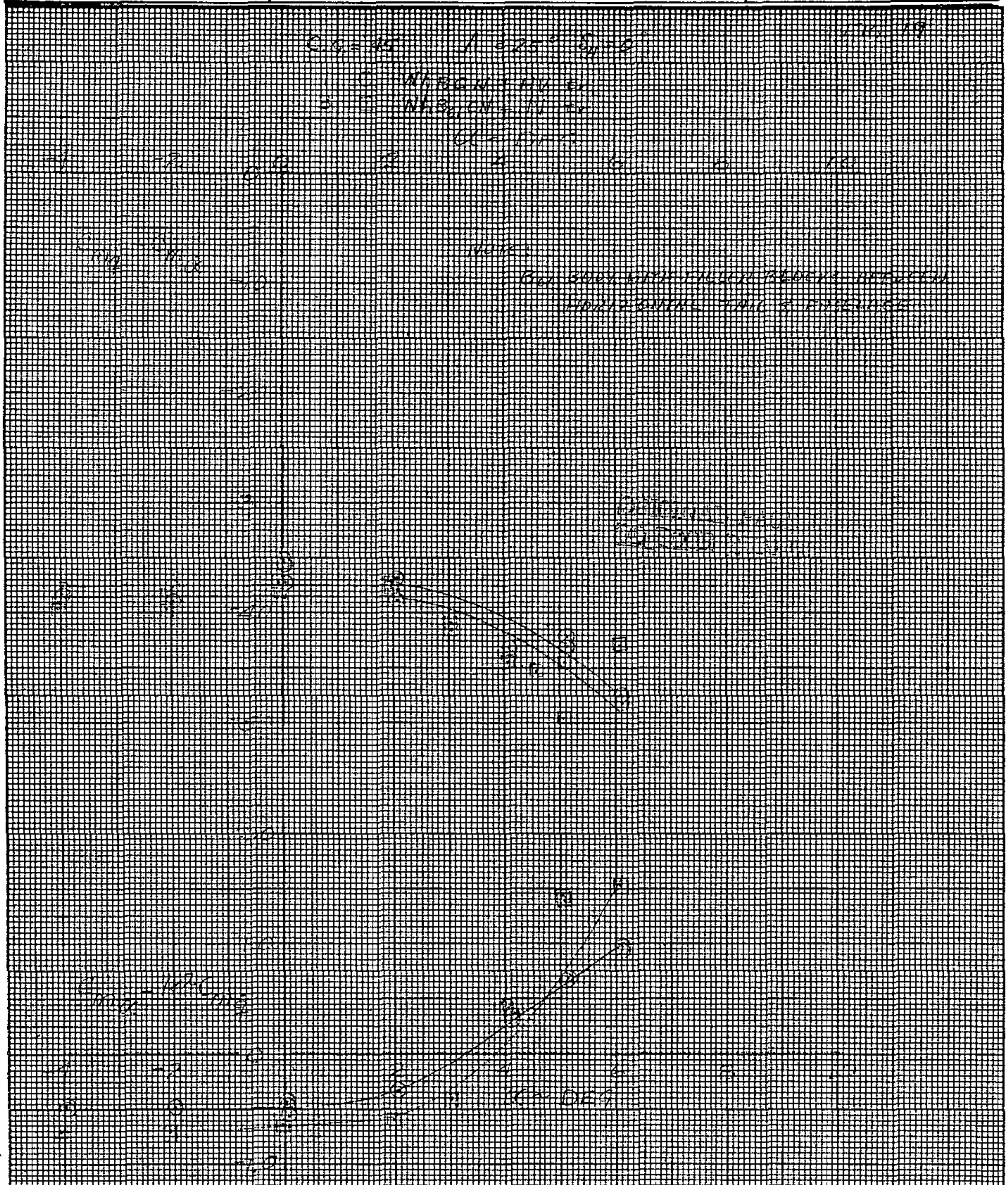

EFFECT OF FILLER BLOCKS
ON DAMPING IN PITCH DERIVATIVES

FIG. 20

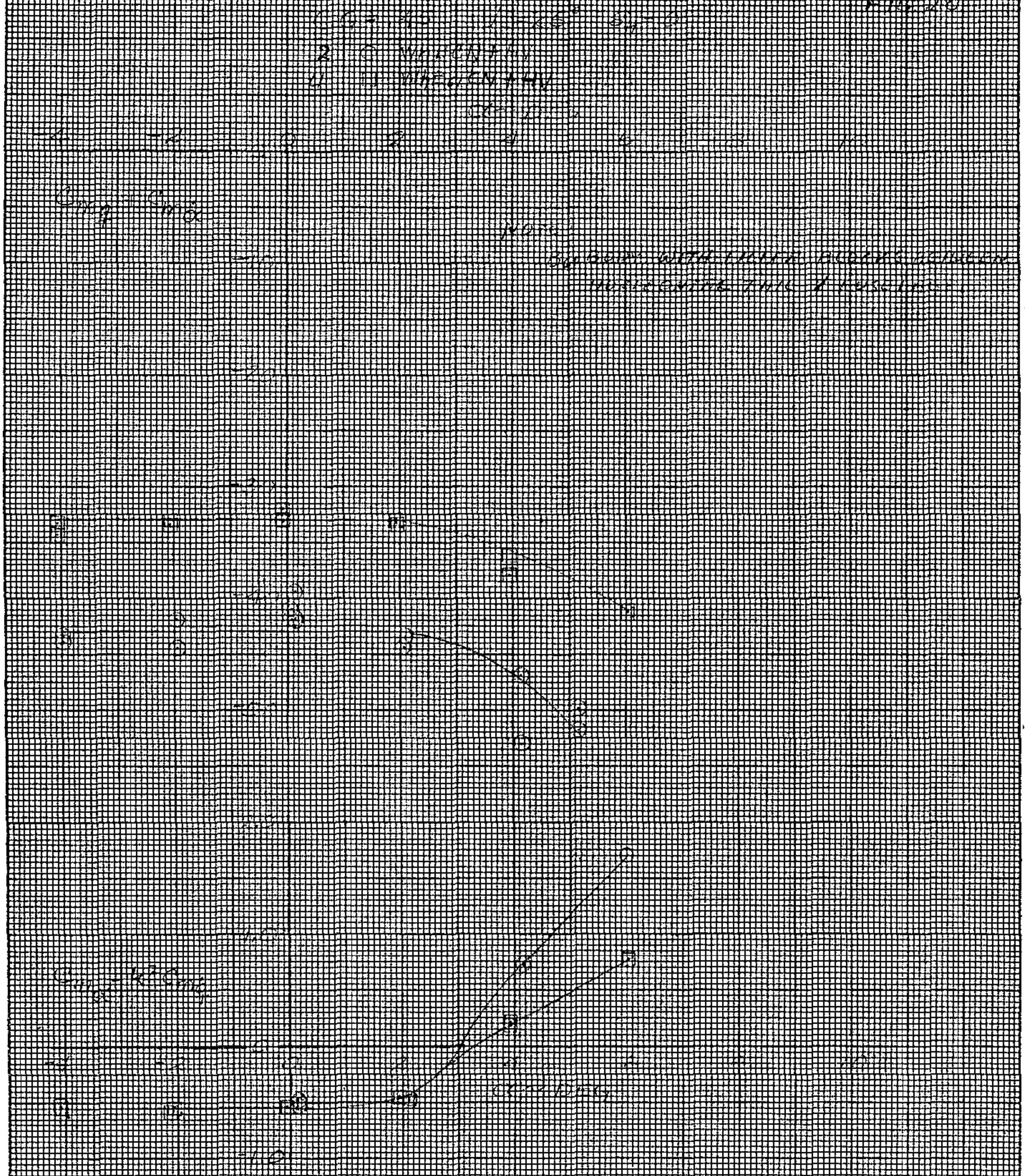

EFFECT OF [illegible] ON DAMPING IN PITCH DERIVATIVES

TEST NO. 936

FORM 1021-S REV 10-70

PREPARED BY: C.L.D	Los Angeles Division North American Rockwell	PAGE NO 47 OF 145
CHECKED BY:		REPORT NO NA-72-82
DATE: 11-5-71		MODEL NO.

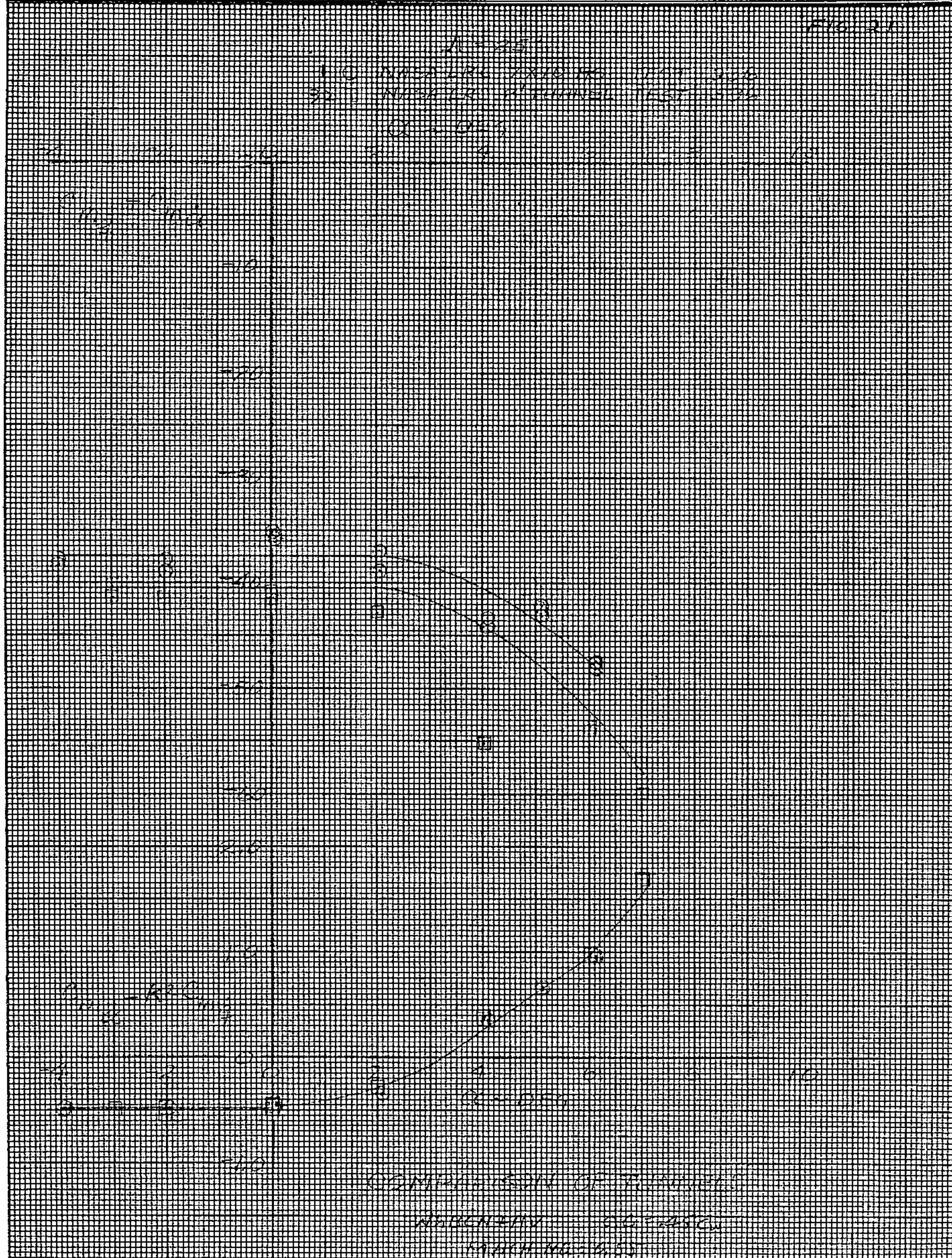

FORM 1021-S REV 10-70

PREPARED BY: C.L.D	Los Angeles Division North American Rockwell	PAGE NO. 48 OF 145
CHECKED BY:		REPORT NO NA-72-82
DATE: 11-5-71		MODEL NO.

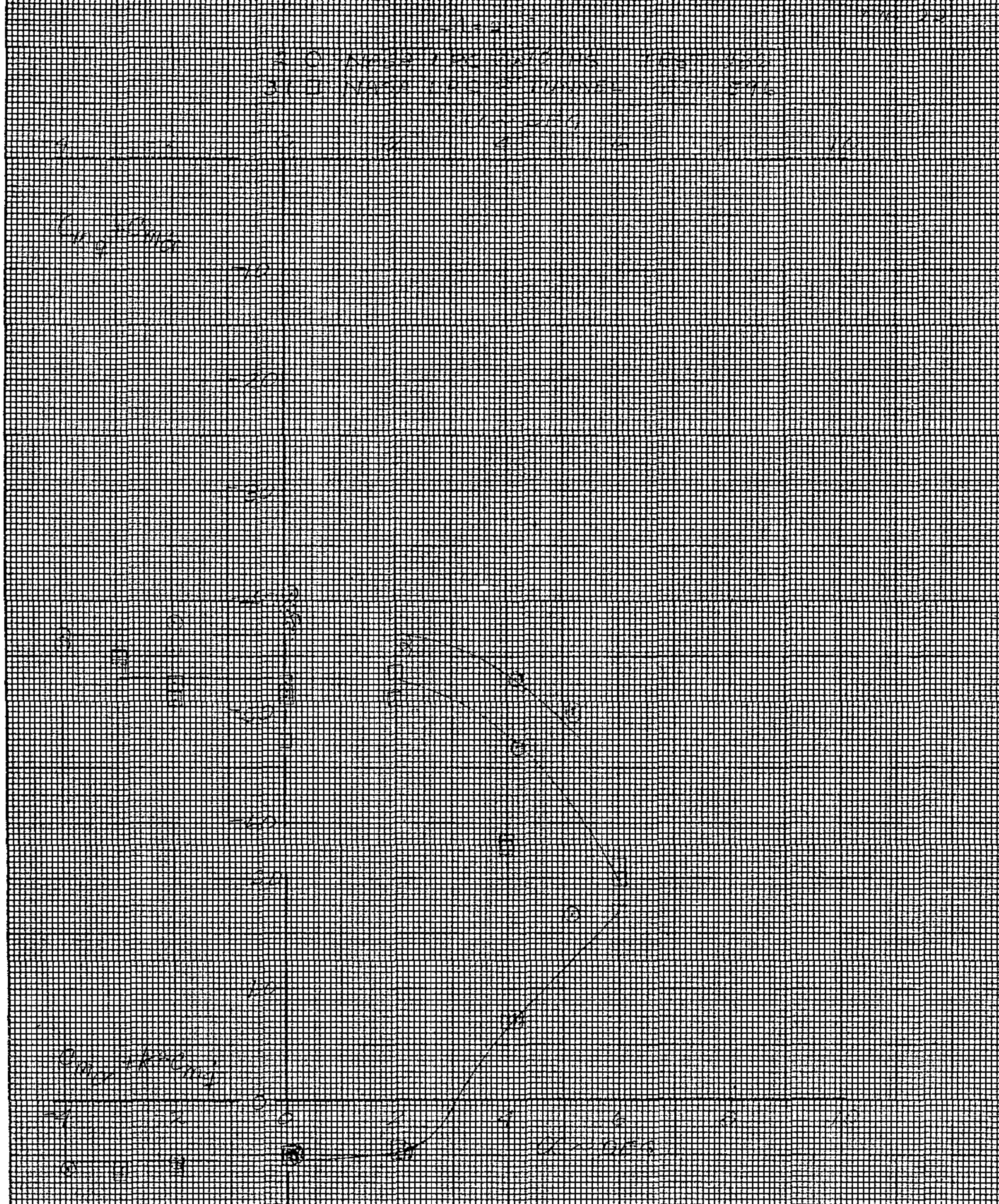

COMPARISON OF TUNNEL

MACH NO. = 0.70

FORM 1021-8 REV 10-70

PREPARED BY:

CHECKED BY:

DATE:

Los Angeles Division
North American Rockwell

REPORT NO NA-72-82

MODEL NO.

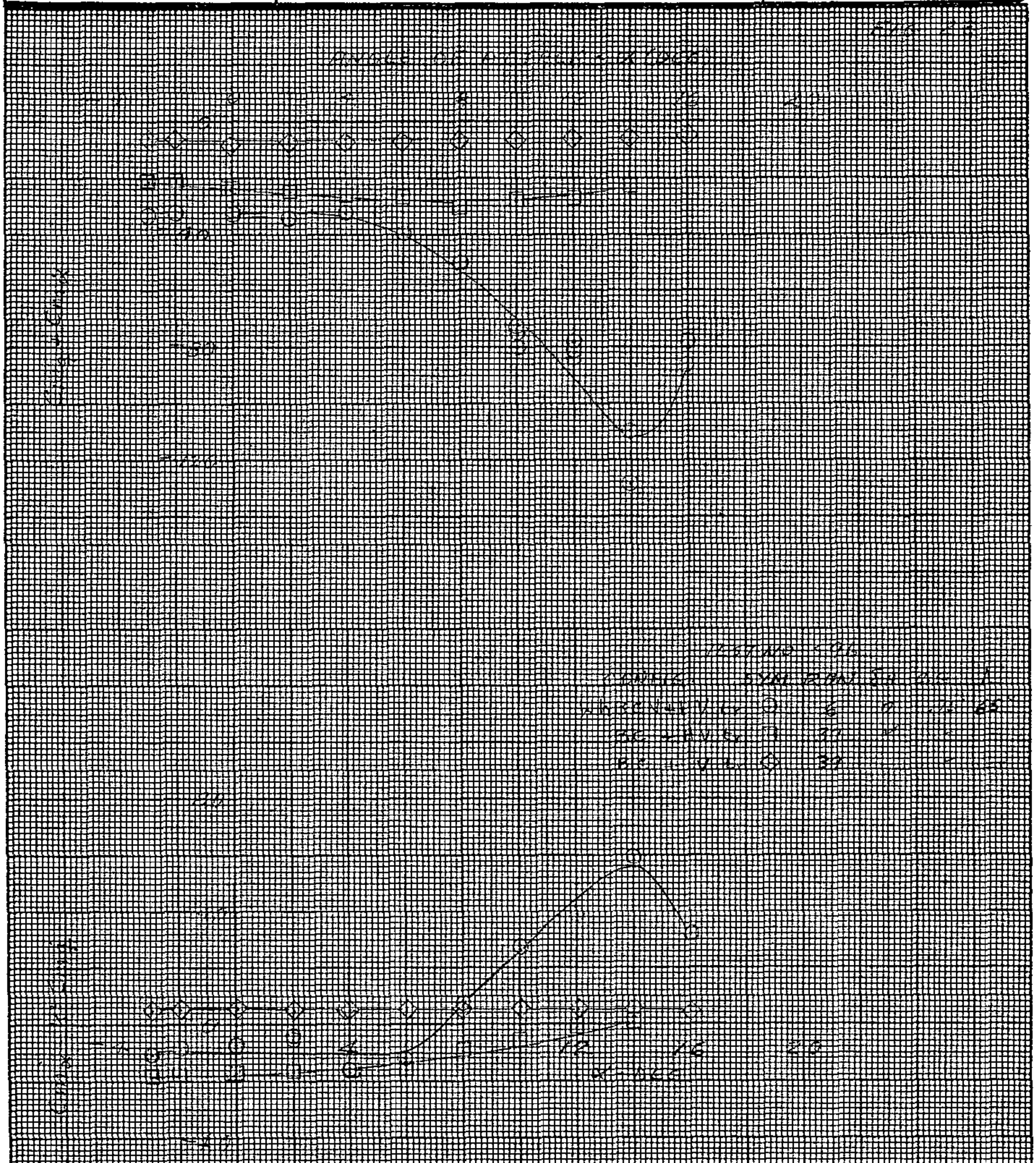

DAMPING IN PITCH DERIVATIVES

COMPONENT BUILD-UP

MACH NO .55

FORM 1021-S REV 10-70

PREPARED BY:	Los Angeles Division North American Rockwell	PAGE NO. 50 OF 145
CHECKED BY:		REPORT NO NA-72-82
DATE:		MODEL NO.

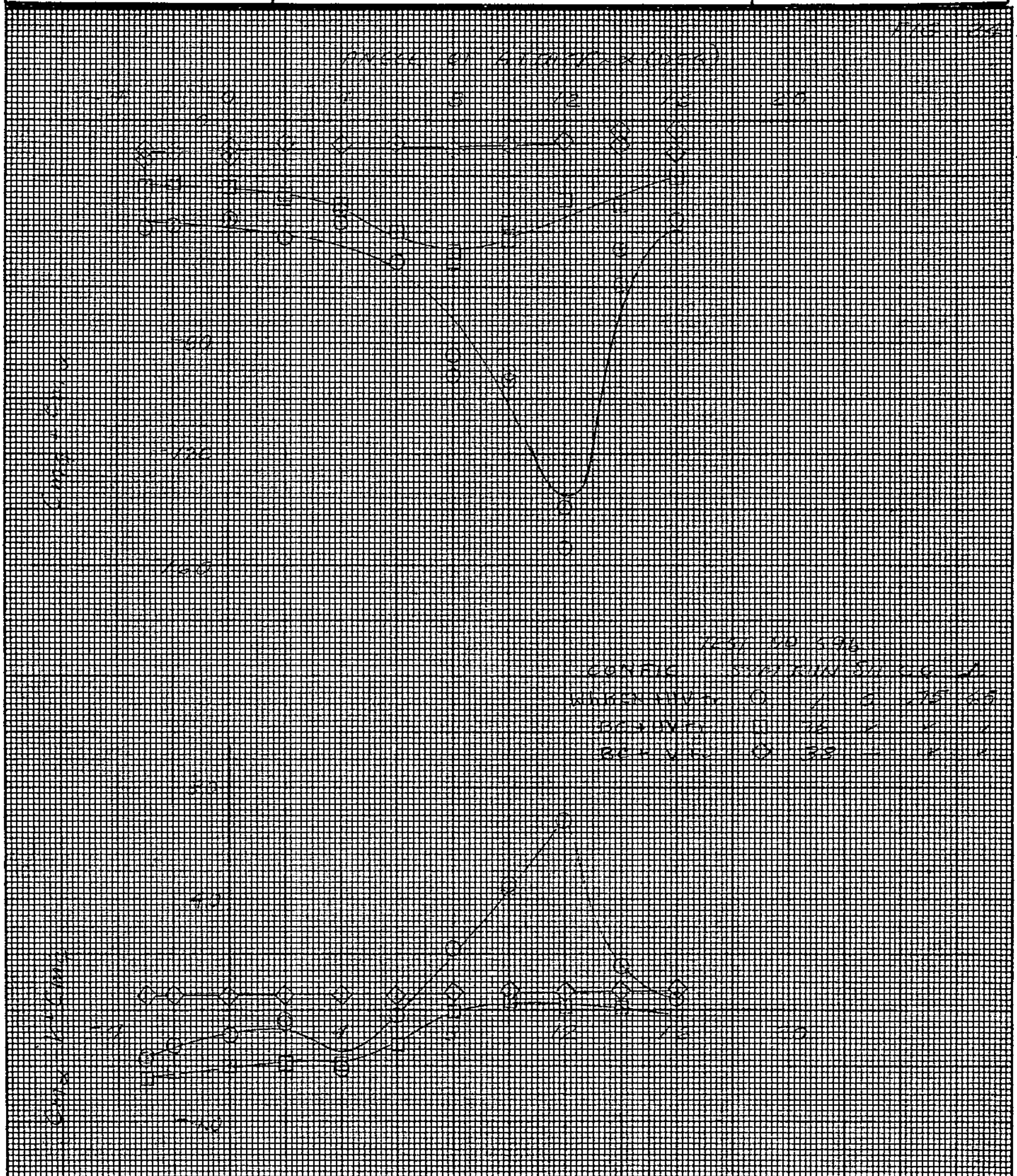

DAMPING IN PITCH DERIVATIVES

COMPONENT BUILD-UP

FORM 1021-S REV 10-70

PREPARED BY:	Los Angeles Division North American Rockwell	PAGE NO. 51 OF 145
CHECKED BY:		REPORT NO NA-72-82
DATE:		MODEL NO.

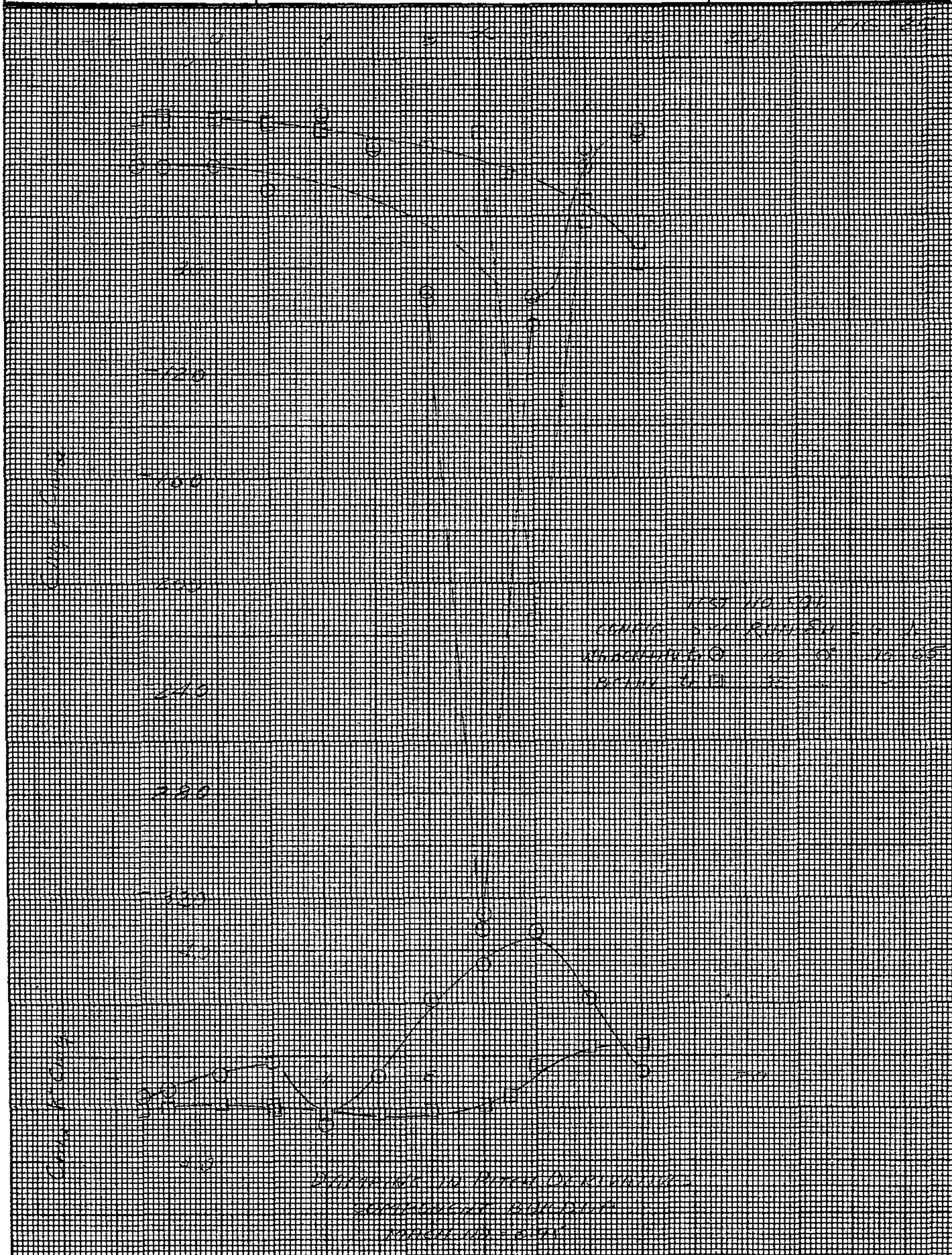

FORM 1021-S REV 10-70

PREPARED BY:	Los Angeles Division North American Rockwell	PAGE NO 52 OF 145
CHECKED BY:		REPORT NO. NA-72-82
DATE:		MODEL NO

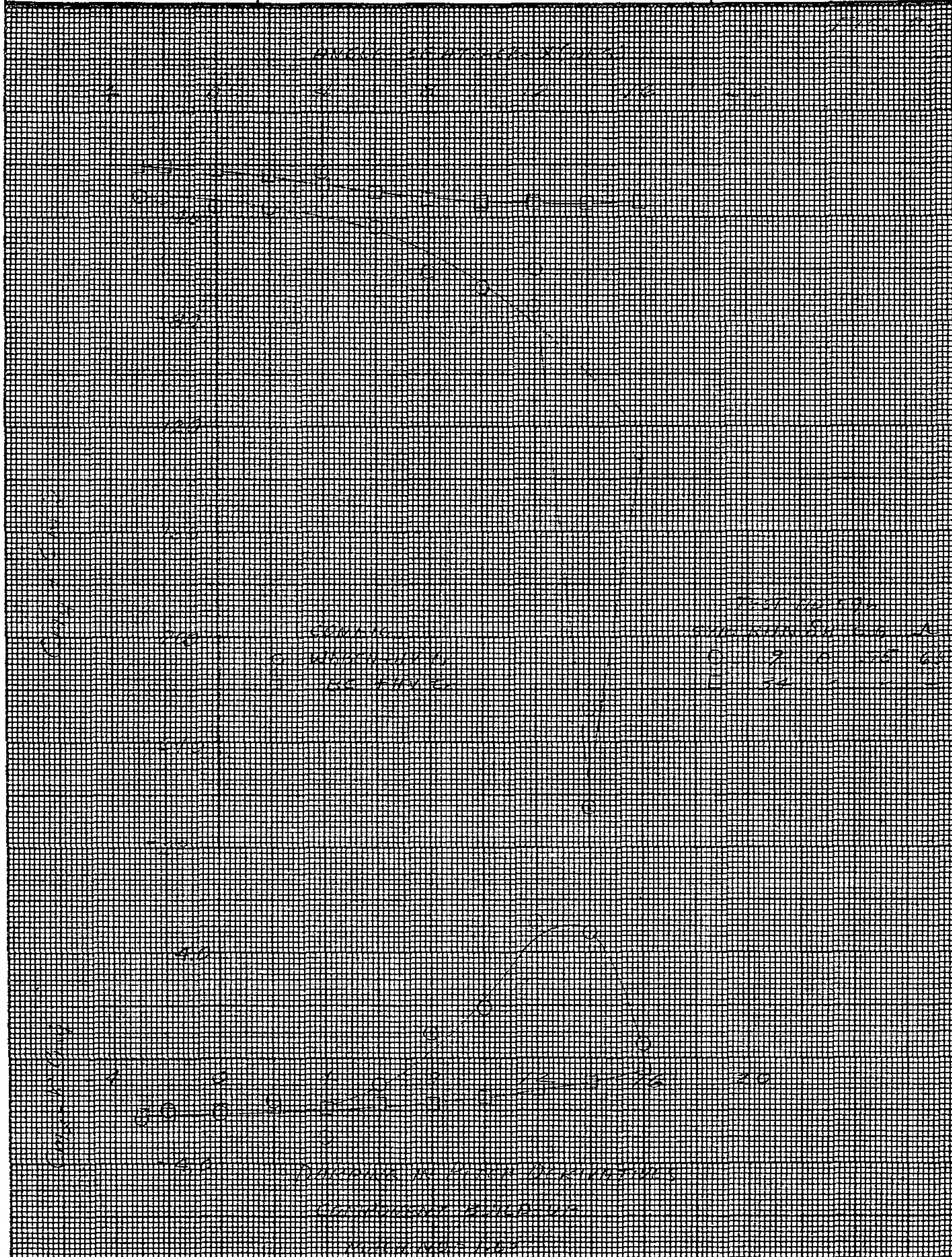

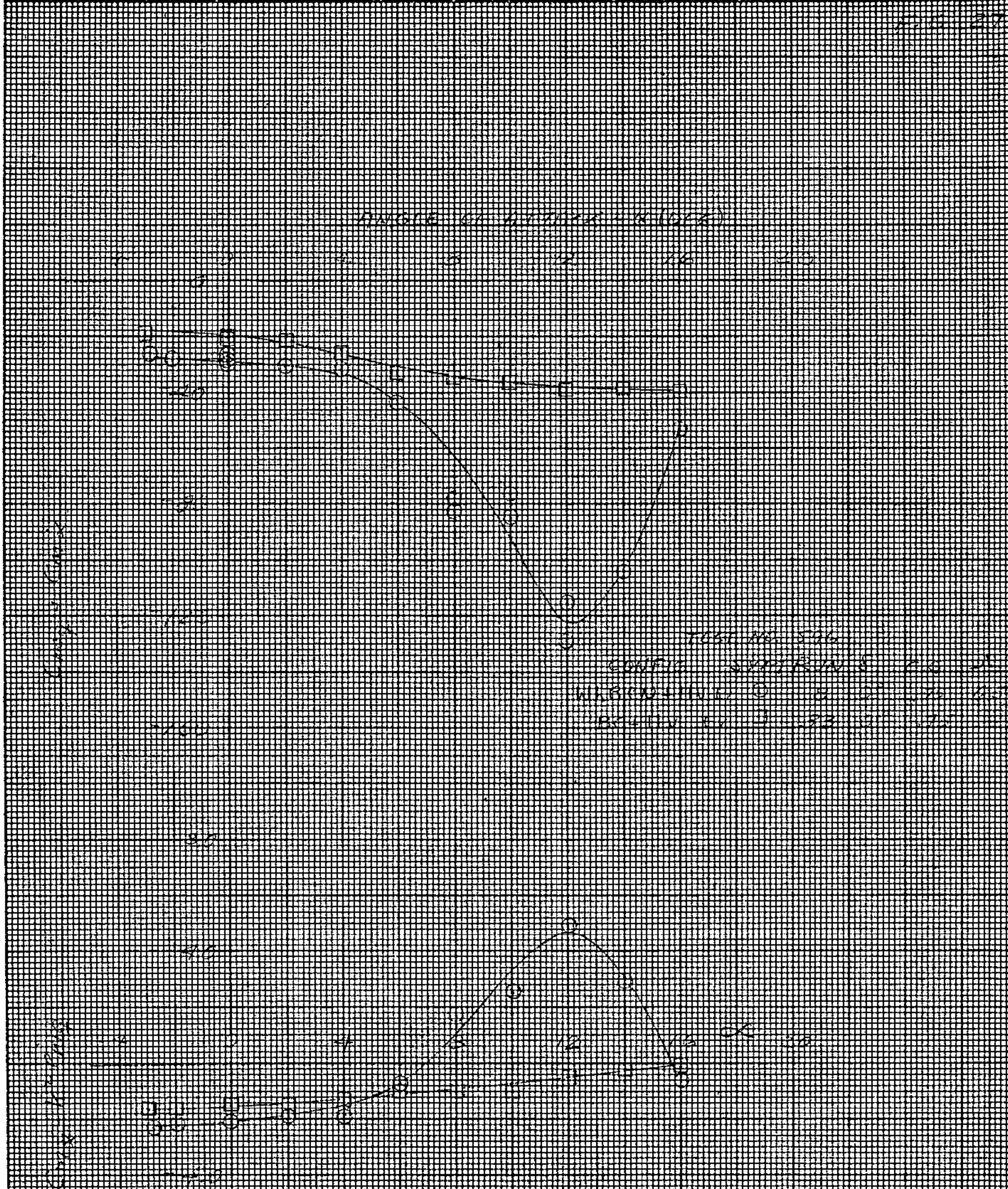

DAMPING IN PITCH DERIVATIVES

COMPONENT BUILD UP

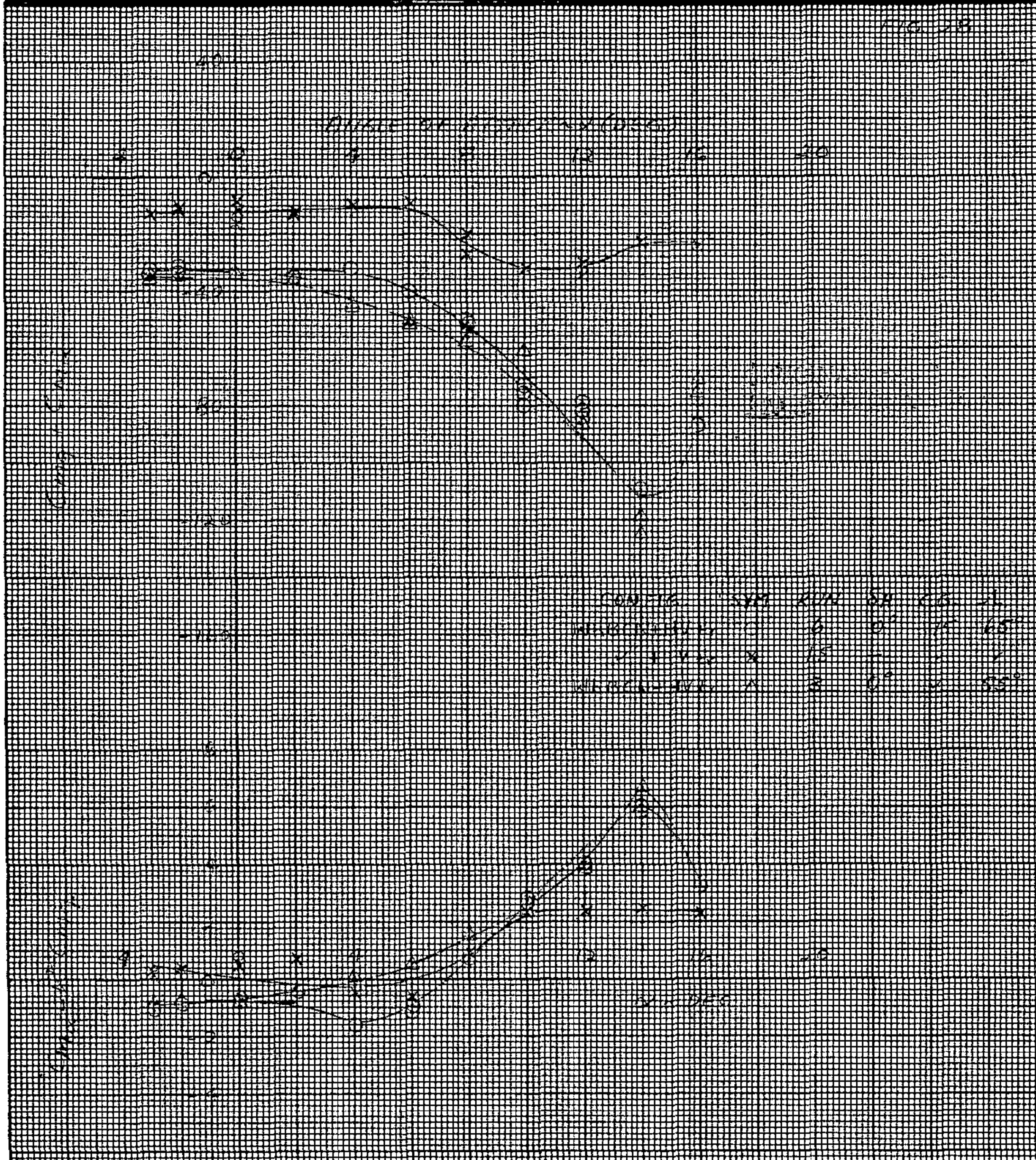

EFFECT OF WING L.E. SWEEP ON DAMPING IN PITCH

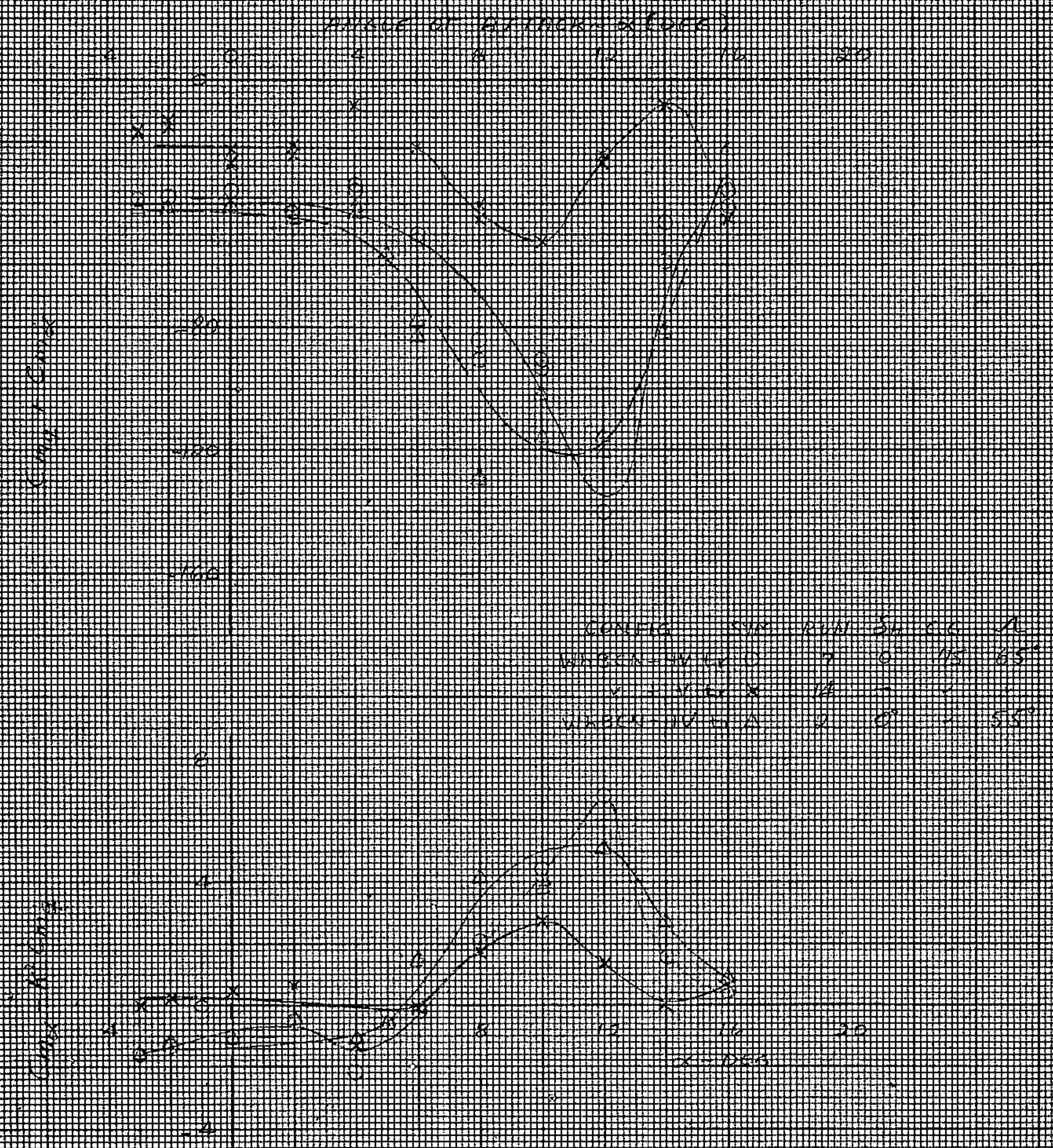

EFFECT OF WING L.E. SWEEP ON DAMPING IN PITCH

HORIZONTAL TAIL ON & OFF MACH NO = 0.85

ARC TEST NO 596

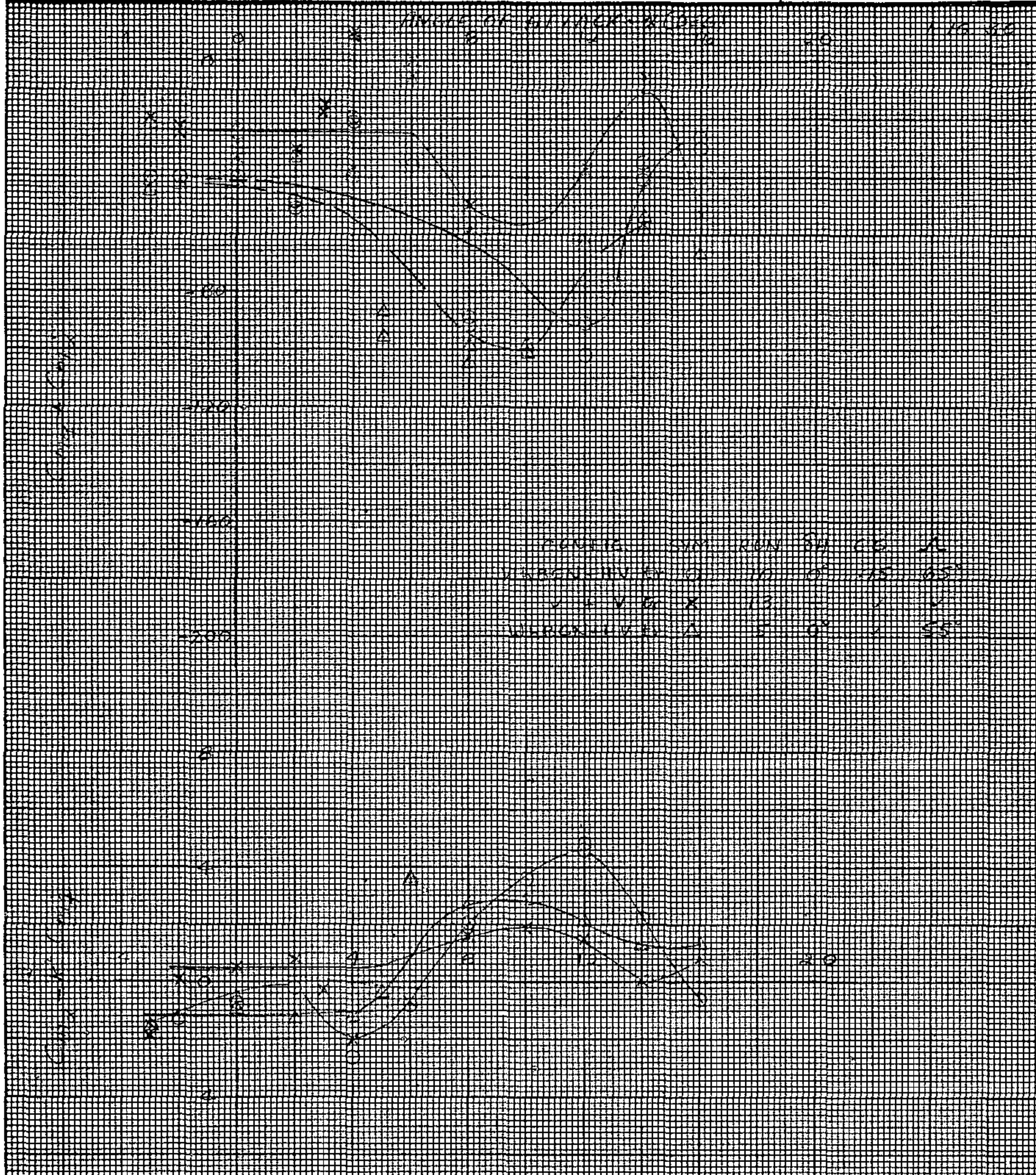

EFFECT OF WING LE SWEEP ON DAMPING IN PITCH

HORIZONTAL TAIL ON & OFF MACH NO = 0.95

LRC TEST NO. 596

FORM 1021-B REV 10-70

PREPARED BY:	Los Angeles Division North American Rockwell	PAGE NO. 57 OF 145
CHECKED BY:		REPORT NO NA-72-82
DATE:		MODEL NO.

FIG. 31

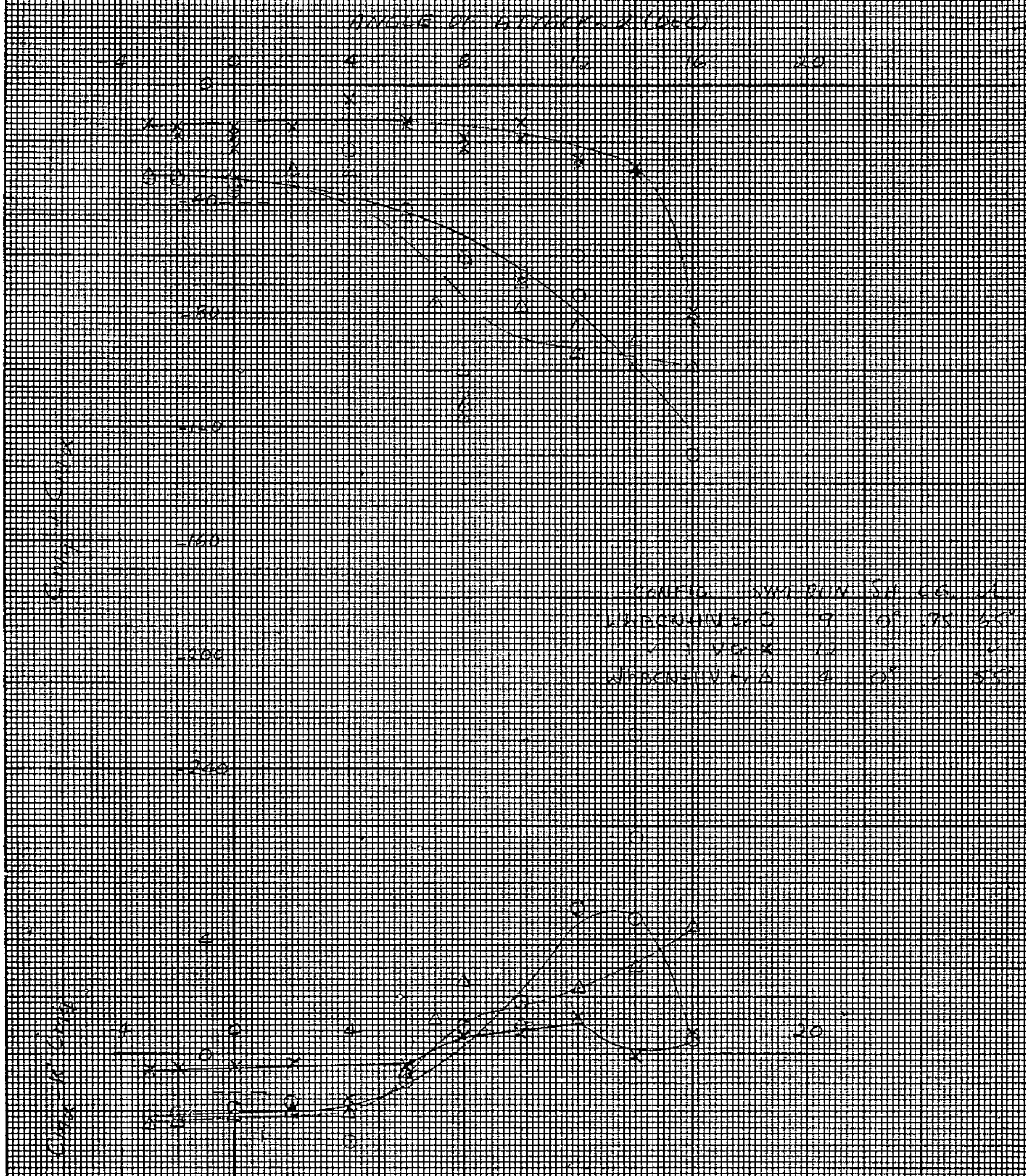

EFFECT OF WING L.E. SWEEP ON DAMPING IN PITCH

HORIZONTAL TAIL ON & OFF. MACH No = 1.05

LRC TEST No. 576

FORM 1021-S REV. 6-69

PREPARED BY:	North American Aviation / Los Angeles North American Rockwell	PAGE NO. 58 OF 145
CHECKED BY:		REPORT NO NA-72-82
DATE:		MODEL NO.

FIG. 32

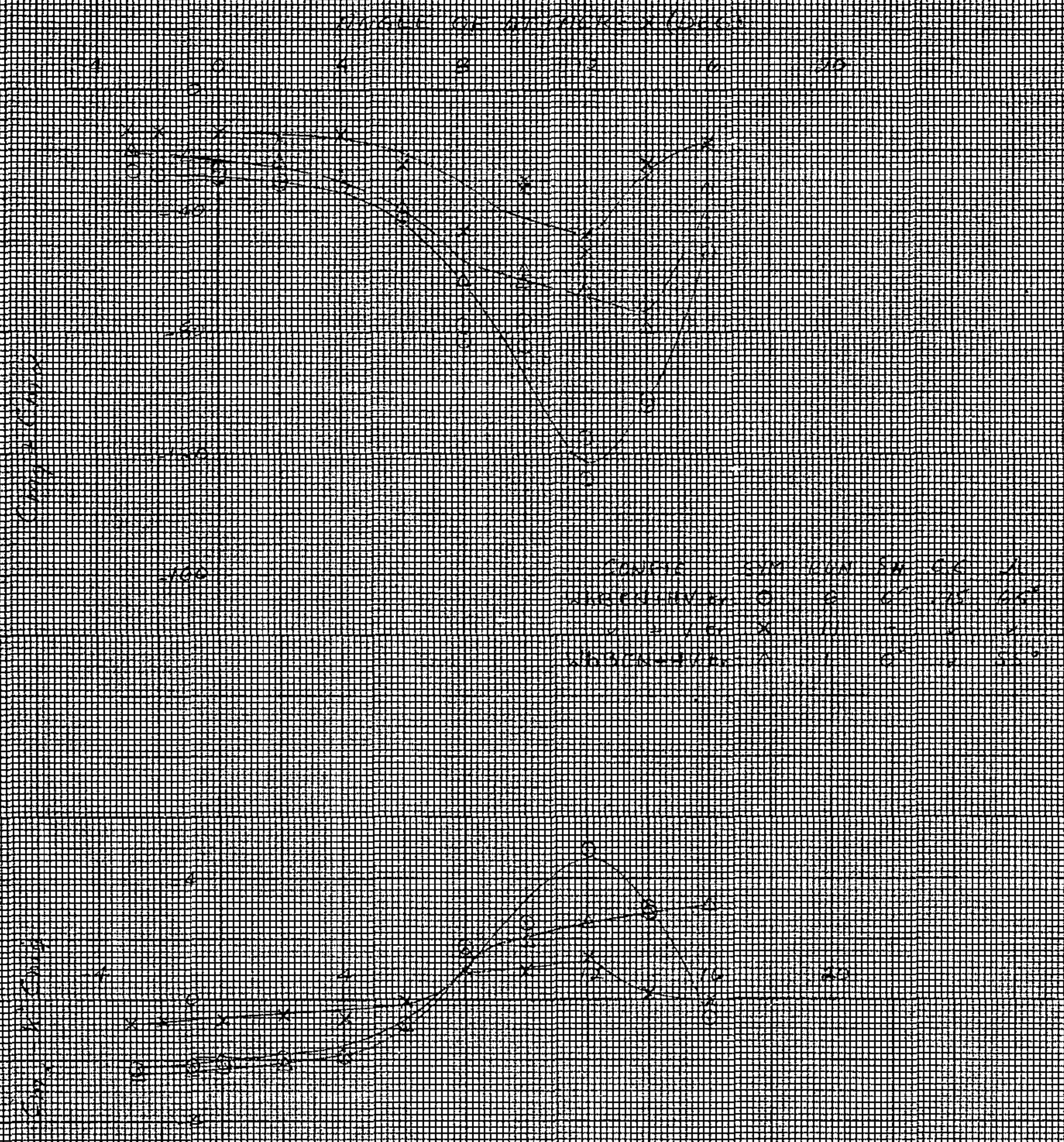

EFFECT OF WING L.E. SWEEP ON DAMPING IN PITCH

HORIZONTAL TAIL ON & OFF   MACH NO. 1.2

LRC TEST NO 596

FORM 1021-S REV 6-69

PREPARED BY:	North American Aviation / Los Angeles North American Rockwell	PAGE NO 59 OF 145
CHECKED BY:		REPORT NO. NA-72-82
DATE:		MODEL NO.

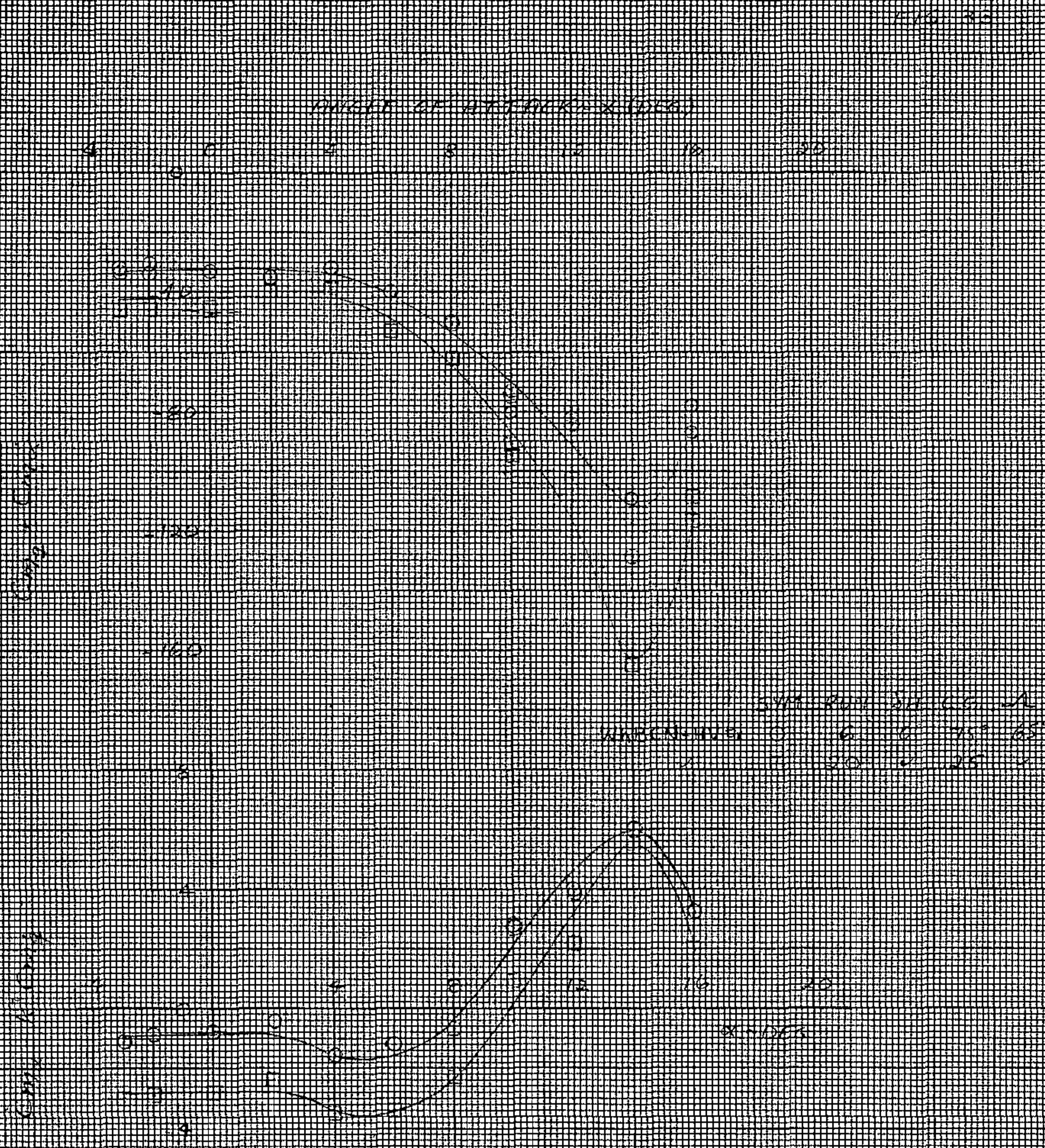

EFFECT OF C.G. LOCATION ON DAMPING IN PITCH

HORIZONTAL TAIL ON MACH No. = 0.55

LRC TEST No. 596

FORM 1021-S REV 10-70

PREPARED BY:	Los Angeles Division North American Rockwell	PAGE NO 60 OF 145.
CHECKED BY:		REPORT NO NA-72-82
DATE:		MODEL NO.

FIG. 14

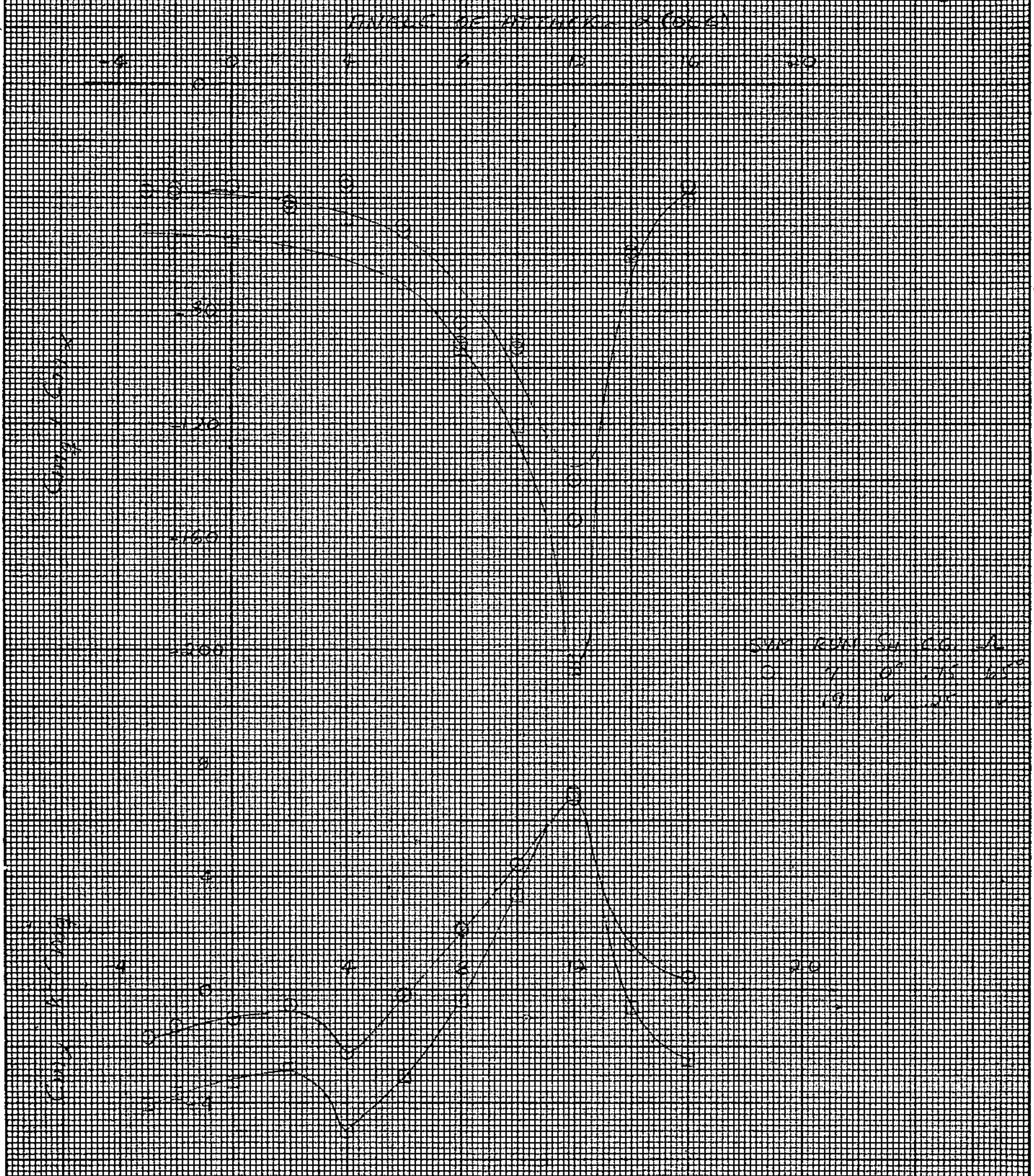

EFFECT OF C.G. LOCATION ON DAMPING IN PITCH

HORIZONTAL TAIL ON MACH No = 0.85

WRRTRUE

LRC TEST No. 596

FORM 1021-S REV 10-70

PREPARED BY:	Los Angeles Division North American Rockwell	PAGE NO. 61 OF 145
CHECKED BY:		REPORT NO NA-72-82
DATE:		MODEL NO

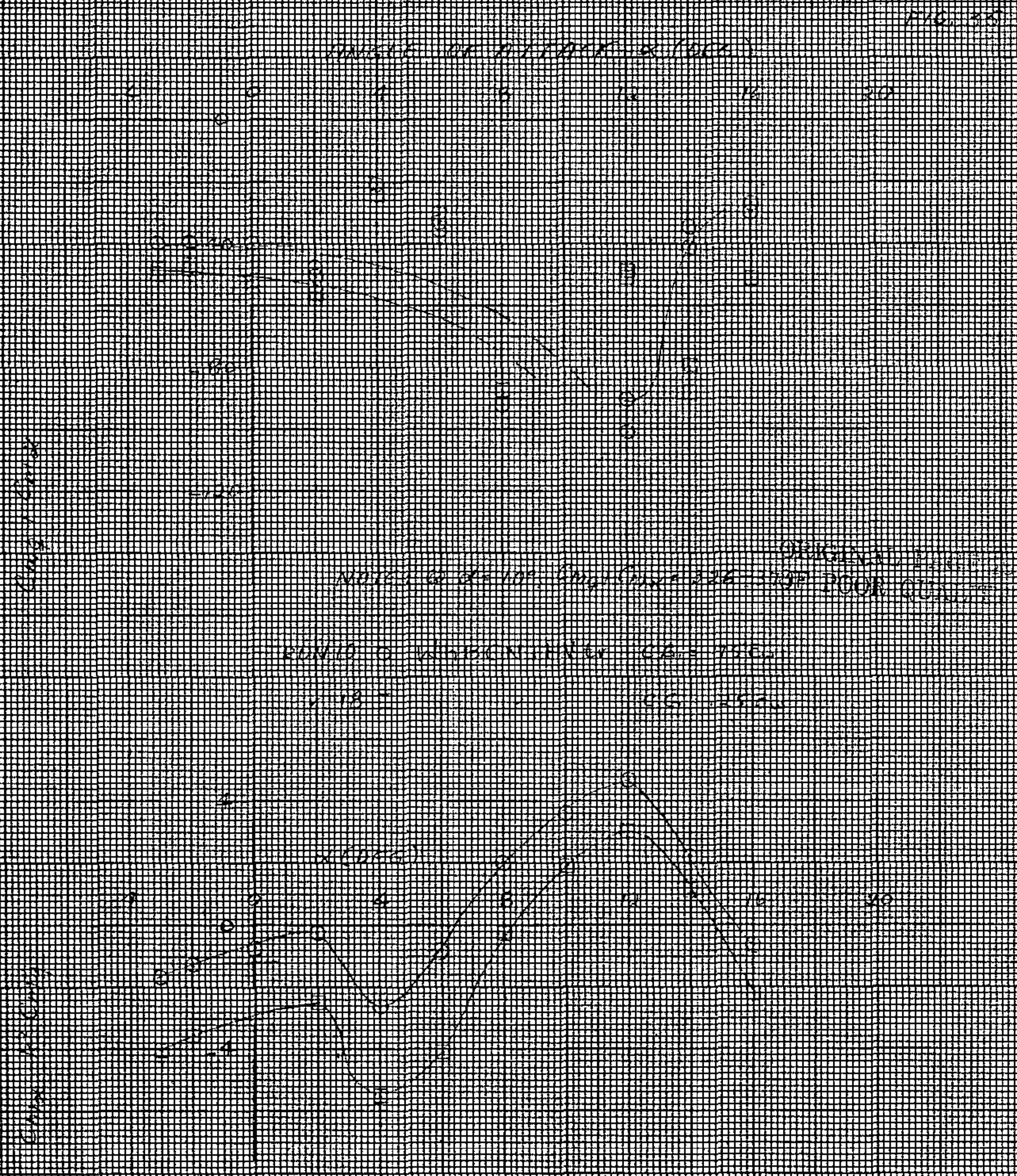

EFFECT OF C.G. LOCATION ON DAMPING IN PITCH

TAIL OFF

MACH NO = 0.95

LRC TEST NO 596

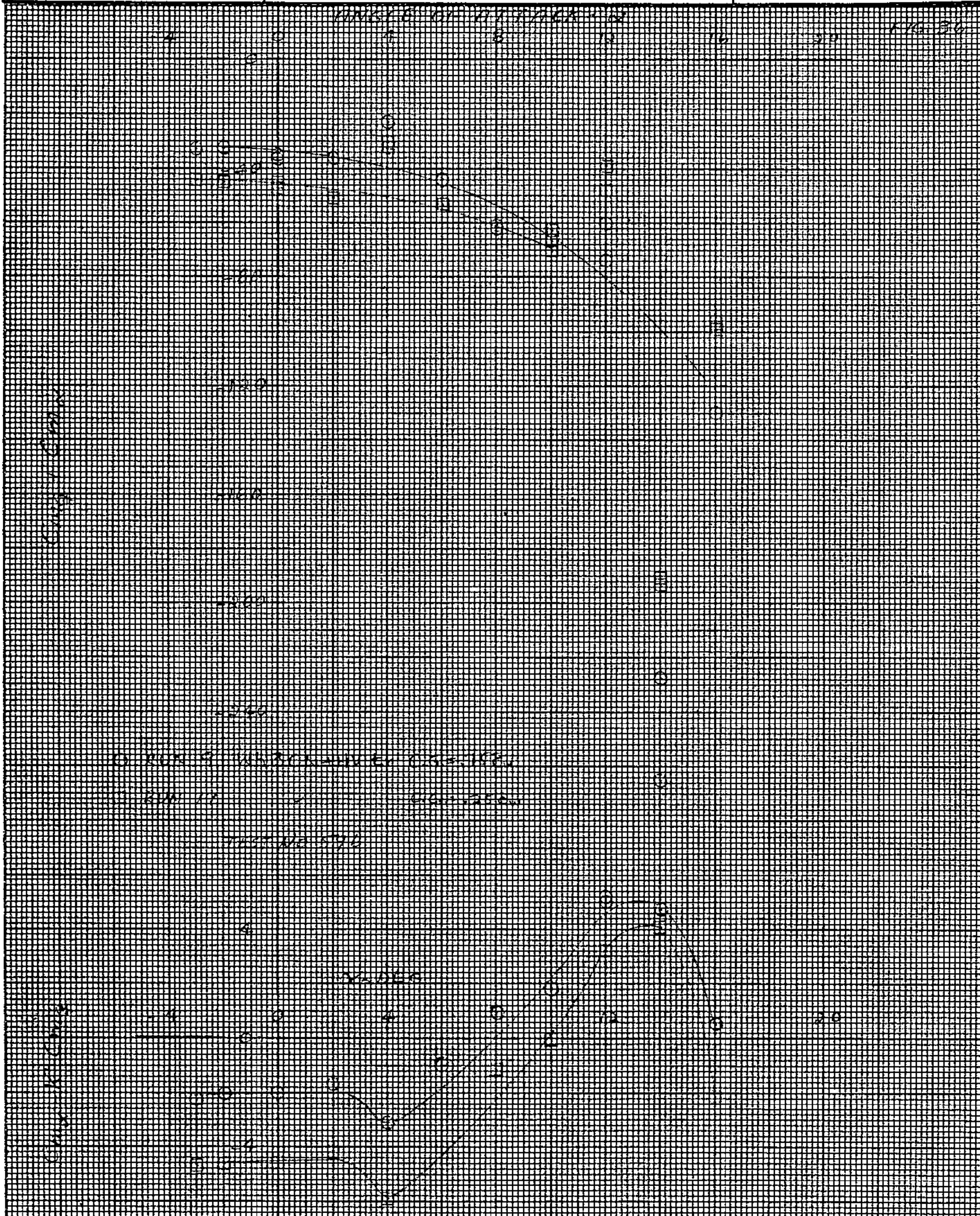

EFFECT OF C.G. LOCATION ON DAMPING IN PITCH
TAIL ON Λ = 65°
MACH NO. = 1.63

FIG. 37

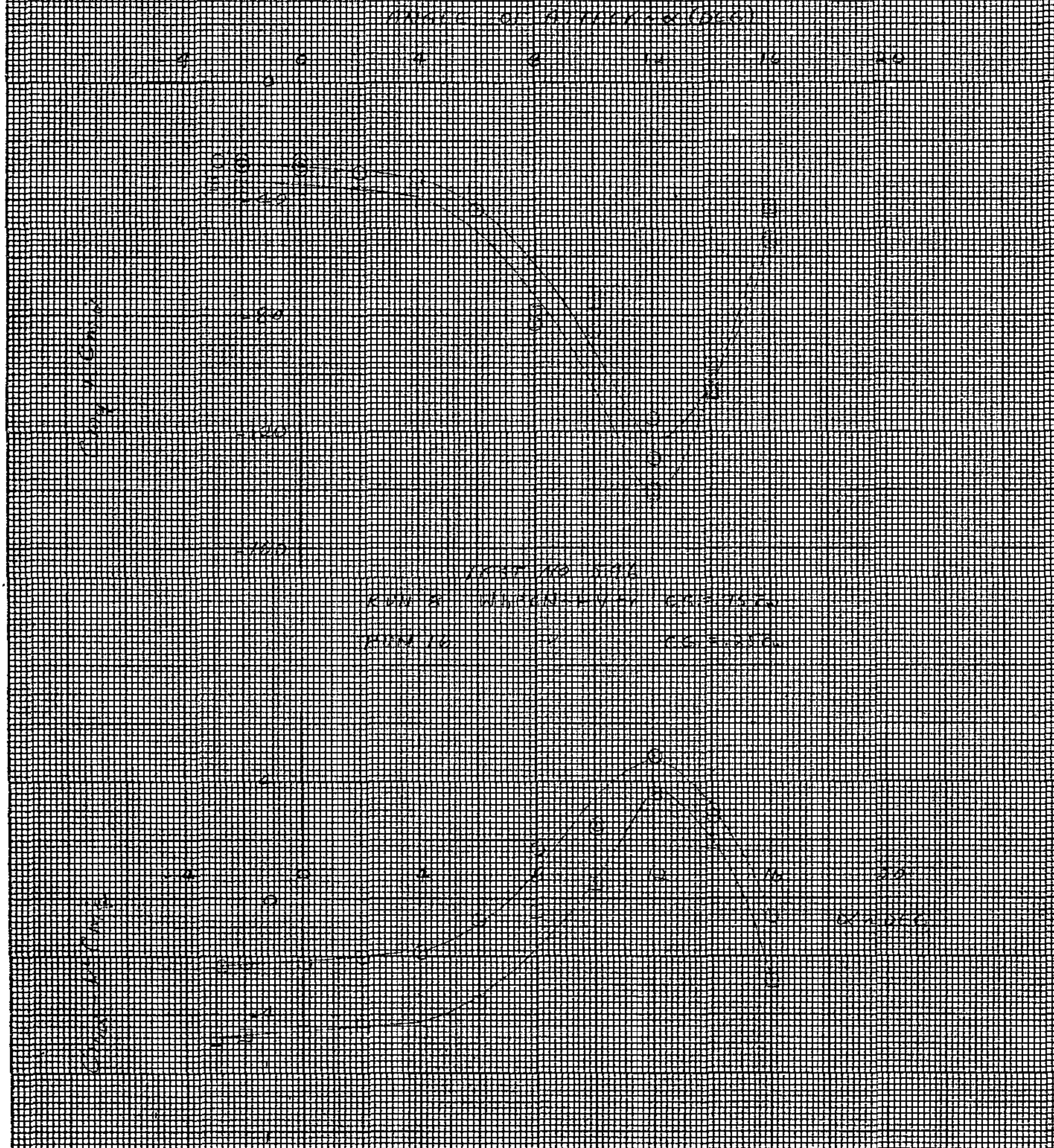

EFFECT OF C.G. LOCATION ON DAMPING IN PITCH

FORM 1021-S REV 10-70

PREPARED BY:	Los Angeles Division North American Rockwell	PAGE NO 64 OF 145
CHECKED BY:		REPORT NO NA-72-82
DATE:		MODEL NO.

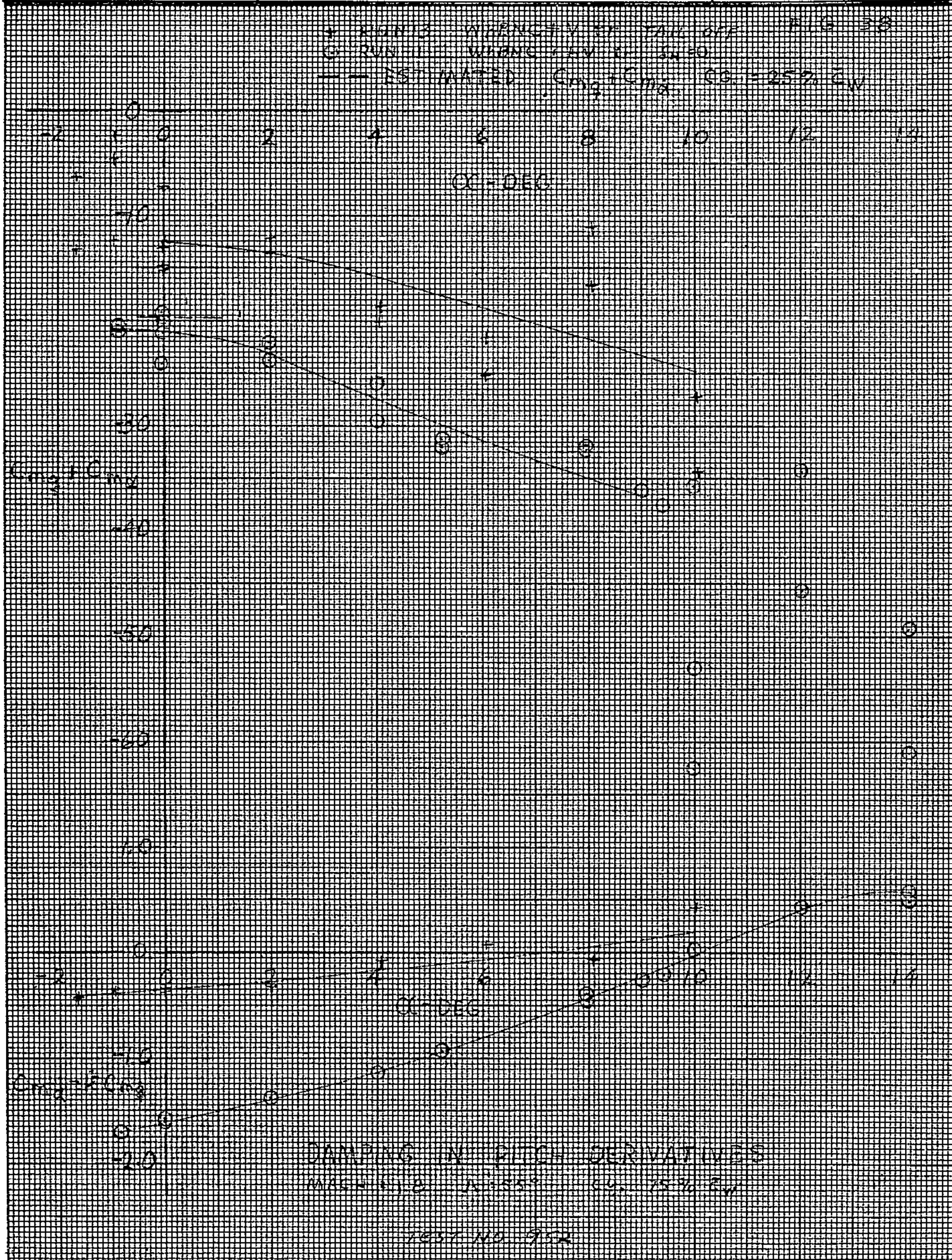

FORM 1021-S REV 10-70

PREPARED BY:	Los Angeles Division North American Rockwell	PAGE NO. 65 OF 145
CHECKED BY:		REPORT NO NA-72-82
DATE:		MODEL NO

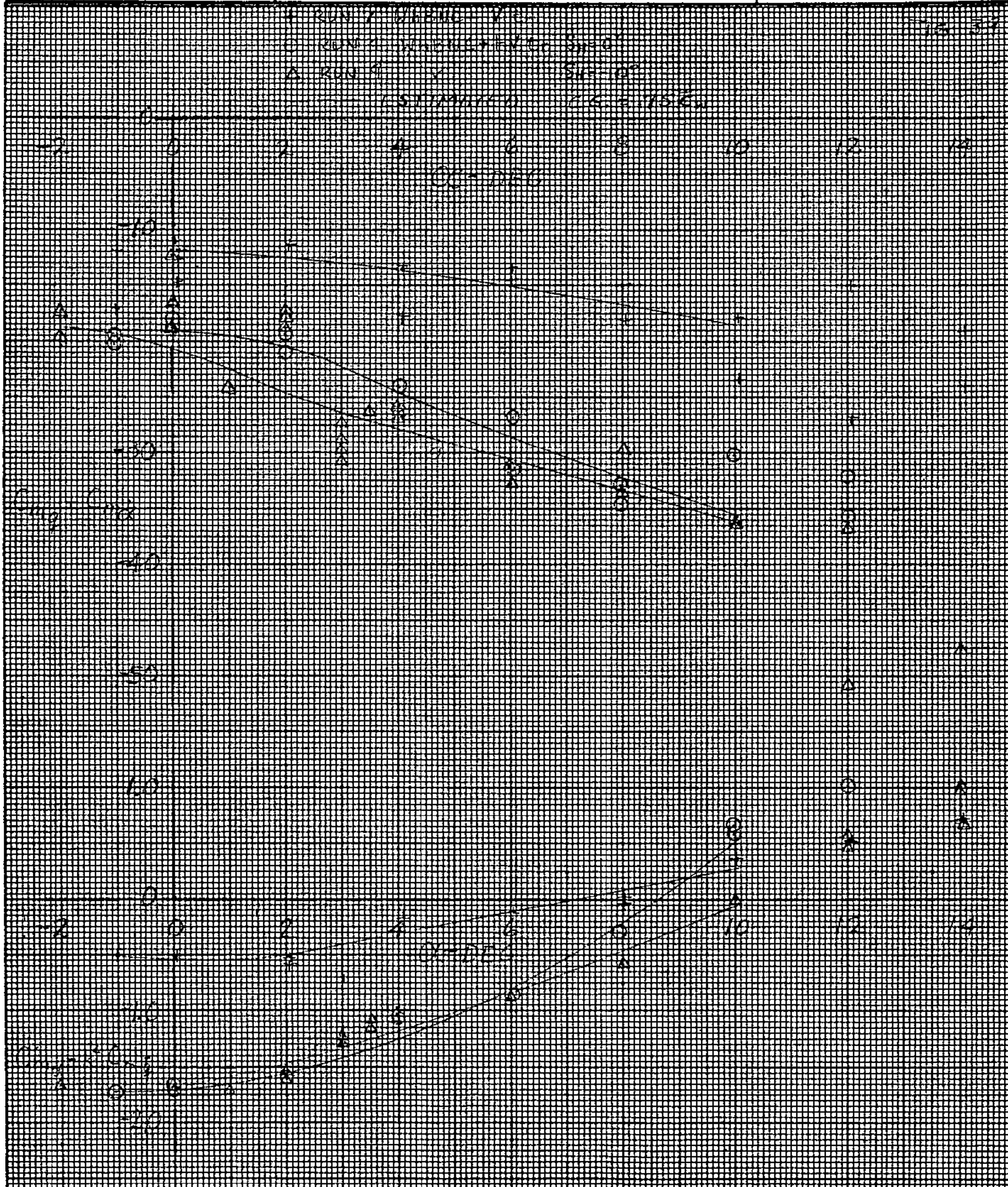

DAMPING IN PITCH DERIVATIVES

FORM 1021-S REV 10-70

PREPARED BY:	Los Angeles Division North American Rockwell	PAGE NO 66 OF 145
CHECKED BY:		REPORT NO. NA-72-82
DATE:		MODEL NO.

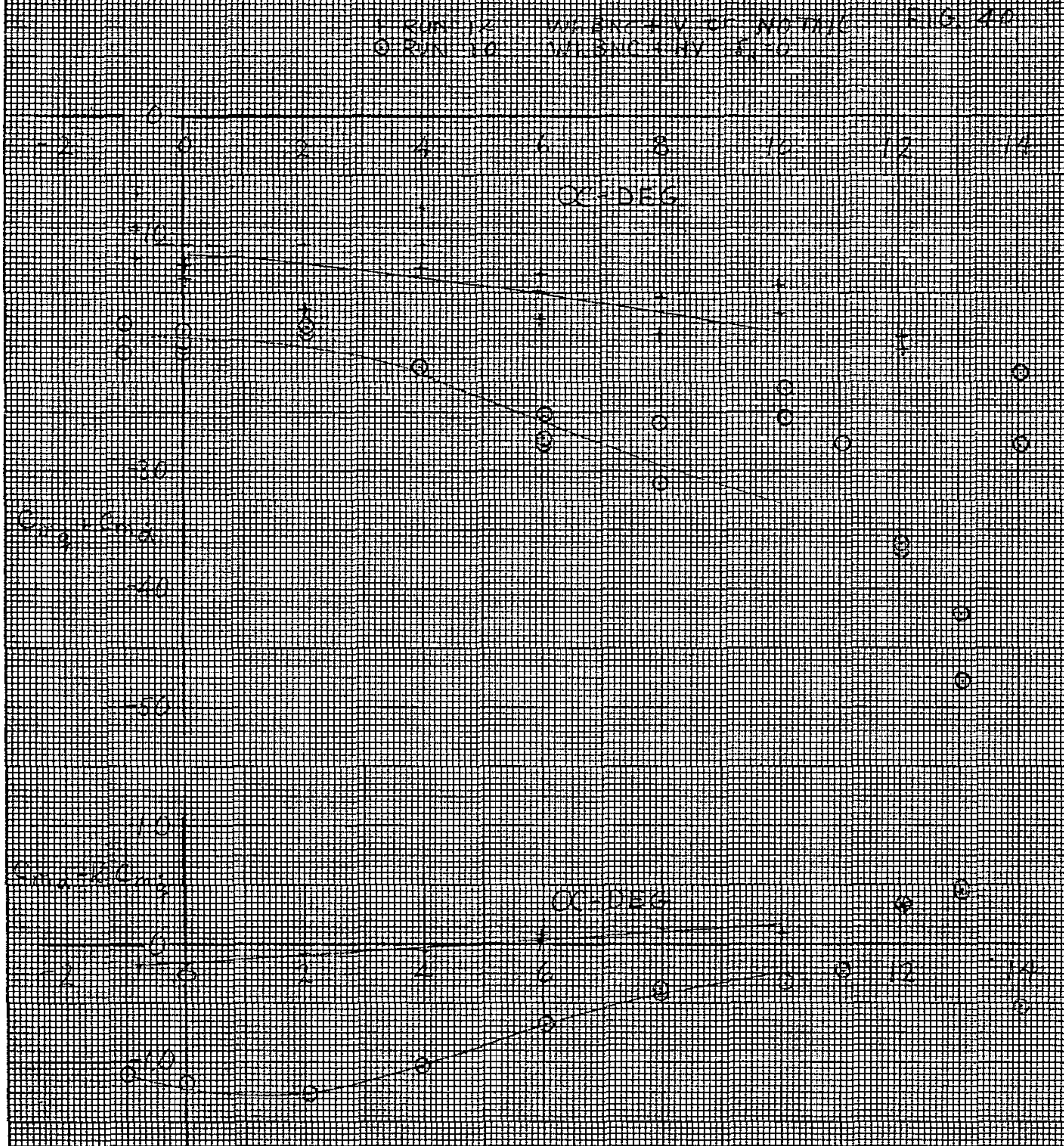

DAMPING IN PITCH DERIVATIVES

MACH = 2.16 Λ = 55° C.G. 75 % $\bar{c}_w$

TEST NO. 951

FORM 1021-6 REV. 10-70

PREPARED BY:	Los Angeles Division North American Rockwell	PAGE NO. 67 OF 145
CHECKED BY:		REPORT NO NA-72-82
DATE:		MODEL NO.

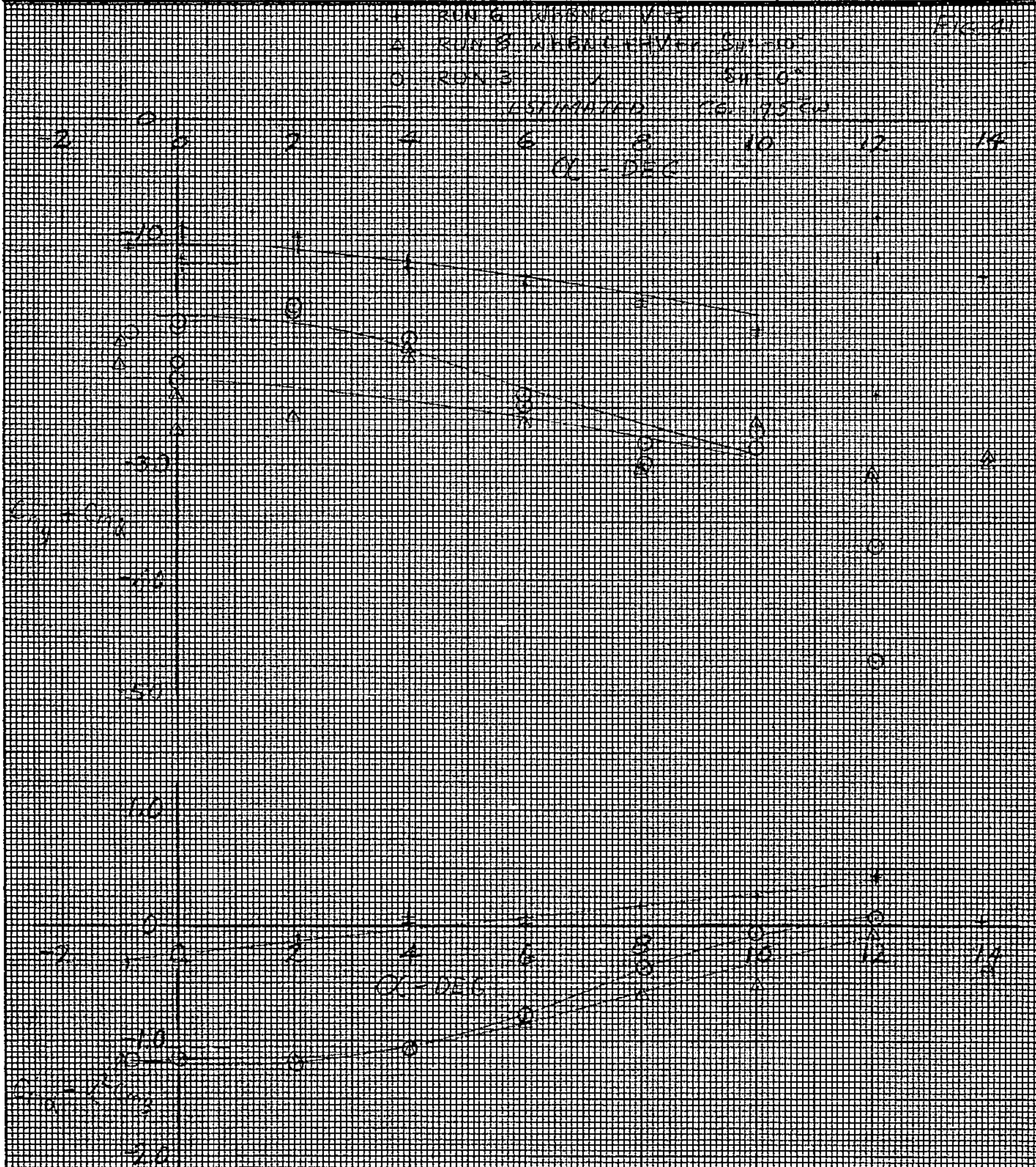

DAMPING IN PITCH DERIVATIVES

LRC TEST NO. 952

FIG. 42

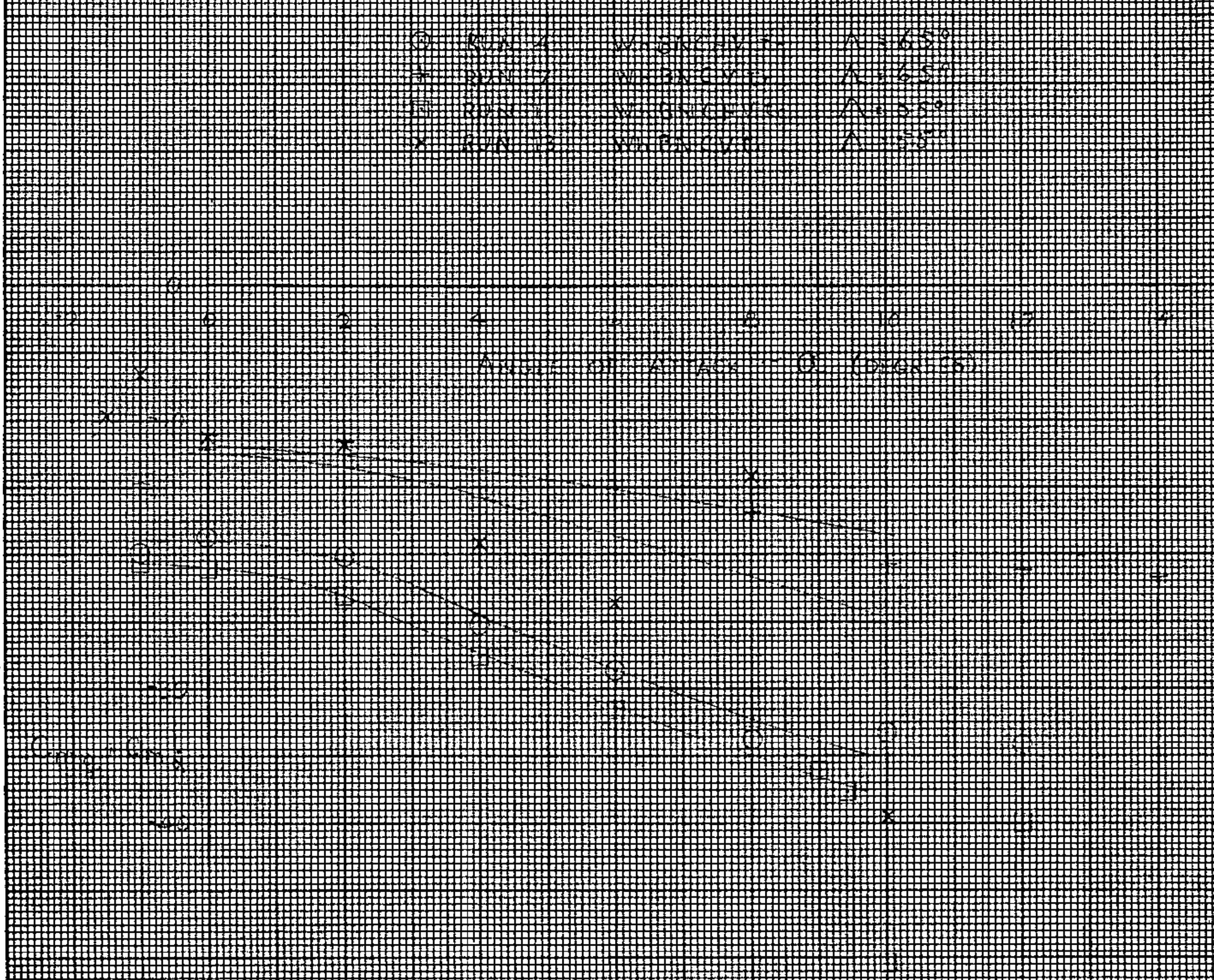

ORIGINAL PAGE
OF POOR QUAL

EFFECT OF SWEEP ON DAMPING IN PITCH DERIVATIVES

MACH NO. = 1.6

FORM 1021-S REV 10-70

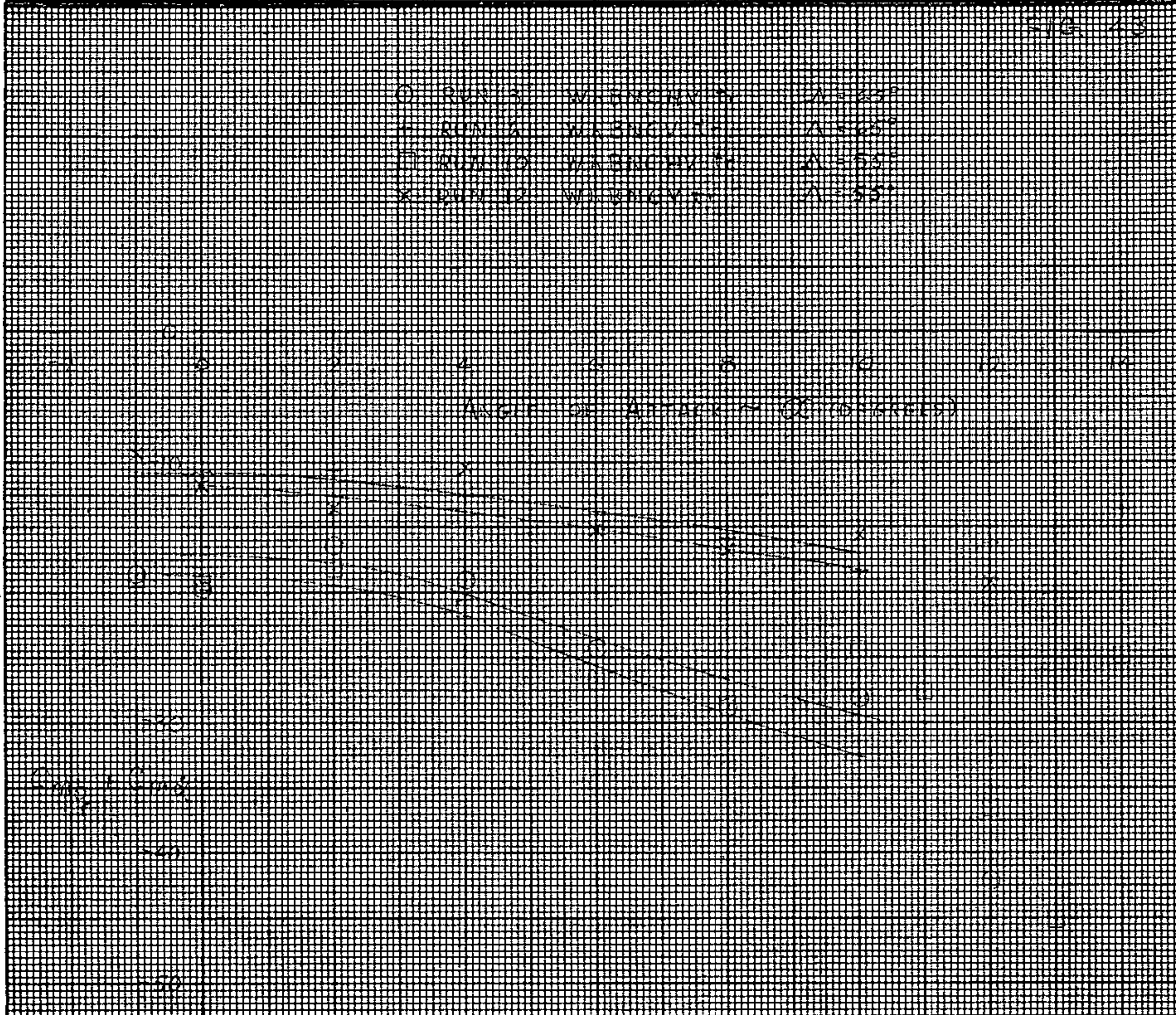

Effect of Sweep on Damping in Pitch Derivatives

Mach No. = 2.16

FORM 1021-S REV 10-70

PREPARED BY:	Los Angeles Division North American Rockwell	PAGE NO 70 OF 145
CHECKED BY:		REPORT NO: NA-72-82
DATE:		MODEL NO

FIG. 44

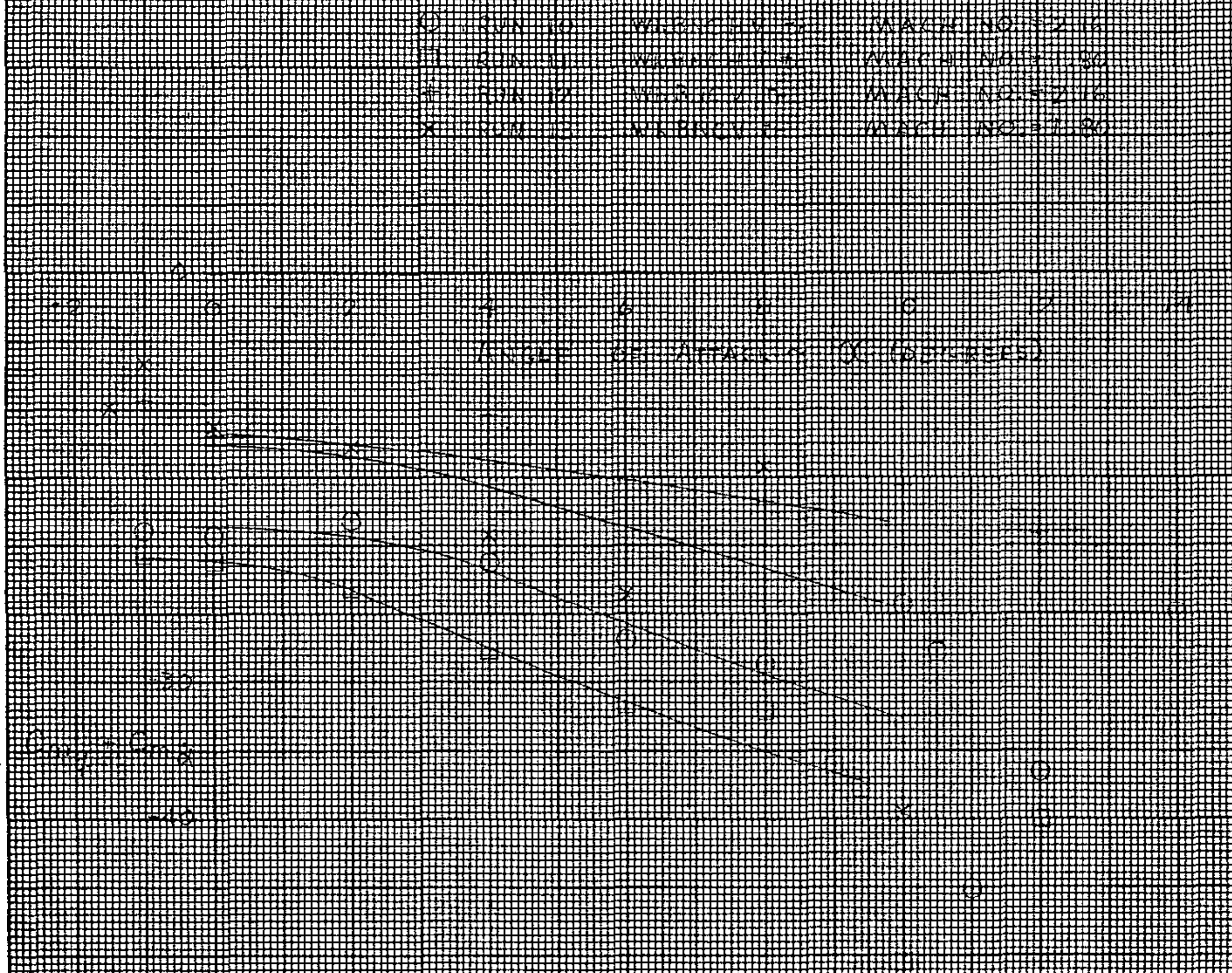

FORM 1021-S REV 10-70

PREPARED BY:	Los Angeles Division North American Rockwell	PAGE NO. 71 OF 145
CHECKED BY:		REPORT NO. NA-72-82
DATE:		MODEL NO

FIG. 45

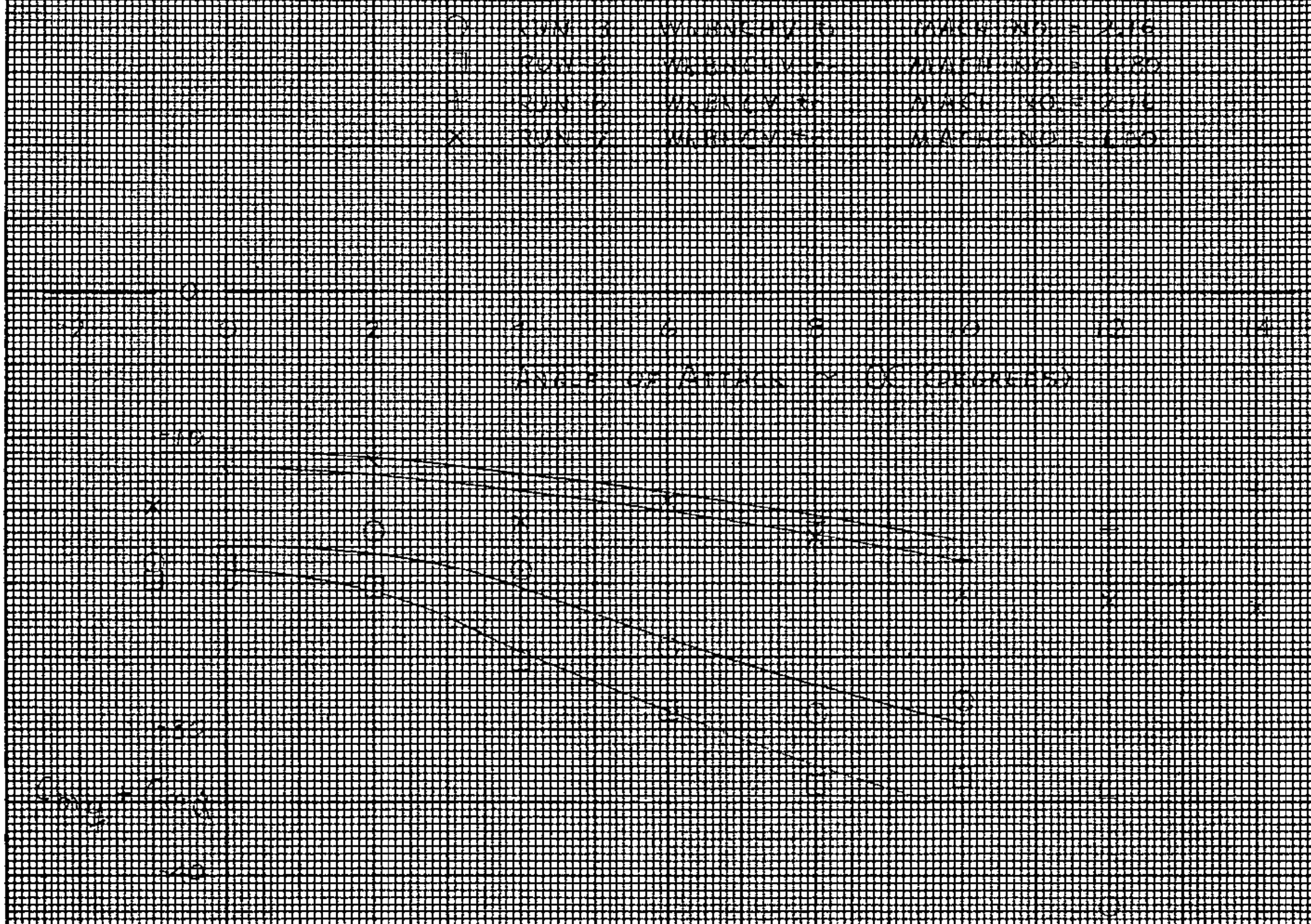

EFFECT OF MACH NUMBER VARIATION ON DAMPING IN PITCH DERIVATIVES

$\delta_H = 0$ $\Lambda = 65°$ c.g. = 75.9% $\bar{c}_w$

TEST NO. 930

FIG 46

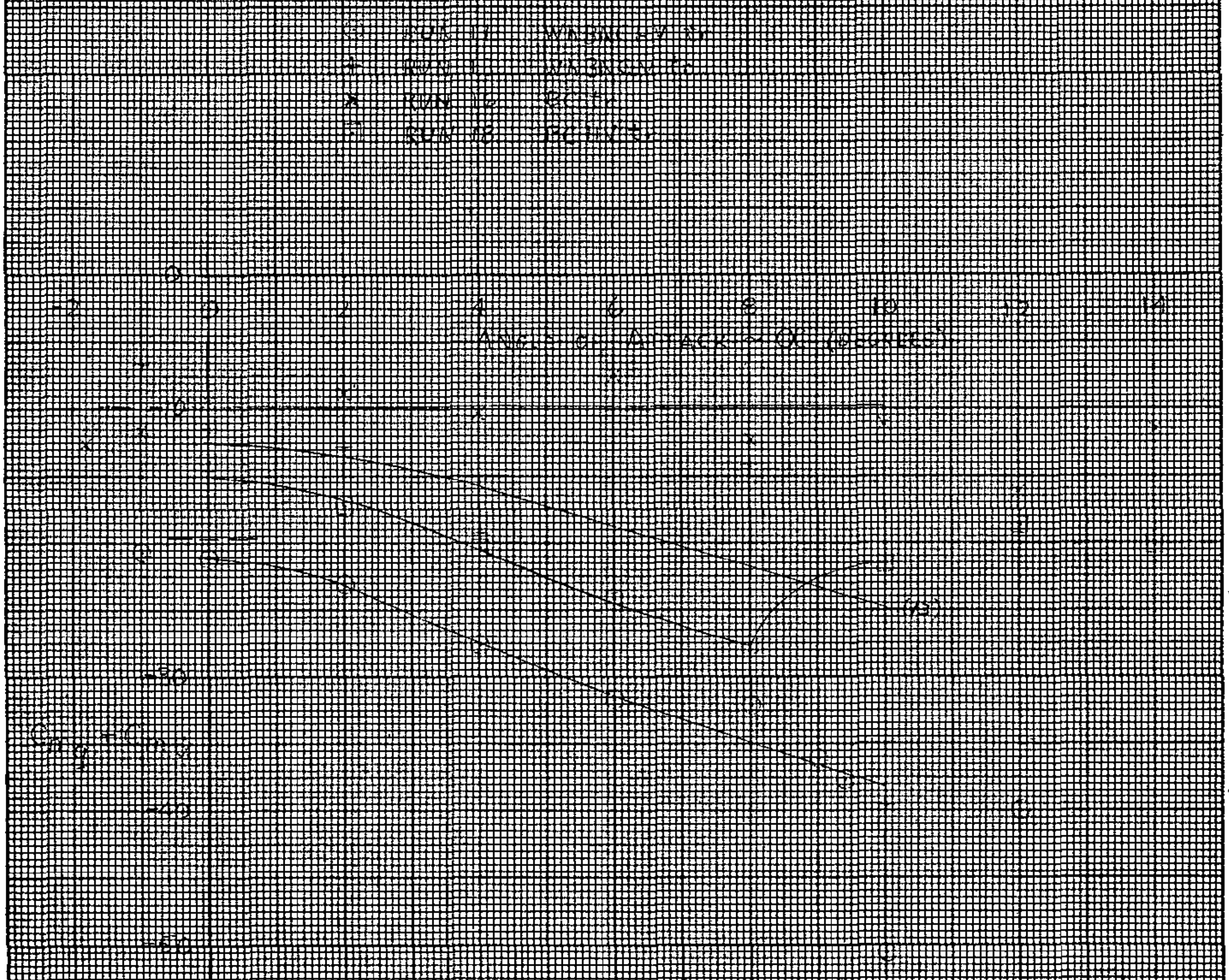

EFFECT OF COMPONENT BUILD-UP ON DAMPING IN PITCH DERIVATIVES

FORM 1021-S REV 10-70

PREPARED BY:	Los Angeles Division North American Rockwell	PAGE NO 73 OF 145
CHECKED BY:		REPORT NO. NA-72-82
DATE:		MODEL NO.

FIG 47

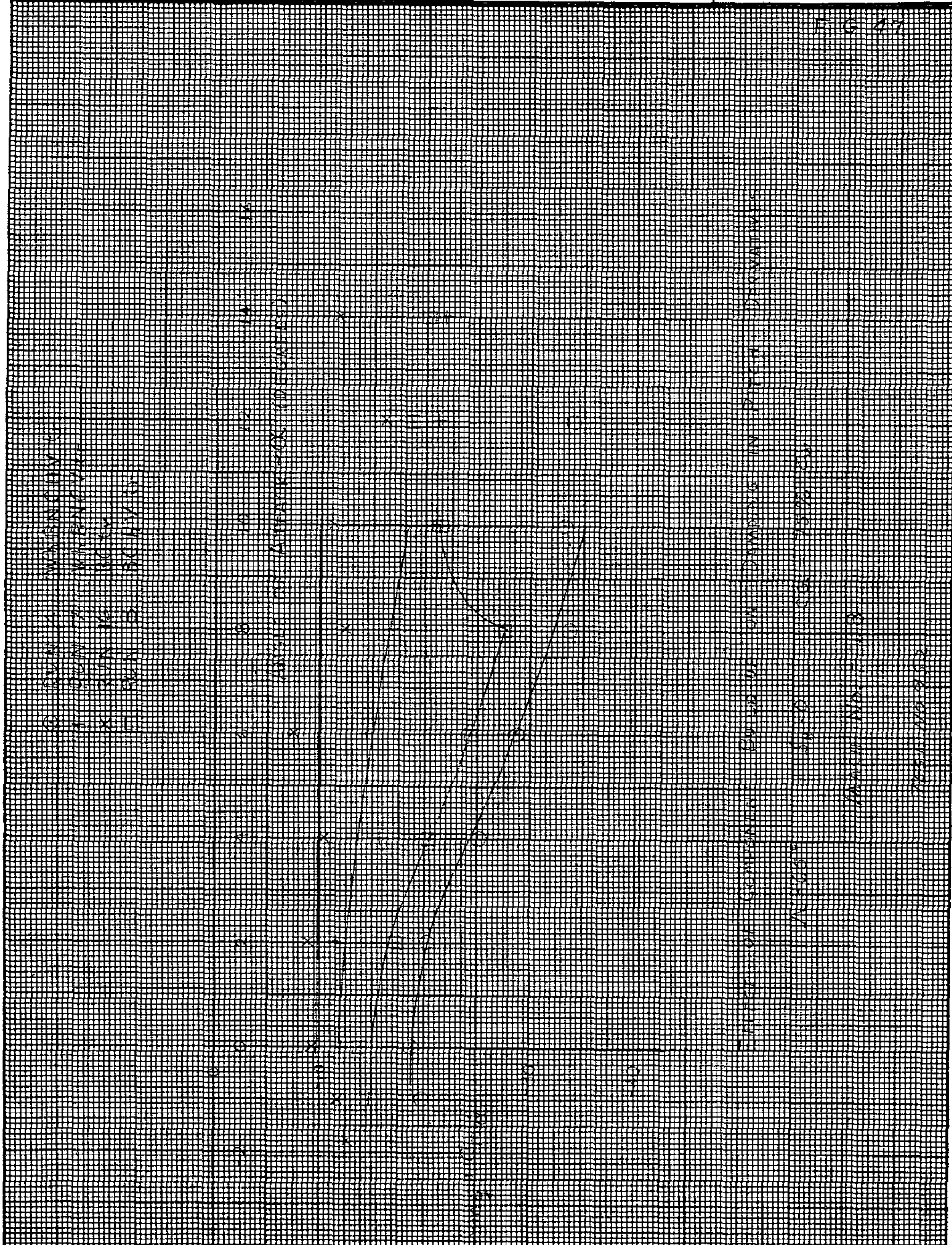

FIG 43

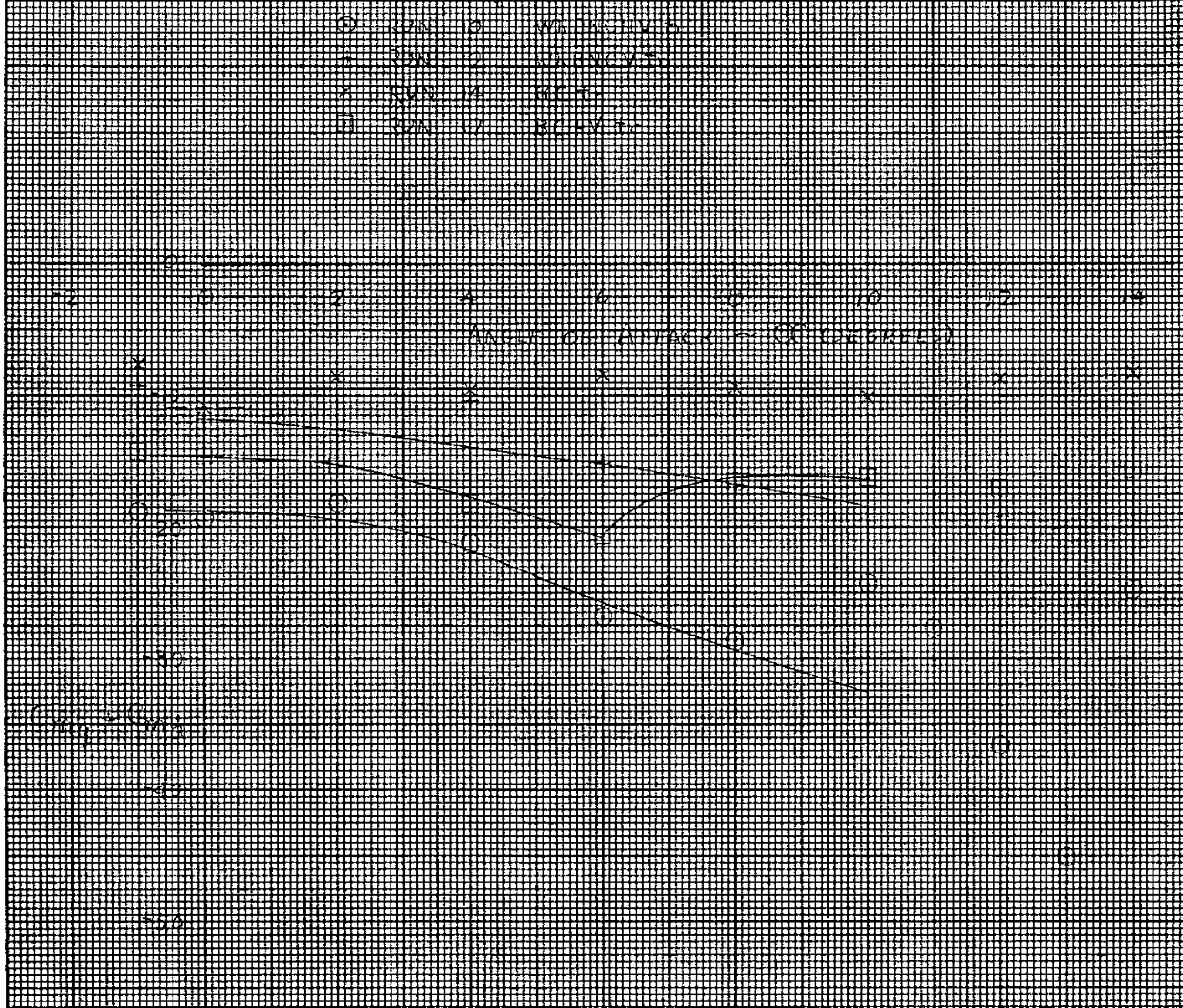

EFFECT OF COMPONENT BUILDUP ON DAMPING IN PITCH DERIVATIVES

MACH NO = 3.4

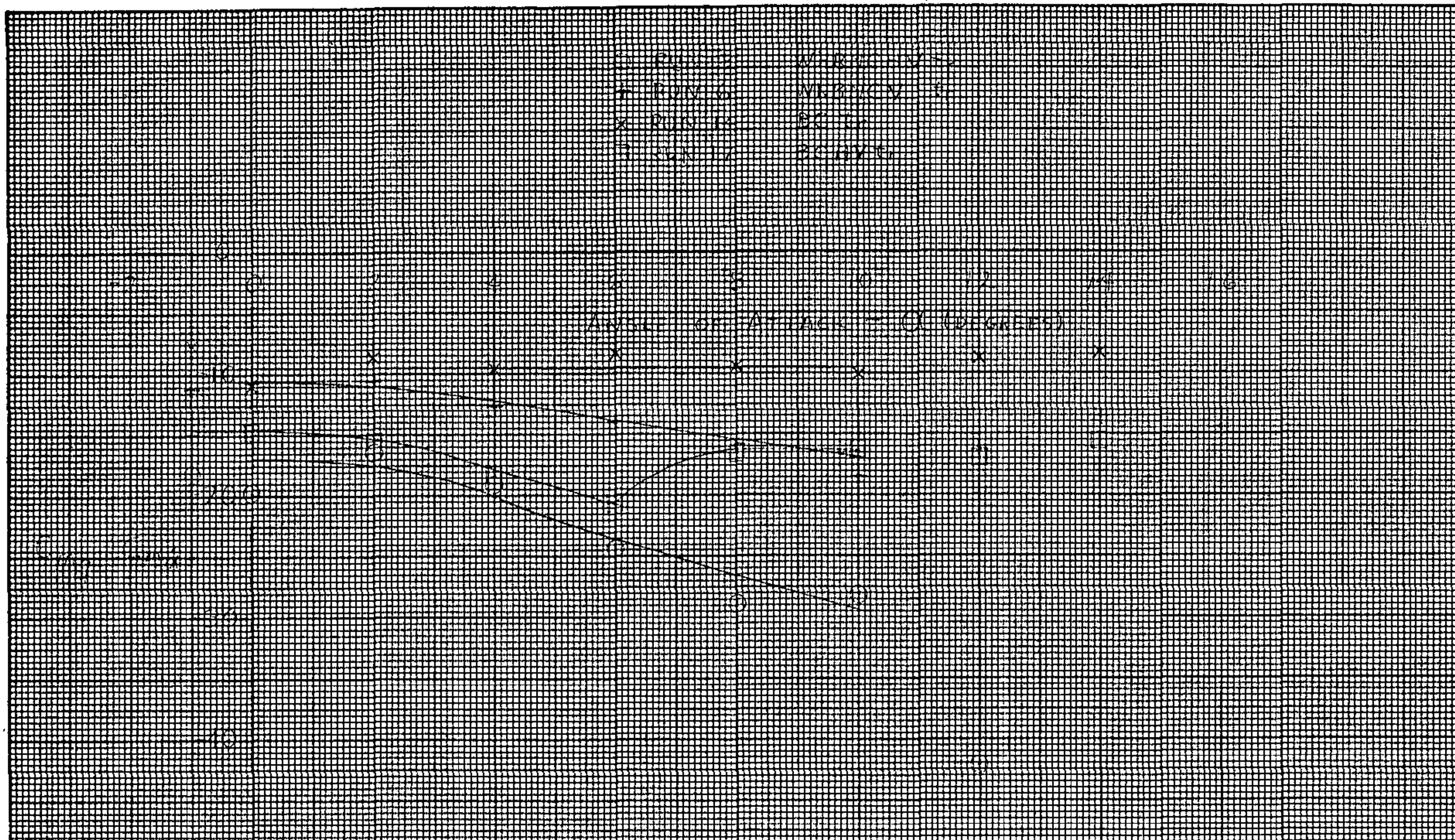

EFFECT OF COMPONENT BUILDUP ON DAMPING IN PITCH DERIVATIVES

MACH No.

TEST NO. 952

FIG 46

FORM 1021-S REV. 10-70

PREPARED BY:	Los Angeles Division North American Rockwell	PAGE NO 76 OF 145
CHECKED BY:		REPORT NO NA-72-82
DATE:		MODEL NO.

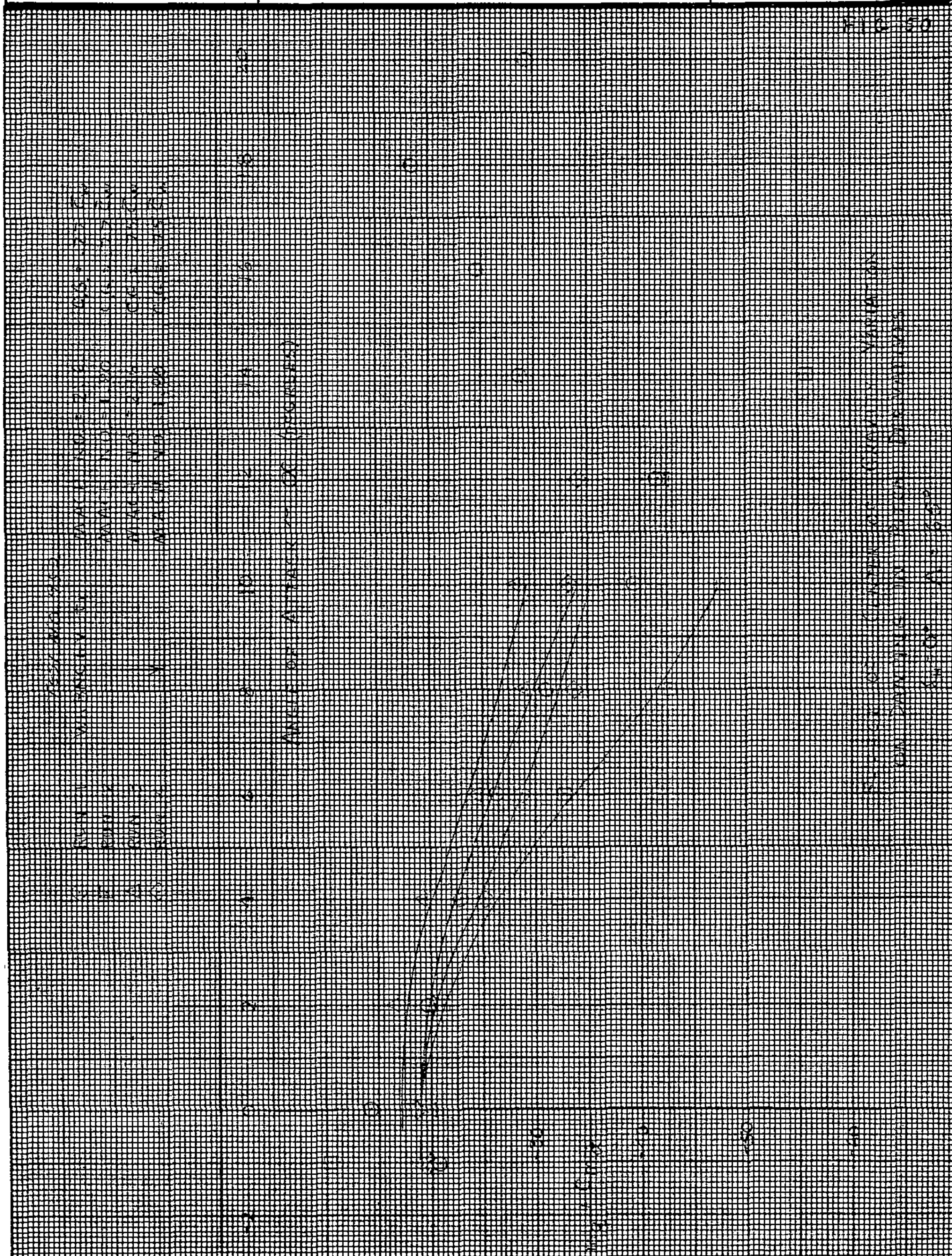

FIG 50

FIG. 51

○ RUN 11 − RUN 13 MACH NO. = 1.80
□ RUN 10 − RUN 12 MACH NO. = 2.16
— — — ESTIMATED HORIZONTAL INPUT

		δ_H	Λ	M	C.G.
RUN 10	WBNC + HV +	0°	55°	2.16	25% $\bar{c}_w$
RUN 11	+ HV	0°		1.80	
RUN 12	+ −V	—		2.16	
RUN 13	+ −V	—		1.80	

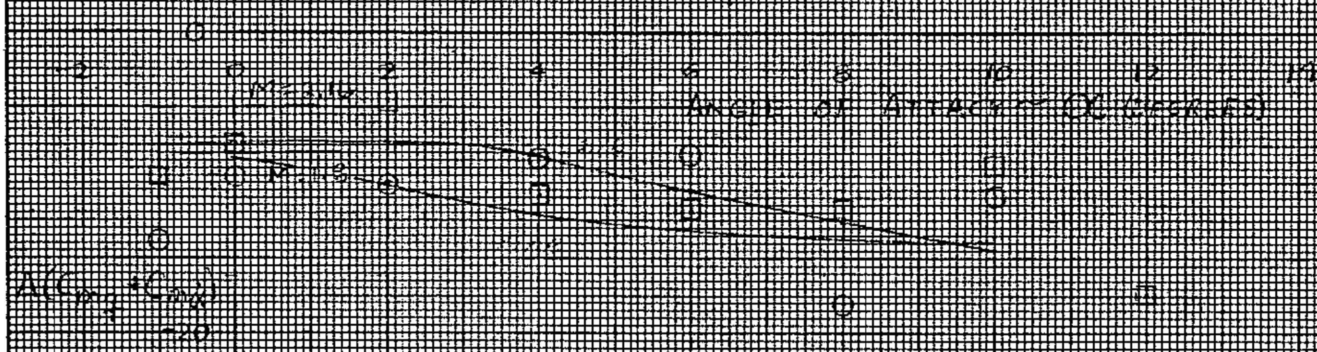

HORIZONTAL TAIL INPUT INTO DAMPING IN PITCH
DERIVATIVES — WING-ON

TEST NO. 332

FIG. 32

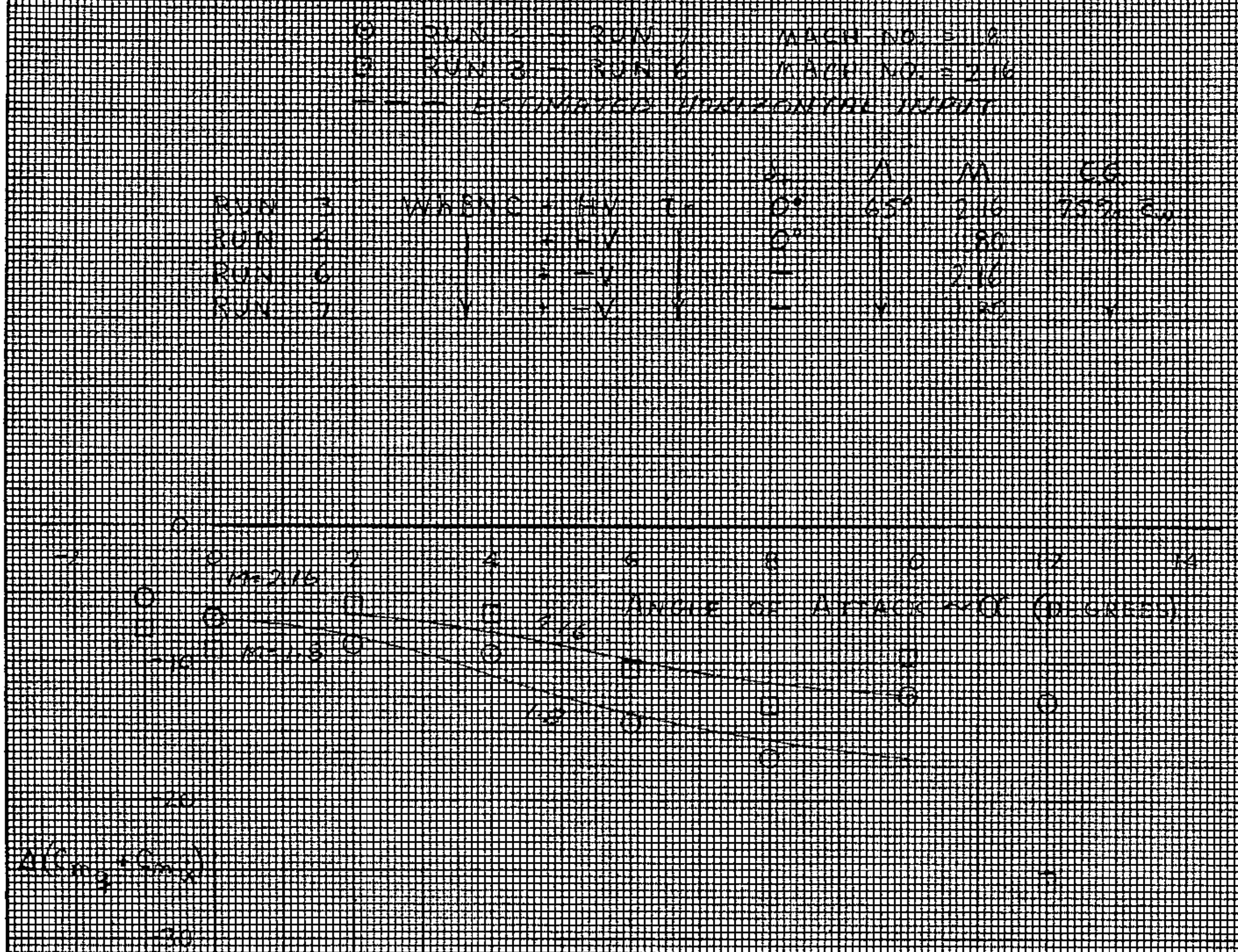

HORIZONTAL TAIL INPUT INTO DAMPING IN PITCH DERIVATIVES
— WING ON

TEST NO. 752

FIG 53

○ RUN 18 − RUN 16 MACH NO. = 1.8
□ RUN 17 − RUN 14 MACH NO. = 2.16

		δ_H	M	C.G.
RUN 14	BC + — + t_F	—	2.16	70 % $\bar{c}_w$
RUN 16	BC + — + t_F	—	1.80	
RUN 17	BC + HV + t_F	0°	2.16	
RUN 18	BC + HV + t_F	0°	1.80	

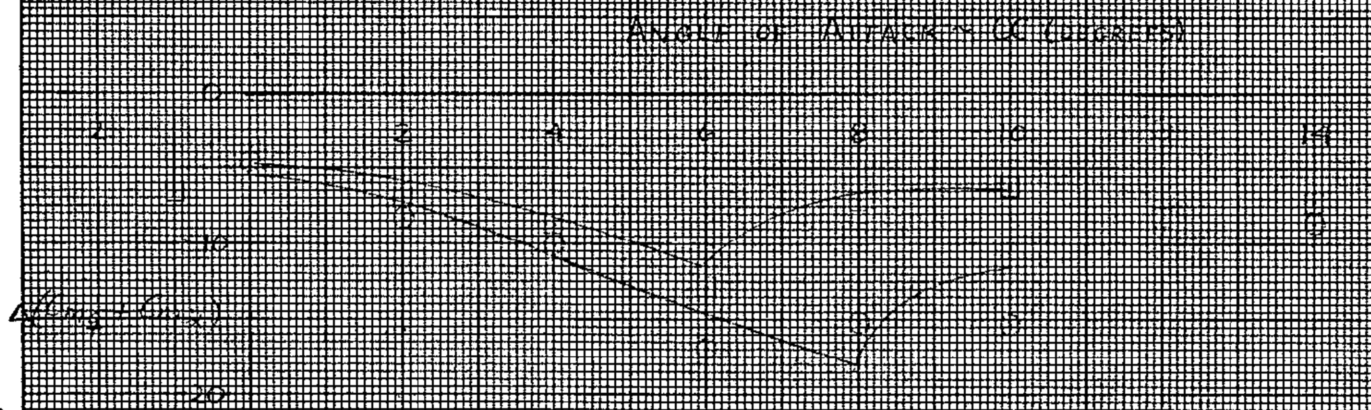

HORIZONTAL TAIL INPUT INTO DAMPING IN PITCH DERIVATIVES
— WING OFF

TEST NO. 953

FORM 1021-S REV. 10-70

PREPARED BY:	Los Angeles Division North American Rockwell	PAGE NO. 80 OF 145
CHECKED BY:		REPORT NO NA-72-82
DATE:		MODEL NO.

FIG. 54

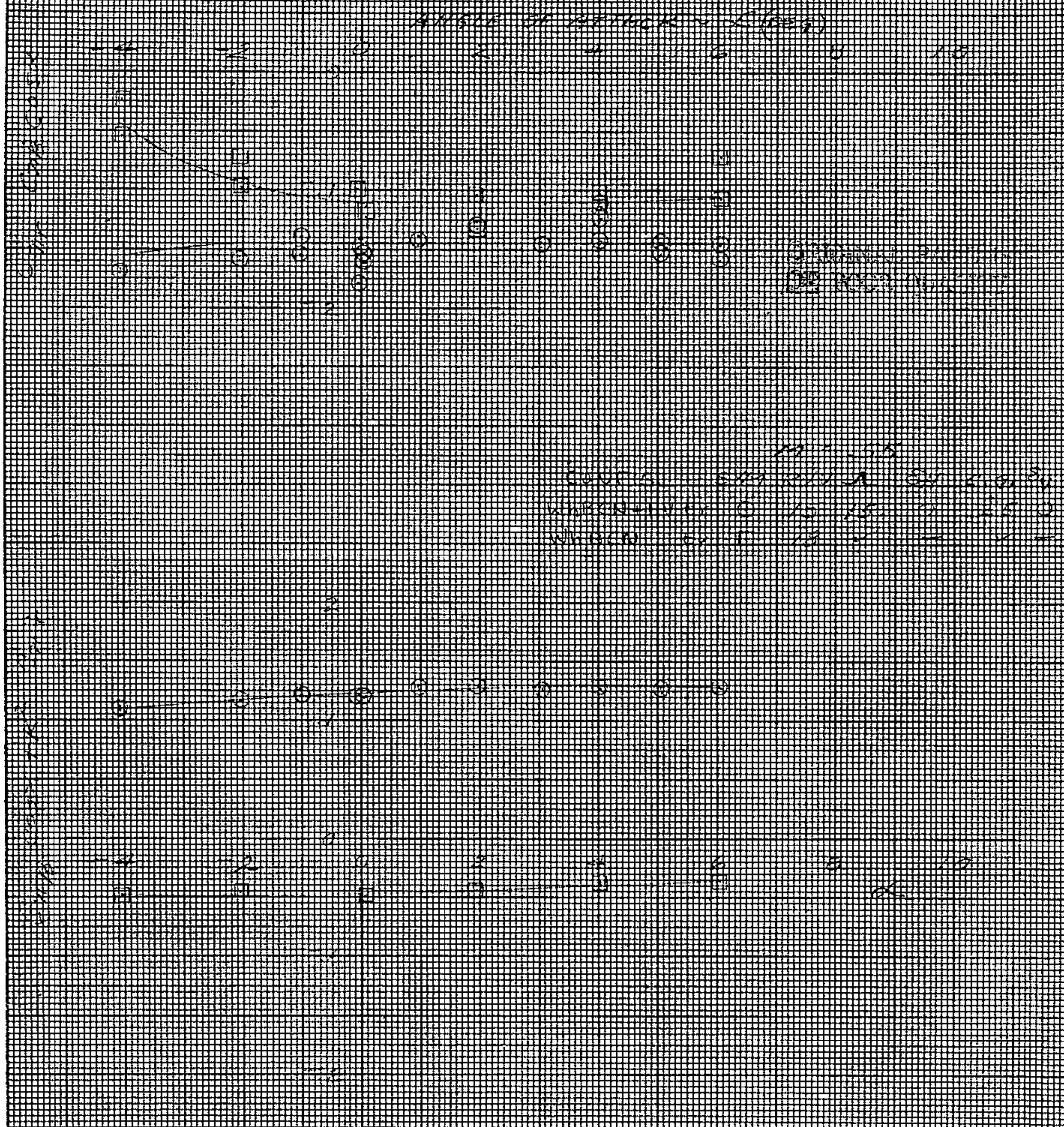

$\Lambda = 15^\circ$ $M = .65$

TEST NO 734

FORM 1021-S REV. 10-70

PREPARED BY:	Los Angeles Division North American Rockwell	PAGE NO. 81 OF 145
CHECKED BY:		REPORT NO NA-72-82.
DATE:		MODEL NO.

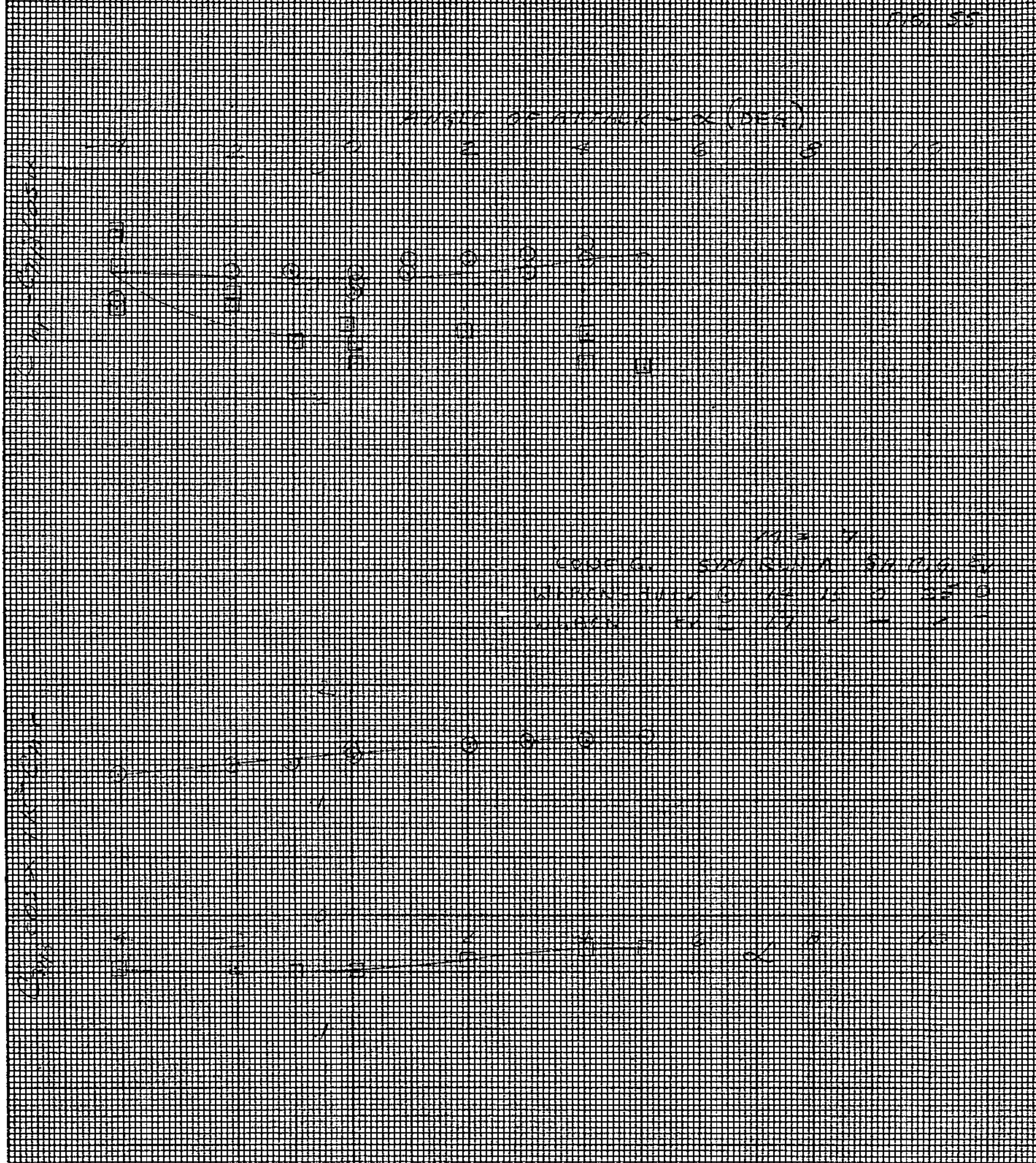

$\Lambda = 15°$ M = 7.0

TEST NO 934

FORM 1021-S REV. 10-70

PREPARED BY:	Los Angeles Division North American Rockwell	PAGE NO. 82 OF 145
CHECKED BY:		REPORT NO. NA-72-82
DATE:		MODEL NO.

FIG. 56

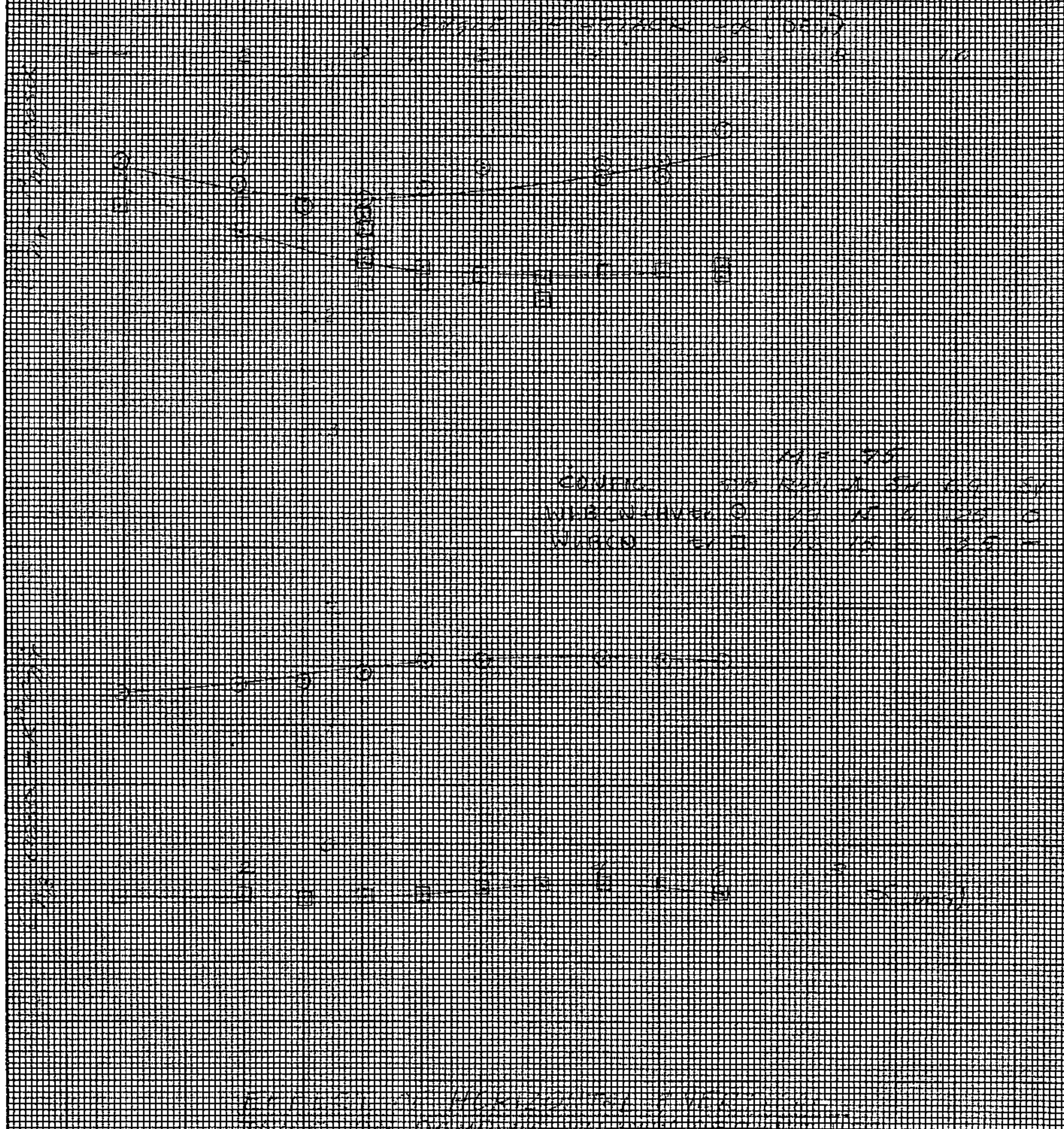

Λ = 15° M = .70

TEST NO. 734

FORM 1021-S REV 10-70

PREPARED BY:	Los Angeles Division North American Rockwell	PAGE NO. 83 OF 145
CHECKED BY:		REPORT NO NA-72-82
DATE:		MODEL NO.

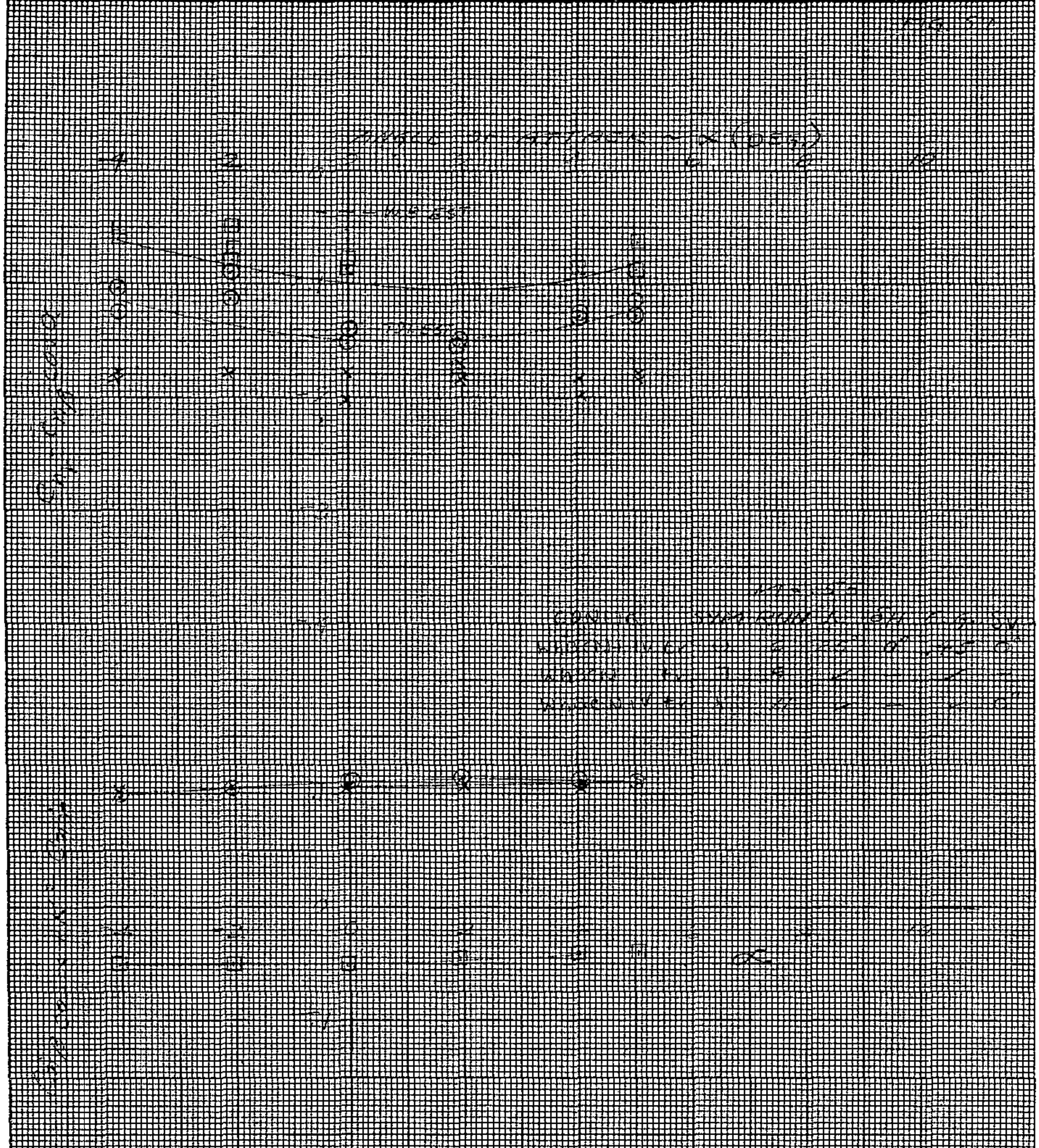

EFFECT OF HORIZONTAL & VERTICAL TAIL ON [illegible]
[illegible] OF YAW DERIVATIVES

$\Lambda = 25°$ $M = 0.55$

LRC TEST NO. 931

FIG. 58

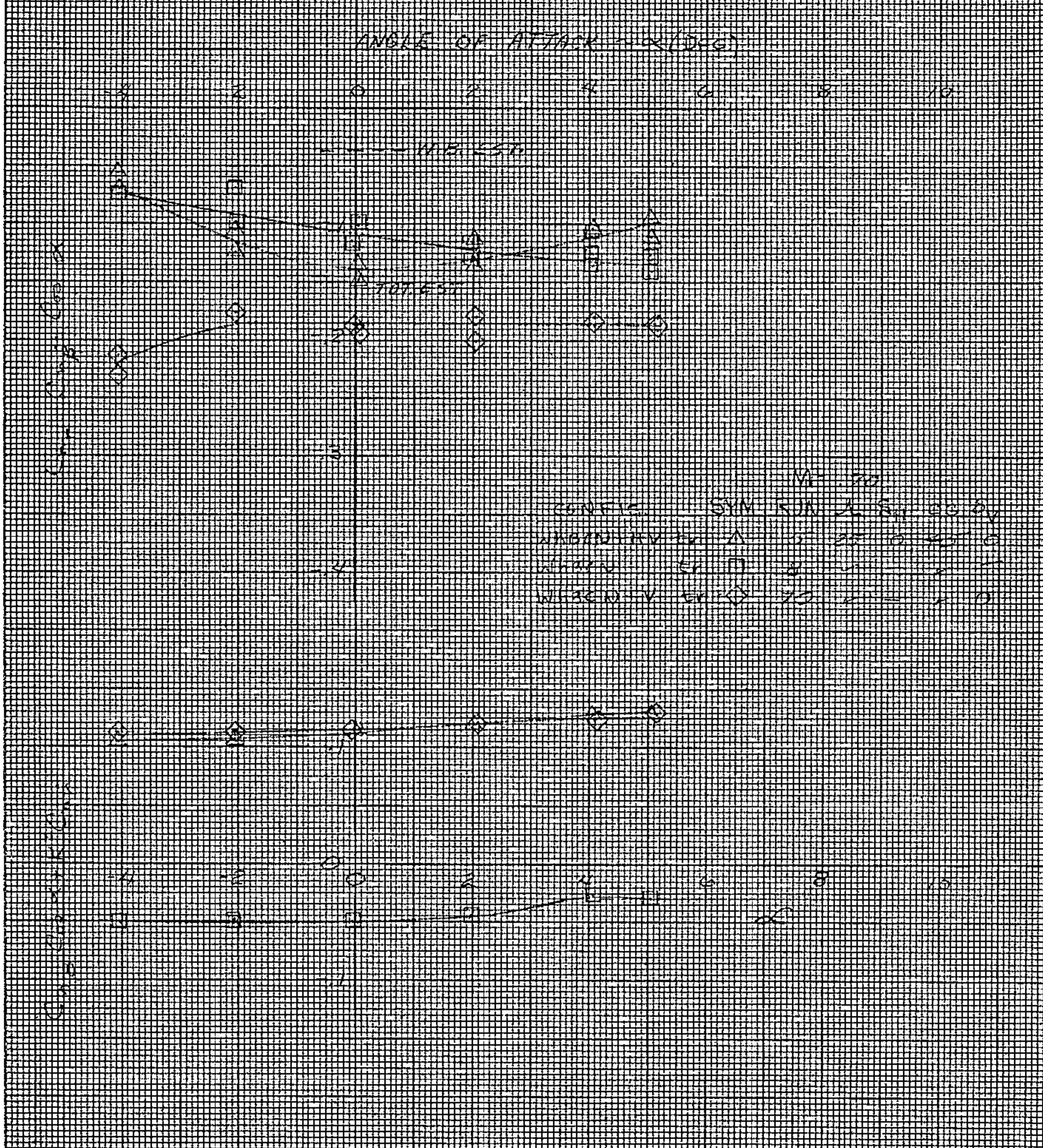

EFFECT OF HORIZONTAL & VERTICAL TAILS
ON DAMPING IN YAW DERIVATIVES
Λ = 25

MACH NO = 0.70

TEST NO. 934

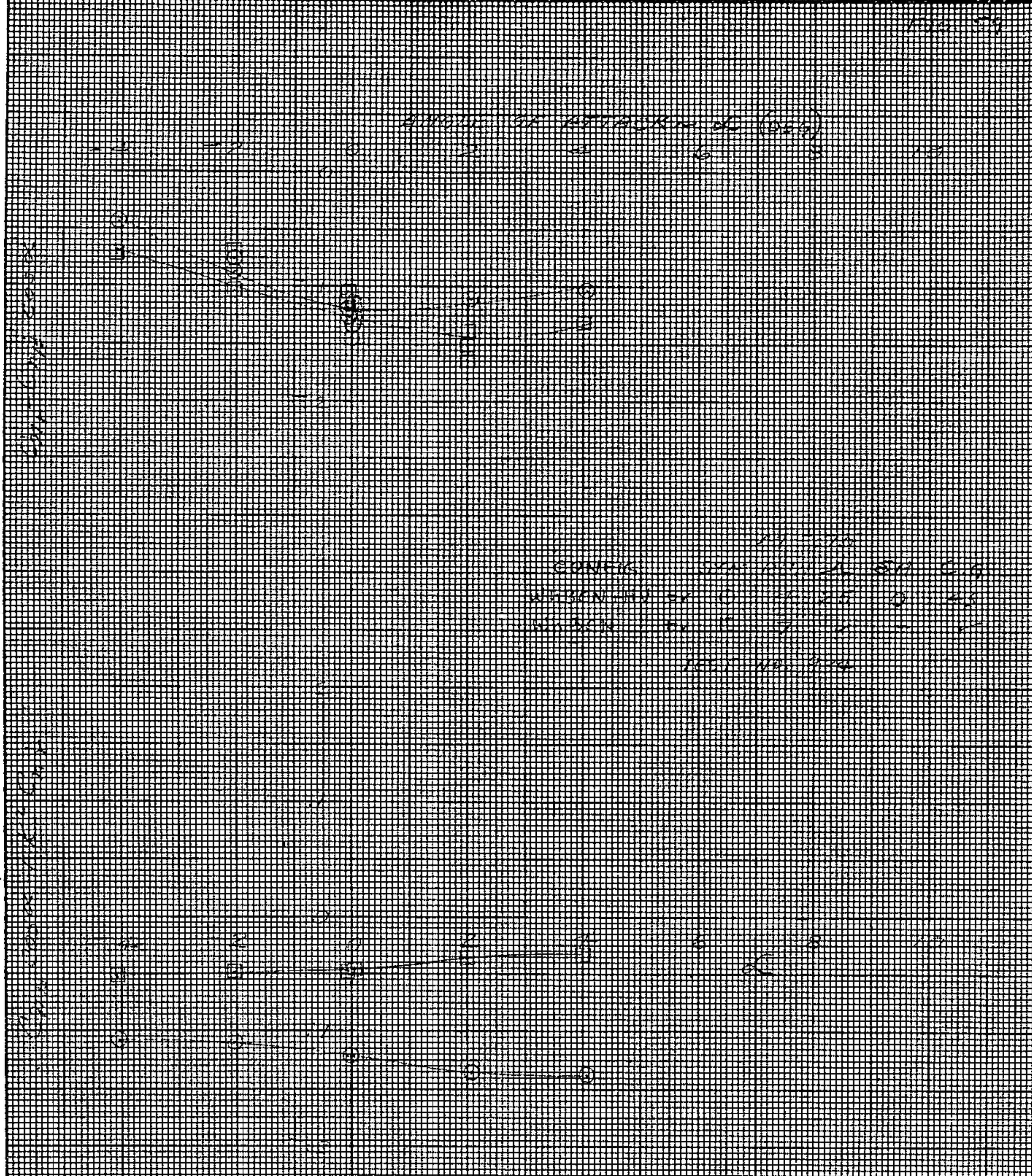

EFFECT OF [illegible] VERTICAL TAILS ON DAMPING [illegible]

Λ = 25°

MACH NO. = .75

FIG 66

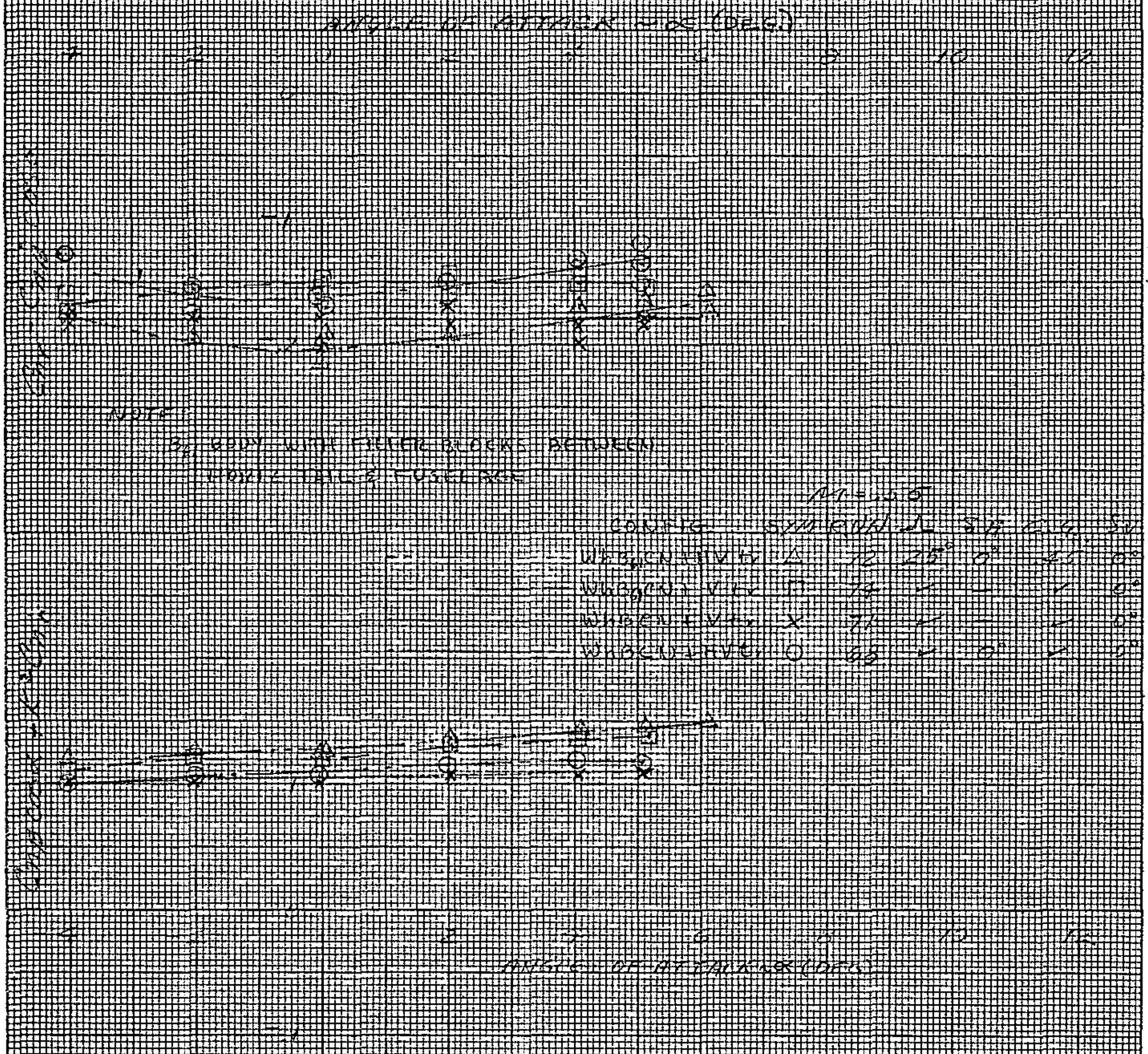

EFFECT OF FILLER BLOCKS ON
DAMPING IN YAW DERIVATIVES
Λ = 25° M = 0.35

TEST NO. 934

FORM 1021-S REV 10-70

PREPARED BY:	Los Angeles Division North American Rockwell	PAGE NO. 87 OF 145
CHECKED BY:		REPORT NO. NA-72-82
DATE:		MODEL NO.

FIG. 61

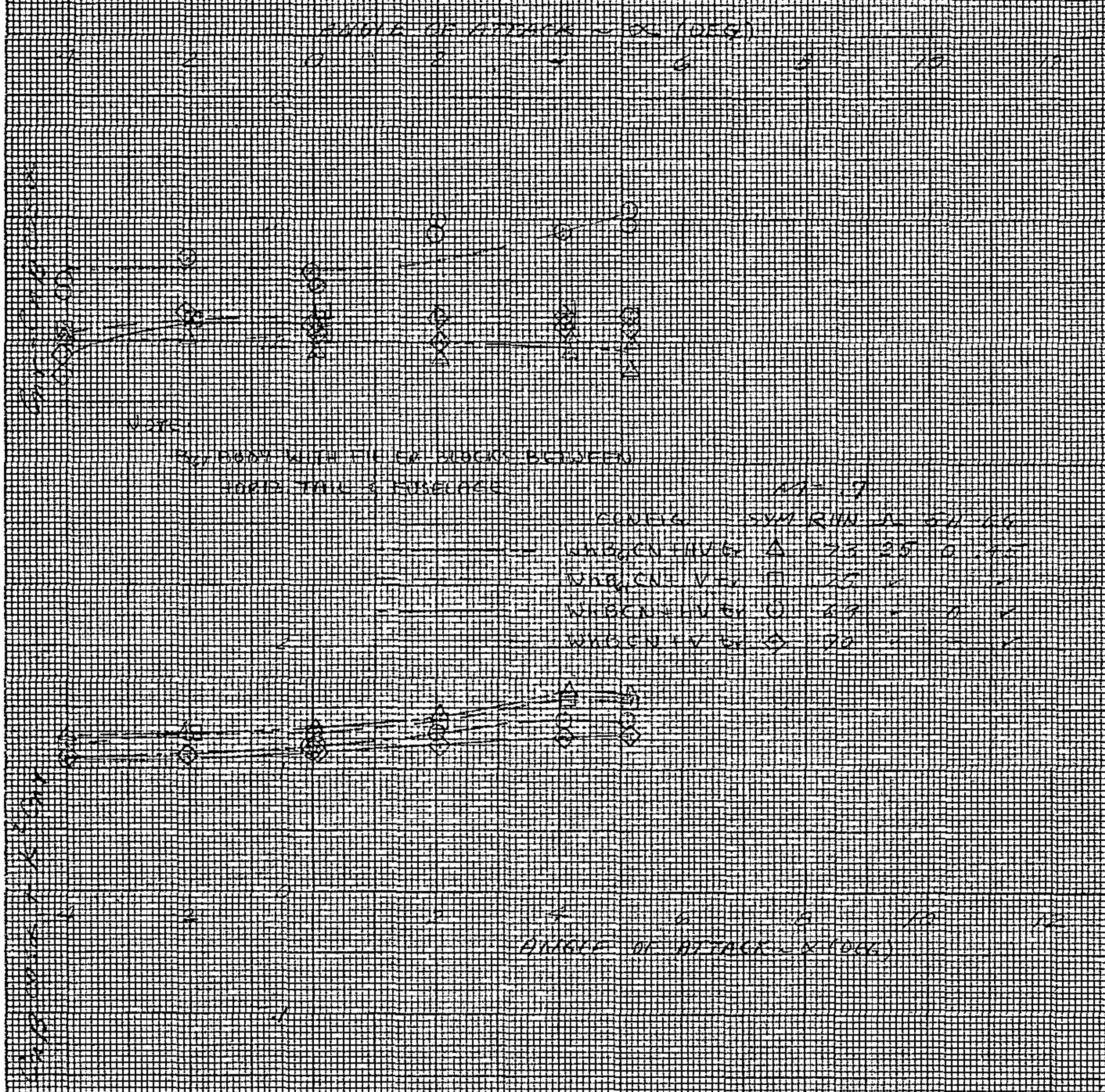

EFFECT OF FILLER BLOCKS ON
DAMPING IN YAW DERIVATIVES
M = 0.70
TEST NO. 734

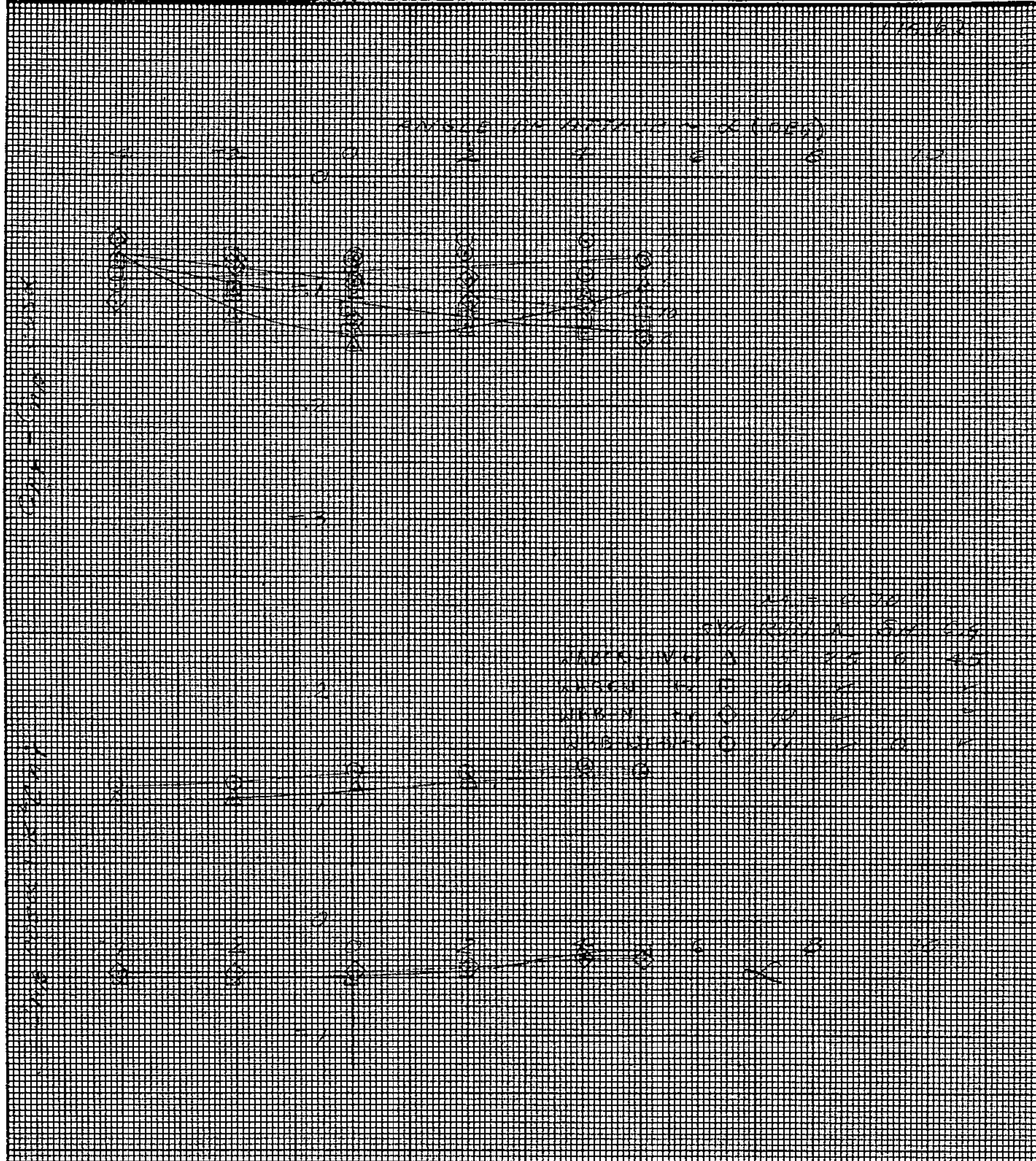

EFFECT OF SMC VANE, HORIZONTAL & VERTICAL TAILS ON DAMPING IN YAW DERIVATIVES

MACH = 0.70   Λ = 25°

TEST NO. 734

FORM 1021-S REV 10-70

PREPARED BY:	Los Angeles Division North American Rockwell	PAGE NO 89 OF 145
CHECKED BY:		REPORT NO. NA-72-82
DATE:		MODEL NO.

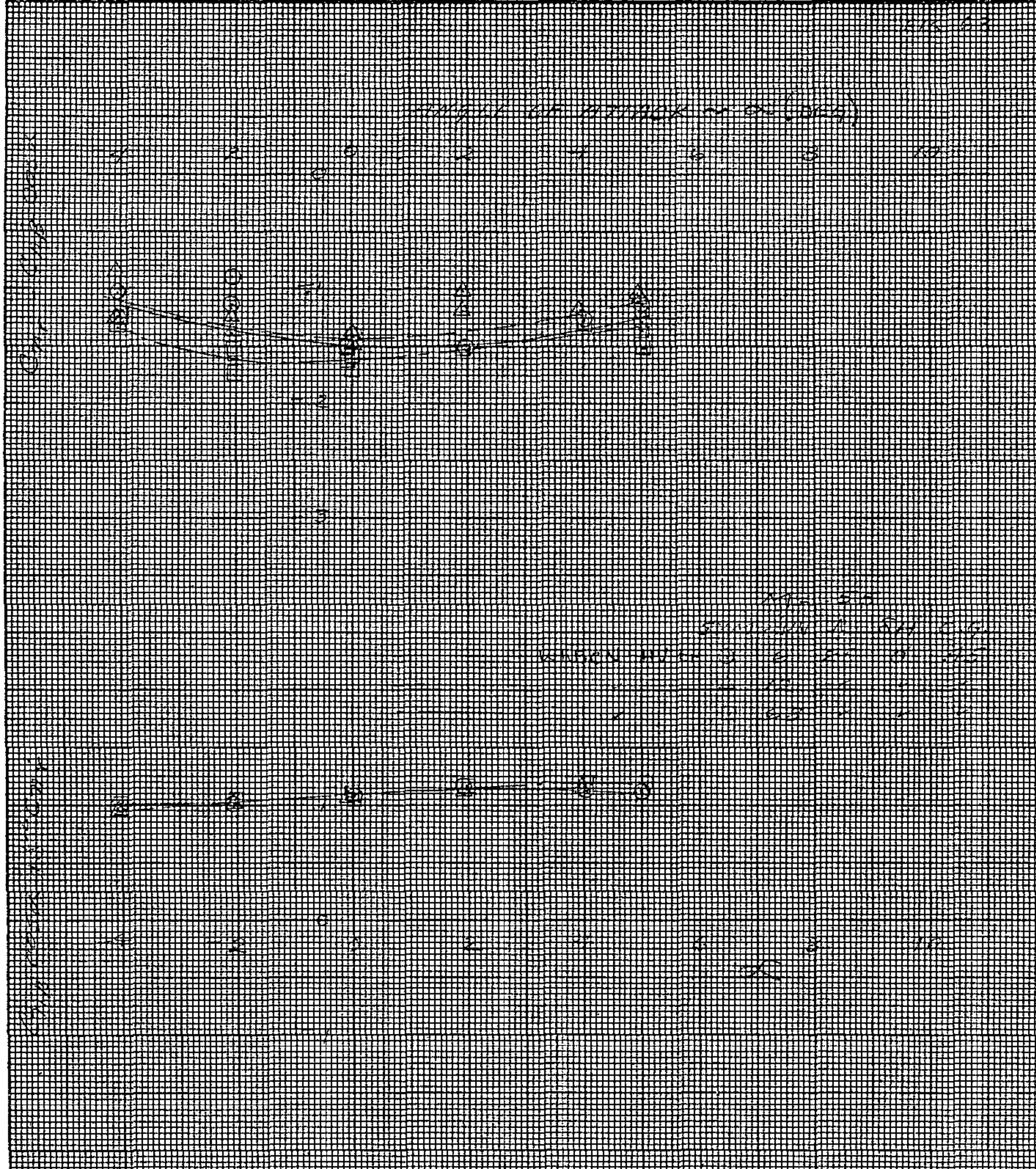

DAMPING IN YAW DERIVATIVES
DATA PRELIMINARY
A-25
MACH NO. 0.65
TEST NO. 934

FORM 1021-S REV 10-70

PREPARED BY:	Los Angeles Division North American Rockwell	PAGE NO 90 OF 145
CHECKED BY:		REPORT NO NA-72-82
DATE:		MODEL NO

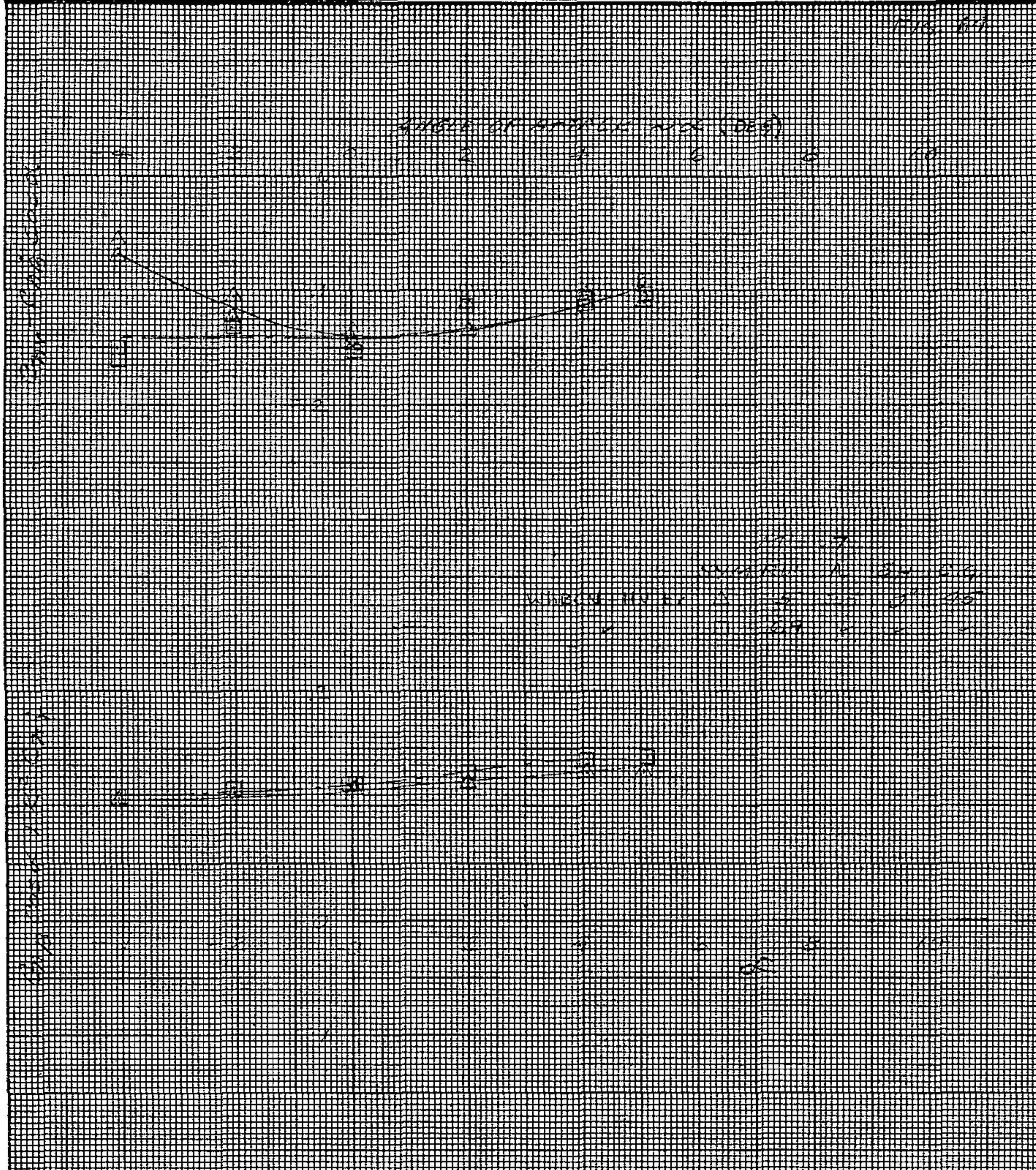

DAMPING IN YAW DERIVATIVE

DATA REPEATABILITY

$\Lambda = 25°$

MACH NO = 0.7

TEST NO 439

FORM 1021-S REV 10-70

PREPARED BY:	Los Angeles Division North American Rockwell	PAGE NO. 91 OF 145
CHECKED BY:		REPORT NO NA-72-82
DATE:		MODEL NO.

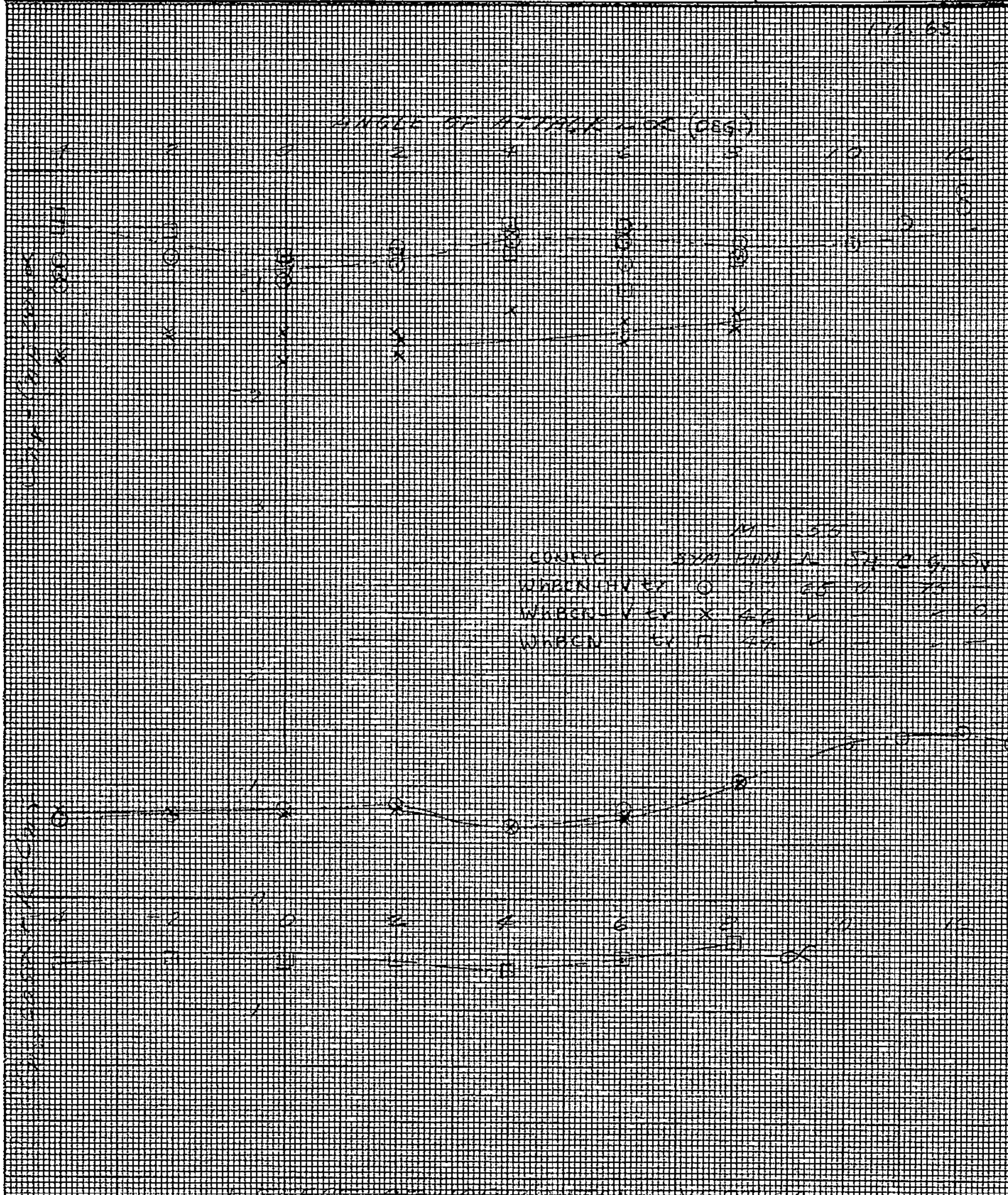

TEST NO. 934

FORM 1021-S REV. 10-70

PREPARED BY:	Los Angeles Division North American Rockwell	PAGE NO 92 OF 145
CHECKED BY:		REPORT NO. NA-72-82
DATE:		MODEL NO

FIG. 66

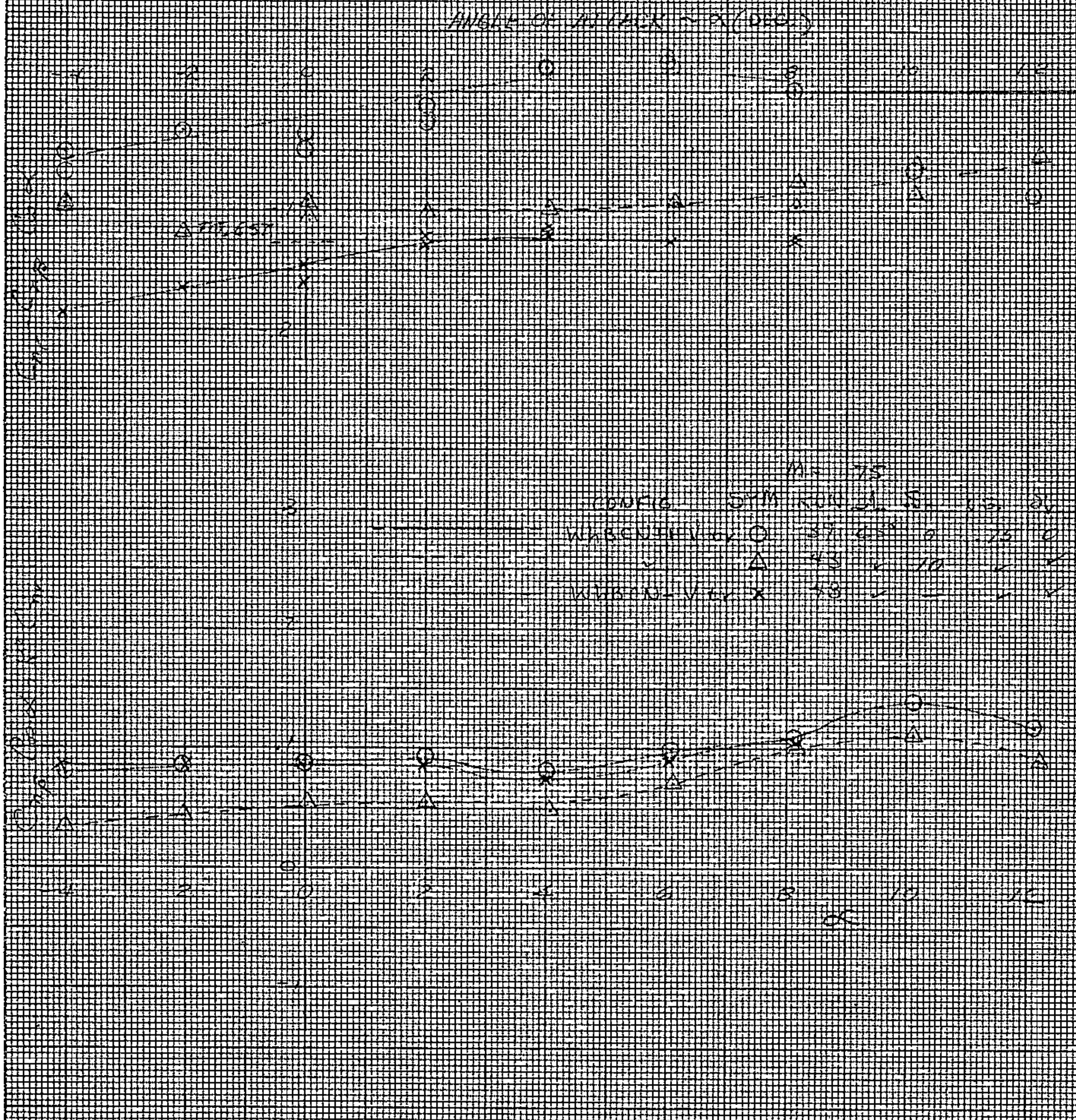

EFFECT OF HORIZONTAL & VERTICAL TAILS
ON DAMPING IN YAW DERIVATIVES

Λ = 65° MACH = 0.75

TEST NO. 934

FORM 1021-S REV. 10-70

PREPARED BY:	Los Angeles Division North American Rockwell	PAGE NO. 93 OF 145
CHECKED BY:		REPORT NO NA-72-82
DATE:		MODEL NO.

FIG. 67

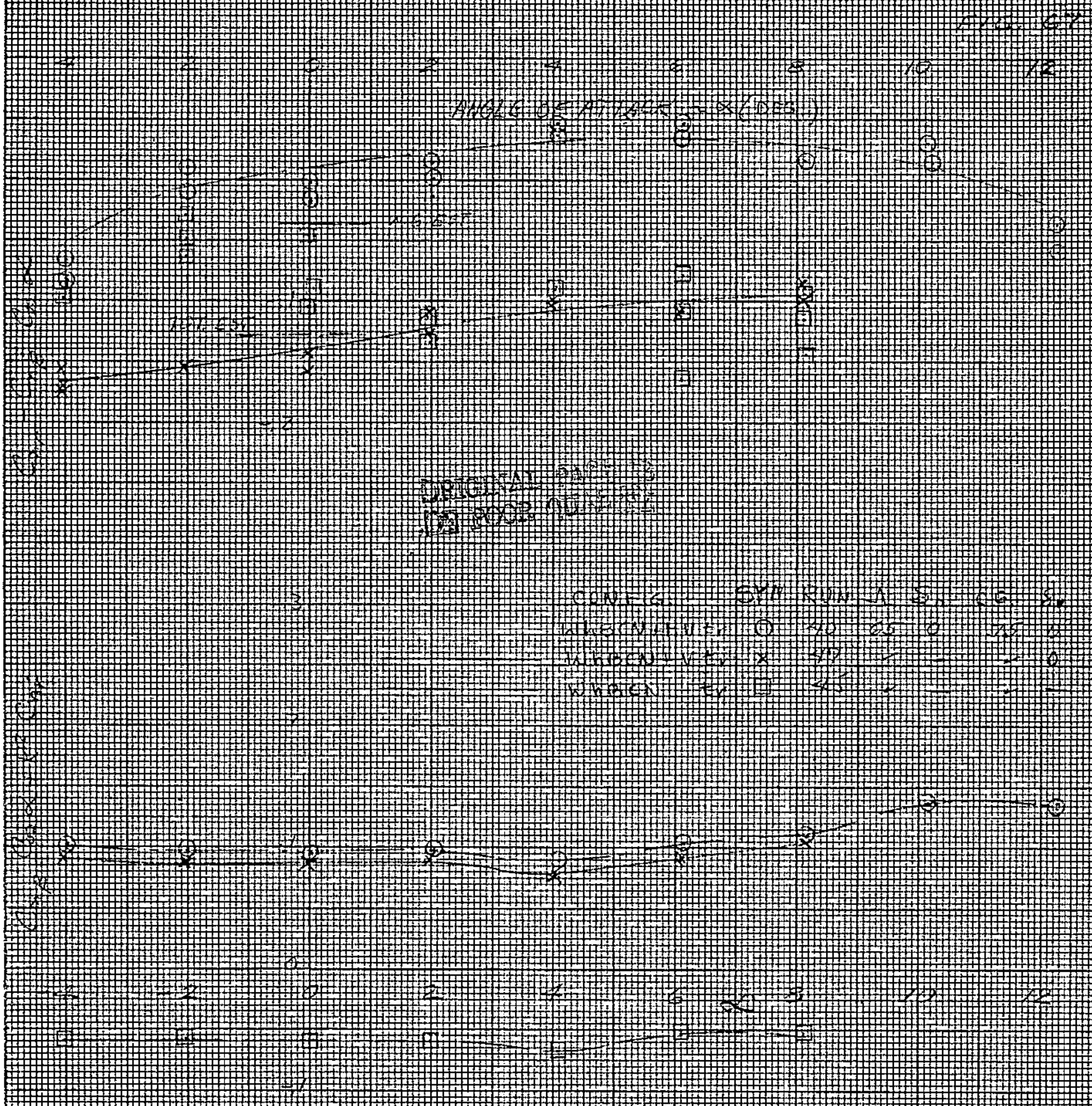

EFFECT OF HORIZONTAL AND VERTICAL TAILS
ON DAMPING IN YAW DERIVATIVES

Λ = 65° MACH NO. = 0.80

TEST NO. 934

FORM 1021-5 REV. 10-70

PREPARED BY:	Los Angeles Division North American Rockwell	PAGE NO. 94 OF 145
CHECKED BY:		REPORT NO. NA-72-82
DATE:		MODEL NO

FIG 68

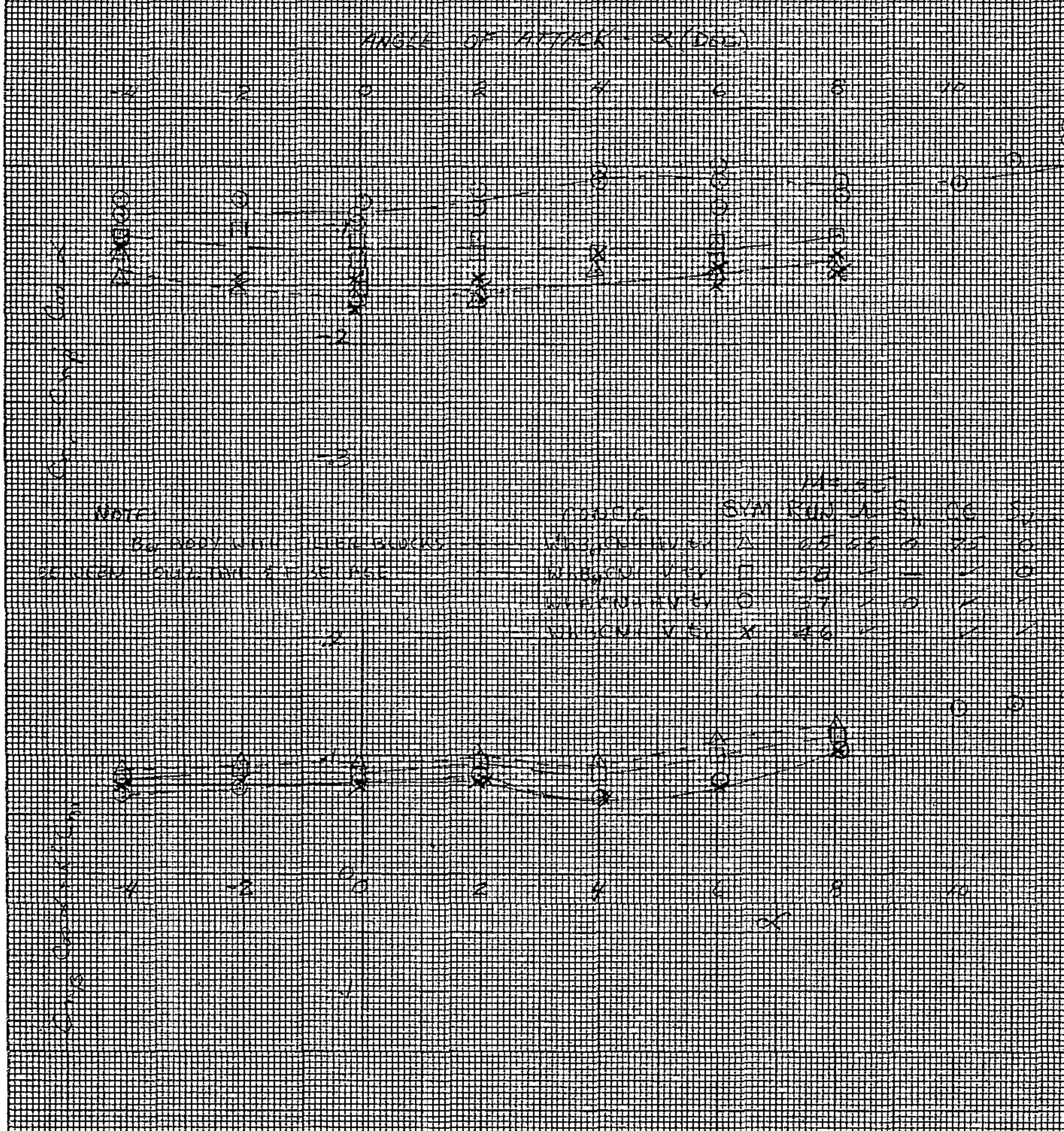

EFFECT OF FILLER BLOCKS ON
DAMPING IN YAW DERIVATIVES

M = 0.35 Λ = 65°

TEST NO. 934

FIG. 69

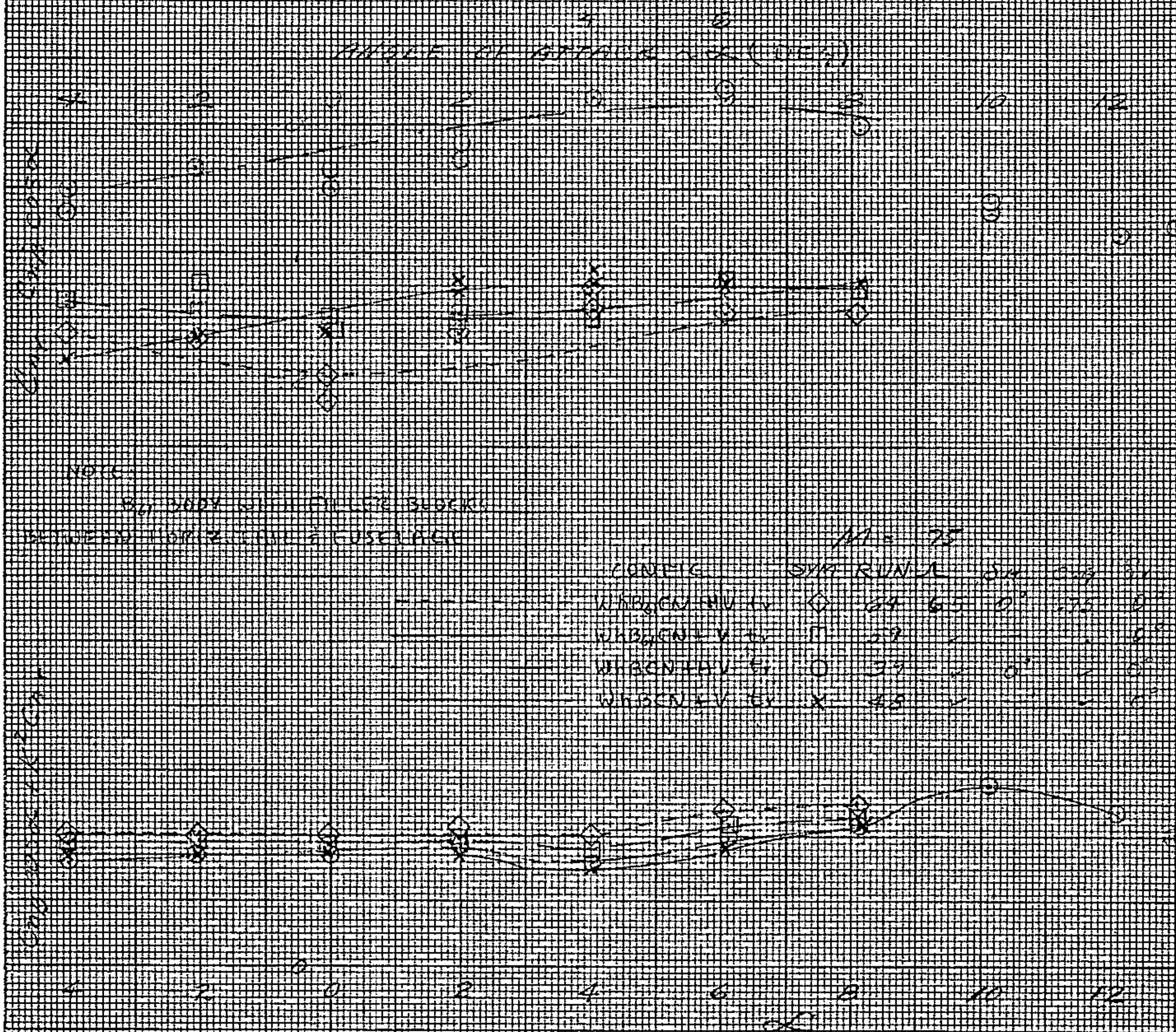

EFFECT OF FILLER BLOCKS ON
DAMPING IN YAW DERIVATIVES
Λ=45° M=0.75

TEST NO. 934

FORM 1021-S REV 10-70

PREPARED BY:	Los Angeles Division North-American Rockwell	PAGE NO 96 OF 145
CHECKED BY:		REPORT NO NA-72-82
DATE:		MODEL NO.

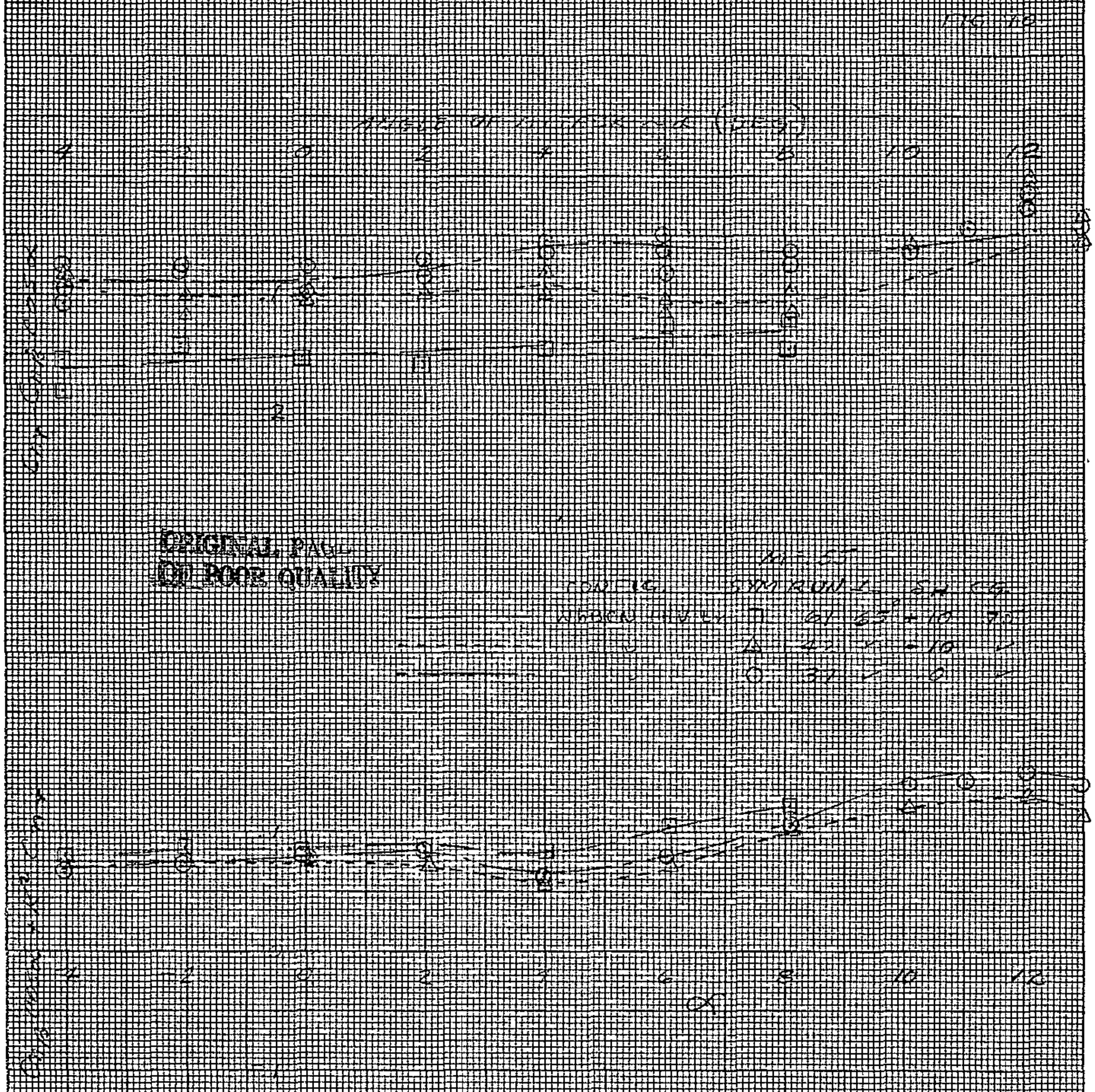

EFFECT OF HORIZONTAL TAIL DEFLECTION
ON DAMPING IN YAW DERIVATIVES
$\alpha = 65°$ M 0.55
TEST NO. 934

FIG. 71

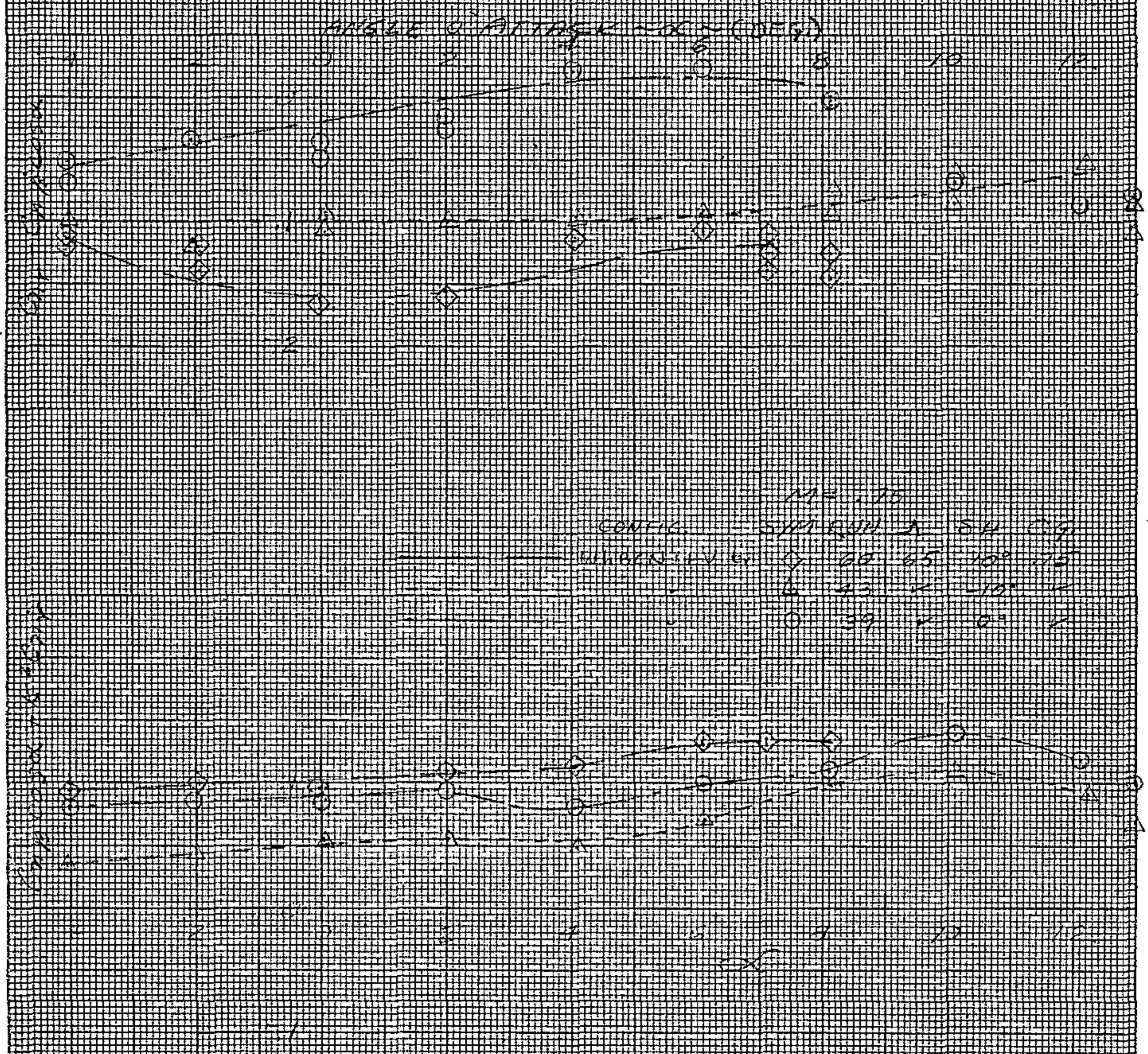

EFFECT OF HORIZONTAL TAIL DEFLECTION
ON DAMPING IN YAW DERIVATIVES
Λ = 65° M = 0.75

TEST NR 934

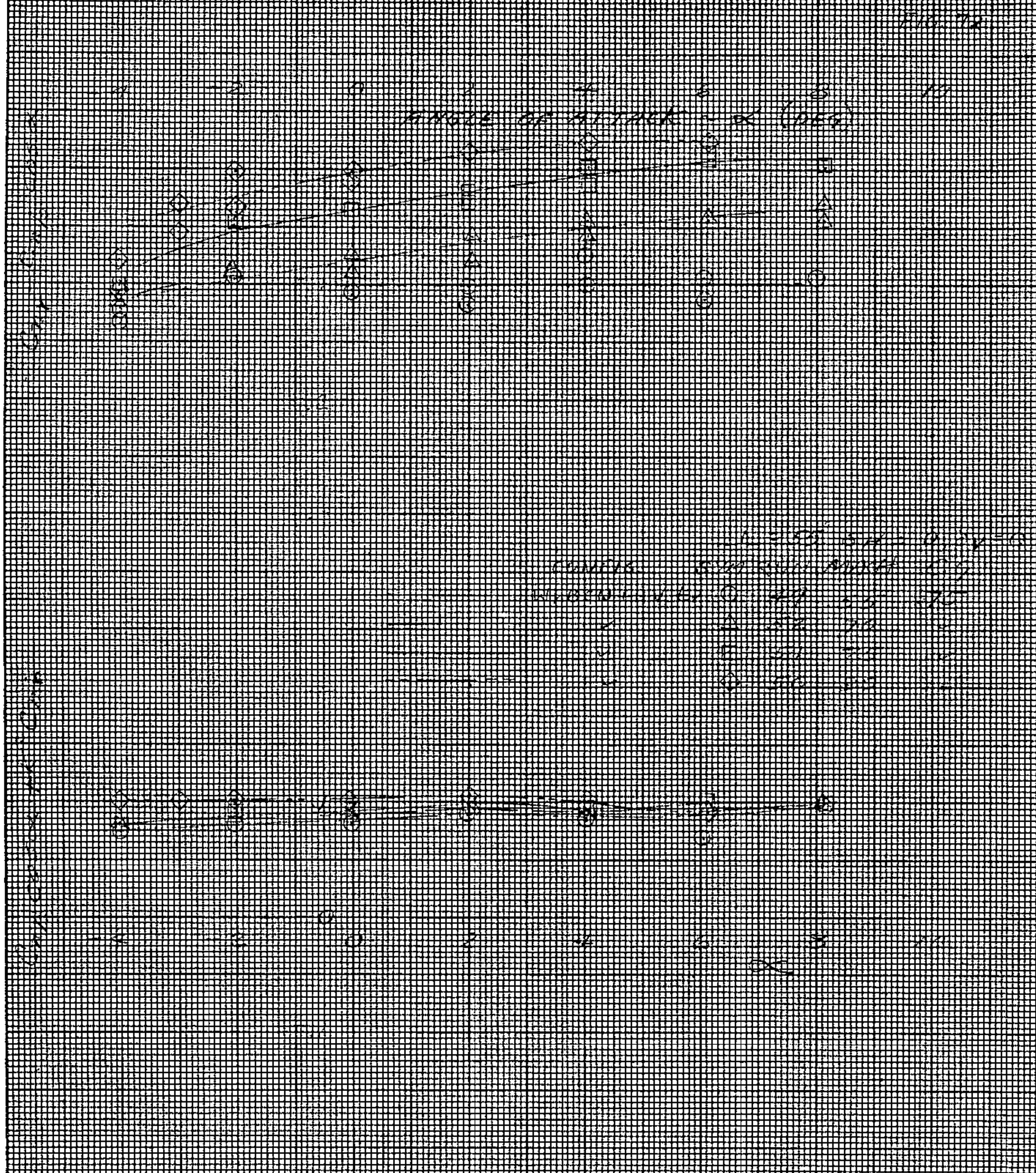

EFFECT OF MACH NUMBER
ON DAMPING IN YAW DERIVATIVES
Λ = 56°

TEST NO. 9??

FORM 1021-S REV. 10-70

PREPARED BY:	Los Angeles Division North American Rockwell	PAGE NO 99 OF 145
CHECKED BY:		REPORT NO NA-72-82
DATE:		MODEL NO.

FIG. 75

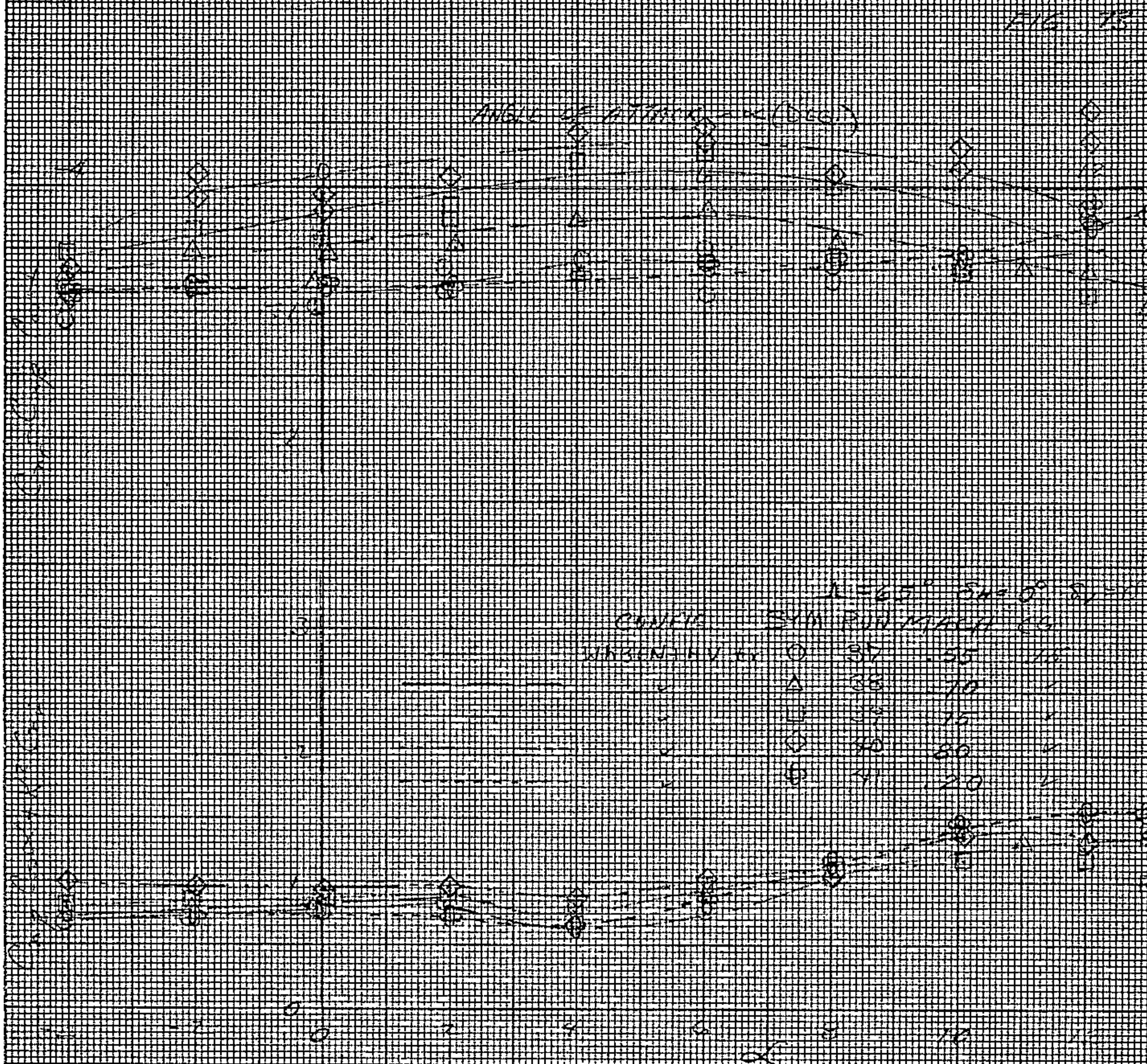

EFFECT OF MACH NUMBER
ON DAMPING IN YAW DERIVATIVES
Λ = 65°

TEST NO. 334

FORM 1021-S REV 10-70

PREPARED BY:	Los Angeles Division North American Rockwell	PAGE NO. 100 OF 145
CHECKED BY:		REPORT NO NA-72-82
DATE:		MODEL NO.

FIG 74

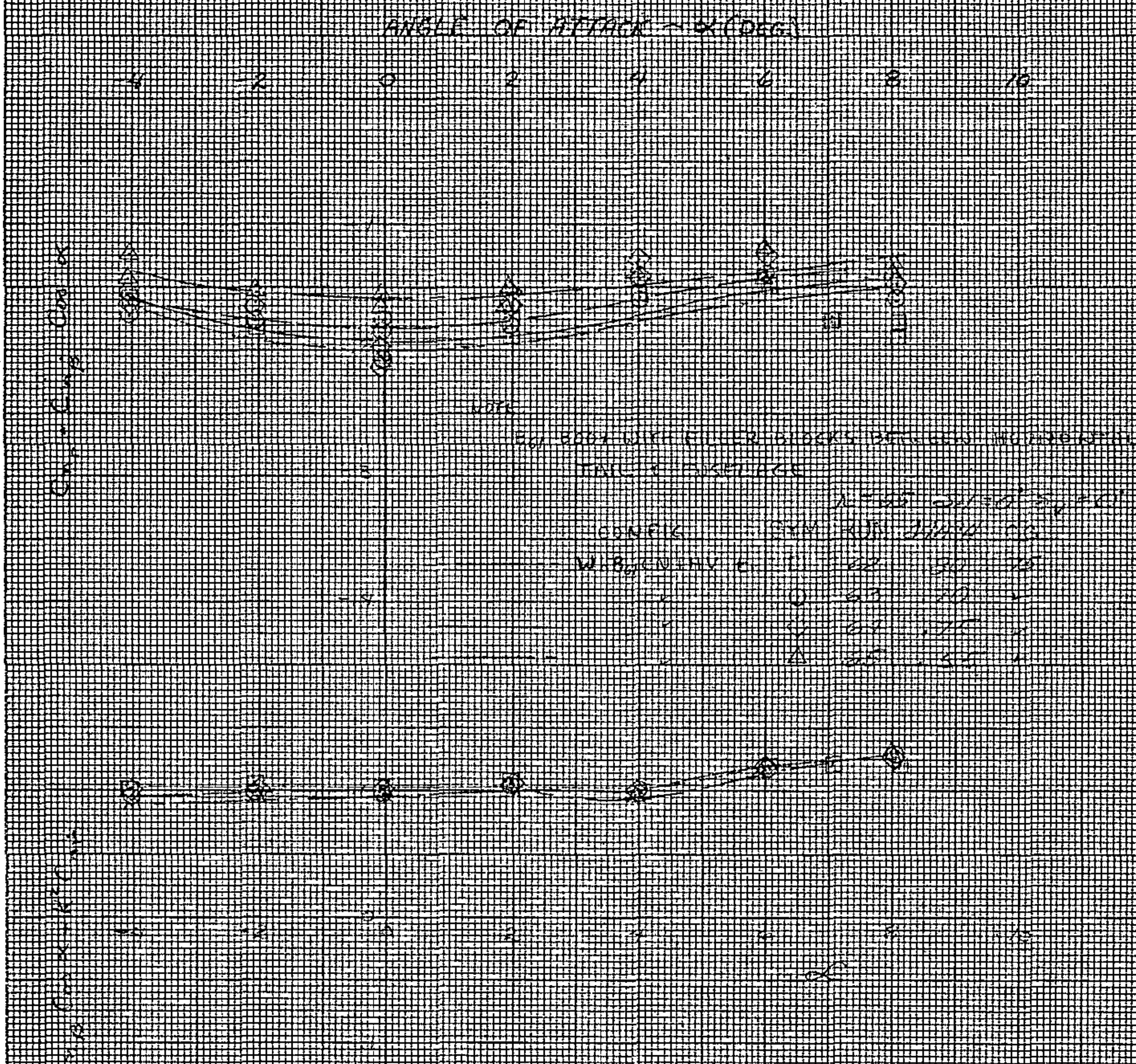

EFFECT OF MACH NUMBER ON DAMPING IN YAW DERIVATIVES

Λ = 25°

TEST NO. 934

FIG. 75

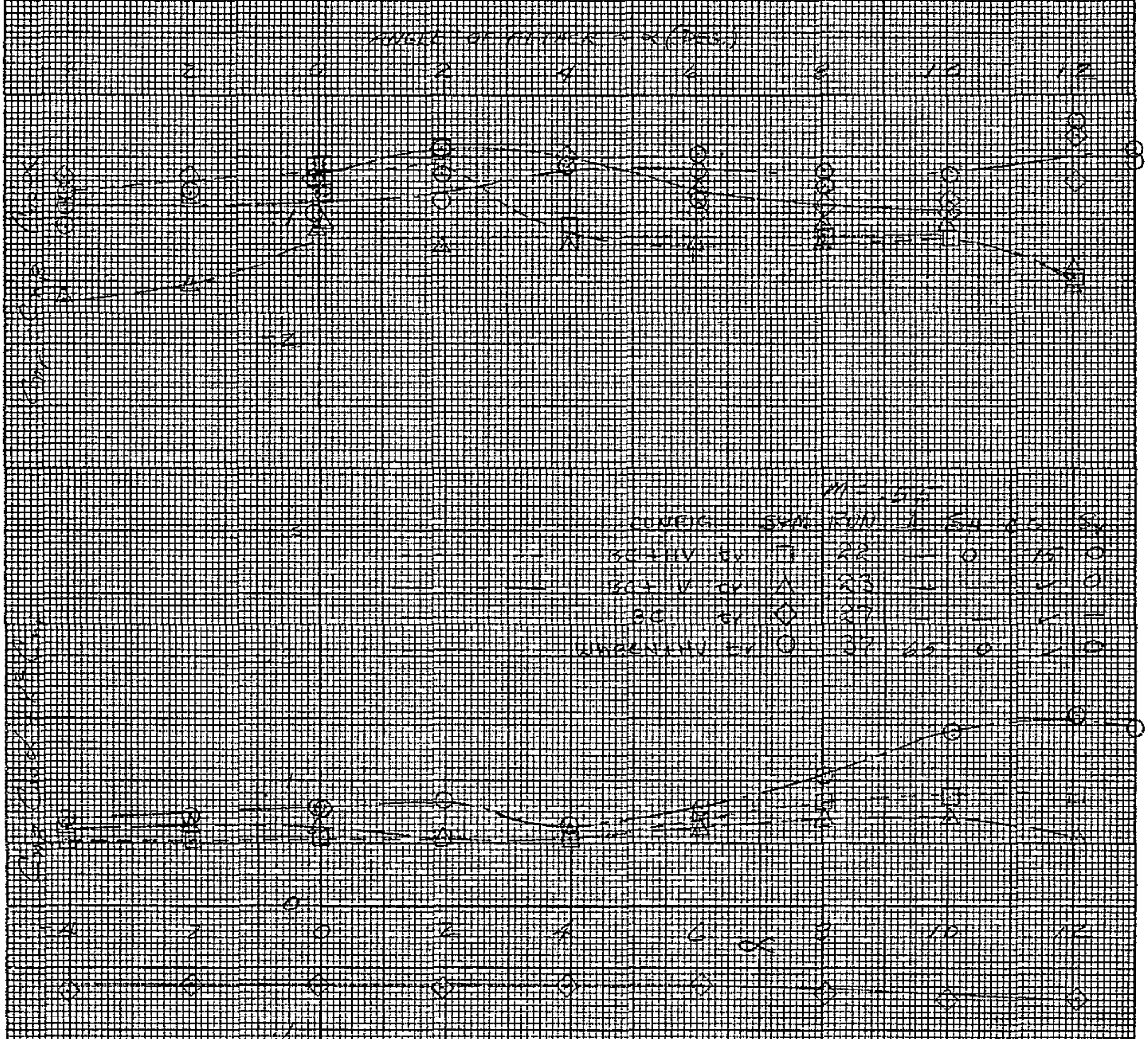

COMPONENT BUILDUP

MACH NO = 0.55

TEST NO. 934

FORM 1021-S REV. 10-70

PREPARED BY:	Los Angeles Division North American Rockwell	PAGE NO 102 OF 145
CHECKED BY:		REPORT NO NA-72-82
DATE:		MODEL NO.

FIG. 76

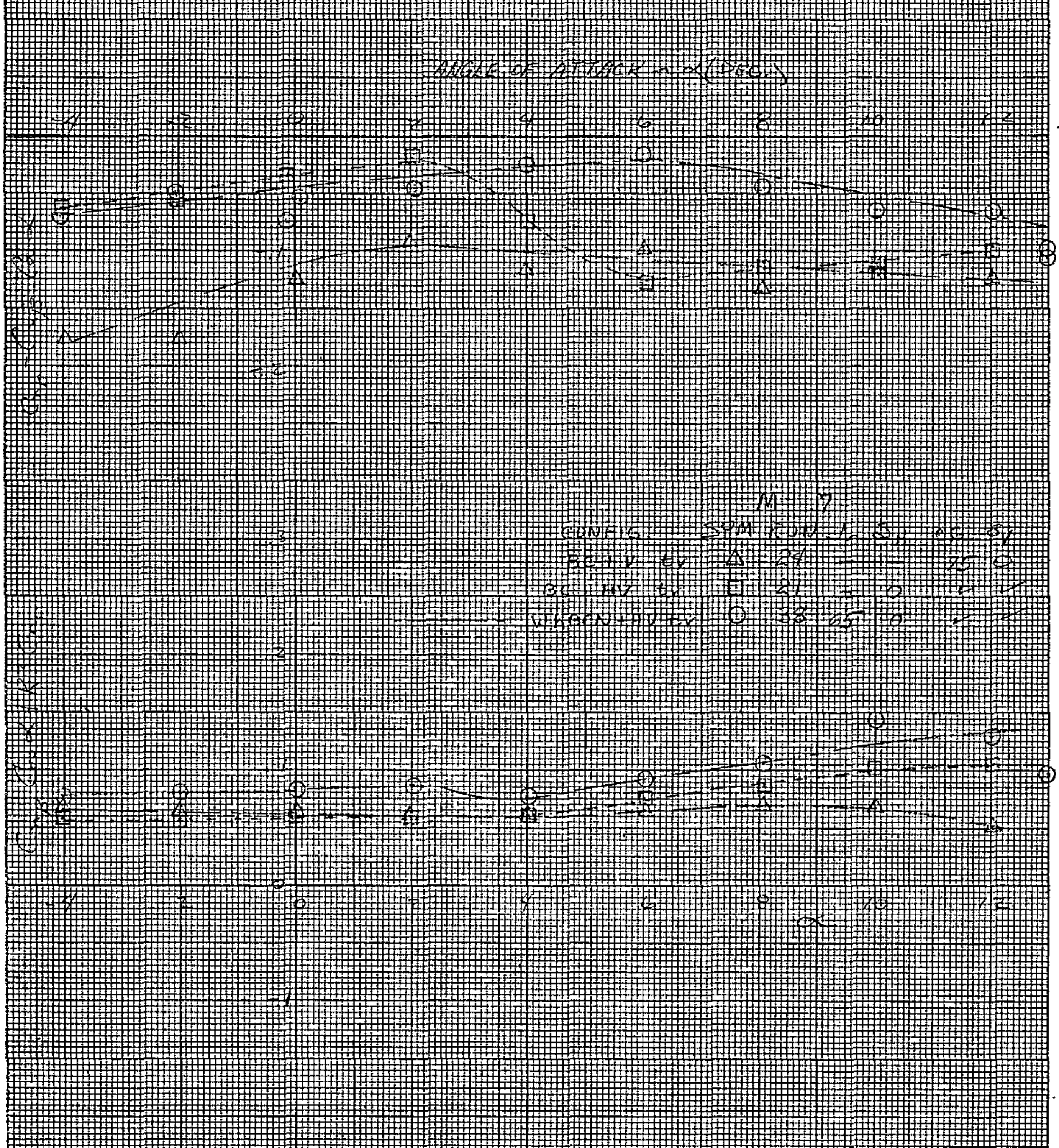

COMPONENT BUILD-UP

$C_L - C_{m}$

MACH NO = 0.2

TEST NO. 934

FORM 1021-S REV 10-70

PREPARED BY:	Los Angeles Division North American Rockwell	PAGE NO. 103 OF 145
CHECKED BY:		REPORT NO NA-72-82
DATE:		MODEL NO.

FIG. 77

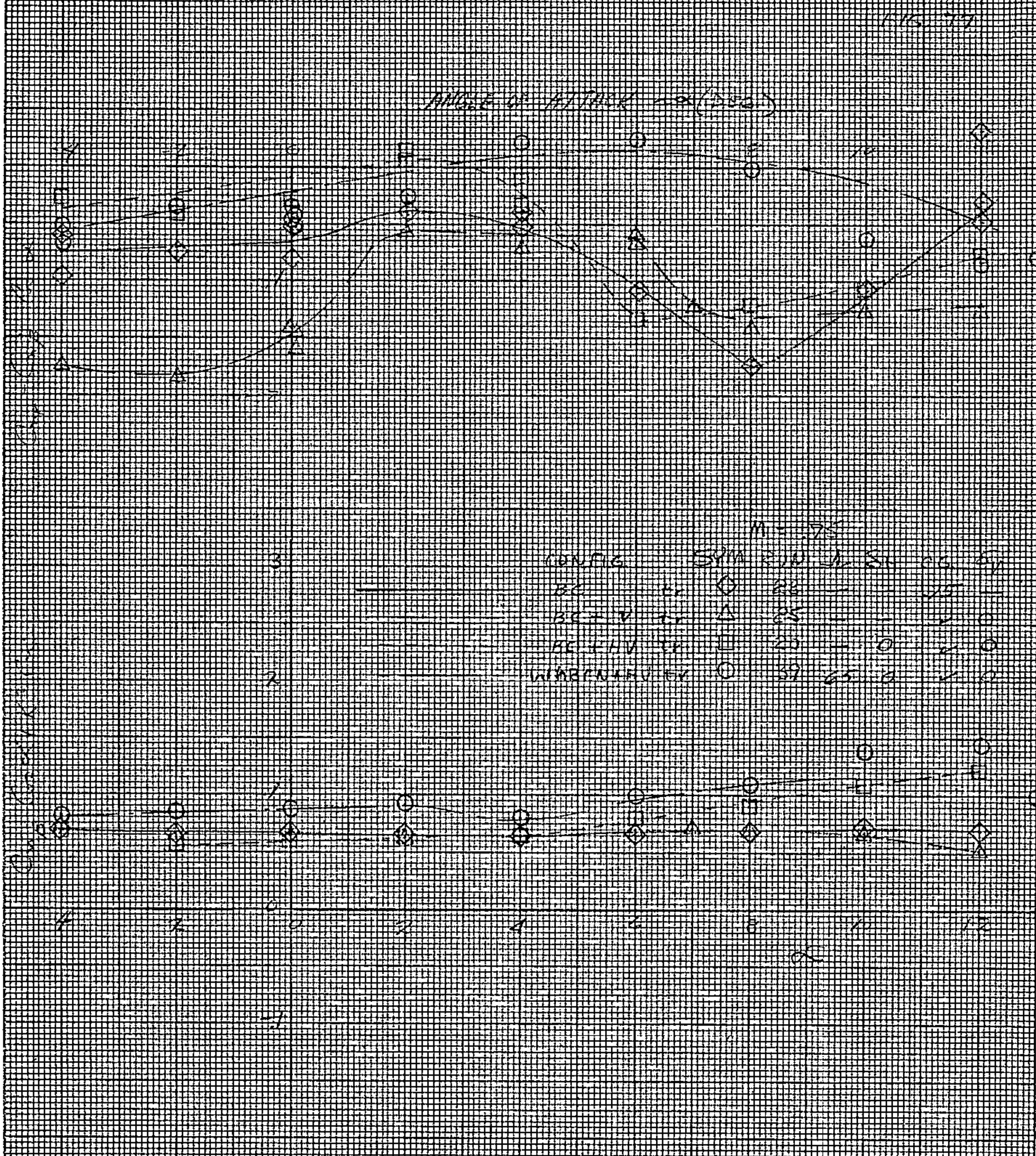

COMPONENT BUILD-UP

Λ = 65°

MACH NO = 0.75

TEST NA 734

FIG. 78

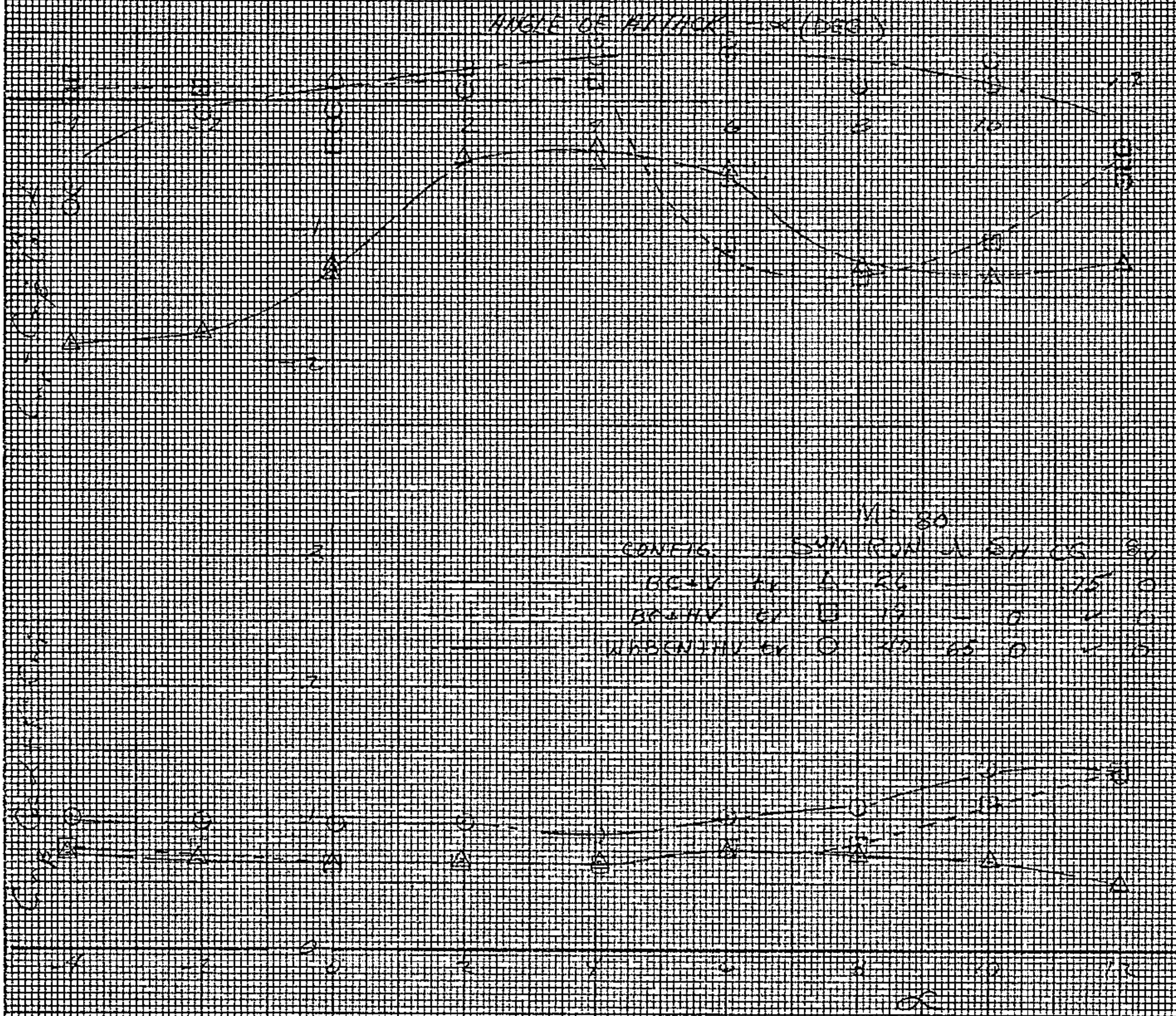

COMPONENT BUILD UP
Λ = 65°

MACH NO. = 0.80

TEST NO. 734

FORM 1021-S REV 10-70

PREPARED BY:	Los Angeles Division North American Rockwell	PAGE NO. 105 OF 145
CHECKED BY:		REPORT NO. NA-72-82
DATE:		MODEL NO.

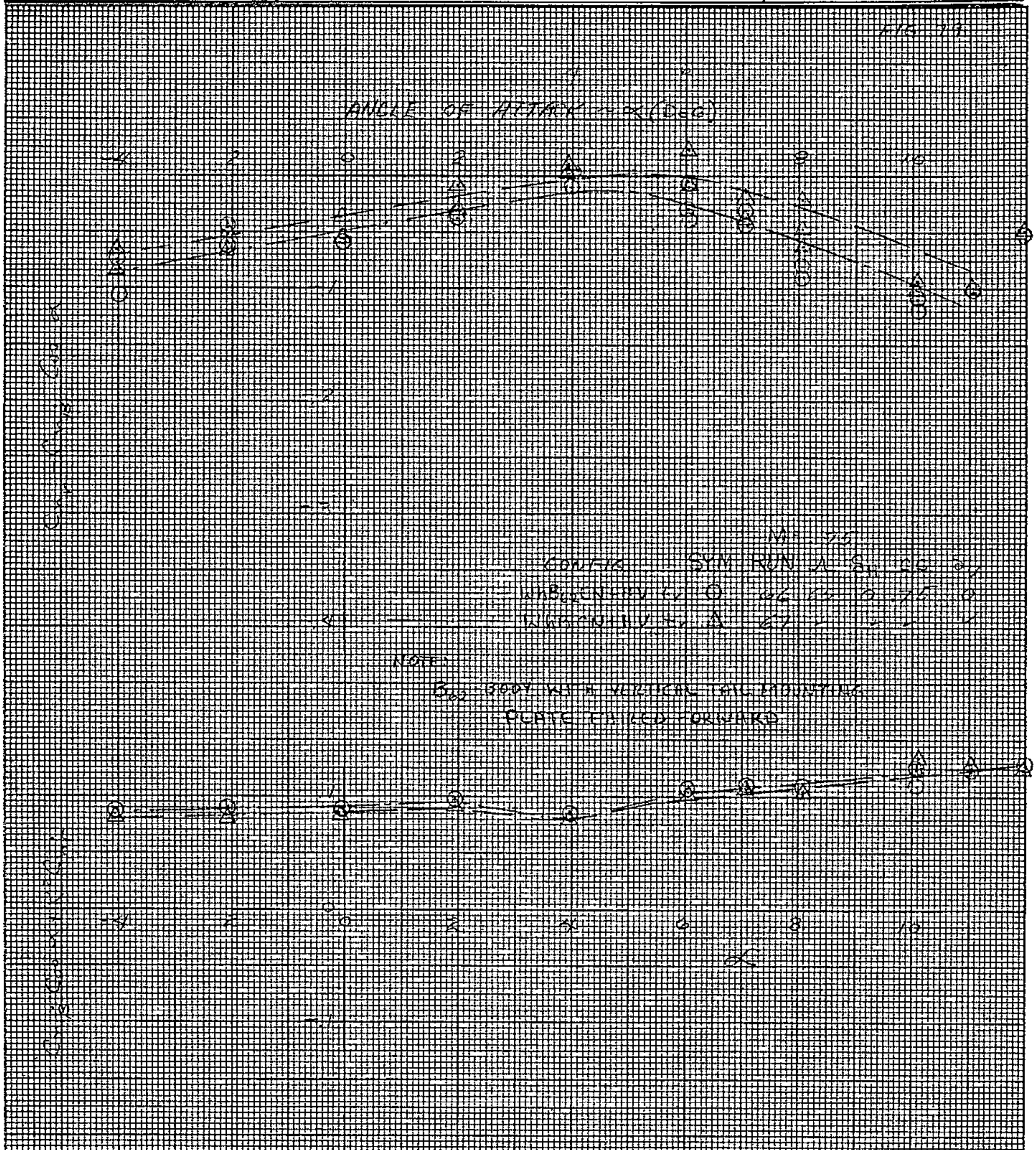

COMPARISON OF BODIES

MACH NO. = 0.75

TEST NO. 934

FIG 20

EFFECT OF SWEEP & STEEL ROD ON THE
ROLLING & YAWING DERIVATIVES

MACH NO. = 0.55

TEST NO. 954

FORM 1021-S REV. 10-70

PREPARED BY:	Los Angeles Division North American Rockwell	PAGE NO. 107 OF 145
CHECKED BY:		REPORT NO NA-72-82
DATE:		MODEL NO

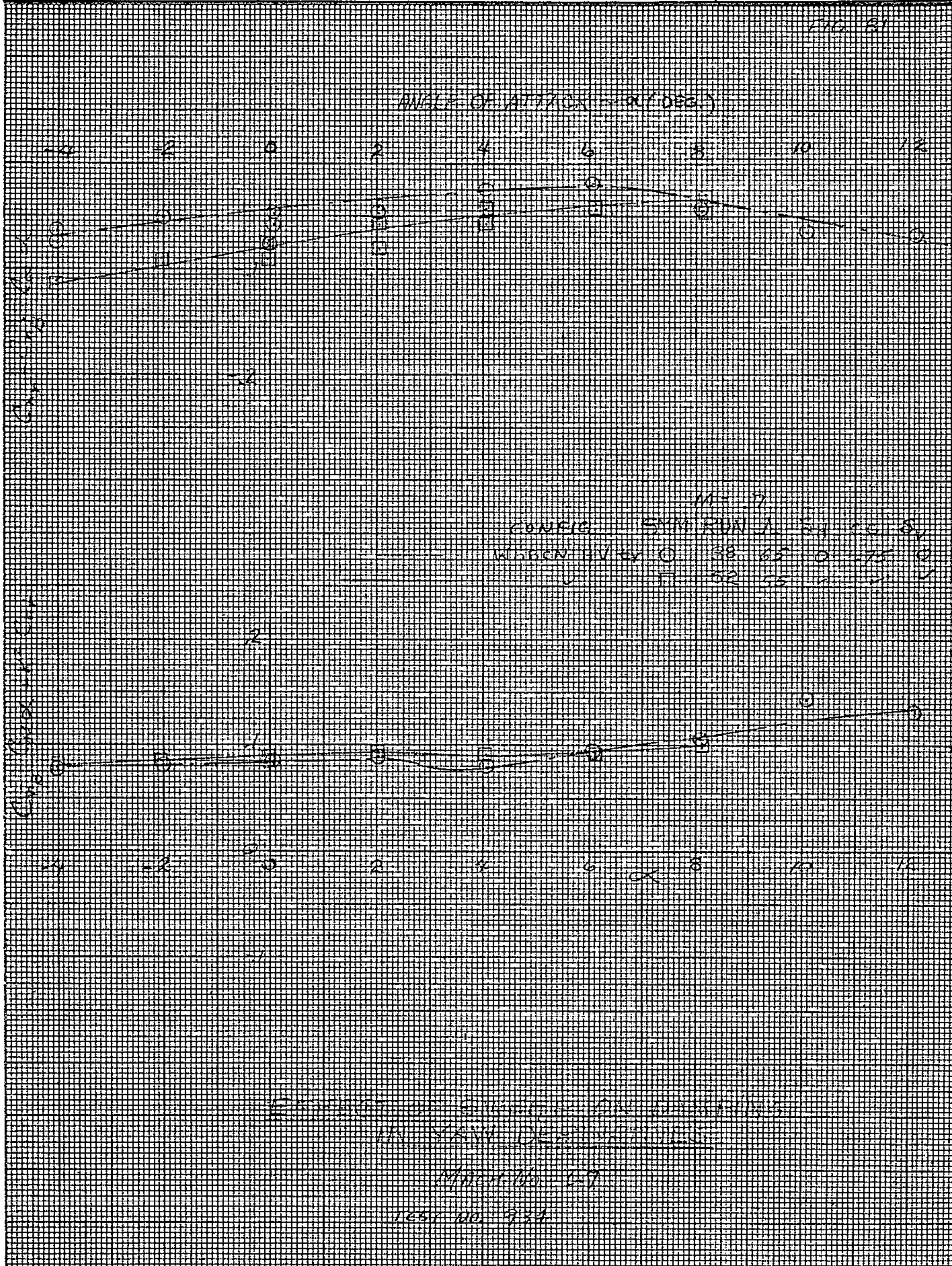

FORM 1021-S REV 10-70

PREPARED BY:	Los Angeles Division North American Rockwell	PAGE NO. 108 OF 145
CHECKED BY:		REPORT NO NA-72-82
DATE:		MODEL NO.

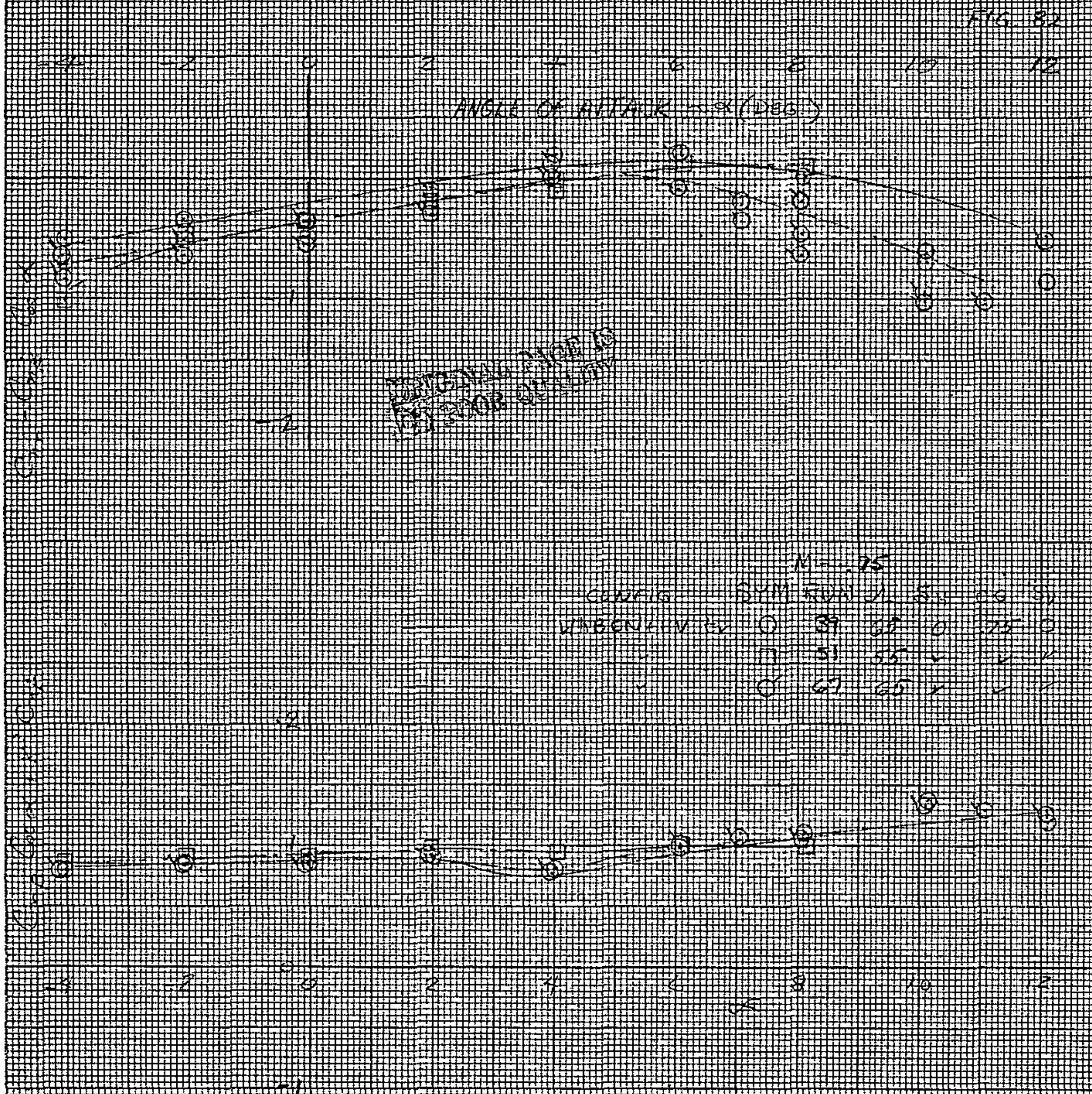

EFFECT OF SWEEP
ON DAMPING IN YAW DERIVATIVES

MACH NO = 0.75

TEST NO. 934

FORM 1021-S REV 10-70

PREPARED BY:	Los Angeles Division North American Rockwell	PAGE NO. 109 OF 145
CHECKED BY:		REPORT NO. NA-72-82
DATE:		MODEL NO.

FIG. 83

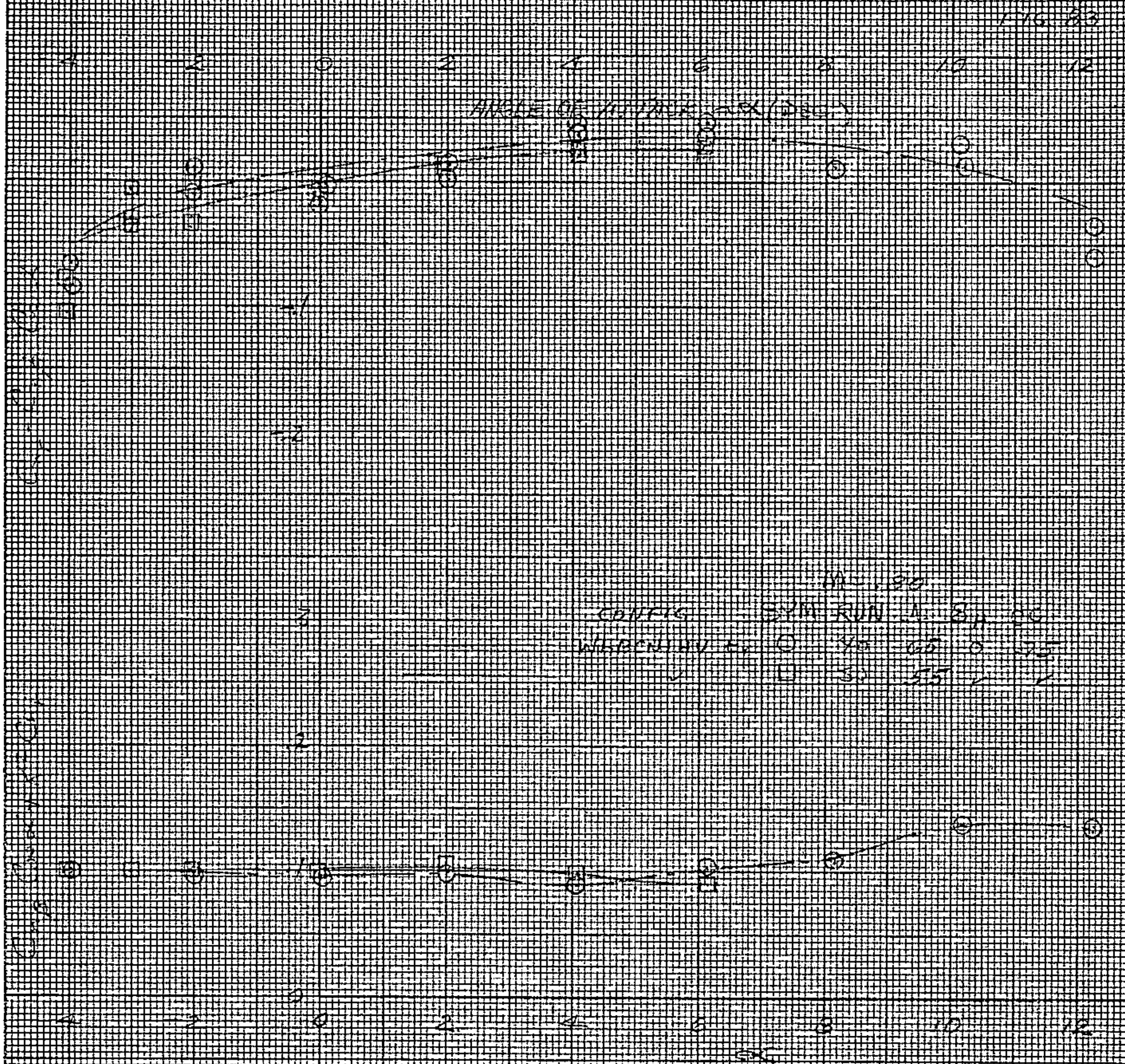

EFFECT OF SWEEP
ON DAMPING IN YAW DERIVATIVES

MACH NO. = .80

TEST NO. 934

FORM 1021-5 REV 10-70

PREPARED BY:	Los Angeles Division North American Rockwell	PAGE NO. 110 OF 145
CHECKED BY:		REPORT NO. NA-72-82
DATE:		MODEL NO.

FIG. 84

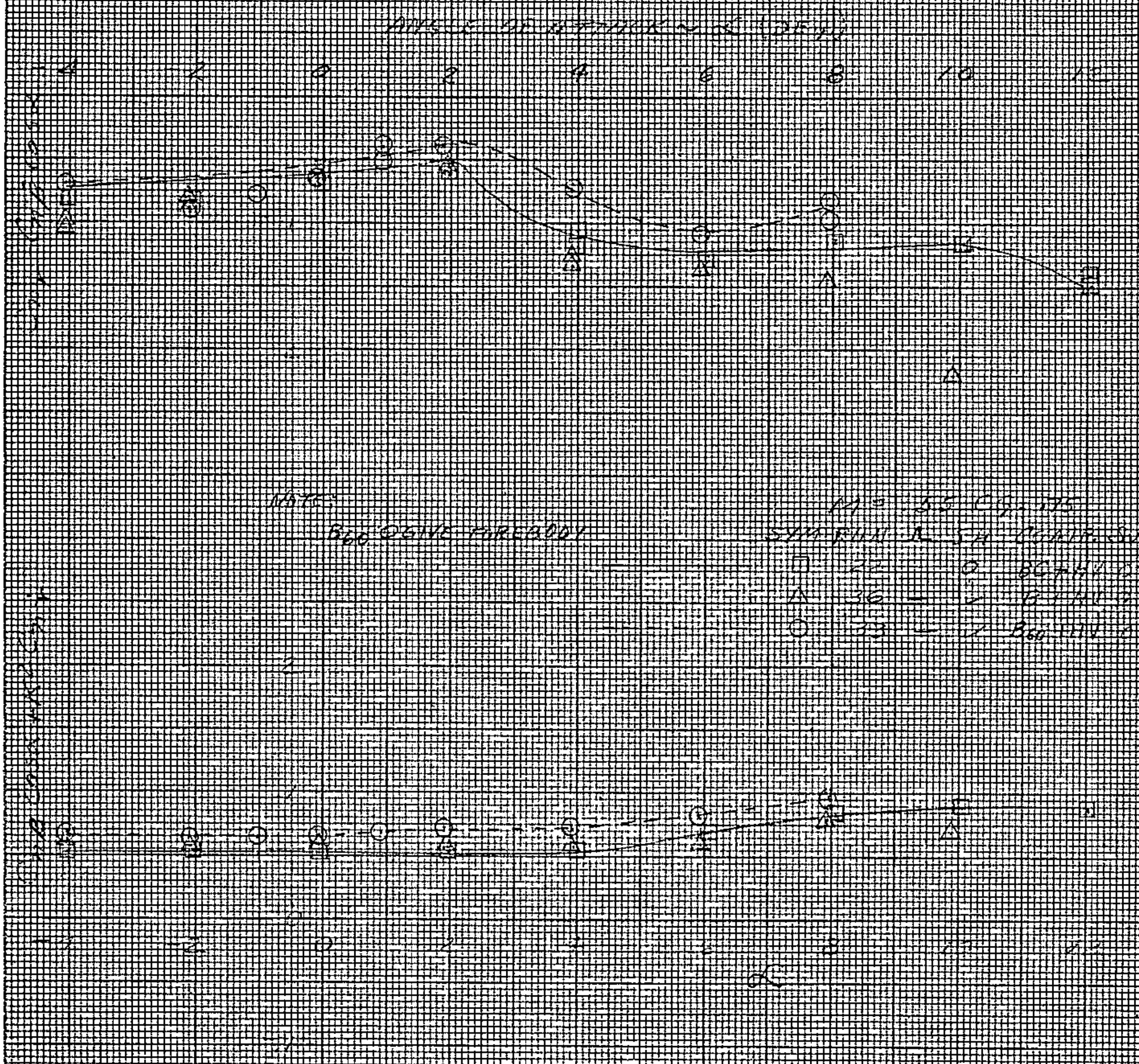

COMPARISON OF VARIOUS BODIES

MACH NO = 0.55

TEST NO. 932

FIG. 85

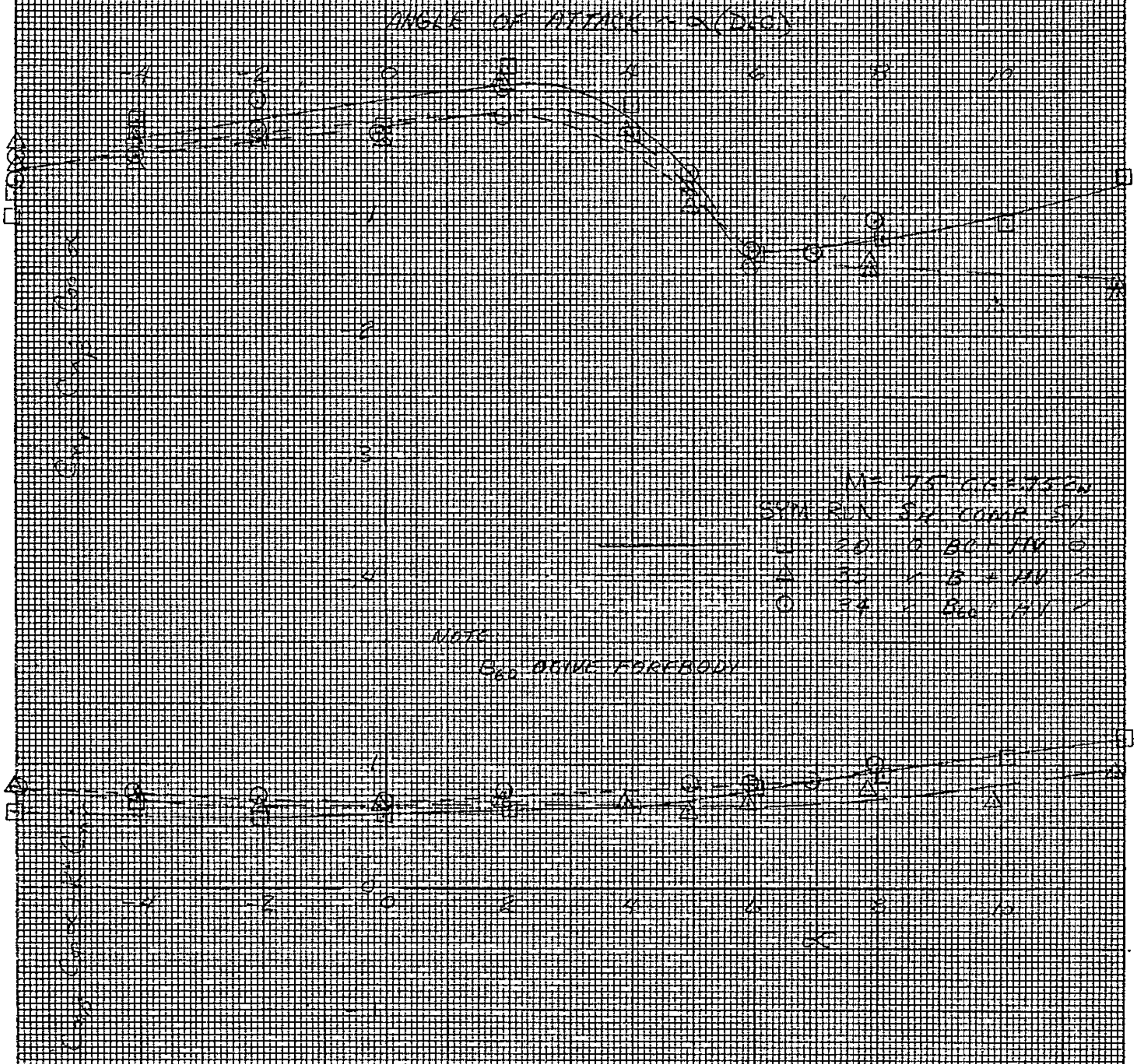

COMPARISON OF [illegible]

MACH NO = 0.75

TEST NO. 934

FORM 1021-S REV. 10-70

PREPARED BY:	Los Angeles Division North American Rockwell	PAGE NO. 112 OF 145
CHECKED BY:		REPORT NO NA-72-82
DATE:		MODEL NO.

FIG. 86

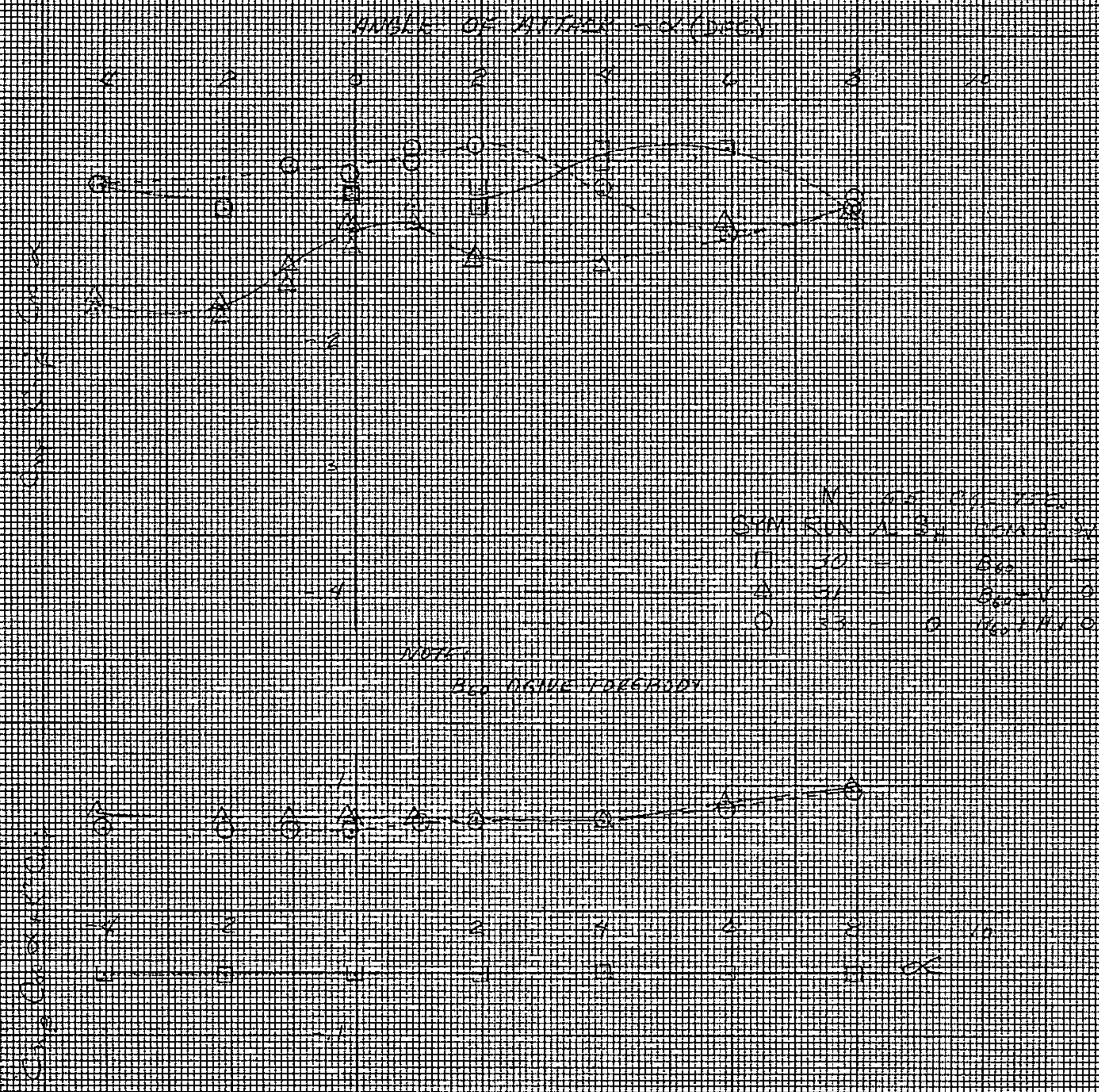

COMPONENT BUILDUP

MACH NO. = 0.55

TEST NO. 934

FIG. 57

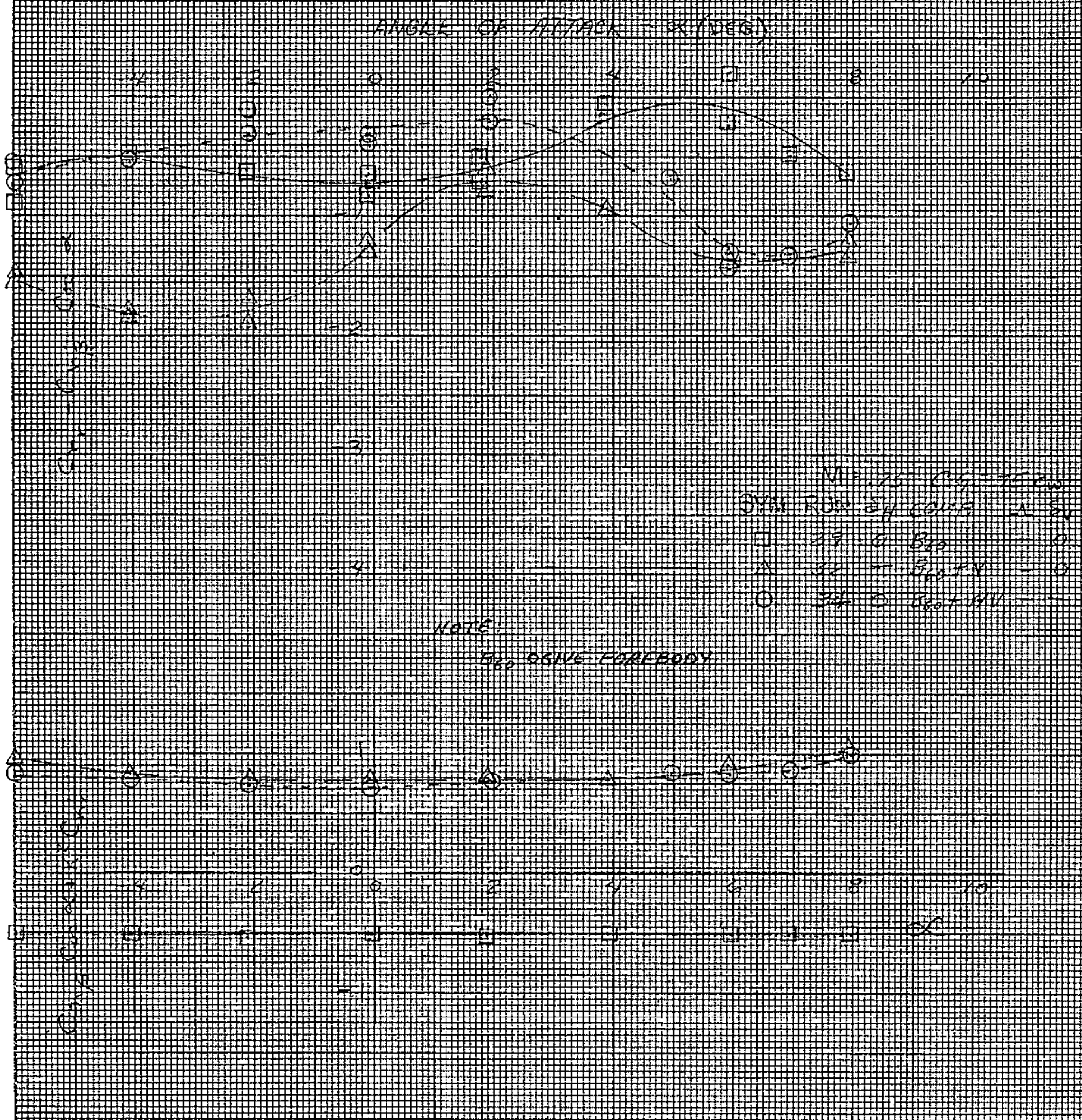

COMPONENT BUILD-UP

MACH NO = 0.75

TEST NO. 934

FORM 1021-S REV 10-70

PREPARED BY:	Los Angeles Division North American Rockwell	PAGE NO 114 OF 145
CHECKED BY:		REPORT NO NA-72-82
DATE:		MODEL NO.

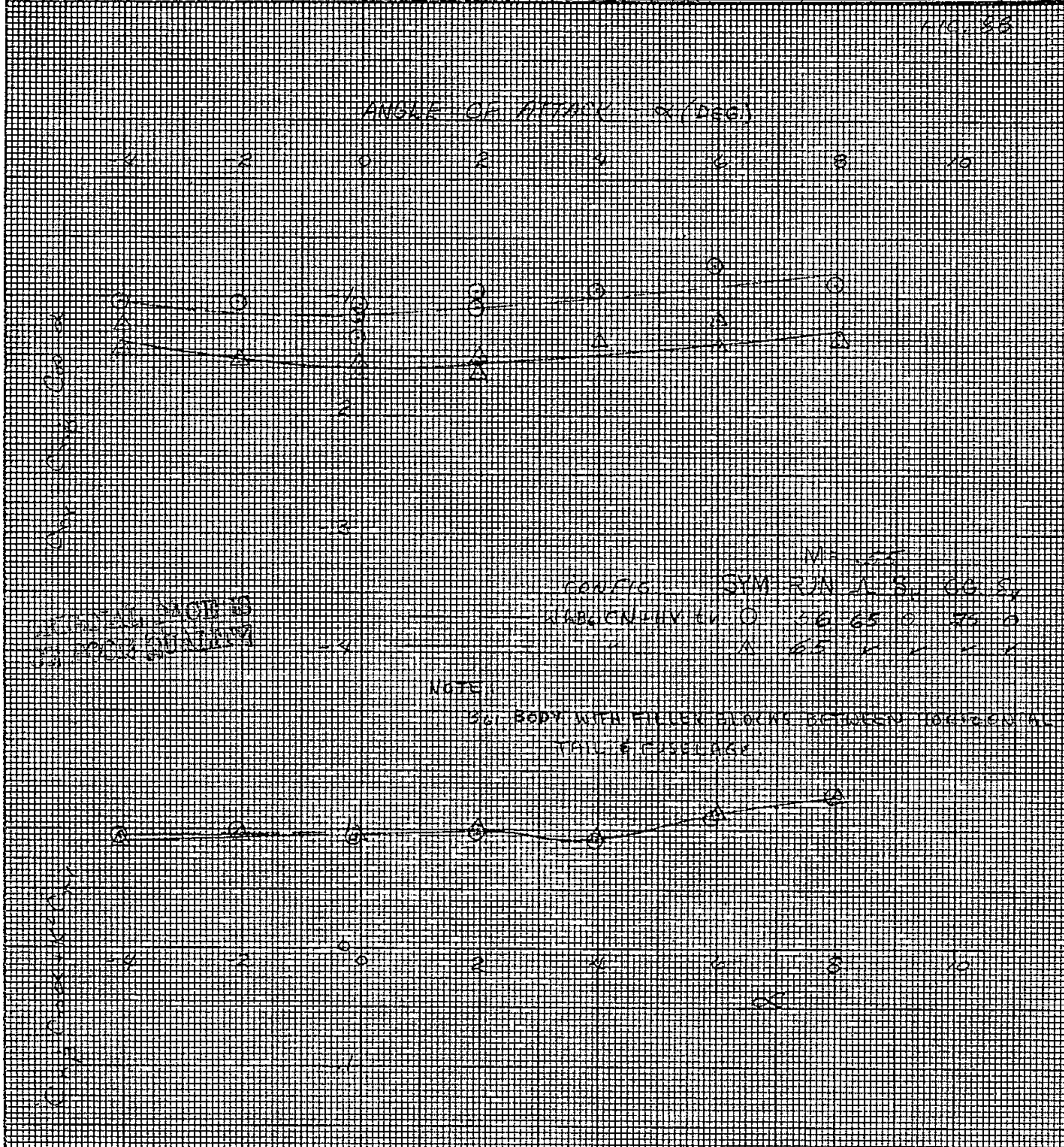

DATA REPEATABILITY

Λ = 65°

MACH NO = 0.55

FORM 1021-S REV. 10-70

PREPARED BY:	Los Angeles Division North American Rockwell	PAGE NO. 115 OF 145
CHECKED BY:		REPORT NO NA-72-82
DATE:		MODEL NO.

FIG. 83

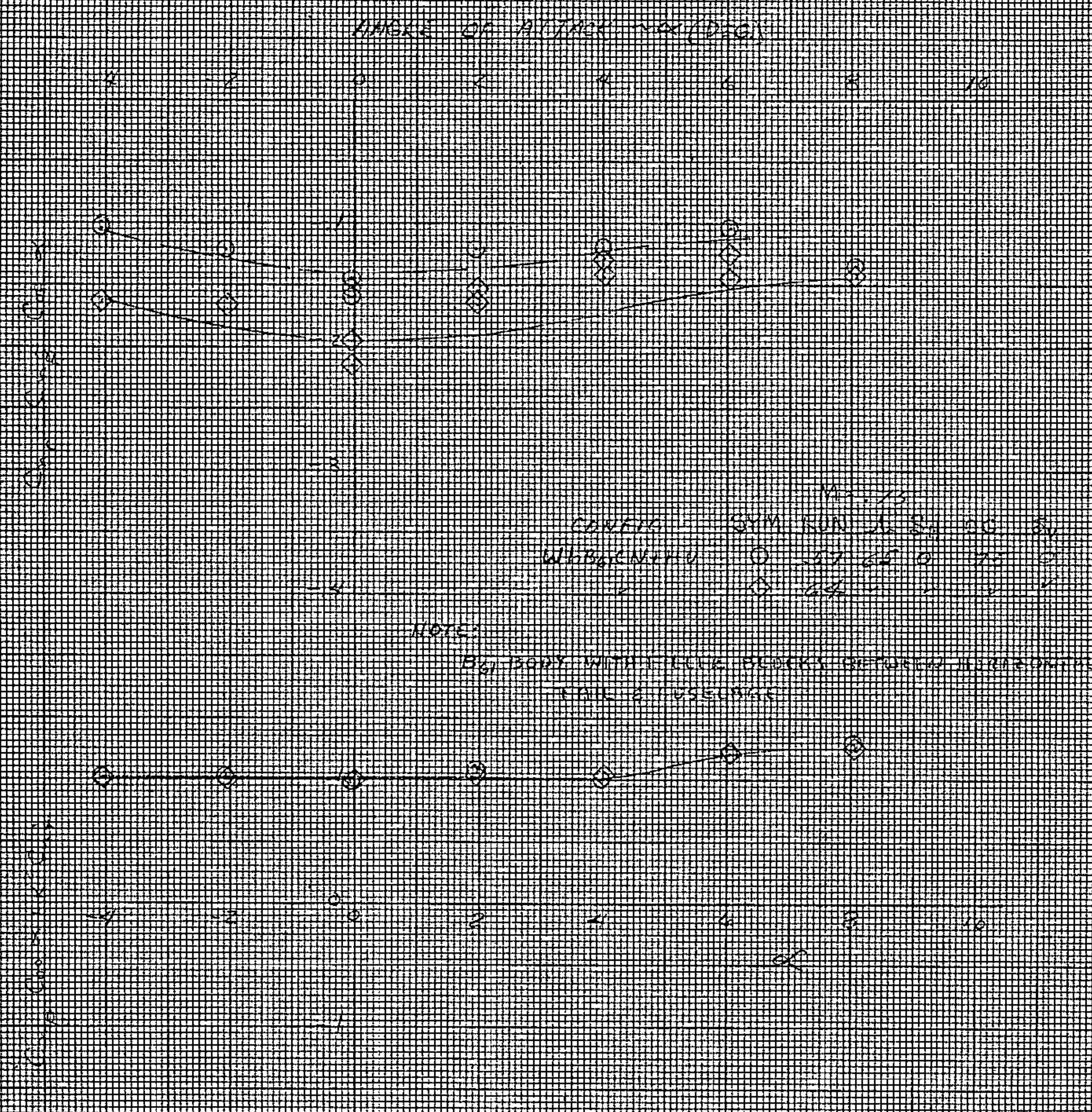

DATA REPEATABILITY

Λ = 65°

MACH NO. = 0.75

TEST NO. 934

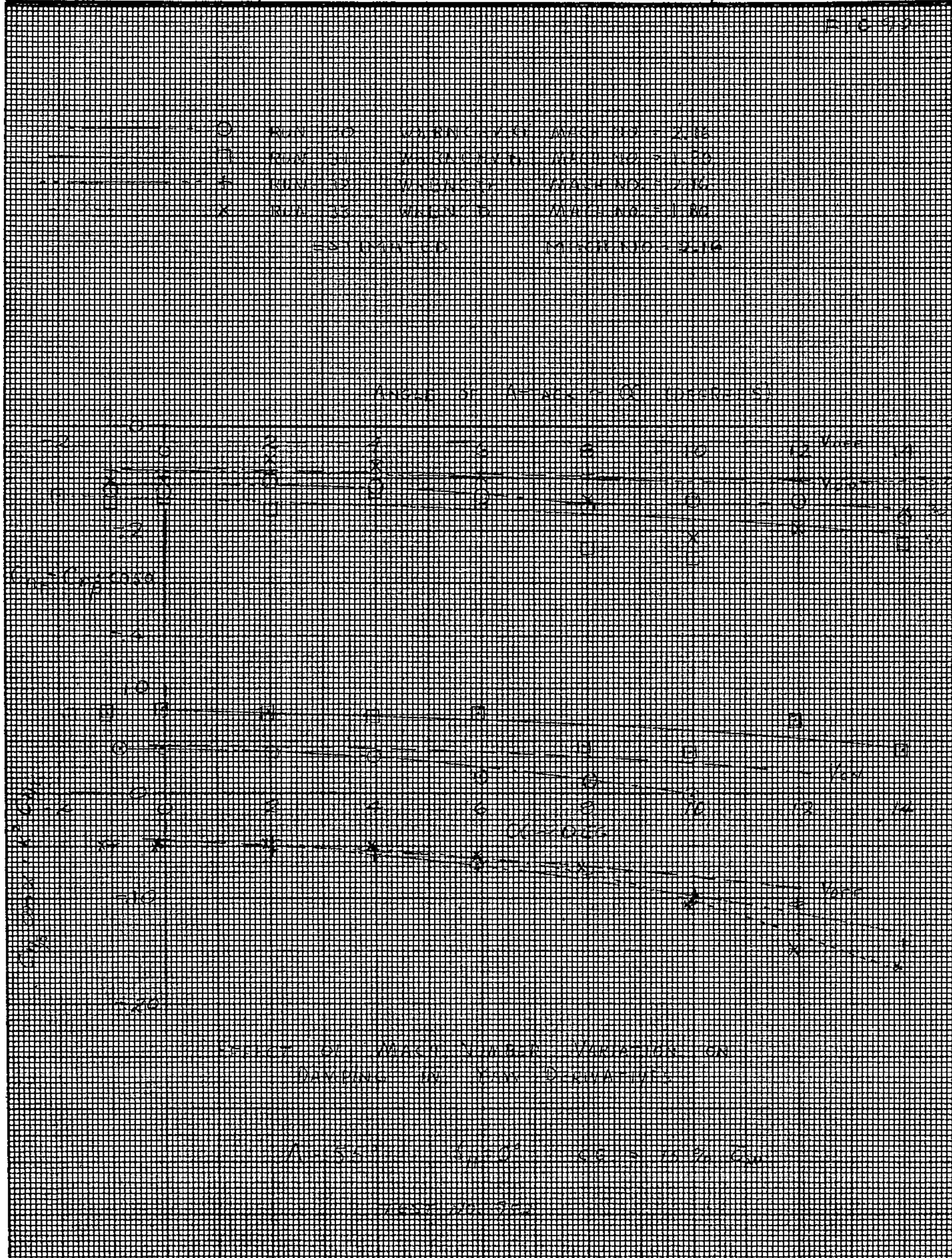
ANGLE OF ATTACK = α (DEGREES)
-2
0
2
4
6
8
10
12
14
-4
-10
-20
EFFECT OF MACH NUMBER VARIATION ON
DAMPING IN YAW DERIVATIVES

FORM 1021-S REV. 10-70

PREPARED BY:	Los Angeles Division North American Rockwell	PAGE NO. 117 OF 145
CHECKED BY:		REPORT NO. NA-72-82
DATE:		MODEL NO.

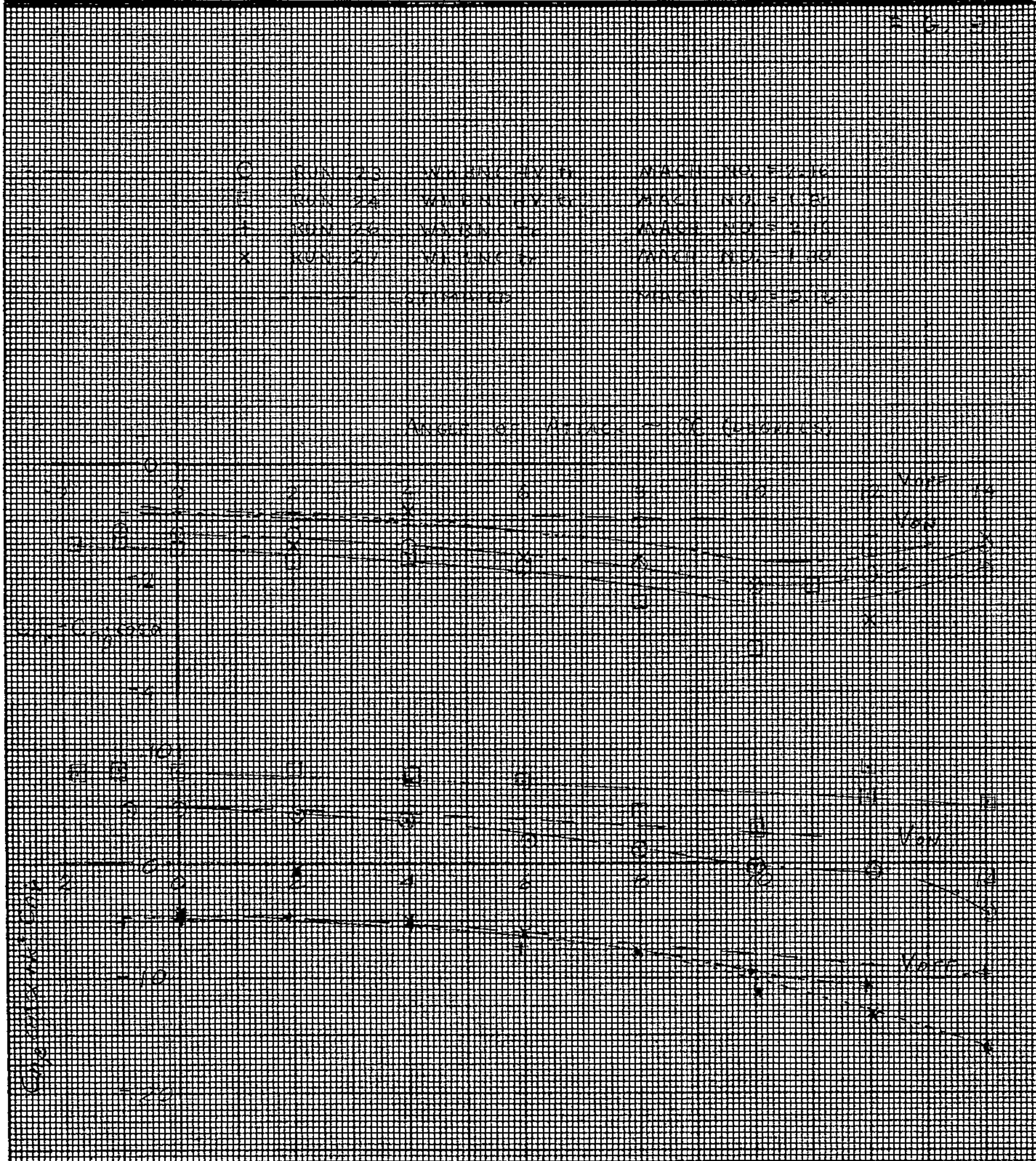

EFFECT OF MACH NUMBER VARIATION
ON DAMPING IN YAW DERIVATIVES
$\delta_F = 0$ $\Lambda = 63°$ C.G. = 75% l_W

FORM 1021-S REV. 10-70

PREPARED BY:	Los Angeles Division North American Rockwell	PAGE NO. 118 OF 145
CHECKED BY:		REPORT NO NA-72-82
DATE:		MODEL NO.

FIG 92

EFFECT OF SWEEP VARIATION ON DAMPING IN YAW DERIVATIVES

δ = 5°   CG = .35 $\bar{c}_w$

MACH No. 1.8

TEST No. 752

FORM 1021-S REV 10-70

PREPARED BY:	Los Angeles Division North American Rockwell	PAGE NO. 119 OF 145
CHECKED BY:		REPORT NO. NA-72-82
DATE:		MODEL NO.

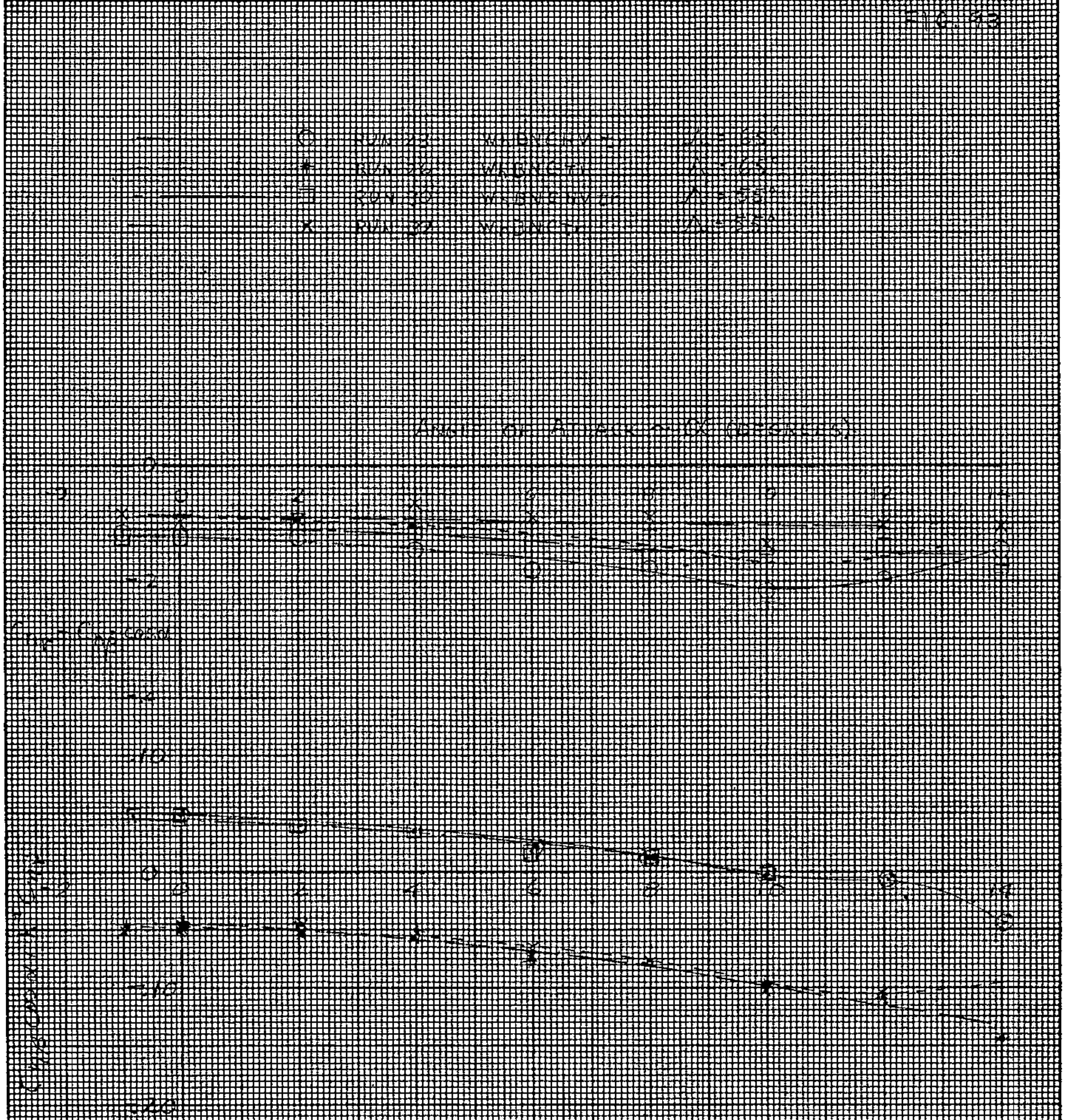

EFFECT OF SWEEP VARIATION ON DAMPING IN YAW DERIVATIVES

FIG. 94

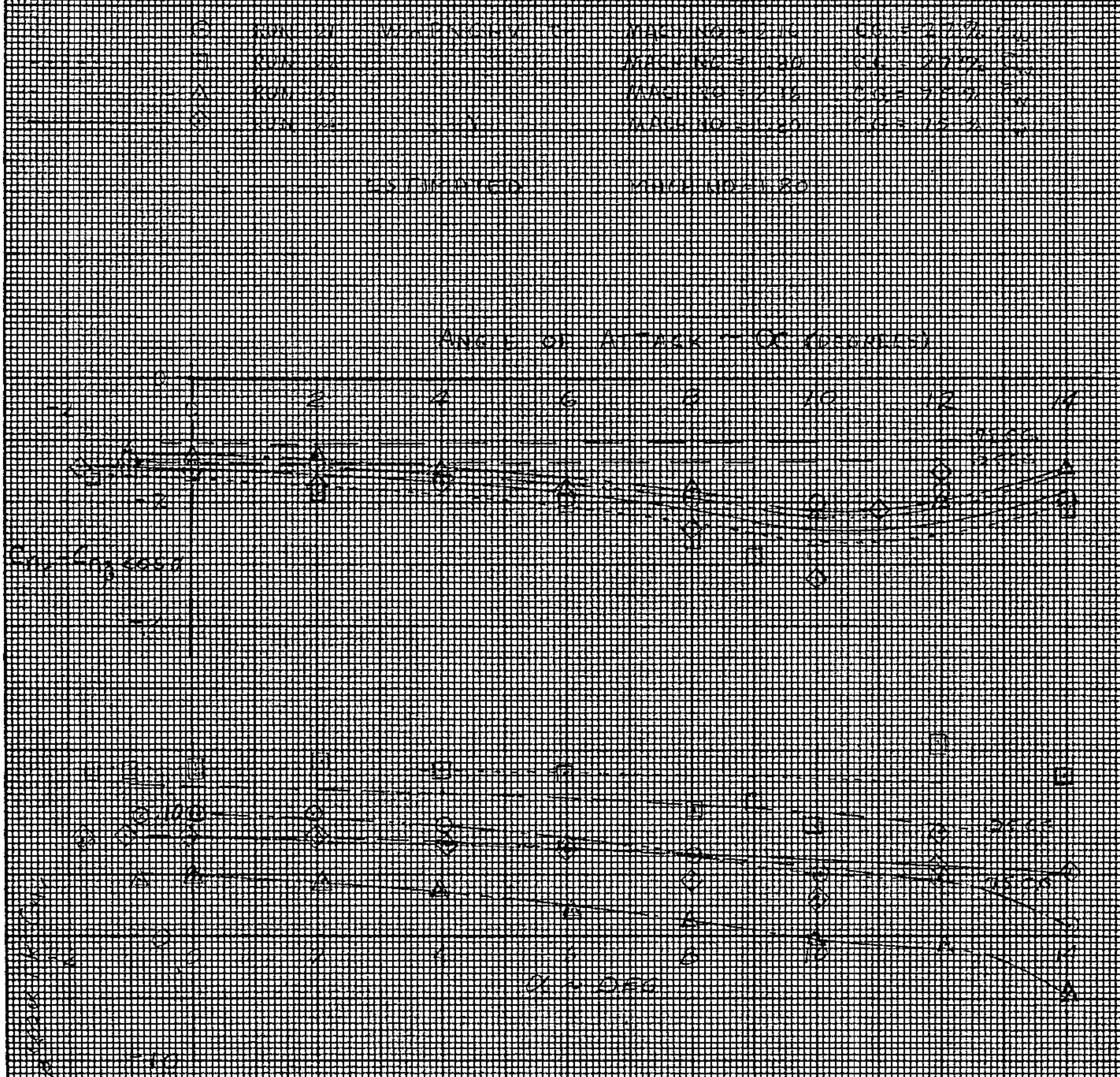

EFFECT OF CENTER OF GRAVITY POSITION
ON DAMPING IN YAW

Λ = 65°

FORM 1021-S REV. 10-70

PREPARED BY:	Los Angeles Division North American Rockwell	PAGE NO. 121 OF 145
CHECKED BY:		REPORT NO. NA-72-82
DATE:		MODEL NO.

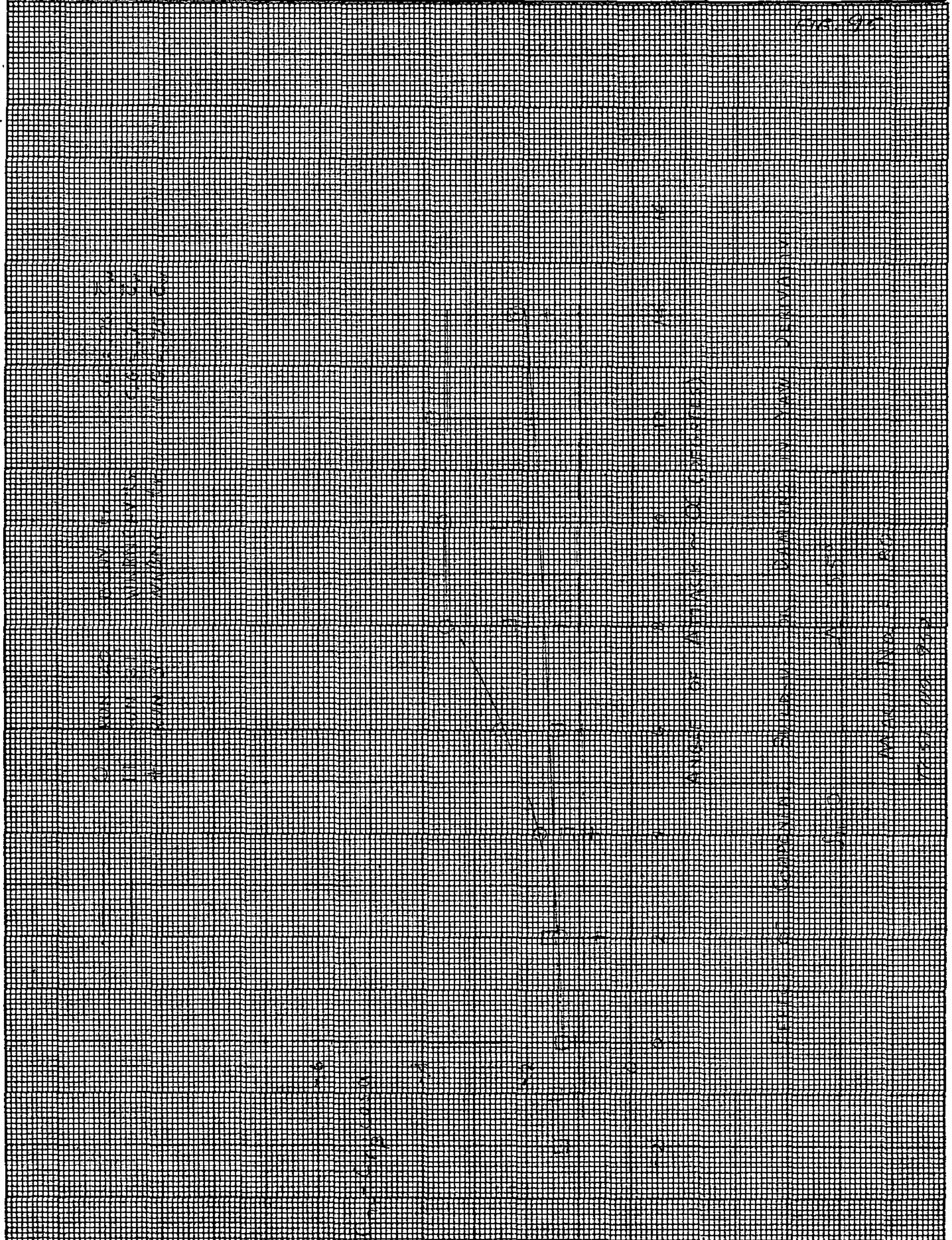

FORM 1021-8 REV. 10-70

PREPARED BY:	Los Angeles Division North American Rockwell	PAGE NO. 122 OF 145
CHECKED BY:		REPORT NO NA-72-82
DATE:		MODEL NO.

FIG 96

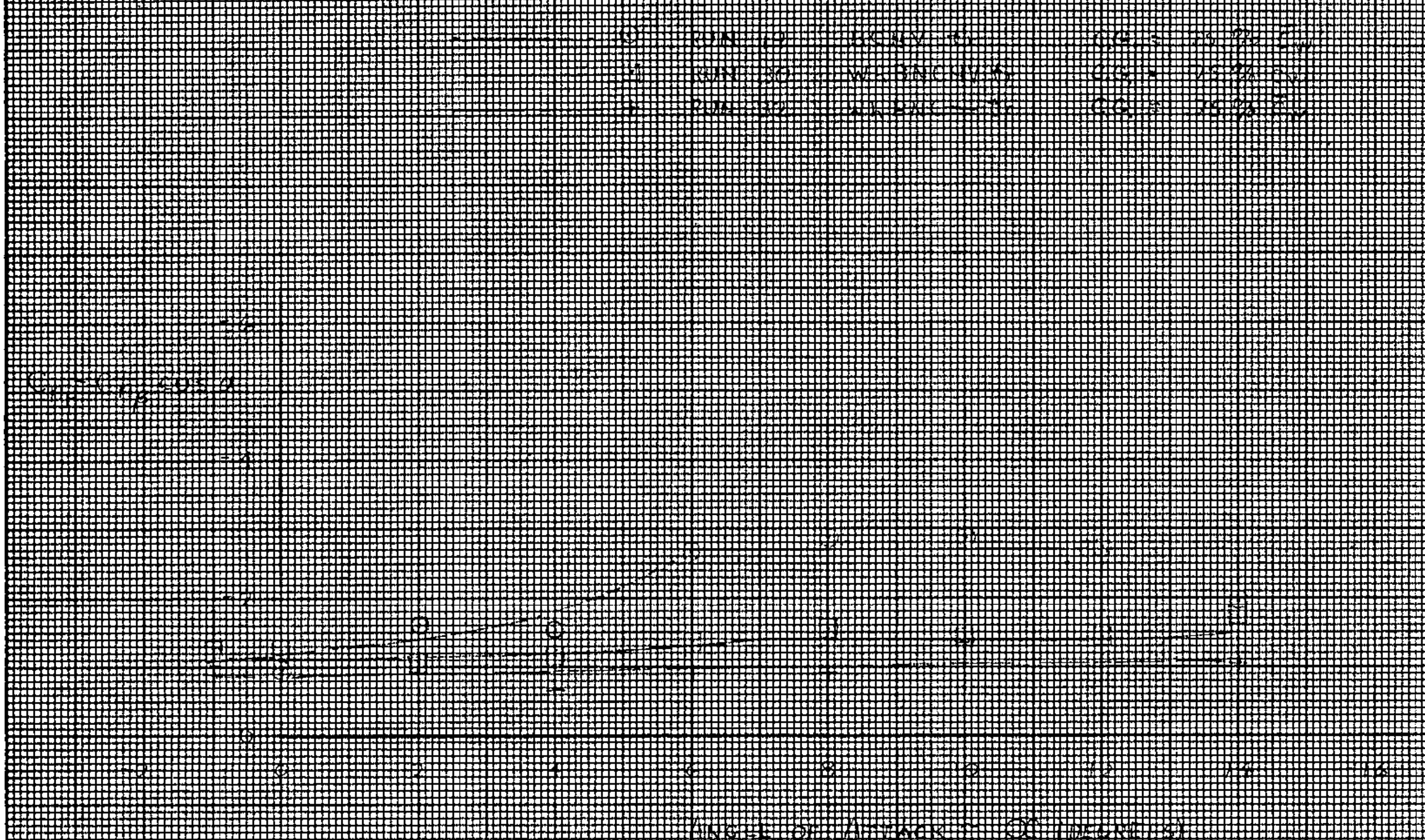

EFFECT OF COMPONENT BUILD-UP ON DAMPING IN YAW DERIVATIVES

$\delta_r = 0$ $\Lambda = 56°$

MACH NO. = 2.16

TEST NO. 982

FORM 1021-S REV. 10-70

PREPARED BY:	Los Angeles Division North American Rockwell	PAGE NO 123 OF 145
CHECKED BY:		REPORT NO NA-72-82
DATE:		MODEL NO.

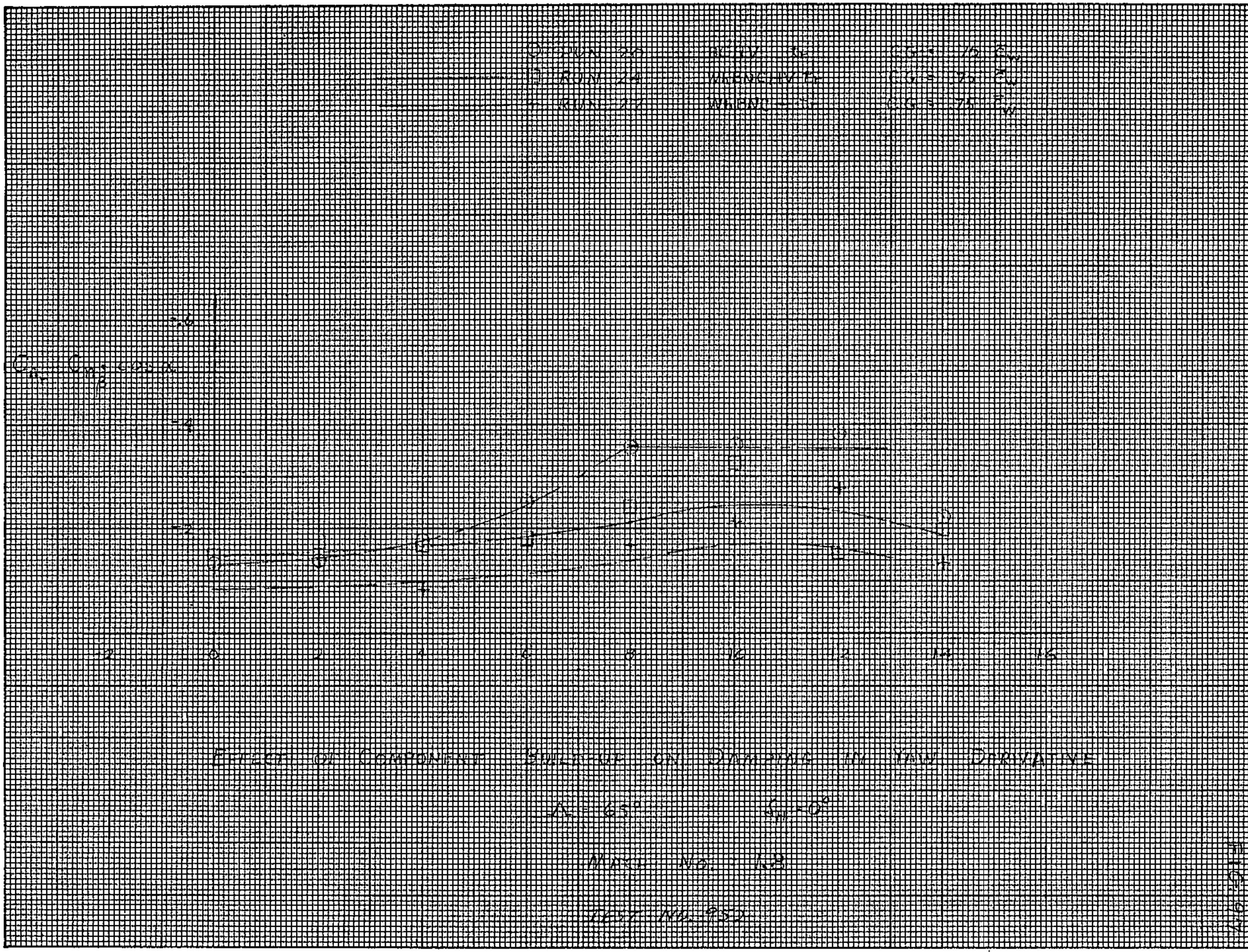

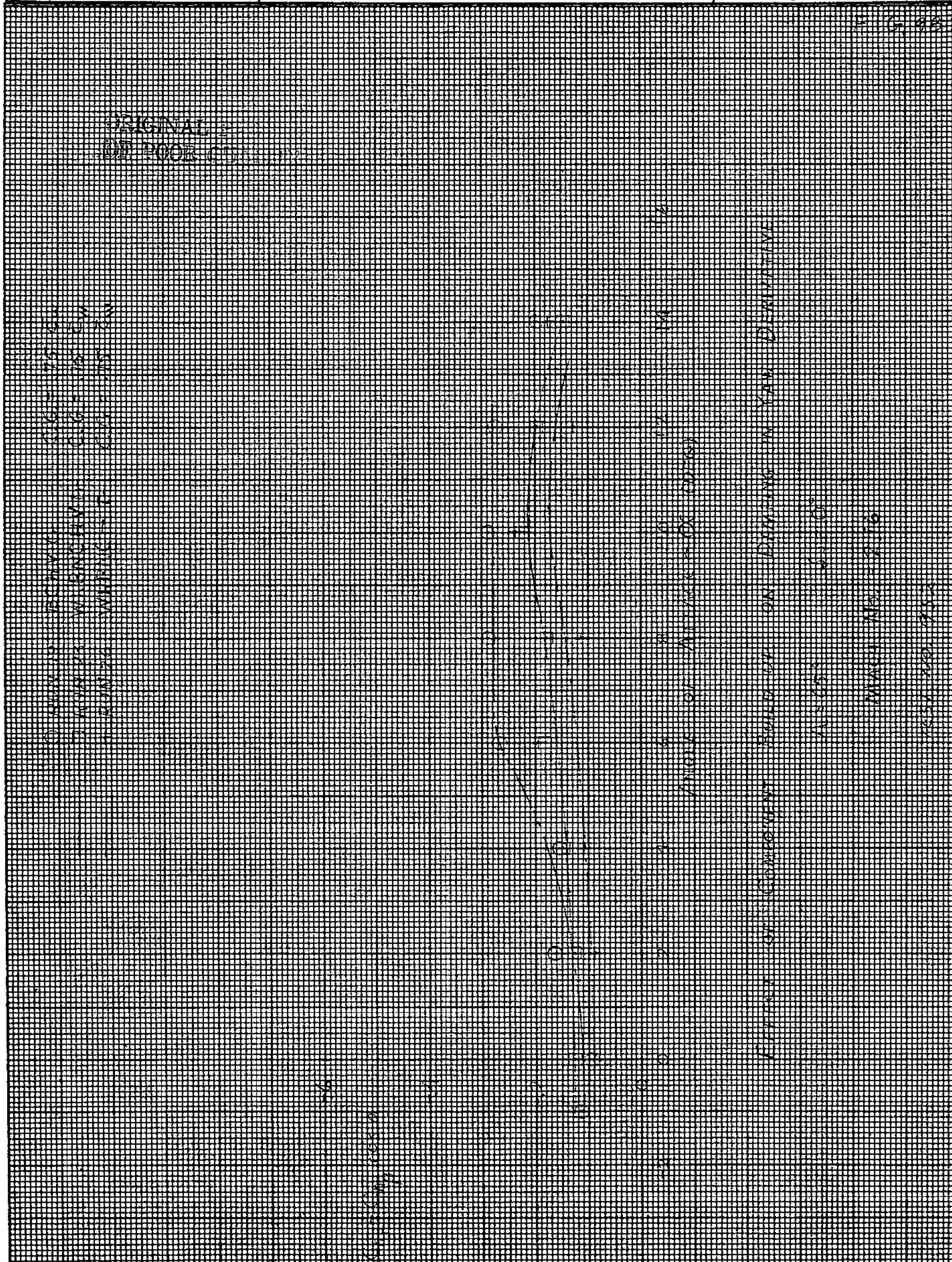
ANGLE OF ATTACK ~ α (DEG)
-2
0
2
4
6
8
10
12
14
16
EFFECT OF COMPONENT BUILD UP ON DAMPING IN YAW DERIVATIVE
MACH NO. = 2.16

FORM 1021-S REV. 10-70

PREPARED BY:	Los Angeles Division North American Rockwell	PAGE NO. 125 OF 145.
CHECKED BY:		REPORT NO. NA-72-82
DATE:		MODEL NO

FIG 49

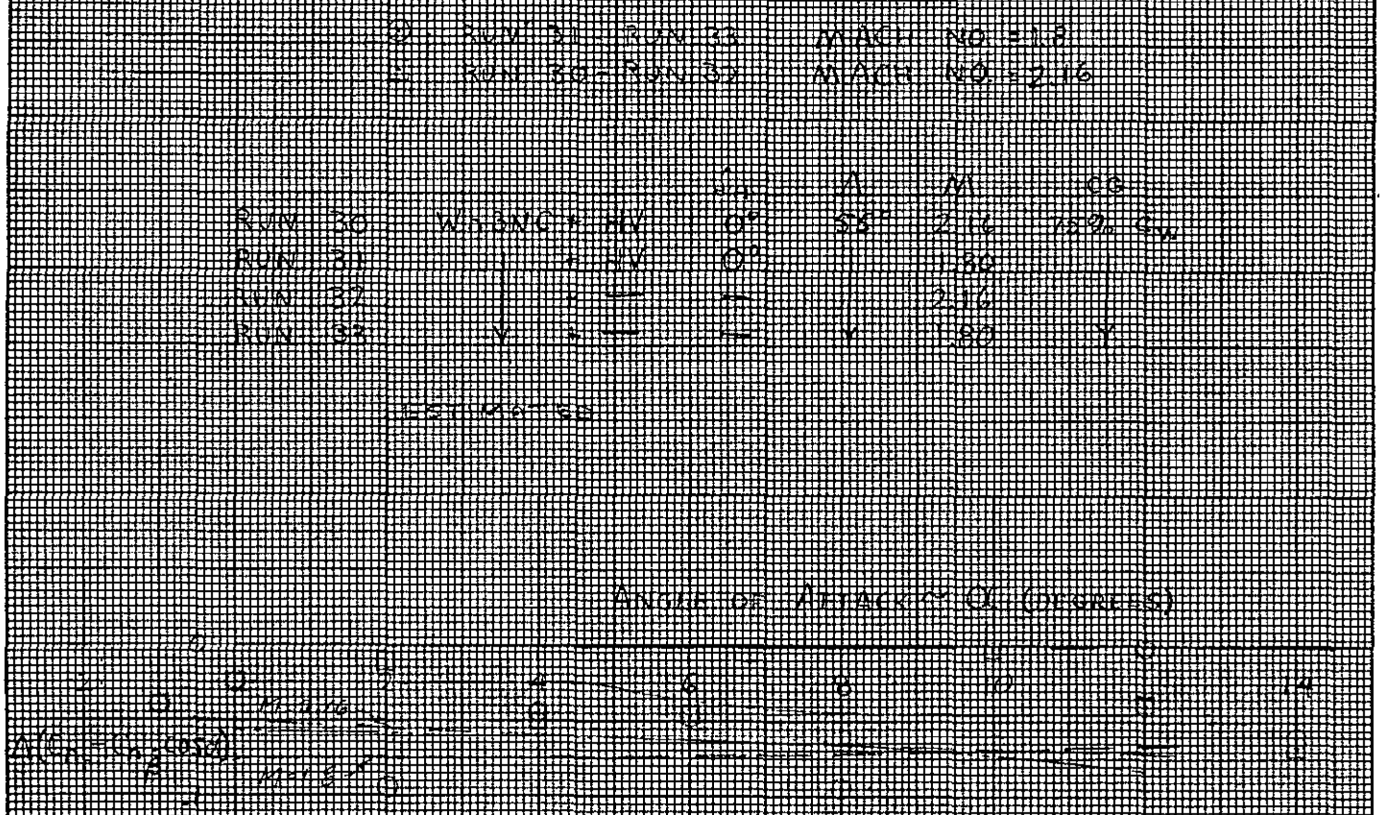

VERTICAL TAIL INPUT INTO DAMPING IN YAW DERIVATIVES

Λ = 55°

TEST NO 952

FIG 102

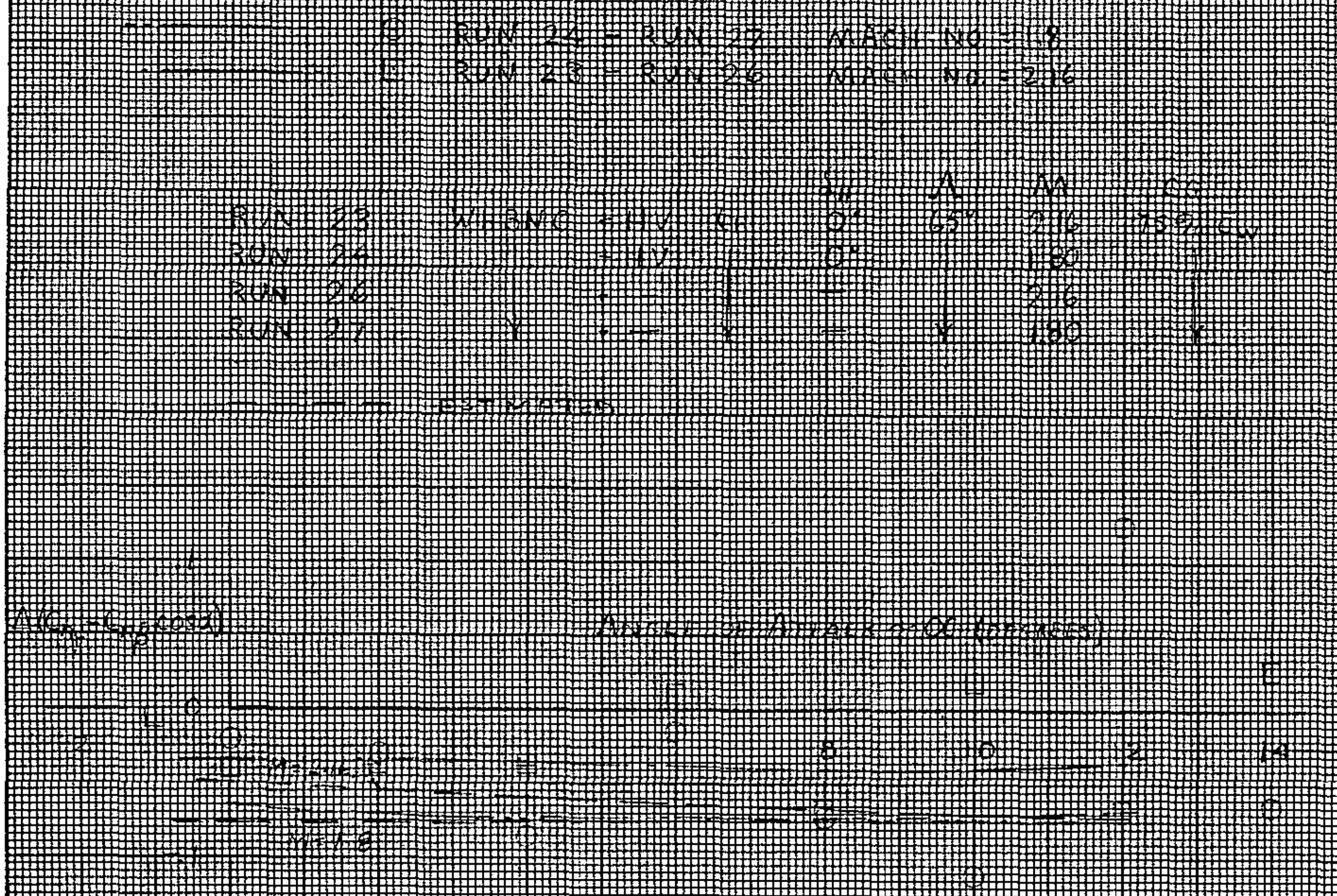

VERTICAL TAIL INPUT INTO DAMPING IN YAW DERIVATIVES

Λ = 65°

TEST NO. 952

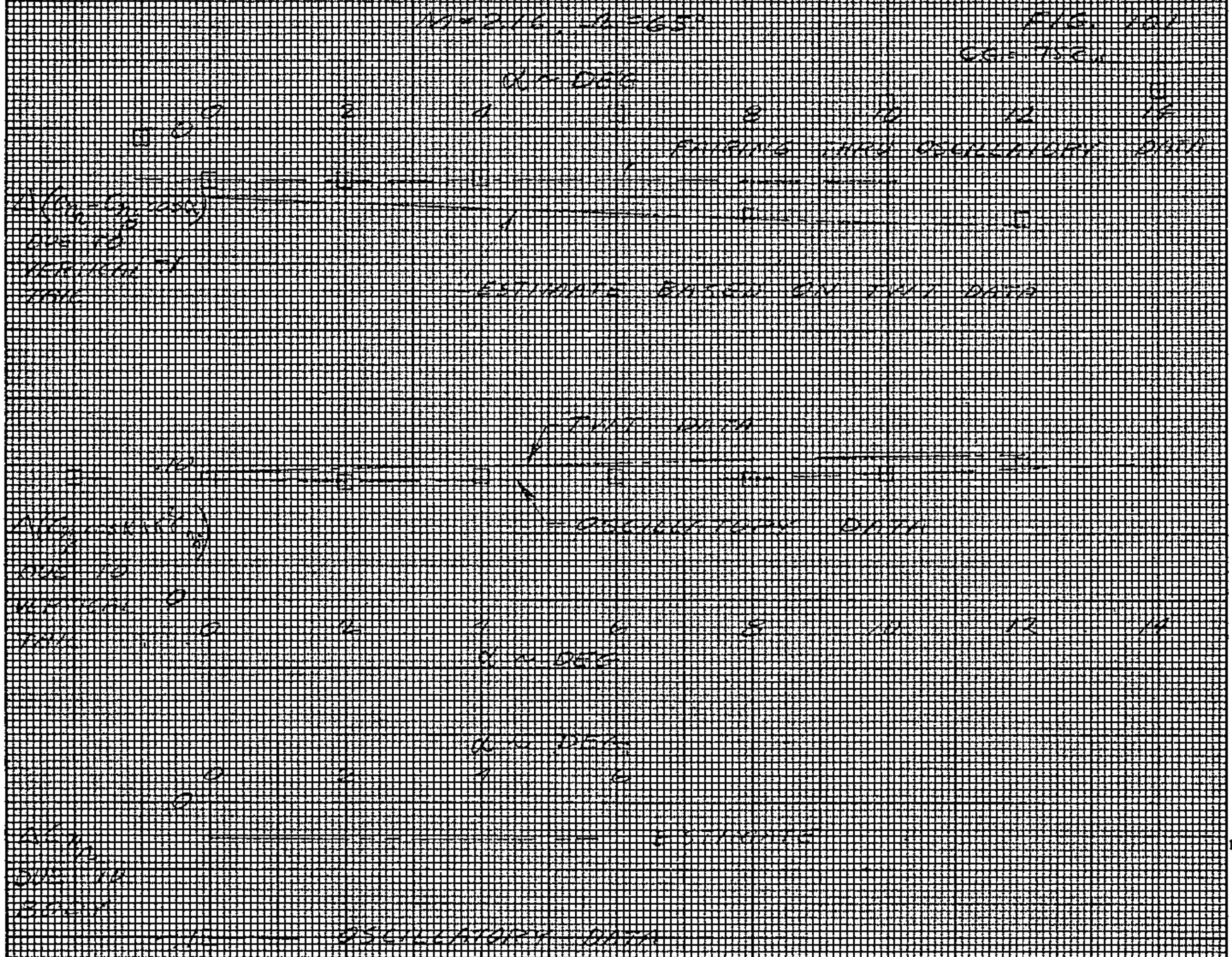

COMPARISON OF YAW DATA WITH ESTIMATES
$M = 2.16$
$\Lambda = 65°$

TEST NO 952

FORM 1021-S REV 10-70

PREPARED BY:	Los Angeles Division North American Rockwell	PAGE NO. 128 OF 145
CHECKED BY:		REPORT NO. NA-72-82
DATE:		MODEL NO.

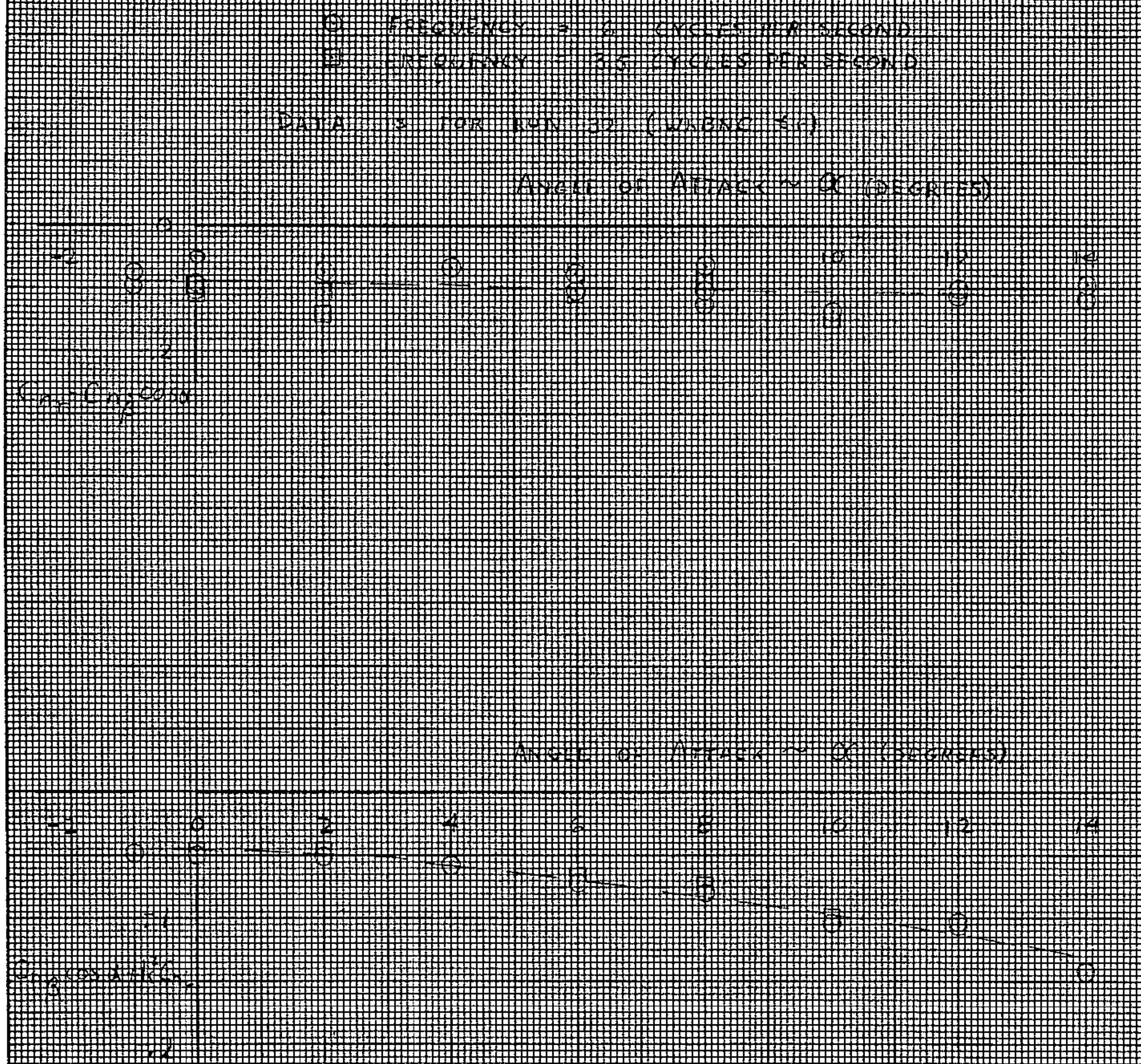

DATA SENSITIVITY TO CHANGE IN OSCILLATORY FREQUENCY

MACH No = 2.16

TEST NO 952

FORM 1021-8 REV. 12-67

PREPARED BY:	LOS ANGELES DIVISION NORTH AMERICAN ROCKWELL CORPORATION	PAGE NO: 129 OF 145
CHECKED BY:		REPORT NO NA-72-82
DATE:		MODEL NO.

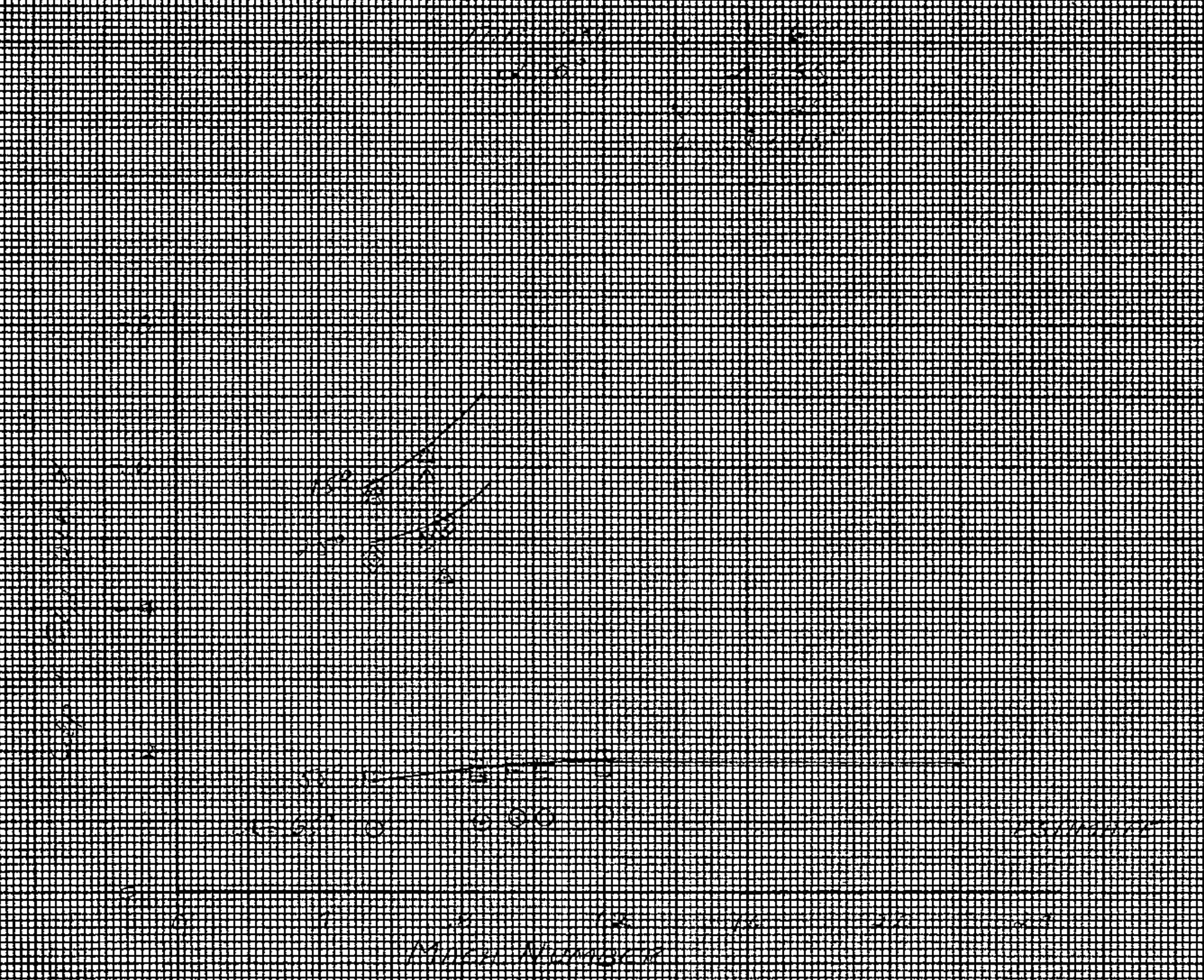

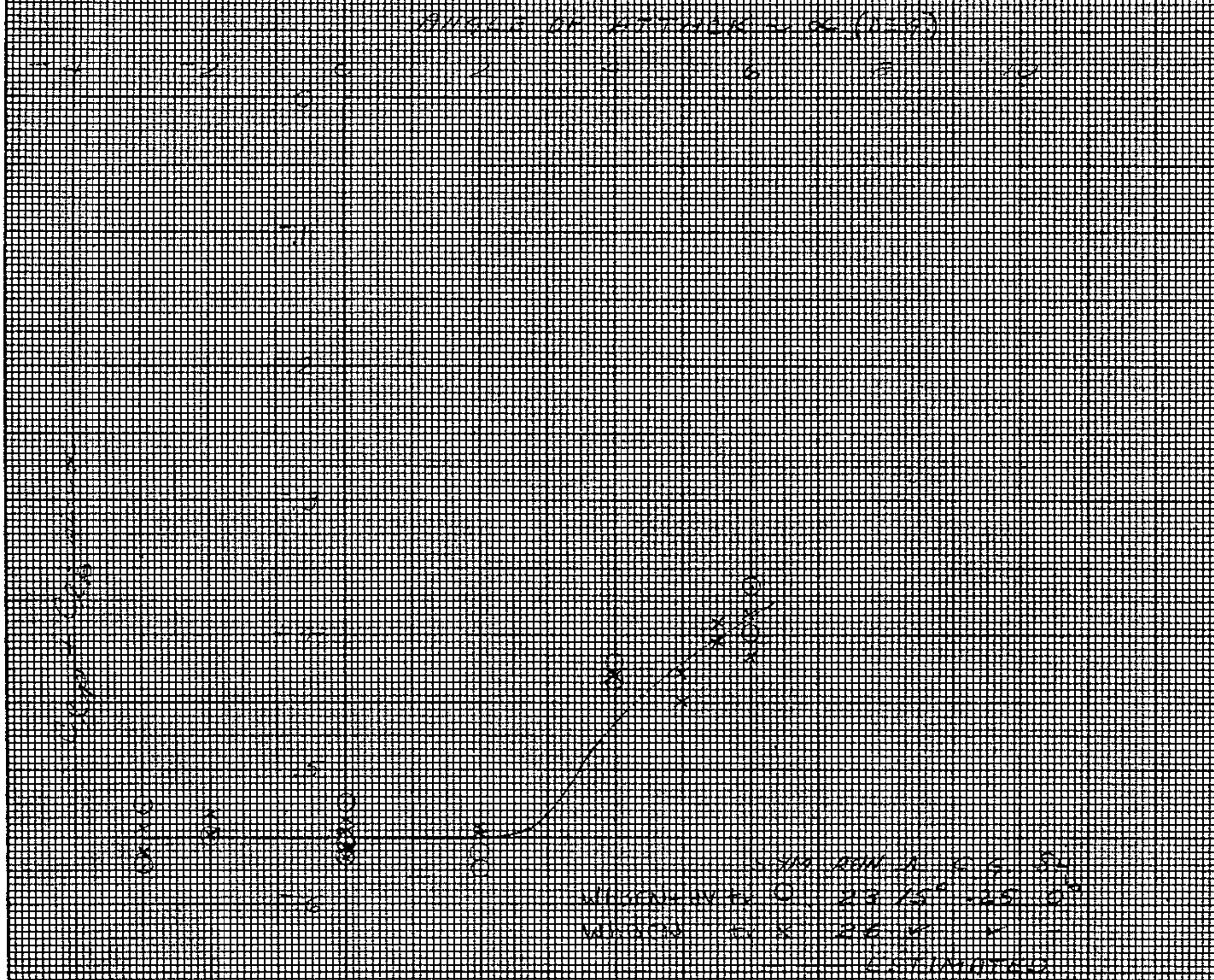

DAMPING IN ROLL DERIVATIVE

HORIZONTAL TAIL ON & OFF

Λ = 15° MACH NO. = .55

TEST NO. 590

FORM 1021-S REV. 10-70

PREPARED BY:	Los Angeles Division North American Rockwell	PAGE NO. 131 OF 145
CHECKED BY:		REPORT NO NA-72-82
DATE:		MODEL NO.

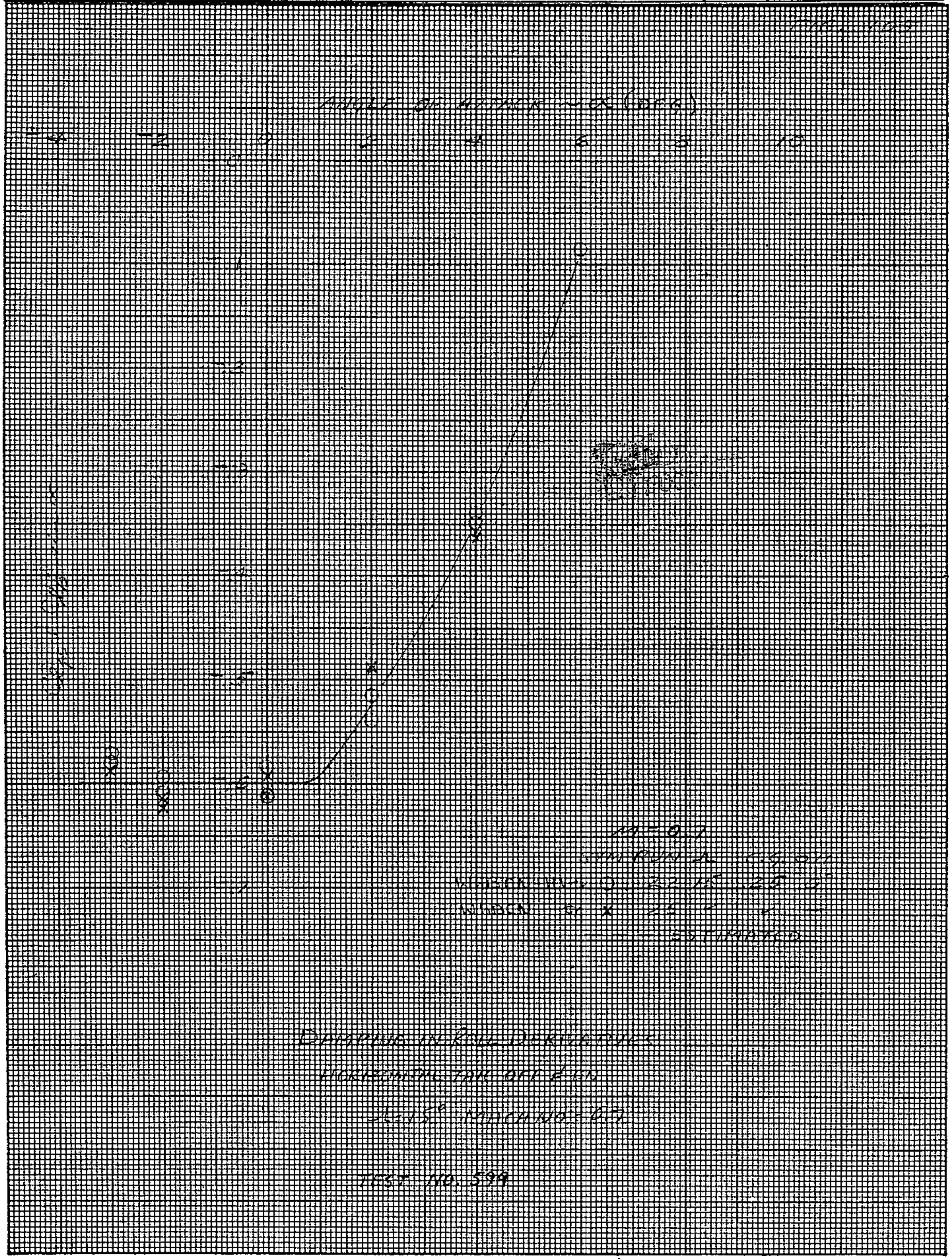

FORM 1021-S REV. 10-70

PREPARED BY:	Los Angeles Division North American Rockwell	PAGE NO 132 OF 145
CHECKED BY:		REPORT NO NA-72-82
DATE:		MODEL NO.

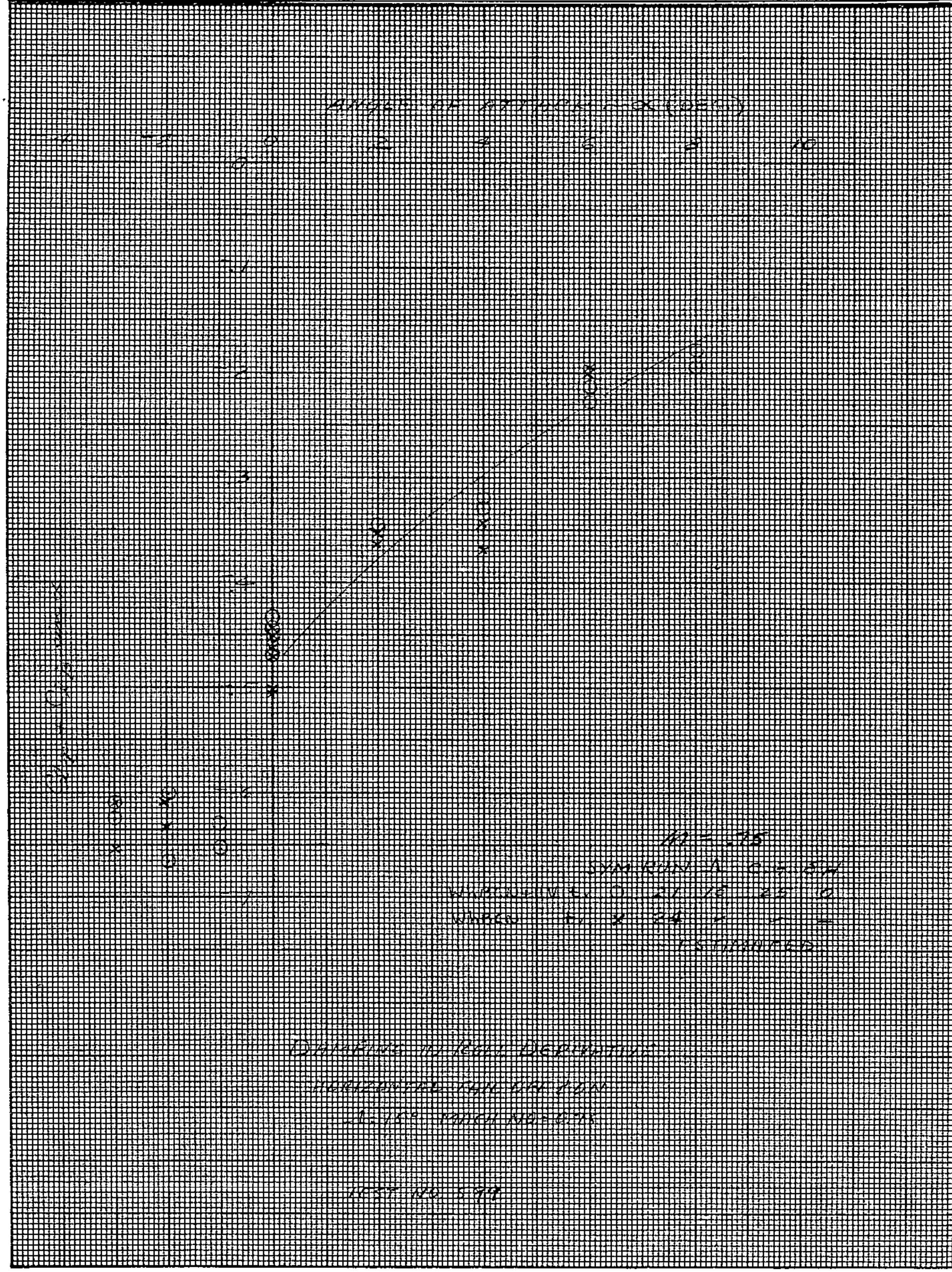

FIG. 107

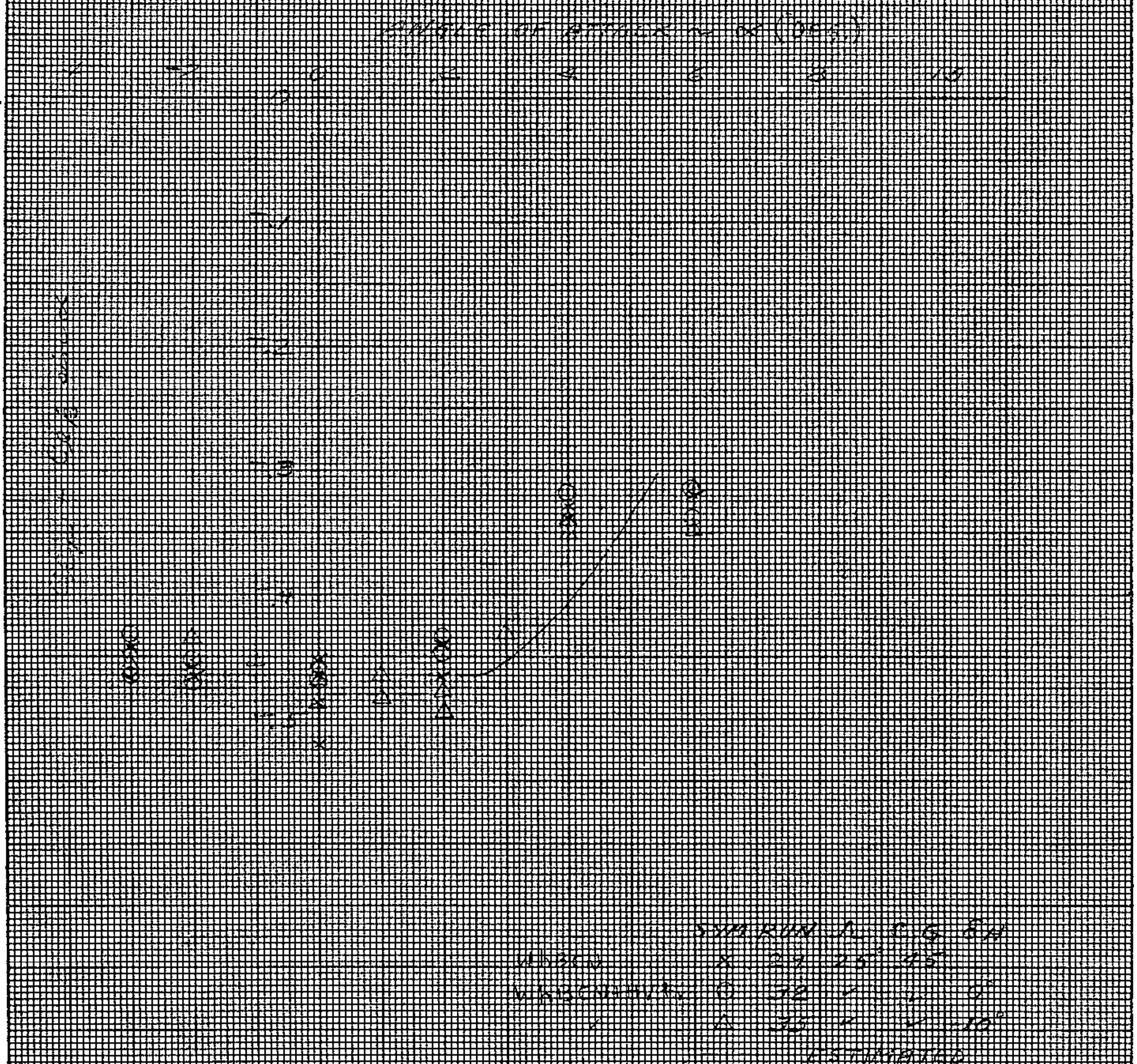

DAMPING IN ROLL DERIVATIVES

HORIZONTAL TAIL EFFECT

$\Lambda = 25°$ MACH NO = .55

TEST NO. 599

FORM 1021-S REV 10-70

PREPARED BY:	Los Angeles Division North American Rockwell	PAGE NO. 134 OF 145
CHECKED BY:		REPORT NO NA-72-82
DATE:		MODEL NO.

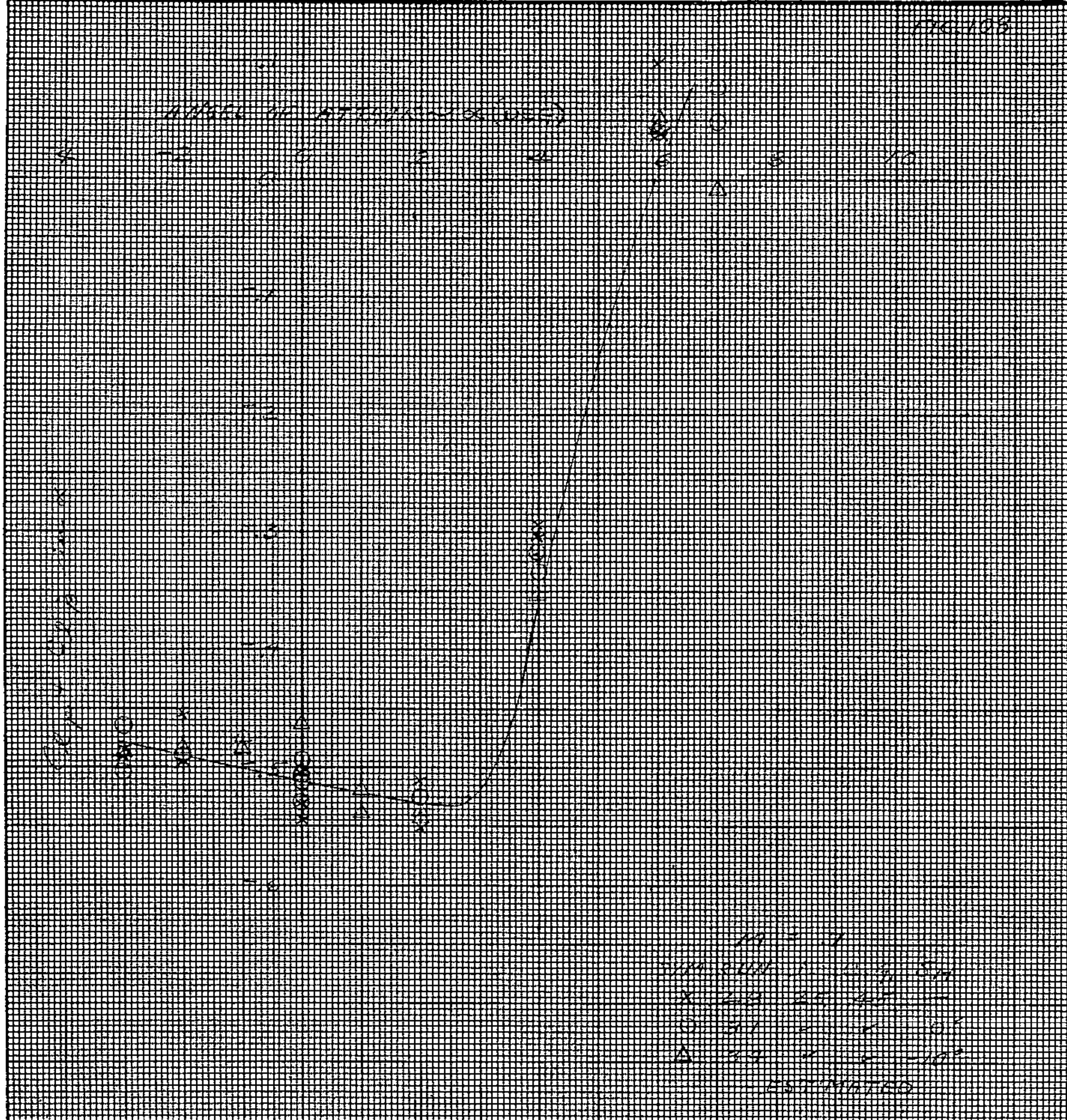

HORIZONTAL TAIL EFFECT

TEST NO. 597

FIG. 105

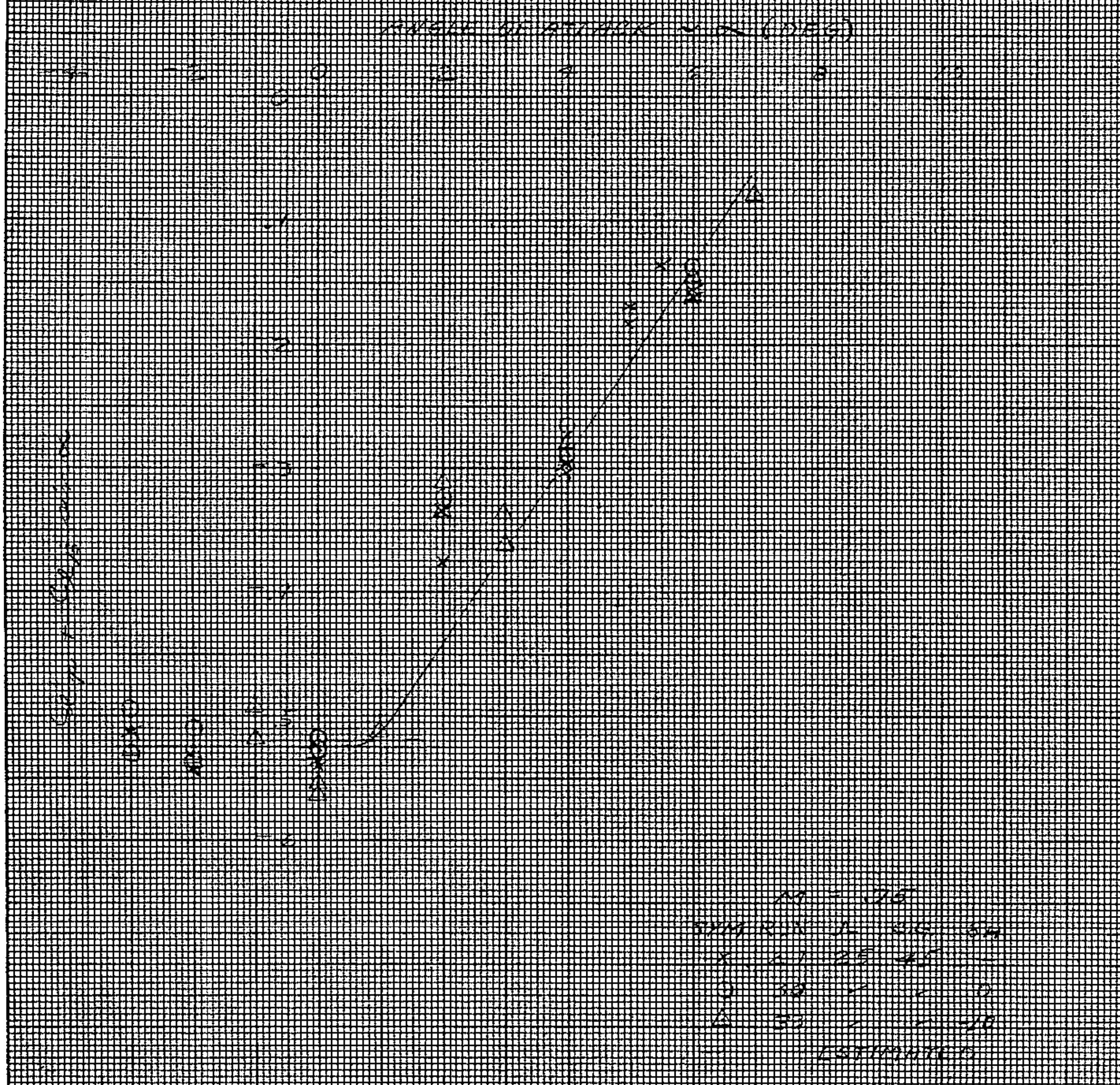

DAMPING IN ROLL DERIVATIVES
HORIZONTAL TAIL EFFECT
L=255 MACH NO=.075

TEST NO. 599

FORM 1021-S REV. 10-70

PREPARED BY:	Los Angeles Division North American Rockwell	PAGE NO 136 OF 145
CHECKED BY:		REPORT NO NA-72-82
DATE:		MODEL NO.

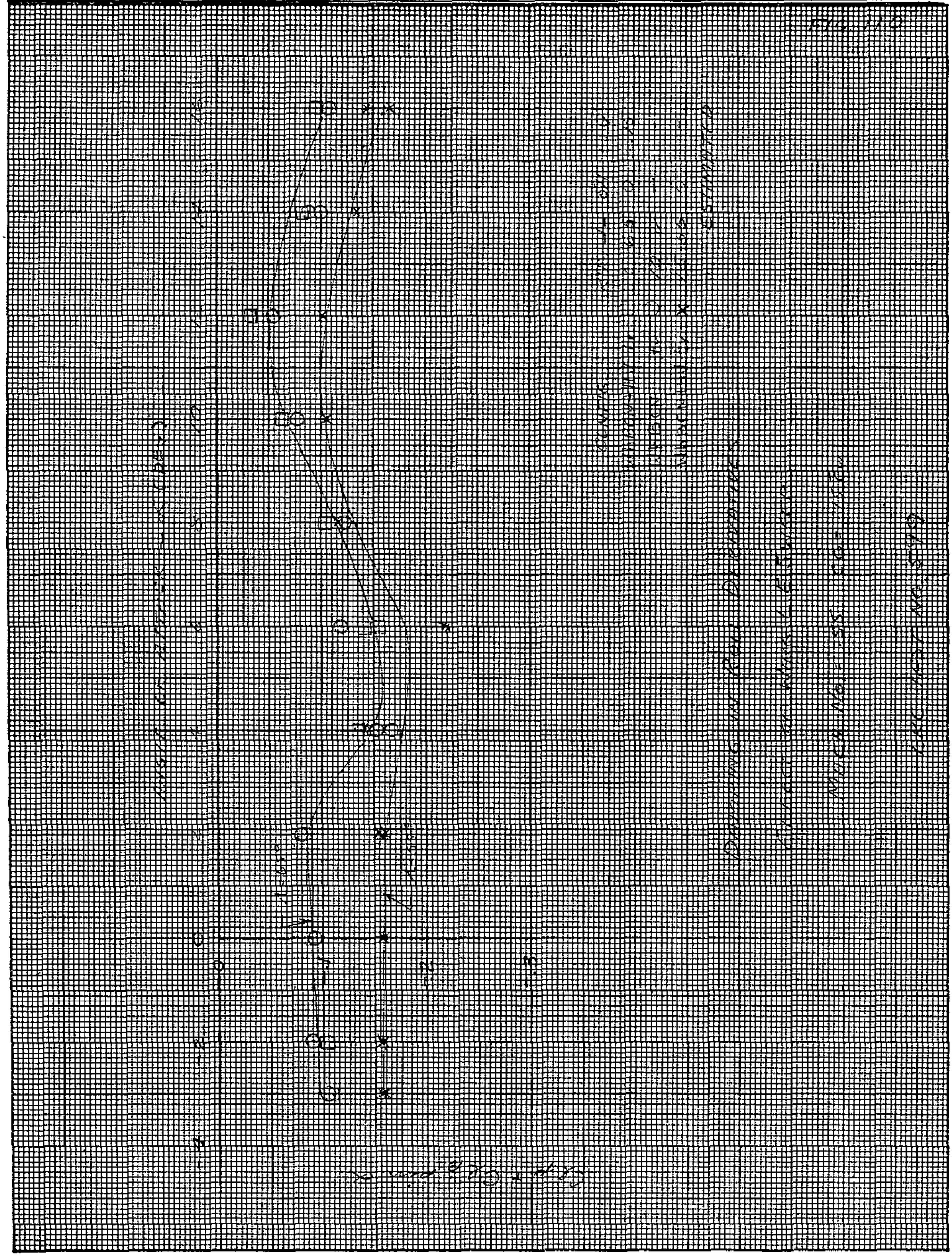

FORM 1021-S REV 10-70

PREPARED BY:	Los Angeles Division North American Rockwell	PAGE NO. 137 OF 145
CHECKED BY:		REPORT NO NA-72-82
DATE:		MODEL NO.

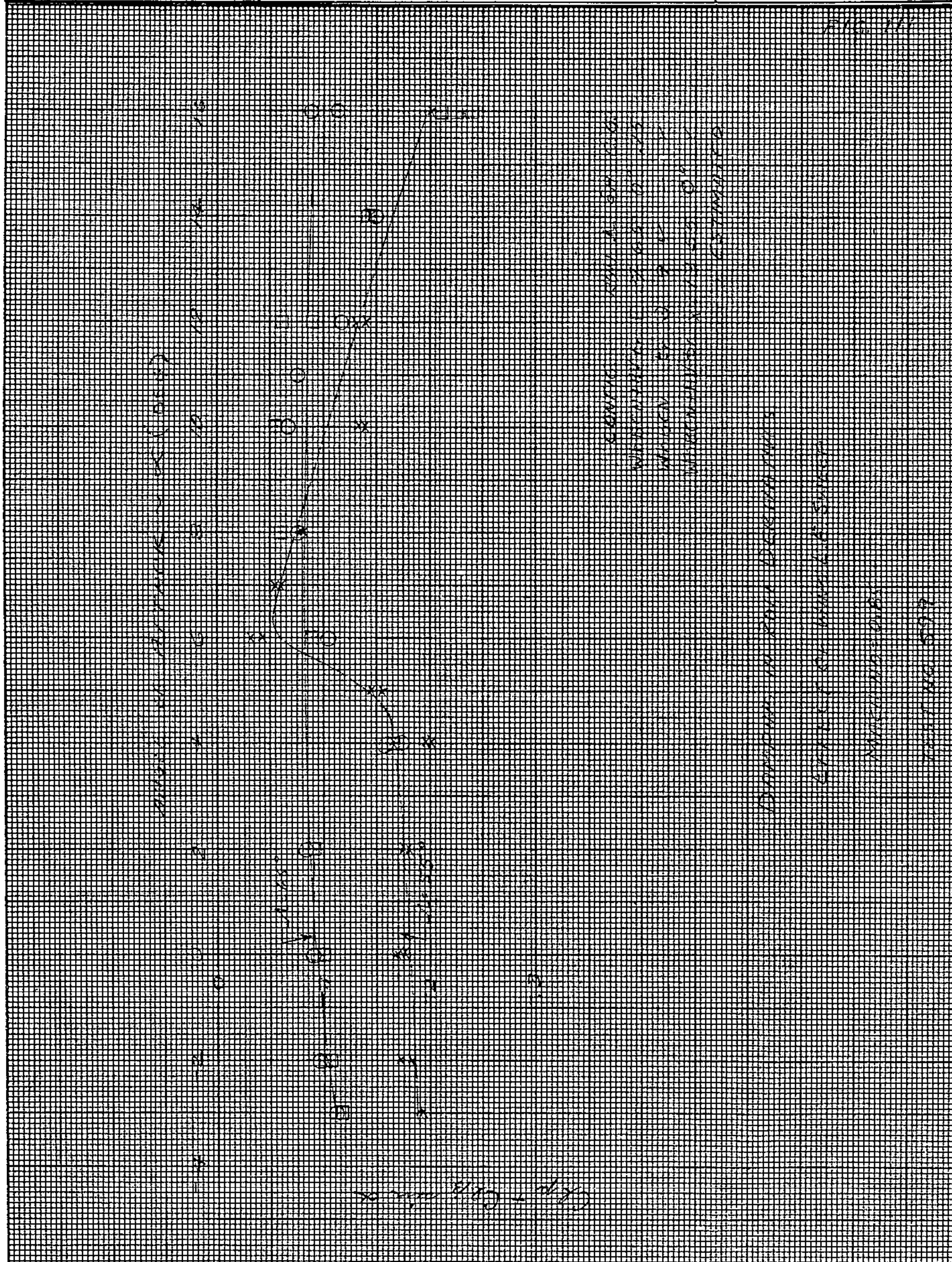

FORM 1021-S REV. 10-70

PREPARED BY:	**Los Angeles Division** North American Rockwell	PAGE NO. 138 OF 145
CHECKED BY:		REPORT NO. NA-72-82.
DATE:		MODEL NO.

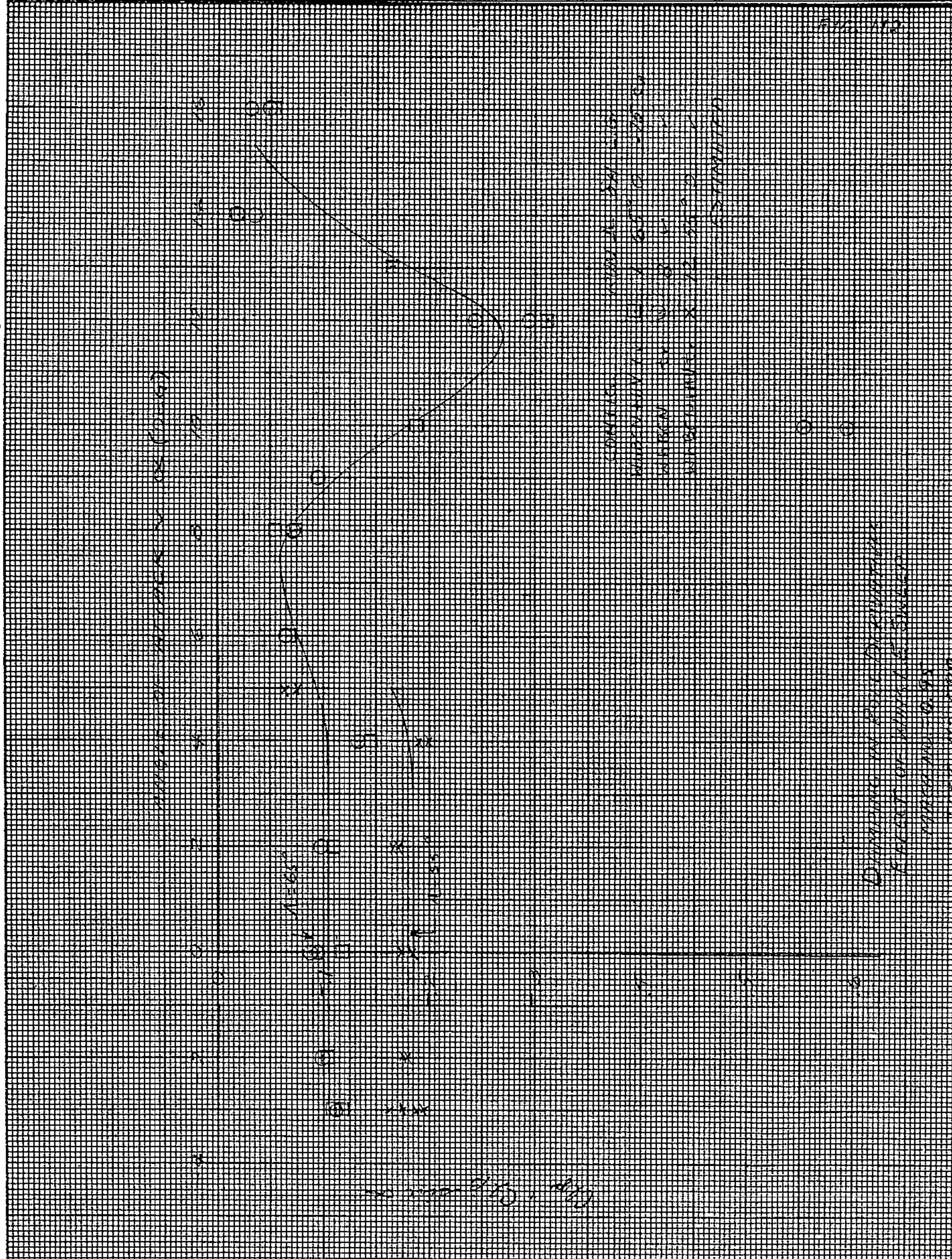

FORM 1021-S REV 10-70

PREPARED BY:	Los Angeles Division North American Rockwell	PAGE NO. 139 OF 145
CHECKED BY:		REPORT NO NA-72-82
DATE:		MODEL NO.

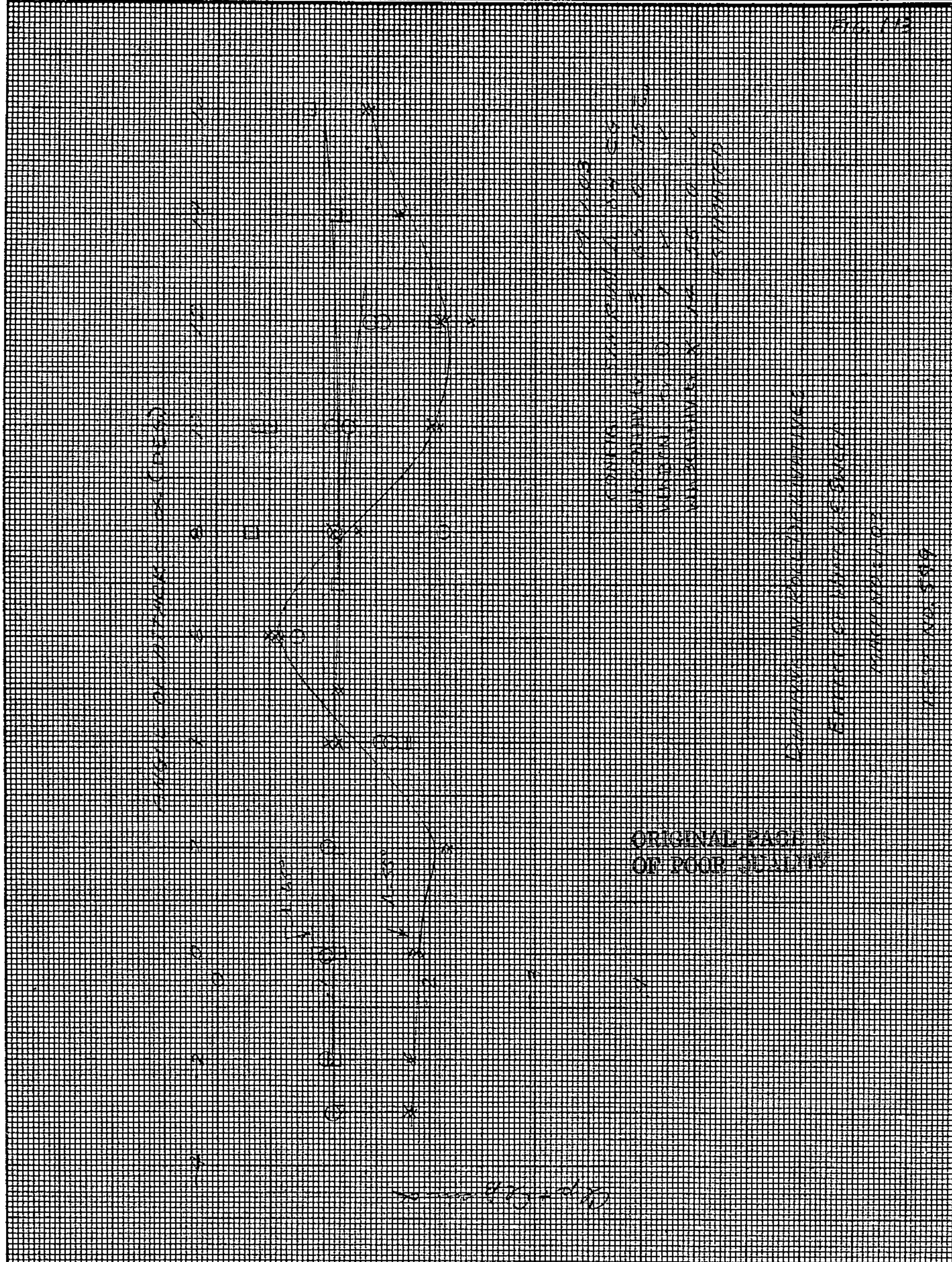

FORM 1021-S REV 10-70

PREPARED BY:	Los Angeles Division North American Rockwell	PAGE NO. 140 OF 145
CHECKED BY:		REPORT NO. NA-72-82
DATE:		MODEL NO

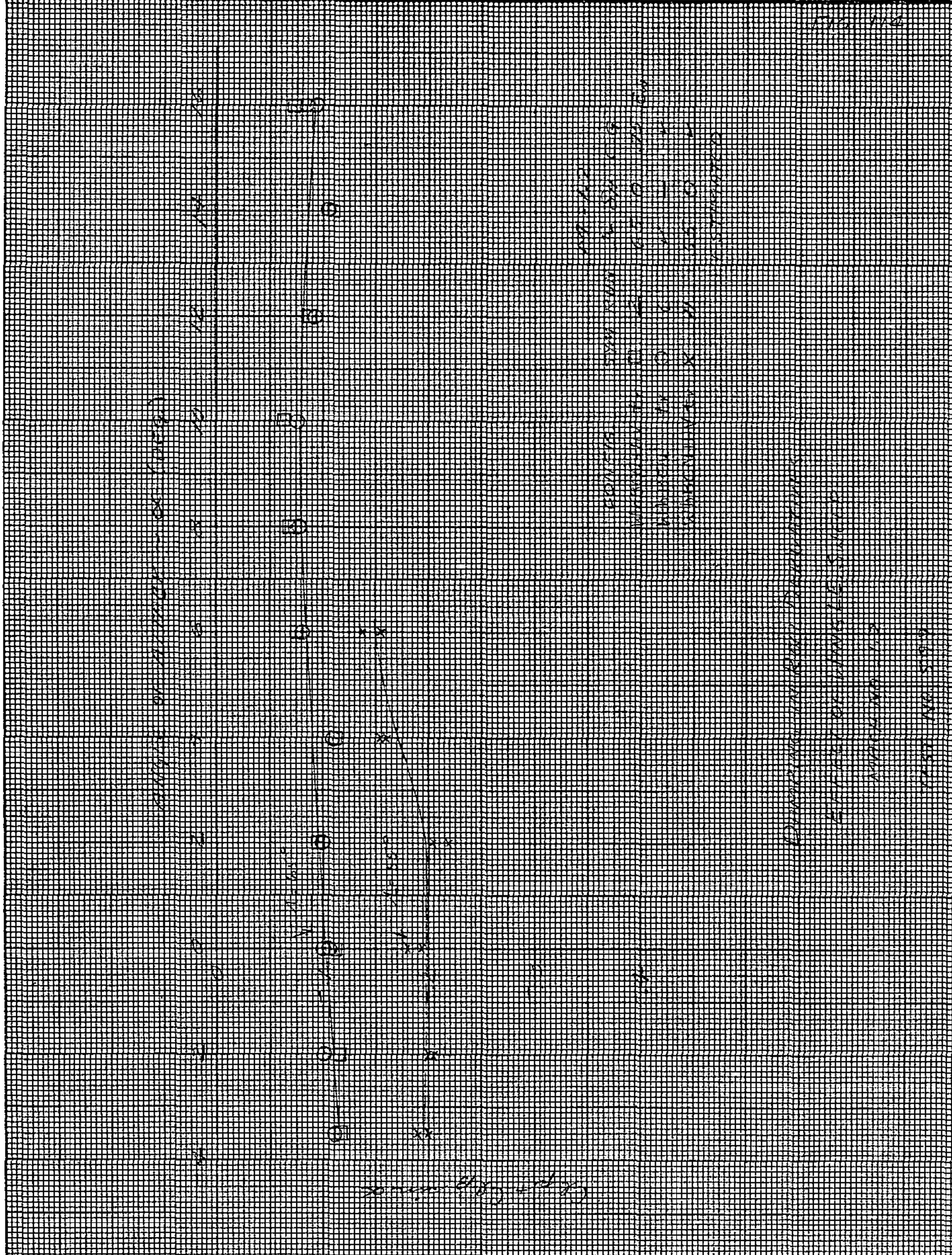

FORM 1021-S REV 10-70

PREPARED BY:	Los Angeles Division North American Rockwell	PAGE NO. 141 OF 145
CHECKED BY:		REPORT NO NA-72-82
DATE:		MODEL NO.

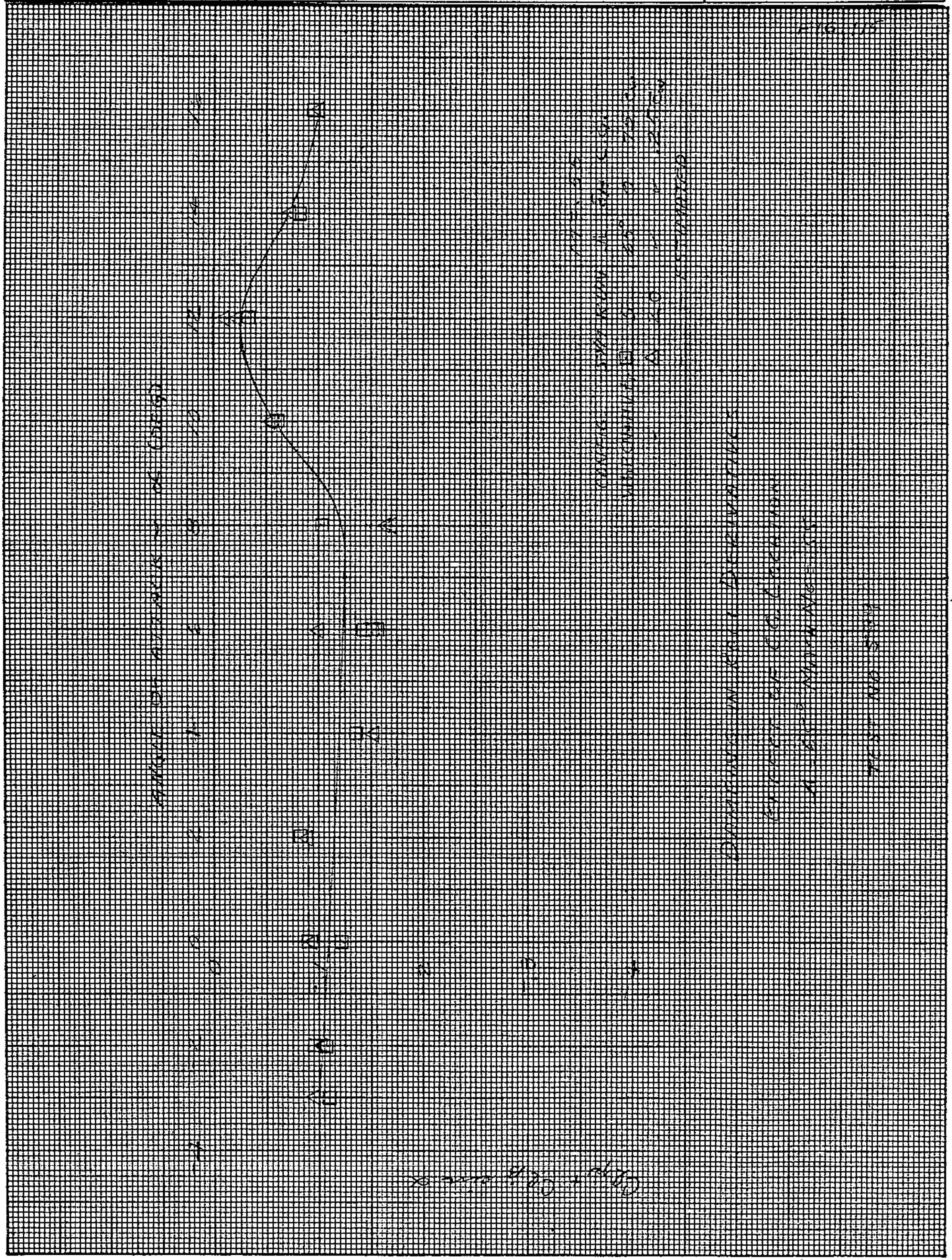

FORM 1021-S REV 10-70

PREPARED BY:	Los Angeles Division North American Rockwell	PAGE NO 142 OF 145
CHECKED BY:		REPORT NO NA-72-82
DATE:		MODEL NO.

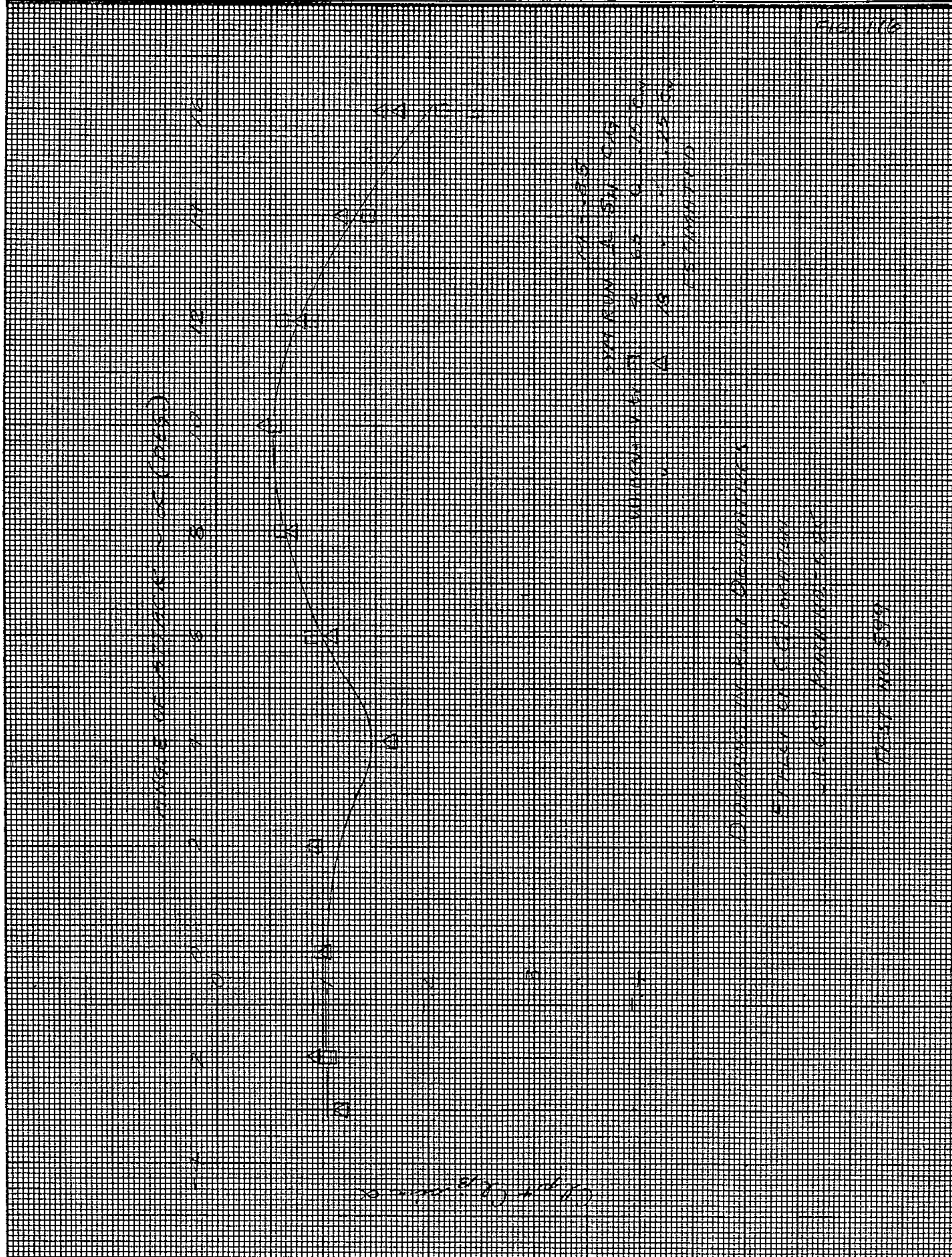

FORM 1021-S REV 10-70

PREPARED BY:	Los Angeles Division North American Rockwell	PAGE NO. 143 OF 145
CHECKED BY:		REPORT NO NA-72-82
DATE:		MODEL NO

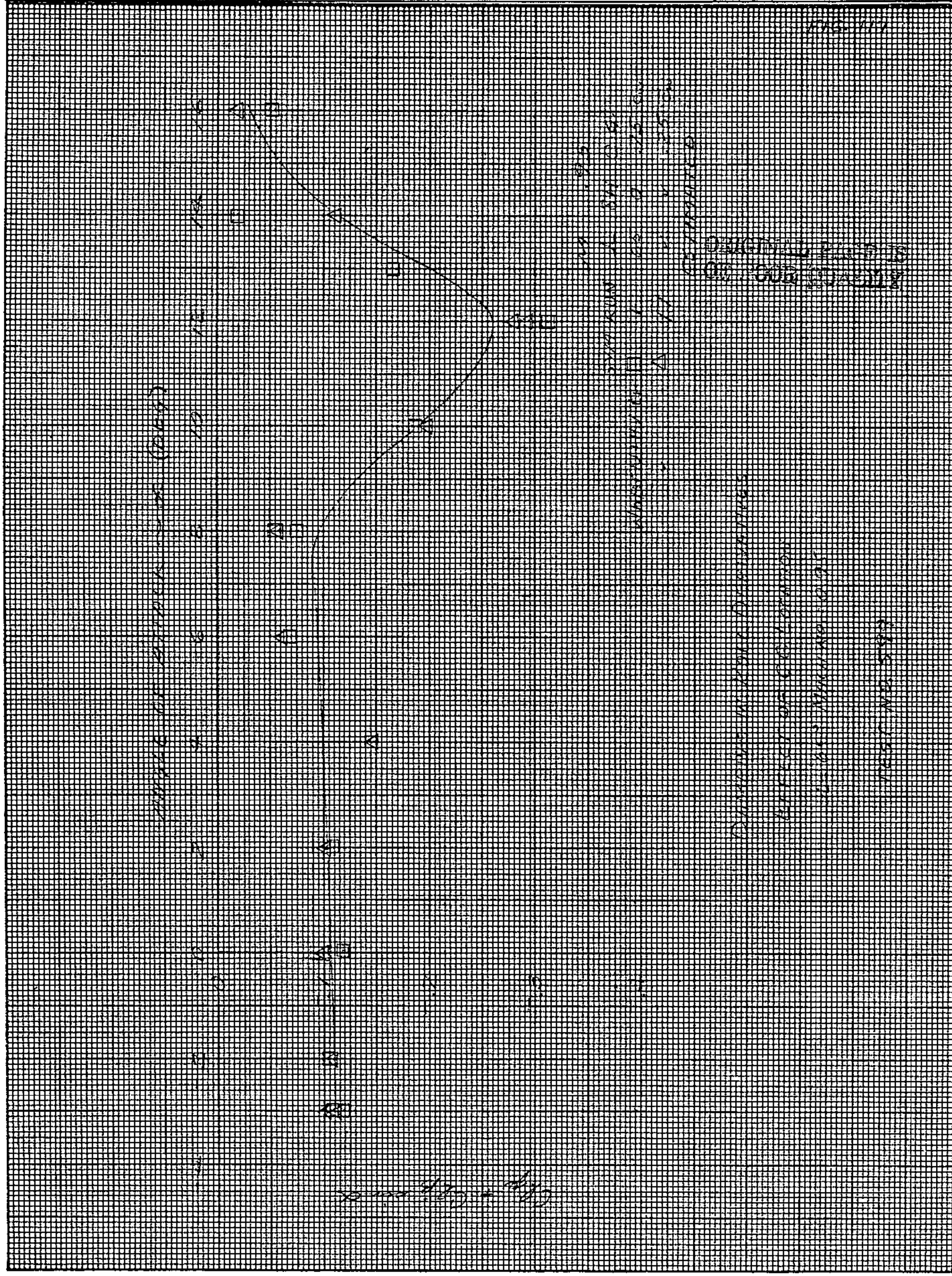

FORM 1021-S REV. 10-70

PREPARED BY:	Los Angeles Division North American Rockwell	PAGE NO. 144 OF
CHECKED BY:		REPORT NO NA-72-82
DATE:		MODEL NO.

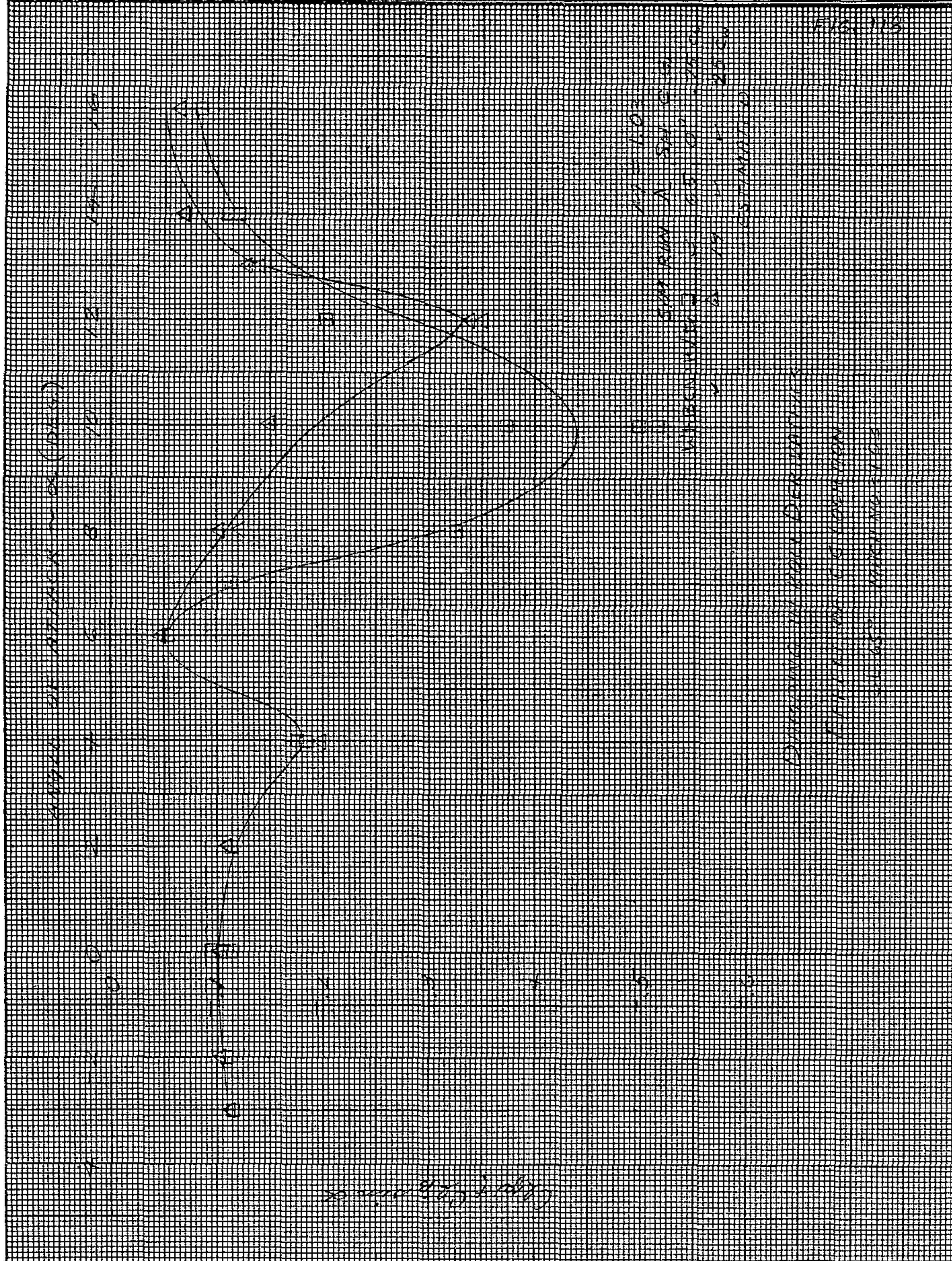

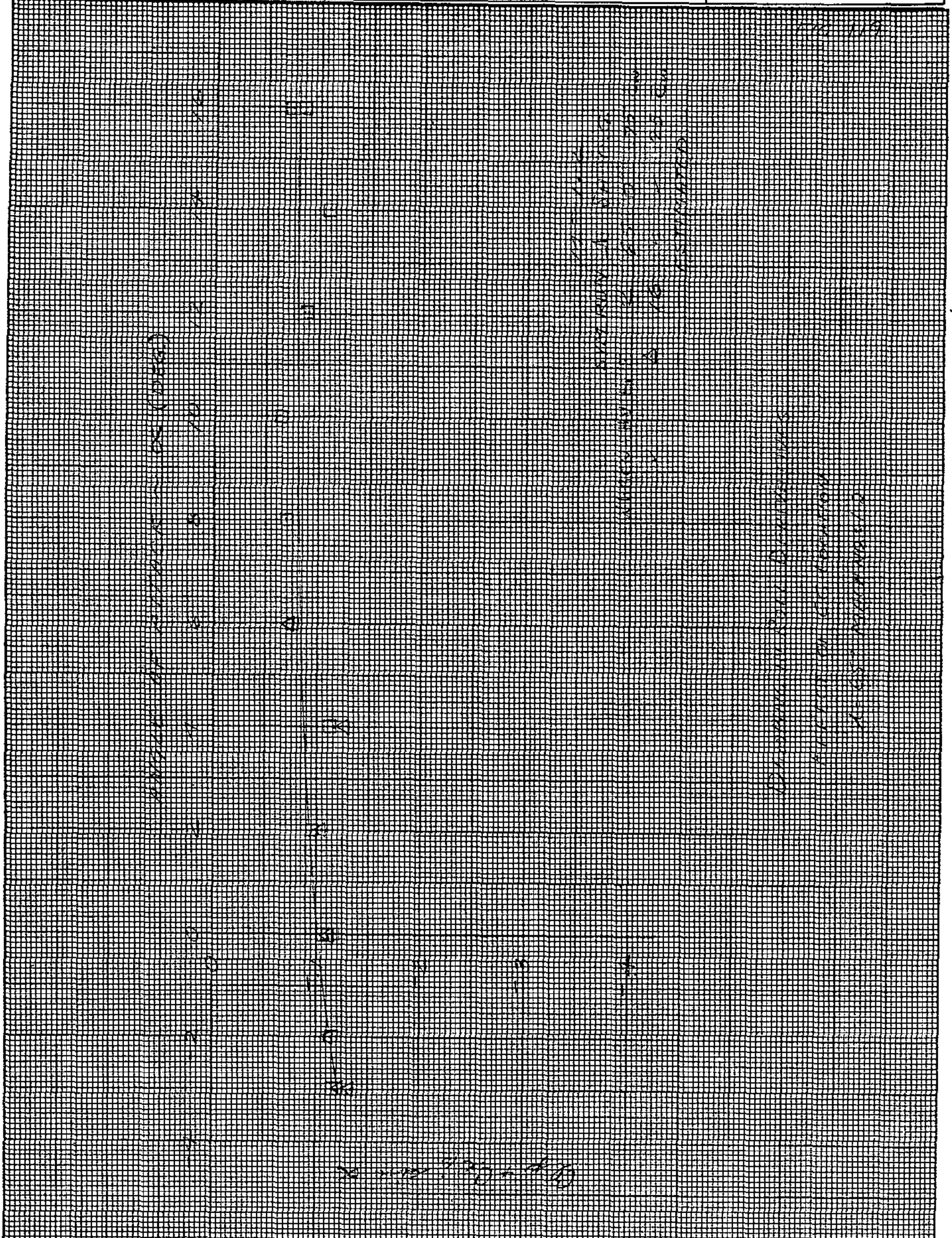
ANGLE OF ATTACK ~ α (DEG)